DIGITAL SIMULATION OF A FOUR-WINDING, UNIFORM AIR-GAP, ROTATING AC ELECTRICAL MACHINE FOR DYNAMICAL ANALYSIS STUDIES

by

Thomas H. Einstein

B.S. University of New Hampshire
(1954)

M.S., Case Institute of Technology
(1961)

SUBMITTED IN PARTIAL FULFILLMENT OF THE

REQUIREMENTS FOR THE DEGREE OF

MECHANICAL ENGINEER

at the

MASSACHUSETTS INSTITUTE OF TECHNOLOGY

May 1969

Signature of Author .. ..
Department of Mechanical Engineering, May 23, 1969

Certified by .....
Thesis Supervisor

Accepted by ....
Chairman, Departmental Committee on Graduate Students

DIGITAL SIMULATION OF A FOUR-WINDING UNIFORM AIR-GAP ROTATING AC ELECTRICAL MACHINE FOR DYNAMICAL ANALYSIS STUDIES

by

THOMAS H. EINSTEIN

Submitted to the Department of Mechanical Engineering
on May 23, 1969 in partial fulfillment of the
requirements for the Degree of Mechanical Engineer

ABSTRACT

In this thesis a mathematical model is developed for digital computer simulation of a four-winding, uniform air-gap rotating AC electrical machine. The four coil windings of the basic machine are assumed to be sinusoidally distributed in space around the air-gap circumference, and consist of two magnetically orthogonal rotor windings and a similar pair of magnetically orthogonal stator windings.

The simulation developed in this thesis differs from most other conventional simulations of rotating electrical machinery in that the machine is modeled directly in terms of the physical winding currents, flux linkages, and voltages, rather than in terms of transformed variables defined on a suitably rotating dq reference frame.

The simulation presented here is unique in two respects. First of all the problem of magnetic saturation in the machine is treated at a very fundamental level in the development of the machine model equations. The non-linearity of the magnetic energy storage due to saturation is represented in terms of a magnetic coenergy function. It is shown that for the case of the uniform air-gap machine with sinusoidally distributed windings, the effects of magnetic saturation do not give rise to harmonic components in the winding currents or voltages. Consequently, the effects of saturation on machine performance can be rigorously represented in terms of an equivalent linear machine.

The second unique feature of the present simulation is its generality in terms of its ability to model machines having unsymmetric and/or an aribtrary number of open circuited windings. Consequently, the machine model of this thesis may be used to simulate single-phase machinery, machines connected to external networks which contain solid state components, unbalanced faults and the effects of opening or reclosing of circuit breakers. A machine having less than four windings can be considered as a four-winding machine having several of its windings open-circuited; therefore such machines can also be simulated using the model of this thesis, as long as the existing windings satisfy the conditions of orthogonality and sinusoidal distribution.

The most serious problem inherent in the digital simulation of rotating electrical machinery appears to be the limitation imposed on

the maximum allowable time step-size used in the computation by the value of the smallest physical time constant in the machine system being simulated.

The basic problem of modeling a multi-machine system for simulation is to choose and combine the mathematical models of the individual machines and network components in the system so that the input/output causality requirements of each of these component models are satisfied upon interconnection with the rest of the system. Three methods of simulating systems composed of two or more electrically interconnected machines are described:

1. The machine interconnection network contains resistive or capacitive shunt impedance elements. The individual machines in the system are represented by conventional single machine models which have integration causality, such as the model of this thesis.

2. At least one machine in the system is simulated by a model having derivative causality (current in/voltage out). Such a formulation involves the use of computational differentiation in the simulation.

3. The equations of the individual machine models in the system are analytically combined with those of the interconnection network in order to eliminate the need for computational differentiation.

It appears that either of the latter two methods described above must be used for the simulation of directly interconnected machine systems - systems in which the interconnection network contains no resistive capacitative shunt impedances.

Three examples of single machine simulation, and two examples of two-machine system simulation are described, and simulation results for these examples are presented. The single machine simulations include transient performance of induction motors during start-up and acceleration, and the transient response of a synchronous motor to step changes in mechanical load. The two-machine system examples consist of an induction motor interconnected to an alternator, and the response of the system during starting of the induction motor is given.

Thesis Supervisor: Henry M. Paynter
Title: Professor of Mechanical Engineering

ACKNOWLEDGMENTS

First of all, I would like to thank my thesis advisor Professor H. M. Paynter for originally having stimulated my interest in the topic of rotating electrical machinery, and for his subsequent guidance and intellectual stimulation during the research for and preparation of this thesis. In particular, the basic method of approach to the modelling of electrical machinery in this thesis has been very strongly influenced by many of Professor Paynters conceptual ideas regarding the modelling of electromechanical devices for simulation.

I would also like to thank Professor D. C. Kamopp for taking the time to critically review much of the material in this thesis, particularly the sections regarding computational causality and the simulation of multi-machine systems. His suggestions and corrections were invaluable and their inclusion resulted in an immeasurable improvement in the readability, clarity, and coherence of much of the material in Chapter 2.

I would also like to express my sincere appreciation to my typist, Mrs. Susan Daly, for her efficiency, impeccable neatness and accuracy, and for her patience during the inevitable difficult moments that arise when racing against time to meet a deadline.

Finally, I would like to express my gratitude to the National Science Foundation for its financial support during the first two of three years of graduate study and research at MIT, and to Lincoln Laboratory for their financial support during this past year.

TABLE OF CONTENTS

CHAPTER I

INTRODUCTION

1.1 Background

In recent years there has been a revival of interest in the dynamical performance of rotating electrical machinery, from both a practical and a theoretical point of view. Much of the current research in this field appears to be focused on the dynamical performance of alternating current machinery, in particular the common synchronous and induction machines which are predominant in the majority of industrial electromechanical energy conversion applications. The renewed interest in the dynamic performance of these two types of machines appears to have been motivated primarily by the following two recent developments. First, the recent application of solid state devices, such as high power SCR's, in circuits for continuous speed control of AC machinery has demanded the development of new methods of analyzing the performance of rotating machines, even in the steady state. This is so because the existing steady state theory, based on phasor diagrams, etc., is strictly applicable only for constant frequency sinusoidal terminal voltages whereas the introduction of solid state power control devices results in the application of terminal voltages and the creation of winding currents which differ markedly from constant frequency sinusoids. Secondly, the disasterous Northeast Blackout of November 1965, indicated that the current level of understanding of the dynamic interaction between interconnected machines in a power system during a severe transient disturbance left much to be desired. One might say that the effect of the Northeast Blackout on the electric power industry was analogous to that of Sputnik on the aerospace industry some eight years earlier.

1.2 Synopsis

The objective of this thesis is the development of a digital simulation model for the dynamic performance of a four winding uniform air-gap rotating electrical machine. Because of the practical importance of AC machinery and the difficulty of analyzing the general dynamic performance of most AC machines in contrast to that of DC machines, the model to be developed will be applied only to the dynamic simulation of AC machines which have either slip-rings or squirrel cage rotors. A slight modification of this model would also provide for the simulation of either AC or DC commutator machines, however, no examples of such applications will be given in this thesis. Typical examples of practical machines whose dynamic performance can be simulated by the model of this thesis are most squirrel cage induction motors and round-rotor synchronous machines, however, the model does not provide for the simulation of salient pole machines.

The model developed for the single machine is also used as a component in the development of a dynamic simulation of a system composed of two electrically interconnected round-rotor machines. Typical practical problems that can be investigated with this two-machine dynamic simulation are the starting of an induction motor powered by an alternator and the transient or accelerating performance of two synchronous machines connected in parallel to a common bus. It is shown that there are certain unique computational difficulties associated with the dynamical simulation of multi-machine systems that are not generally encountered in the dynamical simulation of single machines.

1.3 Definition of Machine Dynamical Performance

Since the purpose of the simulation model to be developed is the investigation of dynamic performance, it is appropriate to define "dynamic performance" of a rotating machine, particularly in contrast to its "steady-state" performance. A clarification of the meaning of "dynamical performance" is especially necessary with respect to the performance of AC machinery, where strictly speaking, the applied terminal voltages are always time varying, even during steady state operation. In brief, the "dynamical performance" of a rotating machine is defined as its performance for any operating conditions other than "steady state". The "steady-state" performance of an AC machine is defined as its performance for constant speed operation with sinusoidal armature terminal voltages of constant magnitude and frequency in the limit as $t \to \infty$. There are three separate conditions expressed in the above definition; (1) constant speed, (2) sinusoidal voltages of constant frequency and magnitude, and (3) in the limit as $t \to \infty$, which implies that the effects of all initial transients have decayed.

Condition (2) in the above definition of steady state operation appears somewhat arbitrary in that it restricts steady state operation of an AC machine to operation in the presence of sinusoidal terminal voltages only. Thus constant speed operation of an AC machine with impressed voltages that are periodic but non-sinusoidal, as for example a rectangular voltage waveform, is not considered steady state in the sense of the above definition. This restriction in the definition of steady state operation of an AC machine to conditions for which the impressed voltages are sinusoidal is consistent with the conventional

concepts of steady-state equivalent circuits and phasor diagrams, and indeed these concepts only approximately represent the performance of the machine when the impressed voltages are non-sinusoidal.

Having thus defined "steady-state" performance of AC machinery, the "dynamical performance" of a machine is defined as its performance under any or all of the following conditions.

1) Operation during electrical transients, such as sudden short circuits, sudden changes in applied terminal voltages, etc.
2) Operation while rotor speed is changing - for example, the starting of a motor, the hunting of synchronous machines, etc.
3) Operation for non-sinusoidal impressed voltages - as occurs for example, when the machine is connected to a network of solid state devices such as rectifiers, inverters, or cycloverters.

In the following, frequent reference is also made to the "dynamical equations" of a machine. These "dynamical equations" refer to the basic equations of motion of the machine viewed as an electromechanical system composed of coil windings mounted on movable mechanical structures which have finite inertia. For any machine these equations of motion consist of the following; a constitutive relation between the flux linkages of the coil windings in the machine and the currents through those windings, an expression for the electromagnetic torque as a function of the coil flux linkages and currents, a voltage equation for each coil winding which expresses the derivatives of the coil flux linkage in terms of the instantaneous impressed terminal voltage and the resistive voltage drop in the winding, and finally a mechanical torque balance equation for the rotor structure. These relations are usually expressed as a system of four or more coupled non-linear

differential equations which are soluble by elementary methods only in certain special cases. In general the solution of these "dynamical equations" requires the use of an analog or digital computer. The familiar algebraic equations for the steady state operation of an AC machine, which are the basis of phasor diagrams and steady state equivalent circuits, are the steady state (as $t \to \infty$) solutions of these "dynamical equations" for the special case of constant rotor speed and sinusoidal impressed voltages of constant magnitude and frequency.

1.4 Dynamical Analysis of Rotating Electrical Machinery

Although methods for the dynamical analysis of most common types of DC machinery are straightforward and have been well established for many years, the situation for AC machinery, which though far more important in applications, has not been nearly as satisfactory. The reason for this discrepancy is that the dynamic analysis of DC machinery is far simpler and more straightforward than that for AC machines. The relative ease of dynamic analysis of DC machines is due to the fact that for most practical DC machinery, there is very little dynamical interaction between armature and field circuits. As a result of this decoupling between armature and field dynamics, the differential equations which describe the dynamical performance of a DC machine may be broken down into several sets of independent and uncoupled ordinary differential equations, each of which is seldom of higher than second order, and which are thus amenable to direct solution by elementary methods.

Unfortunately, for most AC machinery because there are strong dynamical interactions due to the electromagnetic coupling between armature and field circuits, the dynamical equations of motion for the

AC machine do not decouple into simple isolated sets of first and second order ordinary differential equations, as in the case of the DC machine. Consequently, the computation of the transient performance of an AC synchronous or induction machine generally entails the solution of a strongly coupled system of non-linear differential equations which are at least fourth order but usually sixth order or higher. In general, the solution of such a system of equations is feasible only with the aid of an analog or digital computer. Only when severely restrictive assumptions are made concerning the nature of the solution, as for example, balanced steady-state operation under constant frequency sinusoidal excitation, do the equations of motion for the AC machine reduce to the point where their solution may be achieved by manual methods. Indeed the solution of the equations of motion for the AC machine for steady-state, constant frequency sinusoidal operation form the basis of the well known "steady-state equivalent circuits" for such machines. However, it should be re-emphasized that solutions for the transient response of AC machines can usually only be approximately obtained by manual methods, and then only in certain circumstances such as symmetrical short circuits. In general, the solution for the transient response of an AC machine requires the use of an analog computer or numerical methods on a digital computer.

The relative simplicity of the equations of motion for a DC machine may be considered as resulting from the resolution of the magnetic fields produced by the armature and field windings along orthogonal axes which remain stationary in the machine. Independent machine voltage equations may then be written for each of these orthogonal axes. Indeed for the simplest common DC machine having only a single field

winding and a single pair of brushes, with the brush axis orthogonal to the axis of the field winding, the magnetic fields produced by the field and armature windings will always be mutually orthogonal and thus have no mutual coupling between them. Because of the resultant absence of mutual coupling between the armature and field windings for such a machine, dynamical voltage equations for the two windings will be uncoupled first order differential equations. Although the situation is slightly more complicated for DC machines with series field or compensating winding and/or multiple brush axes, the resulting dynamical equations are still usually sufficiently decoupled to permit their solution by elementary methods.

The relative simplicity with which solutions to the dynamical equations for a DC machine could be obtained, led to the development, in the late 1920's of a technique for transforming the dynamical equations of an AC synchronous machine into those of an equivalent DC machine. This technique was developed by Park in 1928 and is the basis for the well known dq transformation. The dq transformation may be viewed either as a physical transformation of a balanced AC machine into and equivalent DC commutator machine having two orthogonal stator windings and two sets of brushes on orthogonal axes, or merely as a mathematical transformation of the machine's equations of motion. From either point of view, the objective of this transformation is to simplify the dynamic equations of the machine and the analysis of its transient performance. For many practical machines the physical interpretation of this transformation, in terms of an equivalent dc machine, corresponds to analysis of the machine from the familiar viewpoint of a rotating magnetic field.

One of the principal complications in the dynamical equations of AC machines is that the mutual inductances between the different windings on the rotor and stator of the machine are functions of the rotor angle, with the result that sines and cosines of the rotor angle appear in the voltage equations for each of the windings. Since this rotor angle is a continually varying function of time, the resulting equations will have time varying coefficients in addition to being strongly intercoupled. Note that this problem does not exist in DC commutator machines whose brush axes are fixed. The mathematical simplification resulting from application of the dq transformation is that for many practical AC machines this rotor angle dependency of the equations of motion can be eliminated by use of the transformation. Another way of saying this is that because the transformed equations of motion are those of the equivalent DC machine, they do not contain trigonometric functions of the rotor angle. However, it should be pointed out, AC machines do exist whose equations cannot be simplified by application of this transformation. Perhaps the simplest example of such a machine is the single-phase alternator. No transformation can be found which eliminates the angle dependency of the equations for this machine.

Although the dq transformation was originally developed for the purpose of simplifying the dynamic analysis of balanced polyphase synchronous machines, its application in the analysis of other types of balanced polyphase AC machinery also results in similar simplification of the machine's dynamic equations. In general, application of the dq transformation simplifies the transient analysis of polyphase AC machines which are balanced and whose armature windings are connected to either a balanced impedance network or a balanced polyphase sinusoidal voltage

source. The tremendous importance assumed by the dq transformation in the last forty years is primarily due to the fact that the above conditions are satisfied, at least in principle, in most practical applications of polyphase AC machinery. Consequently, the dynamical analysis of such machines is tremendously simplified by transformation of the machine equations into dq coordinates. Although the dq transformation may be applied to equations of any AC machine, when the machine or the voltage sources and loads to which it is connected are unbalanced, or if the voltage sources are non-sinusoidal, the resulting transformed equations often become no simpler to analyze than the original ones, with the result that use of the transformation in those cases offers little or no analytical advantages. For example, although the use of the transformation considerably simplifies the dynamical analysis of a balanced polyphase synchronous machine, it provides no simplification in the analysis of a single phase alternator, as the latter may be considered as an unbalanced two-phase synchronous machine - the machine being unbalanced because one of the two armature phase windings is open circuited. In certain situations where the machine is asymmetric or where the applied terminal voltages are either non-sinusoidal or unbalanced, although the form of the machine equations may be simplified by application of a properly chosen dq transformation, the resulting simplification of the machine equations is of little practical value, because application of the transformation to the applied terminal voltages then results in their becoming dependent upon the machine's rotor angle. Consequently application of a dq transformation to such problems merely shifts the location of the analytical complexity from machine equations to the resulting expressions for the transformed applied terminal

voltages.

Another situation in which the advantages of applying the transformation are somewhat compromised is the dynamic analysis of a system of independent machines which are electrically interconnected, even when all of the machines and their interconnection network are balanced. Such a system is characterized by independent sets of dynamical equations for each machine in the system together with a set of algebraic constraint equations which represent the effect of the electrical interconnection equations. In this situation, the dq transformed set of system equations consists of machine equations which are independent of rotor angles, and constraint equations representing the interconnection which will be functions of the rotor angle differences between the various machines in the system. In contrast, the original (untransformed) equations for such a system consisted of machine equations which were dependent upon the rotor angles of the various machines, and interconnection constraint equations in which no rotor angles appeared. Thus the rotor angle dependency of the dynamic equations for a system of interconnected machines can never be completely eliminated and such problems almost always require the use of analog or digital computation for their solution. However, the use of the transformation in such problems often leads to a slight simplification in the numerical or analog simulation because the angle dependency is now a function of the difference between the machine rotor angles rather than of their absolute values.

Despite the fact that the dq transformation cannot be used to simplify the dynamical equations of every conceivable machine configuration, its wide acceptance stems from its applicability in a large

number of practical situations where the dynamical problem can be at least approximately represented as that of a single balanced machine operating against either a balanced load or a balanced sinusoidal voltage source (infinite bus). Typical of such problems is the response of a balanced machine to a suddenly imposed balanced short circuit in its armature circuit - in power systems parlance, a three-phase short circuit. The use of the dq transformation in the analysis of such common problems has led to the development of simplified concepts such as "transient reactance" of a machine - an apparent machine reactance used to compute the fundamental frequency currents in a machine in response to transients such as suddenly applied balanced short circuits.

1.5 Equivalent Circuits of Rotating Electrical Machinery

No discussion of the subject of dynamic simulation of rotating electrical machinery would be complete without some mention of the role of steady state equivalent circuits in and the contributions of Gabriel Kron to the dynamic analysis of electrical machinery. Equivalent circuits for representing the steady state performance of AC rotating machinery were in existence prior to 1930. It should be emphasized that these "equivalent" circuits are valid characterizations of the machine only for steady state operation with constant frequency sinusoidal applied terminal voltages. Although such steady state equivalent circuits exist for both balanced and unbalanced AC machinery, these equivalent circuits are not valid representations of machine operation for transient conditions, nor for non-sinusoidal applied terminal voltages. That such steady state equivalent circuits do not provide completely valid representations of a machine's transient performance is perhaps

most clearly illustrated by the use of two different machine reactances - the "synchronous reactance" and the "transient reactance" - in the "equivalent circuit" of a synchronous machine for the representation of the machines steady state and transient performance, respectively. Furthermore in the above illustration, the steady state equivalent circuit provides an exact representation of the machines steady state performance, whereas the "transient equivalent circuit" consisting of an excitation voltage "behind the transient reactance" only approximately represents the machines total transient behavior.

The reason that such equivalent circuits cannot be used to simulate the response of a machine under general transient conditions is that these circuits are derived from the steady state solutions of the machine dynamic equations for constant frequency sinusoidal applied voltages and constant rotor speed. In this respect it should also be noted that a steady state constant frequency sinusoid is defined as having started at $t = -\infty$; therefore the steady state equivalent circuits are also not valid for simulation of starting transients in a machine - the response of a machine when a constant frequency sinusoidal voltage is suddenly applied to the armature terminals. Similarly, the steady state sinusoidal equivalent circuits only approximately represent the steady state operation of a machine when the applied voltages have periodic wave forms which are non-sinusoidal - as for example when the machine is supplied from a solid state inverter or speed control circuit. Such a representation effectively represents the operation of the machine in response to only the fundamental component of the applied waveform. However, an improved simulation of the steady state operation of a machine with periodic but non-sinusoidal applied voltages may often be realized

by a combination of several different sinusoidal steady state equivalent circuits, one circuit for each of the principal frequencies appearing in a harmonic decomposition of the applied wave form.

The role of equivalent circuits in the dynamic analysis of rotating machinery has been exhaustively treated by Kron[10]. The essence of the relation between these equivalent circuits and the general dynamical equations of a machine is that, although the transient performance of a machine cannot be simulated by a steady state sinusoidal equivalent circuit consisting of stationary networks, there is a one-one correspondence between such steady state equivalent circuits and the machine's equations of motion. This means that if the steady state sinusoidal equivalent circuit is known, the general dynamical equations of motion can be written down and vice-versa. This dual relationship between the steady state equivalent circuit and the dynamical equations of motion is very concisely expressed by Kron as follows:

> "The equivalent circuits (in terms of stationary networks) to be developed cannot be set up on a transient analyzer to establish exact solutions of transient problems such as sudden short circuit or acceleration problems .... Nevertheless, all equivalent circuits given (in reference 10) have been so organized that they may be used to write down, not only the sinusoidal, but also the transient and accelerating equations of performance of any rotating machine or group of machines by simple inspection."

Kron realized that exact solutions to transient problems in electrical machinery could only be obtained by actually solving the general dynamical equations for a given machine or system of machines. In the late 1930's he developed a unified method, based on tensorial mathematics, of deriving the dynamical equations of any common industrial rotating electrical machine. Kron's principal contribution to the study of rotating machinery dynamics seems to have been the introduction

of the concept of a "primitive" or generalized machine, and that the various common types of practical machines such as synchronous machines, induction machines, machines with movable brushes, etc., could be viewed merely as different variations of the primitive machine. By using this concept of a primitive machine Kron showed that the dynamical equations of any practical machine could be systematically obtained from those of the "primitive machine" by applying appropriate "connection tensor" and "brush shifting" transformations to the equations of the primitive machine. Since the dynamical equations of the primitive machine were invariant, all that was necessary to derive the dynamical equations of the actual machine was the knowledge of the "connection tensor" a matrix which represented the electrical connections between the windings of the actual machine, and if applicable, the appropriate "brush-shifting" transformation which represented the effects of skewed brushes in the actual machine. Kron thus developed a completely systematic, almost mechanical, method of formulating the dynamic equations of most common rotating machines.

The dynamical equations of a rotating machine which are derived by Kron's method appear in operational form and are generally expressed in terms of dq coordinates. Consequently, in many cases, the steady-state performance of an AC machine for sinusoidal terminal voltages may be manually computed from Kron's dynamical equations, merely by evaluating these equations for $s = j\omega$. However, in the general case, solutions to the dynamical equations of a rotating machine can only be obtained by programming these equations on an analog or digital computer, and neither of these devices were available thirty years ago when Kron developed his method. Thus it is not surprising that Kron's work was concentrated

on developing methods of formulating the equations of motion of a machine, rather than in developing methods of actually solving the resultant equations. For the same reasons it is also not surprising that the dynamical equations resulting from Kron's method of formulation sometimes appear in a form which is inconvenient for direct simulation on either an analog or digital computer; this comment is particularly applicable to Kron's formulation of the dynamical equations for a system of several electrically interconnected rotating machines. The fact that Kron's methods merely led to the dynamical equations of a rotating machine rather than to solutions of those equations, and that the form of the resultant equations, particularly in the case of complex systems, was not always amenable to direct implementation on a computer even when analog and digital computers became available, probably has impeded the wider acceptance of Kron's methods in practical engineering circles.

Perhaps Kron's most valuable contribution was his concept of a generalized or primitive machine, and that seemingly dissimilar practical machines as, for example, synchronous and induction machines are merely variations of the same primitive machine. This concept of a generalized machine is really the foundation of the approach to machine simulation taken in this thesis. It will be seen that, for example, the difference between synchronous and induction machines is not reflected so much in the equations of these two types of machines, but rather in the boundary conditions and the specific solution of the equations for each machine.

1.6 Analytical Formulation of Machine Dynamical Equations for Computer Simulation

It was pointed out above that the application of Kron's methods

does not always result in machine dynamical equations which are in a form that is convenient for simulation or computation. It is therefore appropriate at this point to inject a few comments regarding the general problem of formulating the dynamical equations of a physical system from the point of view of facilitating the eventual simulation or numerical solution of these equations. It turns out, perhaps surprisingly, that this is often a formidable problem. The root of this problem lies in the fact that the analytical representation of the behavior of a physical system, in terms of dynamical equations, is generally not unique. A given system may be represented by several different, but equally valid, mathematical models; not all of these however are necessarily equally convenient from a computational point of view. In particular, for purposes of numerical computation or simulation on an analog computer, the system equations should usually be so organized that the need for computational differentiation in the solution of these equations is avoided as much as possible. Except in the rare cases where an analytic solution of the system equations can be obtained, the dynamical relations should be so formulated that their computational solution entails only integration. The use of integration in lieu of differentiation is a well established procedure in analog computer simulation and is also a generally preferred method of numerical solution on a digital computer.

Generally, a "state-variable" formulation of the system equations is one that is convenient for computational implementation. In this formulation the time derivative of each independent system variable is expressed as a function of all the system variables, but not of the derivatives of any of these variables. A detailed discussion of state

variable formulation for the dynamical equations of a physical system is not within the scope of the present discussion but may be found in [13]. In the case of simple first and second order systems, the form of the system equations that is most convenient for computation is usually obvious, however, for higher order systems organization of the system dynamical equations into a form convenient for direct simulation or numerical computation often presents a formidable problem.

The problem of organizing the dynamical equations of a physical system into a form convenient for simulation and computation has been the subject of some recent research. In [12] a systematic procedure is developed for organizing the system equations for simulation and computation using the bond-graph method of modeling a physical system. An introduction to bond-graph methods of modeling physical systems and the role of these bond-graphs in organizing the formulation of the system equations to facilitate computation - or in bond-graph parlance "the assignment of computational causality" - is given in [15].

1.7 Analog vs Digital Computer Simulation of Rotating Electrical Machinery

Most dynamical simulations of rotating electrical machinery have, until recently, been implemented on analog rather than digital computers. This has been partly due to the fact that the availability of commercial electronic analog computers preceded that of digital computers of comparable computing capacity by nearly a decade, and that until recently the analog computer has been the typical means of solving general problems in dynamics and control - particularly those involving electrical circuits or electrical analogs of thermal, mechanical, or fluid systems. Consequently, much of the analog computing lore that had been developed

for the general simulation of dynamics and control problems could be directly applied to facilitate the simulation of rotating machinery dynamics problems. Examples of analog computer simulations of rotating machinery problems are given in [6], [7], [8]. Furthermore, analog computer representations in terms of dynamical block diagrams for a wide variety of rotating electrical machinery may be found in [18].

Another reason for the predominance of analog computer simulations for solving dynamics problems of rotating machinery has been one of economics. Analog computers are much less expensive than their digital counterparts, and once a machine dynamics problem has been set up on an analog computer, the solution of the problem usually procedes in real-time - that is it only takes one second of computer time to compute the response of the system being simulated over one second of problem time. Thus once a problem has been set up on an analog computer the cost of generating solutions on the computer is next to nothing. On the other hand, even on the most recent vintage high speed digital computers, the solution time required for typical machinery dynamics problems is roughly two orders of magnitude longer than on an analog computer - roughly one minute of computing time for every second of problem time. Consequently based upon an approximate cost of $10/min for computation time on a high speed digital computer, the total cost of generating many solutions on a digital computer can become quite expensive. The reason for the much greater speed of the analog machine is effectively due to the fact that an analog computer actually performs many different computations simultaneously, or in parallel, whereas most general purpose digital computers can only work on one computation at a time and thus must compute the necessary operations serially. For example, if a given problem requires

the integration of ten different variables, the necessary computation is performed sinultaneously by ten separate integrators on an analog machine, whereas a digital computer must perform the necessary numerical integrations in sequence for each variable. For the same reason, the required computation time for a problem on analog computer is nearly independent of problem size, whereas on a digital computer the required computation time increases nearly in proportion to the size of the problem. Thus the solution of a large problem on an analog computer takes no more time than for a small problem, whereas on a digital computer the solution of the larger problem requires proportionally more computation time. However, as will be seen, one of the advantages of a digital computer is that it can accommodate much larger problems than would be practical to simulate on an analog computer.

Despite the economic advantages that appear to be associated with the use of analog computers, there has been a recent trend towards the increased use of digital computers for solving problems in rotating machinery dynamics, particularly for problems involving a system of many electrically interconnected machines [11], [15]. The advantages offered by the digital computer, despite its significantly greater incremental cost of computation, are briefly: increased flexibility, easier problem set-up, avoidance of scaling problems, and greater reliability. The greater flexibility offered by a digital computer is due to two factors.

First, a digital computer of even medium capacity is generally capable of accommodating much larger problems than most analog computers. The number of available components and operational amplifiers in most analog computer installations is quite limited, but the number of these

elements required in a given problem simulation varies nearly in direct proportion with the problem size. As a result, the simulation of a dynamics problem involving two machines with their associated controllers represents the approximate upper limit on problem size that can be handled on most conventional analog computer installations. In a digital computer, a simulation problem for a large system often only requires slightly more storage (although a much longer solution time) than a similar type of problem for a much smaller system. This compression of problem size on a digital computer is accomplished through the use of subroutines - for example, although a given simulation may require the computation of the sines and cosines of many different angles, the computation for each of these angles is performed by the same physical set of program instructions in the computer, rather than having a different set of instructions compute these quantities for each angle variable. Because of these considerations, the simulation of the dynamic performance of large systems involving many electrically interconnected rotating machines is usually implemented on a digital computer [11], [15].

A second area in which the use of a digital computer offers greater flexibility than an analog computer is in the simulation of non-linear functions such as non-linear machine magnetization curves, transcendental functions, etc. Although analog computer techniques for simulating such non-linearities exist, they are often quite cumbersome, and their use is subject to many restrictions. On the other hand the presence of non-linear functions presents no special problems in a digital computer simulation.

In addition to the increased flexibility offered by digital simulation, digital computer programs are also much easier to set up, debug, and operate than analog simulations. For example, the troublesome necessity of scaling an analog simulation is completely avoided in most modern digital computers which use floating-point arithmetic for scientific computations. Furthermore, digital computer programs can be stored indefinitely on punched cards or magnetic tape, thus enabling these simulation programs to be set-up for operation merely by reading the program deck or magnetic tape back into the computer, a procedure that is both rapid and effortless. On the other hand, for an analog computer, even when the basic simulation is wired into a removable and storable plug-board, set-up of the simulation generally requires manual re-calibration of the operational amplifiers and gain potentiometers each time.

Examples of digital simulations of multi-machine dynamics problems have already been cited. An example of a digital simulation of a single machine and a good discussion of the relative merits of digital vs analog simulation of rotating machinery problems is given in [4].

1.8 Advantages and Limitations of dq Transformation in Machinery Analysis

The original motivation for the development of the dq transformation described earlier was the tremendous simplification in the machine's equations of motion that resulted when the transformation was applied to the equations of a symmetric polyphase machine connected to either balanced loads or a balanced polyphase sinusoidal voltage source. The resultant simplification of the equations enabled approximate

analytical expressions to be derived for the effects on machine performance of commonly occurring transient conditions in power systems such as polyphase symmetrical short circuits. In the days prior to the advent of analog and digital computers, such approximate analytical methods were the only means of determining the effects of such transients on the performance of AC rotating electrical machinery. Approximate analyses of symmetric short circuits in polyphase synchronous and induction machines in terms of dq variables are described in [3].

As was mentioned earlier, the solution of the dynamic equations of a rotating machine in terms of dq variables does not directly yield the instantaneous values of the machine coil or phase variables (voltages and currents) and if these quantities are desired, it is necessary to apply the inverse dq transformation to the solution in terms of dq variables. Application of this inverse transformation effectively re-inserts the rotor angle dependency into the solution in order to produce the instantaneous values of the actual voltages and currents flowing in the physical coils of the machine. However, in many practical applications involving symmetric polyphase machinery, the principal properties of the transient solution which are of interest are the mechanical motion of the rotor, the peak magnitude of the phase currents, and the stability of the system, and all of this information is directly obtainable from the solution expressed in dq coordinates. Thus unless the actual instantaneous values of the phase variables are also required (and they often are not), application of the inverse transformation is not necessary.

Because the dynamic equations of systems consisting of balanced rotating machine, networks, and voltage sources are greatly simplified when expressed in terms of dq coordinates, and since a great many

practical applications involve only such balanced machines and networks, most computer simulations of such systems have been and in all likelihood will continue to be formulated in terms of d-q variables. A typical example of the simulation in terms of dq coordinates of a balanced multi-machine system for power system stability study is given in [11].

It is only for situations in which the machines are asymmetric, the networks to which the machine is connected unbalanced, the voltage sources either unbalanced or non-sinusoidal, or where computation of the instantaneous values of the coil variables is required, such as in the case when semi-conductors are connected to the machine, that the simplifications associated with the use of the dq transformation begin to diminish. However, because of the recent application of solid state devices in circuits for speed control of AC machinery, such formerly unconventional machinery problems are beginning to assume a new importance.

Although the steady state solution of unbalanced systems can sometimes be obtained by the method of symmetrical components, and the method of multiple reference frames may be used to obtain solutions for the steady-state (constant speed) performance of machines in cases where the applied voltages are periodic but not sinusoidal [9], the general transient solution of such problems by manual methods is generally out of the question. When a machine simulation is implemented for solution on either an analog or digital computer, whether or not it should be formulated in terms of dq variables depends entirely upon whether a formulation in dq coordinates offers any computational advantages. Indeed, in certain applications where the instantaneous values of all coil currents must be computed because solid state devices are connected

in series with the machine windings on both sides of the machine, transformation of the machine equations into d-q coordinates only results in further complications, rather than in simplification of the equations.

The problem of determining under what circumstances application of the dq transformation results in a simplification of the equations for a system consisting of unbalanced machines or stationary networks has been investigated by Krause[8]. Recognizing that the primary purpose of the dq transformation was to eliminate time or rotor-angle dependent coefficients from the dynamical equations of the machine, Krause conceived of the dq reference frame as being fixed either in the rotor, or the stator, or rotating at unarbitrary velocity with respect to the stator, usually at synchronous speed or some integral harmonic thereof. For any particular machine problem, that dq reference frame is chosen which results in the greatest simplification of the dynamic equations of the machine. In discussing the problem of simulating unsymmetrical induction machinery in terms of d-q coordinates on an analog computer, Krause[8] implicitly states the rule for choosing the proper dq reference frame for any given machine problem as follows: "If either the stator or rotor of a machine is unsymmetrical, time-varying coefficients will appear in the voltage equations in all (dq) reference frames except the one in the machine where the asymmetry exists." One example of the application of this rule is the following. In problems involving conventional synchronous machines having a single rotor field winding, the dq reference frame is generally fixed to the rotor (whether or not the rotor is salient) with the d axis coincident with the physical axis of the field winding. The rotor circuit in such a machine is unbalanced, even in the absence of saliency, because there is only a single, rather

than two symmetric but orthogonal, windings on the rotor structure. The rotor circuit unbalance in this case may also be viewed as two symmetrical rotor windings connected to an unbalanced external network; the field winding connected to an external voltage source through a finite impedance, the other hypothetical winding, orthogonal to the field, being open-circuited or equivalently connected to an infinite external impedance. Another illustration of this rule is that for an induction machine with asymmetrical stator windings, such as are typical in single phase applications, the angle dependent coefficients are eliminated from the equations of motion only when the dq reference frame is taken as fixed to the asymmetric orthogonal stator windings.

The above "rule" regarding the choice of reference frames may also be extended to the situation where unbalanced external networks are connected to the windings of an otherwise balanced machine. Thus, if an otherwise symmetrical machine has either its rotor or stator windings connected to an external impedance network which is unbalanced, the time varying coefficients in the resultant machine voltage equations disappear only when the dq reference frame is chosen as fixed in the windings to which the unbalanced external impedance network is connected. An example of such a situation is a symmetrical wound-rotor induction motor with unequal rotor resistances. In accordance with the above discussion, when this problem is simulated on an analog computer, [7] the problem is formulated with the dq reference frame fixed to the rotor windings.

A corrolary to the above "rule" for choosing a dq reference frame for ~~in~~ unbalanced or asymmetric problems, such that time varying or angle dependent coefficients are eliminated in the resultant dq transformed

equations, is the following. When unbalanced impedances are connected to, and/or winding asymmetry exists, on both rotor and stator windings of a machine, then no dq reference frame can be found for which the appearance of time varying coefficients in the transformed voltage equations is completely eliminated. A very common example to which illustrates this corrolary is the single-phase alternator. Since this machine has only a single winding, rather than a pair of symmetrical and orthogonal windings, on each structure, both the rotor and stator windings of this machine are considered asymmetrical, with the consequence that application of the dq transformation to the equations of this machine does not result in any simplification. As a result, the general dynamical analysis for this seemingly simple single phase machine is much more difficult than for the case of its balanced polyphase counterpart.

The role of the dq transformation in the computer simulation of dynamical systems composed of rotating electrical machines and stationary impedance networks may be summarized as follows. In the dynamic simulation of such systems, formulation of the equations of motion of each rotating machine in terms of dq coordinates is worthwhile, from the standpoint of simplifying the simulation or numerical computations, only under the following circumstances:

(a) All machines and networks in the system being simulated are balanced.

or

(b) Any network imbalances or machine asymmetries are so restricted such that such asymmetrics appear on only one structure (rotor or stator) of each machine in the system, thus making it possible to find a dq transformation for

each machine that will eliminate time varying coefficients from its equations of motion (although not from the transformed interconnection equations). Note that for the case of a multi-machine system, the above proviso implies that the system asymmetries all lie on the same side of the electrical interconnection between the machines.

and

(c) Computation of the actual instantaneous values of the physical coil voltages and currents of the various machines is not required.

and

(d) Transformation of the voltage sources in the system from physical to dq coordinates presents no serious difficulties. The computational implementation of this transformation is usually not difficult when the voltage sources are constant frequency sinusoids (with DC voltages viewed as zero frequency sinusoids).

Because most practical machinery applications in the past have involved only balanced machines, networks, and sinusoidal voltage sources, dynamic simulations of such applications on both analog and digital computers, have largely been implemented in terms of the dq transformed equations of motion. One of the few exceptions to this general pattern is a recent paper on the simulation of AC machinery with provision for the effects of third harmonics in the space mmf and flux distributions of the machine.[6] The simulation described in that paper was implemented on an analog computer but is unique in that it is formulated in terms of physical coil variables rather than in terms of dq transformed coordinates. The reason given for implementing the simulation in terms of coil variables is that simulation is oriented towards applications

in which the machine's electrical power is derived from solid state inverter or cycloverter systems. As stated in the Introduction of the paper, "Since in matching of electronic devices to electromechanical machines, it is necessary to deal eventually with actual terminal currents, it was felt desirable to develop a simulation which would provide them directly."

1.9 Scope of the Machine Simulation in this Thesis

In this thesis a similar philosophy to that just described will be adopted in that the machine simulations to be developed will be implemented in terms of physical coil variables and no use will be made of dq transformations. Simulation of the machine equations in terms of physical coil variables does complicate the appearance of the mathematical expressions to be computed since the dynamic equations of the machine will contain time varying or rotor angle dependent coefficients. However, such a formulation does provide additional flexibility in that a wide variety of machines can be simulated and no assumptions regarding machine winding symmetry, balanced loads or sinusoidal voltage sources need be made. Consequently, the simulation model developed in this thesis can handle balanced and unbalanced problems with equal ease and is ideally suited for simulation of problems which involve the connection of the machine to solid state devices or other non-linear impedance networks. It is necessary however, to make the following qualification regarding the generality of a simulation implemented in terms of physical coil variables. As might well be suspected, the flexibility of such a simulation is obtained at the following price. Although the simulation to be described may certainly also be used to solve conventional problems involving only balanced machines, impedance networks,

and sinusoidal voltage sources, the solution of such problems in terms of physical coil variables is computationally somewhat less efficient than a simulation in terms of dq transformed equations would be. In particular, the equations of motion of salient pole machines become quite complex when formulated in terms of physical coil variables. Consequently the dynamic simulation of systems involving salient pole machines connected to balanced impedance networks and voltage sources is much simpler and computationally more efficient when formulated in terms of dq variables. Because of the additional computational problems associated with simulation of salient pole machines in terms of physical coil variables, the simulation of salient pole machines is not considered in this thesis.

In addition to being formulated in terms of physical coil variables, the simulation described herein is intended for implementation on a digital computer. Some of the relative merits of digital vs analog simulation were discussed previously, and the principal reason a digital simulation was chosen here, again one of flexibility. With digital simulation, non-linear effects in the machine such as those caused by magnetic saturation can be represented without difficulty. Perhaps the most significant advantage offered by digital simulation is that the simulation can easily be extended to handle systems of several electrically connected machines, whereas such an extension on a medium scale analog computer would be either impossible or impractical. Again, however, one pays a price for such an extension. As will be seen in the ~~chapter~~ section on Simulation of Two-Machine Systems, the simulation of a system of several electrically interconnected poses some serious computational problems which tend to drastically increase the required

computation time, and thus cost of such simulations.

The flexibility provided by a digital simulation is enhanced when the simulation can be conducted on a time-shared digital computer system. In a time-sharing environment, the simulation can be set-up and interactively controlled from a remote computer communications terminal, usually an electric typewriter or a teletype terminal. Such an arrangement provides the person conducting the simulation with an extremely high degree of flexibility at moderate economic cost. Interactive communication between the simulation user and the computer via the remote terminal gives the user complete control over the simulation, even while the simulation itself is actually in progress. For example, the effects of sudden short circuits, both balanced and unbalanced, the opening and reclosing of circuit breakers, etc. may easily be investigated during the simulation run by typing in appropriate commands to the simulation program from the remote communication terminal.

CHAPTER II

ANALYSIS

2.1 The Generalized Machine Model

Although the simulation to be developed is limited to uniform air-gap machines having no more than four indpendent and sinusoidally distributed windings, the analytical model for this simulation will be developed as a special case of a more general model of a rotating electrical machine. The general model from which the specialized machine simulation of this thesis is developed is based upon energy conservation principles. The structure of this general model is independent of number and distribution of windings, uniformity of the air-gap and other magnetic circuit considerations, etc. Such restrictive assumptions are invoked only at the time that the dynamical equations of a specific machine are derived from those of the generalized model. This generalized model may be viewed as an electromechanical multiport having n electrical ports (the terminals of the n coil windings in the machine) and one mechanical port (the rotor shaft).

The electrical variables which define the power flow at each electrical terminal of the model are voltage and current; the corresponding mechanical shaft power variables are torque and speed. A diagram of this multiport generalized machine model is illustrated in Fig. II-1. Furthermore, if it is assumed that all dissipative effects in the machine can be simulated by lumped elements and if magneto-static conditions are assumed, it is possible to decompose this multiport model of the actual machine into a loss-less multiport electromechanical energy converter, and a system of lumped electrical and mechanical impedance networks which connect this loss-less multiport energy

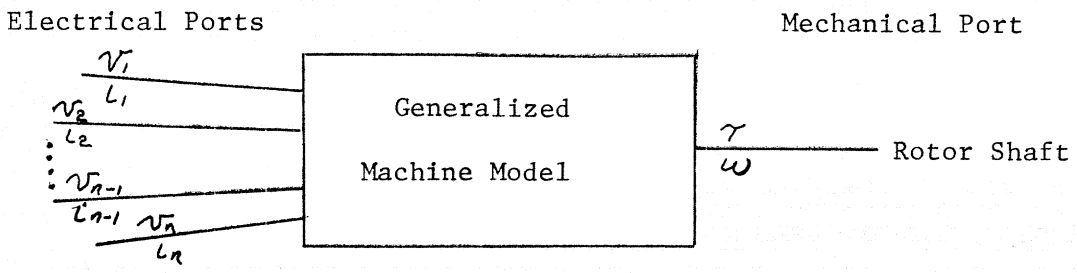

Fig. 2.1 Graphical Respresentation of Generalized Machine Model

converter to the ports of the actual machine model. The additional networks represent all effects that are not directly associated with the magnetic energy storage or electromechanical energy conversion process in the loss-less multiport component of the model, such as resistances of the coil windings and the mechanical inertia and friction of the rotor shaft. The loss-less multiport energy converter, to which these networks are connected, represents the interaction between the mechanical torque and the magnetic flux linkages in the machine. In addition to representing the electromechanical energy conversion process, it also models the storage of magnetic energy in the machine. This decomposition of the model described in Fig. II-1 into a loss-less electromechanical energy converter and a system of external impedance networks is illustrated in Fig. II-2.

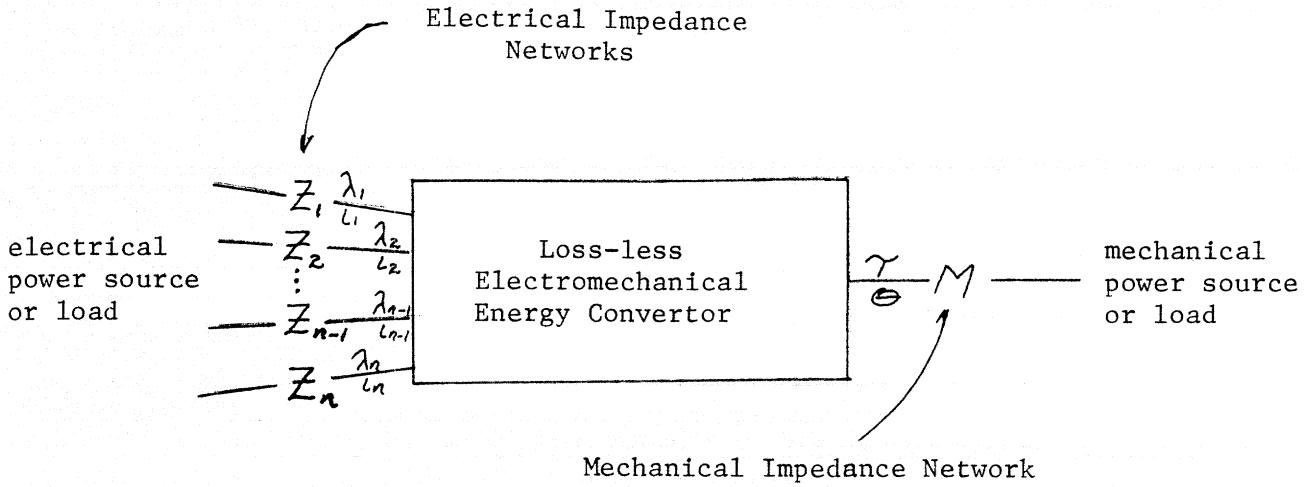

Fig. 2.2 Decomposition of Generalized Machine Model

In the above illustration, the mechanical energy variables are torque, τ, and shaft angle, θ. The corresponding energy variables for the electrical parts are the flux linkages, λ_i, and the coil currents, i_i. Power variables are obtained by using the time rates of change of shaft angle θ and flux linkages λ_i. These are the shaft speed $\omega \equiv \dot{\theta}$ and the induced values of emf, $e_i \equiv \lambda_i^o$ respectively. The mechanical power source or load could be a steam turbine or water wheel, if the machine is used as a generator, or a pump if for example the machine is being used as a motor. The electrical power sources or loads can represent an "infinite bus", interconnections with other machines, etc.

The advantage of the above decomposition of the generalized machine model is that the analysis of the energy conversion process

may be considered separately from that of the attached networks, the latter representing losses, mechanical inertia, etc. Although the analysis of the loss-less multiport is based strictly on the principle of energy conservation, for any specific machine the detailed derivations of the constitutive relations between the mechanical and electrical energy variables often become quite complex because these relations are affected by such factors as nature of the machine's magnetic circuit, number and distribution of windings, magnetic non-linearities etc. On the other hand, the relations for the separated impedance networks which represent winding resistance and shaft inertia are usually quite simple. Thus by separating the generalized model into these two types of components, the analysis of each may be considered independently of the other. The above interpretation of the model for a generalized electrical machine as a combination of a loss-less electromechanical multiport and an external network composed of generalized one and two port impedances is due to H. M. Paynter and D. C. Karnopp.

Because the multiport component of this model is by definition lossless, the algebraic sum of all the incremental energy inputs from each port must equal the increase of energy stored in this device.

$$dW_e = i_i d\lambda_i + \tau d\theta \qquad (1)$$

increase in stored energy	sum of incremental electrical energy inputs	incremental input of mechanical energy

Because a machine usually has several electrical ports (several windings) it is convenient to represent the electrical energy variables λ_i and i, in vector form as follows:

$$\underline{\lambda} \equiv \begin{bmatrix} \lambda_1 \\ \lambda_2 \\ \cdot \\ \cdot \\ \cdot \\ \lambda_n \end{bmatrix} \qquad \underline{i} \equiv \begin{bmatrix} i_1 \\ i_2 \\ \cdot \\ \cdot \\ \cdot \\ i_n \end{bmatrix}$$

In terms of this vector notation Eq. (1) can be written as:

$$dW_e = \underline{i}\tau \; d\underline{\lambda} + \tau d\theta \tag{1a}$$

Because the magnetic energy W_e is a state function, and θ, λ, are independent variables, (1a) is a perfect differential. Thus ~~the~~ W_e is a function of $\underline{\lambda}$ and θ; $W_e = W_e(\underline{\lambda}, \theta)$. In the derivation of the constitutive equations for a specific machine it is often more convenient to work with a magnetic coenergy function W_e^* rather than the energy function W_e. The coenergy function for the present loss-less electromechanical multiport is defined as follows:

$$W_e^* \equiv \underline{i}^T \; \underline{\lambda} - W_e(\lambda, \theta) \tag{2}$$

Upon differentiating (2) and substituting for dW_e from (1a) one obtains the following expression for the differential coenergy:

$$dW_e^* = \underline{\lambda}^T \; d\underline{i} - \tau d\theta \tag{3}$$

The coenergy is a state function and Eq. (3) is also a perfect differential, therefore the coenergy W_e^* is a function of the independent

variables $\underline{i}$ and θ; $W_e^* = W_e^*(\underline{i}, \theta)$. Consequently expressions for the torque, τ, and the winding flux linkages $\underline{\lambda}$ may be obtained as derivatives of the coenergy function $W_e^*(\underline{i}, \theta)$ from (3):

$$\underline{\lambda} = \frac{\partial W_e^*(\underline{i}, \theta)}{\partial \underline{i}} \tag{4}$$

$$\tau = - \frac{\partial W_e^*(\underline{i}, \theta)}{\partial \theta} \tag{4a}$$

Equations (4, 4a) are the basic constitutive relations for the ideal electromechanical multiport component of the machine model illustrated in Fig. 2. It should be emphasized that these equations were derived soley from energy conservation principles and are independent of the magnetic circuit characteristics, or winding distributions of the machine being represented by the model. However, these latter factors are taken into account in the derivation of expressions for W_e^*, $\underline{\lambda}$, and τ for a particular machine as specific functions of the independent variables $\underline{i}$, θ. This determination of the coenergy function W_e^* and its derivatives, the torque and flux linkages, as functions of $\underline{i}$ and θ for a specific machine is dependent upon the details of the spatial distributions of flux and mmf in the machine and is therefore generally not a simple task. Thus equations (4), (4a) are merely a starting point for the derivation of specific expressions of the constitutive relations for τ and $\underline{\lambda}$ as functions of $\underline{i}$ and θ in the analysis of any particular type of rotating electrical machine. The derivation of these expressions for the ideal multiport model of a four-winding smooth air-gap machine with sinusoidally distributed windings is given in Appendix A.

In addition to the generalized constitutive relations for the ideal multiport, the equations of the impedance networks which couple the ideal multiport component to the actual ports of the machine model, as shown in Fig. 2, must also be determined. For simplicity it is assumed that these impedance networks are composed entirely of series elements, however the extension to more complicated network topologies is straightforward. However, the simple series networks are entirely adequate for modelling the effects of winding resistances and rotor shaft inertia. For convenience, and in keeping with the previous definition of the vectors $\underline{\lambda}$ and $\underline{i}$, the applied terminal voltages at the external ports of the model are also defined in vector form:

$$\underline{v} \equiv \begin{bmatrix} v_1 \\ v_2 \\ \cdot \\ \cdot \\ \cdot \\ v_n \end{bmatrix}$$

Thus the equations for the electrical and mechanical impedance networks connected as illustrated in Fig. 2 are:

$$\overset{o}{\underline{\lambda}} = \underline{v} - \underline{Z}\underline{i} \tag{5}$$

$$\tau = \tau_s - M\theta \tag{5a}$$

In Eq. (5) $\underline{Z}$ is the impedance matrix for the electrical network connected between the electrical ports or terminals of the actual machine model and those of the ideal multiport energy conversion component. Similarly M is an operator representing the mechanical impedance of

the rotor structure between the external mechanical power source, or load, and the mechanical port of the ideal multiport component.

Typically, the electrical impedance network $\underline{Z}$ consists merely of the winding resistances of the machine, although series capacitors may also be included in this representation. For reasons of computational convenience to be discussed later, external series inductors are not included in this impedance network but are modelled as part of the machine winding leakage inductances, and are therefore imbedded in the representation of the ~~ideal~~ lossless multiport component. The mechanical impedance operator typically represents only the effects of rotor shaft inertia and friction. For these typical cases, $\underline{Z}$ and M become simply:

$$\underline{Z} = \begin{bmatrix} r_1 & 0 & \cdots & 0 \\ 0 & r_2 & & \vdots \\ 0 & & & \vdots \\ 0 & \cdots & \cdots & r_n \end{bmatrix}$$

Electrical impedance network representation of winding resistance (6)

$$M = J \frac{d^2}{dt^2} + \rho \frac{d}{dt}$$

Mechanical impedance operator for rotor inertia and friction (6a)

J = moment of inertia of rotor assembly

ρ = mechanical friction coefficient of rotor assembly

The complete dynamic equations for the generalized machine model are obtained by combining the constitutive relations (4, 4a) with the network Eqs. (5, 5a). The constitutive relations, which express the eletromagnetic torque and the winding flux linkages as functions of rotor angle and winding currents, represent the ~~ideal~~ lossless electromechanical

energy conversion process of the generalized machine model. The network equations represent the effects of losses and other phenomena such as the mechanical dynamics of the rotor shaft, that are not directly associated with the electromechanical energy conversion process. It should also be noted that the dynamical relations are implicitly introduced soley through the appearance of time derivatives of the state variables in the network equations (5, 5a). The constitutive relations (4, 4a) between the state variables of the ideal multiport component are purely static and time independent as neither time functions nor time derivatives appear in those equations.

In Appendix A specific expressions for the torque and winding flux linkages as functions of rotor shaft angle and winding currents are derived by evaluating the constitutive relations (4, 4a) for the uniform air gap machine with four independent and sinusoidally distributed windings. The resulting expressions for the torque and flux linkages are then combined with the network equations (5, 5a) to obtain a set of dynamical equations for the machine model. These dynamical equations are then organized into a form suitable for numerical computation. The detailed assumptions which more fully describe the uniform air-gap machine being simulated in this thesis are given in the next section.

It should be pointed out the electrical ports of the model in Fig. 1 do not all necessarily correspond to external physical connection terminals on the machine. Each electrical port corresponds to a real or hypothetical winding in the machine. Some windings such as squirrel cage windings, damper bars, and the effect of circulating eddy currents in solid iron rotors are conceptually represented by electrical ports, which although not externally apparent, may be modelled as being

connected to internal impedance networks within the machine - principally the electrical resistances of these windings.

2.2 Assumptions Describing the Machine Simulation to be Developed

The following assumptions define the limitations of the specific machine model to be developed in this thesis. The equations for this specific machine model are derived in Appendix A as a special case of the generalized machine model described in the previous section.

1. The machine has a uniform air-gap such that surfaces of the rotor and stator iron structures are smooth coencentric cylinders. Therefore the characteristics of the machines magnetic circuit are axi-symmetric.
2. The machine has a maximum of four windings arranged in two pairs as follows. Two of the windings are located on the rotor structure and are wound such that their magnetic axes are mutually orthogonal. Similarly, the other two windings are located on the stator structure and are also wound such that their magnetic axes are mutually orthogonal. Two windings are defined as being magnetically orthogonal if they are so located with respect to each other that there is no mutual inductive coupling between them when they are placed in a magnetically isotropic medium. In the case of a two pole machine the physical axes of magnetically orthogonal windings will also be geometrically orthogonal.
3. All windings on the rotor and stator structure are assumed to be sinusoidally distributed in space with respect to the periphery of air-gap. When the windings are so distributed,

the distribution of mmf, resulting from currents flowing in all of these windings, will also be sinusoidal in space with respect to the circular air-gap periphery.

4. Magnetic linearity is not assumed in this analysis. However, it is assumed that the effects of magnetic saturation in the machine's iron structure may be considered on a localized basis - that is that the radial component of flux at any circumferential position along the air-gap periphery is uniquely determined by the local value of the mmf distribution at the position. It is further assumed that the leakage fluxes of each winding are mainly in air and may therefore be represented by constant values of leakage inductances. Finally, it is assumed that the effects of magnetic hysteresis may be neglected.

5. External connections to the rotor windings, when necessary, are made only through slip rings. This assumption effectively limits the application of this simulation to AC machinery. Although only minor modifications need be made to this machine model in order to simulate DC machinery having ideal and continuous commutation, this extension will not be given in this thesis.

A discussion of the above assumptions in terms of the characteristics of common types of AC machinery will more clearly outline some of the practical limitations of this machine model.

Perhaps the most restrictive assumption is that of a uniform air-gap. This assumption precludes the application of the present model to the simulation of salient-pole machines. This assumption is made

primarily for reasons of analytical convenience. Because the present simulation is being formulated in terms of coil variables, rather than in dq coordinates, the introduction of saliency (non-uniformity of the machine's magnetic circuit) would tremendously complicate the derivation of the machine equations, particularly ~~in~~ with respect to the treatment of magnetic saturation.

The second assumption concerning the allowable arrangement of windings in the machine precludes the simulation of machines which have two or more windings on the same structure that are mutually coupled. Such machines are said to have multi-layered windings and include shaded pole induction motors, double-squirrel cage induction motors and synchronous machines with direct axis damper windings. Again this assumption is made primarily for reasons of analytical convenience. However, it should be noted that no assumption was made concerning the symmetry of the windings. Thus machines having asymmetric windings such as split phase induction motors, commonly used for single phase service, may be simulated by the present model. Furthermore, most common round-rotor three phase machines can also be simulated by this model. Most such machines have symmetric phase windings, and any symmetric three phase machine whose neutral terminal is not externally connected may be represented by an equivalent symmetric two-phase machine, and thus by this model.

The third assumption of winding distributions such that the resulting space distribution of mmf is sinusoidal around the circumference of the machine is a reasonable idealization of the actual situation for most practical AC machinery. In practically all common machines, because the coil sides of the windings are distributed into

a finite number of slots, the actual space distribution of mmf is only a stair case approximation to a sinusoid. However, most practical AC machines are designed, within the limits of economics, such that this approximation of a sinusoid is attained as closely as possible in order to minimize undesirable effects such as mechanical vibration and additional copper losses due to the presence of space harmonics. Furthermore, the assumption of a sinusoidal space distribution of mmf in the machine results in a considerable simplification of the analysis, particularly with respect to the treatment of magnetic saturation.

The model developed in this thesis is somewhat unique in that magnetic nonlinearity (saturation) is included in the analysis at the level of the derivation of the expressions for torque and flux linkages in terms of the machine's coenergy function Eq. (4, 4a). This treatment of magnetic saturation is based on the assumption that the stored magnetic energy in the machine is a state function (a unique function of $\underline{i}$ or $\underline{\lambda}$ and θ). Such an assumption is only permissible when the effects of magnetic hysteresis are neglected.

2.3 Derivation of Dynamical Equations for the Four-Winding Uniform Air-Gap Rotating Machine

The constitutive and dynamical network equations for a generalized rotating machine model were given in Section 1 of this chapter. The constitutive relations for torque and flux linkages as functions of rotor angle and coil currents were expressed as derivatives of the machine's coenergy function. The network equations represented the effects of winding resistances and shaft inertia and related the state variables ($\underline{\lambda}$, $\underline{i}$, τ, θ) of the loss-less multiport component to the terminal voltages and shaft torque, at the electrical and mechanical

ports respectively, of the actual machine model. In order to proceed further it is necessary to obtain expressions for the torque and flux linkages as explicit functions of the coil currents and rotor angle. Since relations for torque and flux linkage of the generalized machine were expressed as derivatives of the machine's coenergy function, the required explicit expressions for τ and $\underline{\lambda}$ can be directly obtained if the coenergy function $W_e^*(\underline{i}, \theta)$ of the machine can be determined as an explicit function of the coil currents $\underline{i}$ and the rotor angle θ. The explicit form for the coenergy function of a particular machine depends upon the nature of the machines magnetic circuit, the number and distribution of coil windings, etc.

In Appendix A the magnetic coenergy function for a magnetically non-linear, uniform air-gap machine having four independent and sinusoidally distributed windings is derived and the required expressions for torque, τ, and winding flux linkages, $\underline{\lambda}$, are determined as explicit functions of the coil currents $\underline{i}$ and rotor angle θ.

The magnetic coenergy function $W_e^*(\underline{i}, \theta)$ of the machine is derived from a magnetic field model expressed in terms of flux and mmf rather than in terms of the more primitive flux density and magnetic field intensity variables (B and H). Unlike most machine analyses in which the assumption of magnetic linearity leads to the assumption, by implication, that all of the magnetic energy stored in the machine is concentrated in the air gap, this assumption is not made in the present analysis. Indeed when magnetic saturation occurs, some of the magnetic energy will be stored outside of the air gap in the machine's iron structure. For the case of the saturated machine, a description of the magnetic energy storage in terms of flux and mmf variables is much

simpler from a macroscopic point of view than that in terms of flux density and magnetic field intensity (B and H) would be, since the latter description of magnetic energy storage would require a detailed knowledge of the distribution of B and H not only in the air gap but also throughout the entire iron structure. Furthermore, the description of the machines magnetization characteristics in terms of flux and mmf can be more easily related to actual measurements of voltage and current at the machine terminals than a description of the magnetic field distribution in terms of flux density and magnetic field intensity could be.

The evaluation of the machine's coenergy function in terms of the flux and mmf distributions proceeds as follows. Because of the sinusoidal variation of mmf around the circumference of the machine, the magnetic flux and coenergy densities will also vary around the circumferential periphery of the machine. The resultant distributions of flux and coenergy are most conveniently expressed in terms of lineal densities per unit length along the circumference of the circular air-gap. Because of the assumption that the magnetic flux at a given circumferential position along the air-gap is uniquely determined by the local value of the mmf distribution at that point, the expression for the local value of magnetic coenergy density per unit circumferential length, at position angle ϕ on the air-gap circumference is:

$$w_e^*(\underline{i},\theta,\phi) = \int_0^{F(\underline{i},\theta,\phi)} \Phi[F']dF' \qquad (7)$$

In the above integral, the upper limit is the local value of mmf at position angle ϕ. As indicated, the local mmf is a function of the coil current vector $\underline{i}$, the rotor angle θ, and the position angle ϕ. The function $\Phi(F')$ in the integrand is the magnetization characteristic of the localized magnetic circuit across the air-gap at position angles ϕ and $(\phi + \pi)$, and through the iron in the rotor and stator structures. Thus, $\Phi(F')$ represents the local value of flux per unit circumferential length crossing the air-gap as a function of the local value of mmf. It is significant that, because uniformity of the air gap, the local magnetization characteristic $\Phi(F')$ is independent of position angle in the machine. In other words, the machines magnetic circuit characteristics are axi-symmetric.

The expression for the total magnetic coenergy is obtained by integrating the lineal density from Eq. (7) around the air gap periphery of the machine.

$$W_e^*(\underline{i},\theta) = R \int_0^{\pi} w_e^*(\underline{i},\theta,\phi)d\phi \qquad (8)$$

An explanation of why the integration limits in (8) are 0 to π rather than 0 to 2π is given in Appendix A. The explicit dependence of W_e^* on $\underline{i}$ and θ was introduced through the expression for the mmf distribution, $F(\underline{i},\theta,\phi)$, as the upper limit of the integral in Eq. (7). The derivation of the mmf distribution for a uniform air-gap machine with four independent sinusoidally distributed windings as an explicit function of $\underline{i}$, θ, and ϕ is given in Appendix A. The expression for $W_e^*(\underline{i},\theta)$ obtained from (8) is then differentiated with respect to $\underline{i}$ and θ, as per Eqs. (4,4a) to obtain expressions for the torque, τ, and the winding flux

linkages, λ, as explicit functions of $\underline{i}$ and θ. The details of this development are also carried out in Appendix A.

For the typical electrical rotating machine, the impedances $\underline{Z}$ and M of the electrical and mechanical networks, connected between the lossless multiport component and the electrical terminals and mechanical shaft port of the model (see Fig. 2), merely represent the electrical resistances of the windings and the mechanical inertia and friction of the rotor structure, respectively. Thus in the evaluation of the generalized impedance network equations, Eqs. (5, 5a), for the machine simulation model of this thesis, $\underline{Z}$ and M are defined by Eq. (6, 6a). Equation (5) will be referred to as the "voltage equation" since it relates the terminal voltages to the winding flux linkages. Similarly Eq. (5a) will be referred to as the rotor dynamical equation.

A summary of the constitutive equations for winding flux linkages and torque which are derived in Appendix A for the uniform air-gap machine model of this thesis, together with the voltage and rotor dynamical equations is given below.

Constitutive Relations

1) Flux Linkages

$$\begin{bmatrix} \lambda_a \\ \lambda_b \\ \lambda_f \\ \lambda_g \end{bmatrix} = \left[\begin{array}{c|c|c|c} n_a^2L+\ell_a & 0 & n_an_fL\cos\theta & n_an_gL\sin\theta \\ \hline 0 & n_b^2L+\ell_b & n_bn_fL\sin\theta & -n_bn_gL\cos\theta \\ \hline n_an_fL\cos\theta & n_bn_fL\sin\theta & n_f^2L+\ell_f & 0 \\ \hline n_an_gL\sin\theta & -n_bn_gL\cos\theta & 0 & n_g^2L+\ell_g \end{array}\right] \begin{bmatrix} i_a \\ i_b \\ i_f \\ i_g \end{bmatrix} \qquad (9)$$

n_i number of turns in ith winding

ℓ_i leakage inductance of ith winding

$L = L(F_p)$ air-gap mutual inductance parameter (a function of F_p, because of magnetic non-linearity)

F_p magnitude of air gap mmf wave (see Appendix A)

2) Torque

$$\tau_m = \frac{\lambda_g}{n_g} n_f i_f - \frac{\lambda_f}{n_f} n_g i_g + \left(\ell_d \frac{n_g}{n_f} - \ell_q \frac{n_f}{n_g}\right) i_f i_g \qquad (10)$$

Dynamical Relations

1) Voltage Equations

$$\begin{aligned} \overset{o}{\lambda}_a &= v_a - r_a i_a \\ \overset{o}{\lambda}_b &= v_b - r_b i_b \\ \overset{o}{\lambda}_f &= v_f - r_f i_f \\ \overset{o}{\lambda}_g &= v_g - r_g i_g \end{aligned} \qquad \begin{array}{l} r_a, r_b, r_f, r_g \text{ are} \\ \text{winding resistances} \end{array} \qquad (11)$$

2) Rotor Dynamical Equation

$$\dot{\theta} = \omega$$

$$\dot{\omega} = \frac{1}{J}(-\tau_m + \tau_s - \rho\omega) \qquad (12)$$

J rotor inertia

ρ rotor friction coefficient

τ_s externally applied shaft torque (negative for motor load, positive for generator prime mover torque)

The sign on τ_m in (12) is negative because τ_m is the torque applied to the magnetic field by the rotor in the direction of increasing θ, and therefore the magnetic field applies an equal and opposite torque, $-\tau_m$, to the rotor mechanical structure.

The constitutive relations are quantitatively ~~determined by either~~ evaluated either by specifying $\underline{\lambda}$ and θ and solving for $\underline{i}$ and τ, or alternatively by specifying $\underline{i}$ and θ and solving for $\underline{\lambda}$ and τ. Thus either $\underline{\lambda}$ or $\underline{i}$ or any four independent elements from the components of both $\underline{i}$ and $\underline{\lambda}$, may be chosen as the electrical state variables. The dynamical equations then relate these state variables to the values of terminal voltages and shaft torque which are externally applied to the ports of the machine model. The rotor dynamical equation also requires the assignment of rotor speed ω as an additional state variable. Consequently the state of this machine model is uniquely defined by a total of six state variables: the four components of either $\underline{i}$ or $\underline{\lambda}$ and the two mechanical state variables θ and ω.

2.4 Representation of Magnetic Non-Linearity by the Chordal Inductance Model

The matrix on the right hand side of Eq. (9) is called the machine inductance matrix because its elements represent the self and mutual inductances among the various windings of the machine. The leakage inductances ℓ_i represent the effect of the leakage fluxes for each winding; since these leakage fluxes are assumed to remain unsaturated, the corresponding leakage inductances ℓ_i are assumed constant. The air-gap mutual inductance parameter $L(F_p)$ represents the mutual coupling effect between rotor and stator windings associated with the flux that crosses the air-gap of the machine. The parameter $L(F_p)$ is the constant of proportionality between the air-gap flux and mmf. Because the air-gap flux is affected by saturation in the machine iron structure, the flux is not linearly proportional to the air-gap mmf. Consequently, $L(F_p)$ is not a constant, but as the notation implies, is a function of the magnitude of the air-gap mmf wave F_p. $L(F_p)$ is also referred to as the chordal inductance parameter since its value is proportional to the slope of the chord to the curve representing the functional relation between the magnitude of the fundamental component of the space flux distribution in the machine and the magnitude, F_p, of the sinusoidal mmf space distribution. This relationship is shown in Fig. 2.3.

For a magnetically linear (unsaturated) machine, the relation between flux and mmf would be linear as indicated by the dashed straight line in Fig. 2.3. Because the chord would then coincide with this straight line, the slope of the chord, and consequently the value of $L(F_p)$, is constant for the linear machine. It can be seen from Fig. 2.3 that the chordal slope may be uniquely represented as a function of F_p. A typical plot of $L(F_p)$ as a function of F_p is shown in Fig. 2.4.

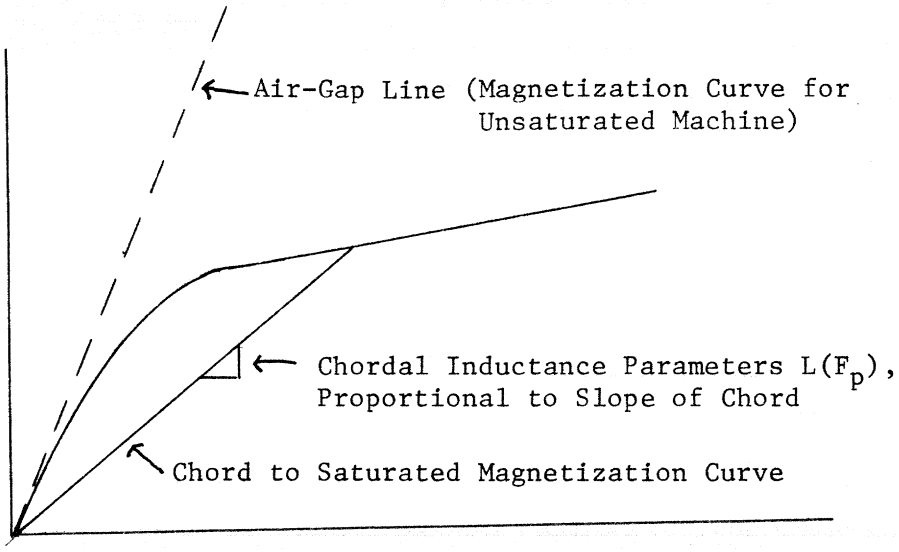

Fig. 2.3 Machine Magnetization Characteristics

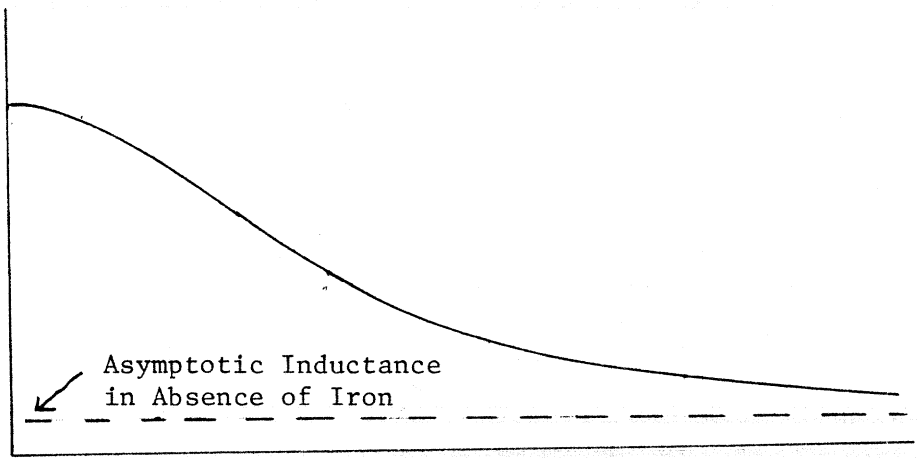

Fig. 2.4 Variation of Chordal Inductance Parameter $L(F_p)$

When $F_p = 0$ the value of $L(F_p)$ is that corresponding to unsaturated conditions in the iron structure of the machine. As F_p increases, the iron begins to saturate, and the value of $L(F_p)$ falls monotonically, asymptotically approaching a finite lower limit which represents the mutual inductance parameter if no iron were present - that is if the machine windings were suspended only in air.

The fact that the overall air-gap magnetization characteristics of this machine may be represented by a single "inductance" parameter, $L(F_p)$, is a consequence of the form of the constitutive relations for the uniform air-gap machine with sinusoidally distributed windings, and is demonstrated in Appendix A. Generally, the relationship for $L(F_p)$ is derived empirically from voltage and current measurements made on the machine under various operating conditions, rather than being derived from the fundamental saturation characteristics and the geometrical configuration of the iron structures and windings of the machine as is done in Appendix A.

Although the mmf space distribution in the machine is assumed sinusoidal and the magnetic circuit is axisymmetric, the resultant space distribution of magnetic flux across the air-gap will only be sinusoidal if the magnetic circuit is linear - that is if there is no saturation of flux at any point in the iron structure of the machine. If the effects of saturation can be assumed to be localized along the air-gap periphery of the in machine, saturation will first occur at the locations of the peaks of the sinusoidal mmf distribution. Therefore, in the event of saturation, the sinusoidal space distribution of mmf will produce a space flux distribution whose shape will be that of a distorted sinusoid with flattened peaks. The distortion of the saturated space

flux distribution can be represented by odd harmonics of the fundamental space sinusoidal distribution. Consequently, the question arises as to what, if any, effects the presence of such space harmonics in the flux distribution will have on the performance of the machine.

The answer, somewhat surprisingly, is that for the uniform air-gap machine having a sinusoidal mmf distribution the presence of space harmonics, due to saturation, in the space flux distribution does not affect the performance of the machine or the harmonic content of its winding currents. This result of course could have been surmised from Eq. (9) which is completely free of any harmonic terms. Furthermore, because of magnetic symmetry, the inductance parameter $L(F_p)$ is also independent of angular position in the machine. Consequently, because space harmonics of the flux distribution do not cause time harmonics in the machine voltages or currents, the performance of the saturated machine may be represented by that of an equivalent linear machine having a purely sinusoidal flux distribution whose magnitude is equal to that of the fundamental frequency component of the actual distorted flux distribution in the saturated machine.

This interesting characteristic of the saturated uniform air-gap machine with sinusoidal mmf distribution is derived in Appendix A as a consequence of the derivation of the constitutive relations for torque and flux linkages. Furthermore, the derivation of this result is independent of the waveform of the winding currents or applied voltages. As is pointed out in Appendix A, this isolation between the effects of space flux harmonics and time harmonics in the winding voltages and currents occurs only because of both (1) uniformity of the air-gap, and (2) sinusoidal space distribution of mmf. Consequently for machine

models in which either of the above two conditions are not satisfied, the performance of the saturated machine cannot be strictly represented in terms of an equivalent linear machine. Furthermore, if either of these conditions are not satisfied, the expression for the saturated air gap mutual inductance can no longer be represented as simply as $L(F_p)$, but will generally also be dependent upon the machine rotor angle θ.

The above result for the uniform air-gap machine with sinusoidal mmf distribution can be summarized by saying that for this machine there is no coupling between the space harmonics of the flux distribution and the time harmonics of the winding currents.

2.5 Choice of State Variables

As was mentioned in Section 3, the machine model of this thesis is characterized by a total of six state variables consisting of four electrical state variables - the four components of the winding flux linkage, $\underline{\lambda}$, or current, $\underline{i}$, vectors, and two mechanical state variables, the angular position, θ, and speed, ω, of the rotor structure. Although the mechanical state variables are fixed, one may choose as electrical state variables any combination of four independent components from the flux linkage $\underline{\lambda}$ and current $\underline{i}$ vectors. As is the practice in many other dynamical simulations of electrical machinery [7], [14], the four components of the flux linkage vector $\underline{\lambda}$ will be chosen as the electrical state variables in the present treatment, rather than the four currents or a combination of currents and linkages. The choice of the winding flux linkages as state variables has several advantages. The first of these is that physically the time behavior of flux linkages in a machine

remains continuous despite discontinuities in the winding currents or sudden changes in machine parameters. This is a result of Lenz's Law which states that flux linkages in a magnetic circuit cannot change instantaneously. Consequently if the winding flux linkages are chosen as state variables, it becomes unnecessary to recompute new initial conditions for these state variables when simulating the effects of sudden changes in the machine environment such as opening and reclosing of circuit breakers or sudden short circuits.

The choice of the flux linkages as state variables also greatly simplifies the analytical treatment of magnetic non-linearity. The additional computational complexities that would be incurred if magnetic non-linearity were treated in terms of the currents as state variables are described in Appendix A.

The choice of the flux linkages as state variables does, however, result in the following computational complication that is particularly significant when the machine equations are formulated in terms of coil variables, as is the case in the present situation, rather than d-q variables. Because the constitutive relation between the flux linkages and winding currents is usually given in terms of an inductance matrix, as in Eq. (9), the use of the flux linkages as state variables requires that the inverse of this matrix be determined in order to compute the currents from the flux linkages. Because this inductance matrix is a function of the rotor angle θ when the machine equations are formulated in terms of coil variables, the computation of the inverse of this matrix is generally not a simple matter. This problem is discussed in detail in Section 8 where it will be seen that a simple form of the inverse of the machine inductance matrix exists only when the coil

windings of the machine are symmetric on both rotor and stator structures. On the other hand, if a dq transformation which removes the rotor angle dependency from the machine inductance matrix can be found, the resulting dq coordinate inductance matrix is usually much simpler to invert than in the present case, even when magnetic non-linearity is accounted for.

2.6 Referral of Winding Variables and Machine Parameters

It is common practice in the analysis of multi-winding electromagnetically coupled devices, such as transformers and various types of AC rotating machinery, to refer the voltages, currents, and impedances of each winding to a common base. This referral process consists of scaling the winding currents and voltages in accordance with the turns ratio of each winding to that of the selected base winding. The referred voltages and flux linkages for each winding are defined as the actual values divided by the value of the winding turns ratio. Similarly, the referred value of current for a given winding is defined as the actual value of current multiplied by the corresponding turns ratio. Consistent with these definitions of referred voltages and currents, the referred values of winding resistance, and leakage inductance or impedance are defined as the actual values of these parameters divided by the square of the corresponding turns ratios. Where the constitutive and dynamical relations for such electromagnetically coupled devices are expressed in terms of referred variables, the resulting equations are considerably simplified in that the appearance of turns ratios or absolute number of winding turns is eliminated. Because of this simplification, most dynamical simulations of electrical machinery are

formulated in terms of such referred variables. Similarly, in the present analysis, the constitutive relations for flux linkage and torque, Eqs. (9), (10) can be greatly simplified by expressing the machine parameters, voltages, flux linkages, and currents in referred form.

The transformation of the machine variables to referred form may either be viewed as a formal mathematical transformation, or may be given a physical interpretation in terms of ideal (loss-less and non-energy storing) transformers connected to the machine winding terminals. A description of the mathematical transformation of the machine equations into terms of referred variables follows. Define the following turns ratio transformation matrix $\underline{N}$.

$$N = \begin{bmatrix} n_a & 0 & 0 & 0 \\ 0 & n_b & 0 & 0 \\ 0 & 0 & n_f & 0 \\ 0 & 0 & 0 & n_g \end{bmatrix}$$

n_a, n_b, n_f, n_g are the turns ratios between the respective machine windings and the selected base winding.

Equations (9), (11) when expressed in vector notation, may be written as:

$$\underline{\lambda} = \underline{L}(\theta)\underline{i} \tag{9}$$

$$\overset{o}{\underline{\lambda}} = \underline{v} - \underline{R}\,\underline{i} \tag{11}$$

Then pre-multiply both sides of these equations by N^{-1}

$$\underline{N}^{-1}\underline{\lambda} = \underline{N}^{-1}\underline{L}(\theta)\underline{N}^{-1}\underline{N}\underline{i} \tag{9a}$$

$$\underline{N}^{-1}\overset{o}{\underline{\lambda}} = \underline{N}^{-1}\underline{v} - \underline{N}^{-1}\underline{R}\underline{N}^{-1}\underline{N}\underline{i} \tag{11a}$$

The referred values of $\underline{\lambda}$, $\underline{v}$, $\underline{i}$, $\underline{L}$, and $\underline{R}$ are designated by a prime and are defined as

$$\underline{\lambda}' \equiv \underline{N}^{-1}\underline{\lambda}$$

$$\underline{v}' \equiv \underline{N}^{-1}\underline{v}$$

$$\underline{i}' \equiv \underline{N}\underline{i}$$

$$\underline{L}'(\theta) \equiv \underline{N}^{-1}\underline{L}(\theta)\underline{N}^{-1}$$

$$\underline{R}' \equiv \underline{N}^{-1}\underline{R}\underline{N}^{-1}$$

These mathematical definitions are identical with those previously given verbally. Finally, in terms of these referred variables, Eq. (9a), (11a) may be written as

$$\underline{\lambda}' = \underline{L}'(\theta)\underline{i}' \tag{9b}$$

$$\overset{o}{\underline{\lambda}} = \underline{v}' - \underline{R}'\underline{i} \tag{11b}$$

Thus the form of Eq. (9b), (11b) in terms of referred variables, is exactly the same as that of the original Eqs. (9), (11). It will be seen subsequently that the principal analytical simplification provided by the referral transformation is in the elimination of the number of winding terms in the expanded form of the referred inductance matrix $\underline{L}'(\theta)$.

Physically the referral process is equivalent to connecting the electrical ports of the machine to ideal (loss-less and non-energy-storms) transformers, each of whose turns ratios is inversely proportional to the number of turns in the machine winding to which they are connected. Consequently, measurements of currents, voltage and impedance made through these hypothetical and ideal transformers will appear to be referred to a common base for all windings - as if all windings had the same number of turns.

Normally, the procedure is to select one of the machine windings as a base and refer the parameters of all other windings to this selected base winding in accordance with the turns ratio of the other windings to that of the selected base winding. However, the selection of a base winding for referral of the winding parameters is arbitrary, and in the development given in Appendix A all winding parameters are referred to a hypothetical single turn base winding.

The use of referred variables may also be applied to the mechanical port of the machine to account for the number of magnetic pole pairs in multipole machines. In this situation the referred mechanical variables are torque and rotor speed. The multipole machine is represented by a hypothetical two pole machine connected to an output shaft through a gear train whose ratio is equal to the number of pole pairs in the actual machine. The torque and speed of the hypothetical two pole machine are the referred values of the corresponding actual variables in the multipole machine, and the pole-pair gear ratio plays the role of an ideal mechanical transformer, analogous to the ideal electrical transformer used for referring the electrical parameters of the machine. Consequently the two-pole machine model developed in this

thesis may be used to simulate the performance of multipole machines by adding an ideal (loss-less and inertia-less) gear train to the rotor shaft.

In reality, the process of expressing machine parameters in terms of referred variables is not as abstract as the above discussion in terms of hypothetical transformers and gear ratios might lead one to believe. For example, when measuring the operating characteristics of a squirrel cage induction motor it is unnecessary to know the turns ratio between the squirrel cage "winding" and the stator winding. Indeed, because of the squirrel cage construction of the rotor winding, the stator/rotor turns ratio for such a machine might even be difficult to define. Furthermore, it would obviously be impractical to make any operating measurements directly on the rotor squirrel cage. The only point in such a machine at which electrical measurements may be conveniently made is at the stator winding terminals. Nevertheless it is possible to obtain derived measurements ~~of values~~ of pertinent rotor parameters, referred to the stator winding, from electrical measurements made only at the stator winding terminals under various operating conditions. Since the dynamical equations of such a machine can be uniquely specified in terms of the resultant referred values of rotor parameters, knowledge of the absolute values of rotor winding impedances is generally not required.

The per-unit system of expressing the voltages, currents, and impedances of machines, transformers and transmission lines in power systems is the ultimate extension of this concept of referred variables.

The definitions of the referred flux linkages, winding currents,

leakage inductances and resistances used in the present analysis are given in Appendix A. The resulting machine equations in terms of these referred variables are given by (13-16) below. These equations may also be considered as the result of applying appropriate turns ratio transformations to the original machine Eqs. (9-12). The simplification resulting from elimination of the appearance of the number of turns, n_i, of the various windings is particularly evident in the constitutive equations for the referred flux linkages and torque. The primes on the variables in Eq. (13-16) indicate the referred form of these variables.

$$\begin{bmatrix} \lambda_a' \\ \lambda_b' \\ \lambda_f' \\ \lambda_g' \end{bmatrix} = \begin{bmatrix} L + \ell_a' & 0 & L\cos\theta & L\sin\theta \\ 0 & L + \ell_b' & L\sin\theta & -L\cos\theta \\ L\cos\theta & L\sin\theta & L + \ell_f' & 0 \\ L\sin\theta & -L\cos\theta & 0 & L + \ell_g' \end{bmatrix} \begin{bmatrix} i_a' \\ i_b' \\ i_f' \\ i_g' \end{bmatrix} \tag{13}$$

Note: For the magnetically non-linear machine L is not constant but is a function of the peak mmf F_p: $L = L(F_p)$.

$$\tau_m' = (\lambda_g' i_f' - \lambda_f' i_g') + (\ell_f' - \ell_g') i_f' i_g' \tag{14}$$

$$\overset{o}{\lambda}_a' = \frac{v_a}{n_a} - r_a' i_a'$$

$$\overset{o}{\lambda}_b' = \frac{v_b}{n_b} - r_b' i_b' \tag{15}$$

$$\overset{o}{\lambda}_f' = \frac{v_f}{n_f} - r_f' i_f'$$

$$\begin{aligned}
\overset{o}{\lambda}_g' &= \frac{v_g}{n_g} - r_g' i_g' \\
\overset{o}{\theta}' &= \omega' \\
\overset{o}{\omega}' &= -\frac{1}{J'}(\tau_m' - \tau_s' + \rho'\omega')
\end{aligned} \tag{16}$$

For future reference, define the induction matrix of Eq. (13) as $\underline{L}(F_p,\theta)$. Furthermore, the matrix $\underline{\Gamma}(F_p,\theta)$ is defined as the inverse of this matrix, thus

$$\underline{\Gamma}(F_p,\theta) \equiv \underline{L}^{-1}(F_p,\theta) \tag{17}$$

With this notation, the relation between flux linkages and currents given by (13) can be expressed in either of the following forms.

$$\underline{\lambda}' = \underline{L}(F_p,\theta)\underline{i}' \tag{18a}$$

or

$$\underline{i}' = \underline{\Gamma}(F_p,\theta)\underline{\lambda}' \tag{18b}$$

2.7 Computational Causality

The set of Eqs. (13-16) constitute a mathematical representation of the physical machine model, expressed in terms of referred variables for analytical and computational convenience. Thus, the dynamical performance of the machine may be simulated, for arbitrary electrical and mechanical operating conditions, by computing the solution to these equations for given electrical and mechanical inputs. However, these equations are sufficiently complex such that their computational solution is, in general, only feasible when performed using either an analog or a digital computer. Consequently, the topic of this section is the organization of these equations for purposes of computation.

Before discussing the computational aspects of the machine simulation, it should be noted that the mathematical model described by Eqs. (13-16) is only one of many different possible mathematical representations of the same physical machine model. In general, a mathematical representation of a given physical model is not unique; many different representations are possible, all of which are of course equivalent, any one being related to any other by a mathematical transformation of variables. For example, in the present case, a different mathematical representation (a different set of equations) of the same machine model would have been obtained had the currents $\underline{i}$ been chosen as the electrical state variables instead of the flux linkages $\underline{\lambda}$. A third possible mathematical representation of the model would have been given by a formulation of the machine equations in terms of d-q variables. However, all of these representations are analytically, although not computationally, equivalent.

The choice of a specific mathematical representation of a physical model for purposes of simulation is usually governed by considerations of computational simplicity and by the problem variables to be computed by the simulation. For example, in the simulation of this thesis the computational advantages of dealing with flux linkages rather than currents, among other factors, lead to the development of the mathematical model described by Eqs. (13-16).

Having selected a given mathematical representation of the physical machine model, the next task is the organization of the resulting model equations for computation. The required computational organization of the model equations is largely determined by which of the problem variables are to be designated as "inputs" to the simulation and which are desired to be computed as "outputs".

Given a system of differential equations, such as Eqs. (13-16), the usual tendency is to implicitly assume that those variables whose derivatives appear explicitly in the equations ($\underline{\lambda}$, ω) are the independent variables which are to be computed as results or outputs of the solution; and any other variables, which are not just algebraic combinations of these independent variables, (for example the voltages $\underline{v}$) are implicitly assumed to be the specified inputs or "forcing functions" of the equations. This is an unnecessarily restrictive designation of input and output variables for a simulation of physical system dynamics. A clearer picture of the designation of inputs and outputs to a mathematical model of a physical system may be obtained by looking at the port variables of the physical model itself (such as Fig. 2.1), rather than at the equations for one particular mathematical representation of the model (Eqs. (13-16)). For example, the machine model of this thesis has

five ports, the four sets of winding terminals and the mechanical rotor shaft. The conditions at each of these ports are completely defined by two variables; an effort or "force" variable, and a flow or "velocity" variable. Thus, for the present machine model, the effort and flow variables at the electrical terminals are the voltages and currents, respectively, and the corresponding variables at the rotor shaft are the torque and speed. This model for the four winding machine is a special case of the n-winding machine model depicted in Fig. 2.1, and is described by the following diagram:

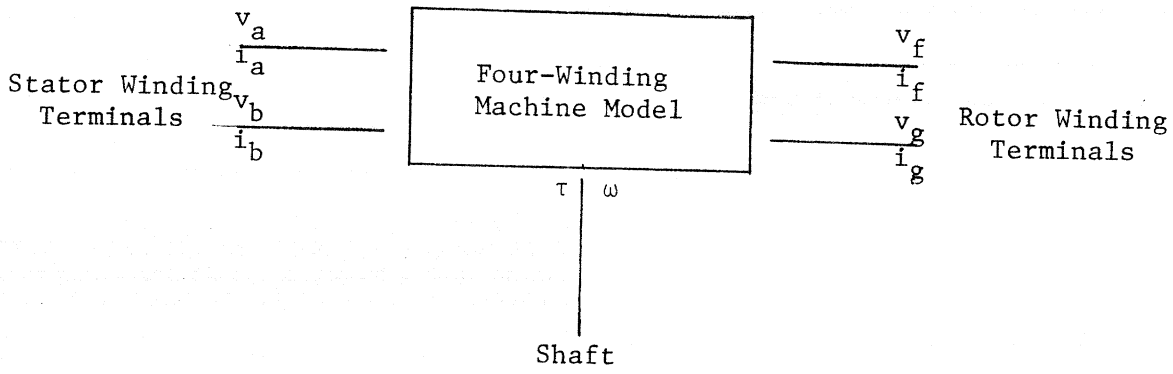

Fig. 2-5 Multiport Representation of 4 Winding Machine Model

At each external port of a physical model, such as that of the four-winding machine illustrated in Fig. 2.5, one and only one of the two variables of each port, either the effort or the flow variable, must be specified as an external input to that port in a simulation. The remaining variables at each port will then be a computed output obtained from the solution of the model equations in the simulation. Since one

input variable must be specified for every port, the total number of input variables to be specified is equal to the number of external ports of the model. The specified input variables may either be explicitly specified, or if the model ports are connected to the ports of an external system, these input variables must be computed outputs generated by a model of that external system.

The designation of input variables (effort, flow) made at each port of the model is the principal determinant of how the model equations are to be organized for computation in a simulation. Generally, if possible, it is desirable to organize the required computations such that the computer solution of the model equations will entail only computational integration - specifically that computational differentiation be avoided. The use of computational differentiation is particularly undesirable in analog computer simulations because of noise problems and limited dynamic range of the operational amplifiers. However, it will be seen that, depending upon which port variables are to be computed as outputs in a simulation, the need for computational differentiation cannot always be avoided.

When a given port of a physical model is associated with an energy storage element imbedded in the model - an inertia or a capacitance - only one of the two variables on that port (effort or flow) can be computed from the model equations without requiring the use of computational differentiation. Computation of the other variable on that port, as an output from a dynamical simulation of the model, will either require the use of computational differentiation, or that the value of the derivative of the input variable be explicitly known. For example, in the present case of electrical machine simulation, although the terminal

currents can be computed from the model equations without using differentiation, computation of the terminal voltages from the solution of the machine model equations will, in general, require the use of computational differentiation, unless the value of the derivative of input current is known explicitly. An example where the value of the derivative of the input is either explicitly known or computable is a situation where it is either known or assumed that the input is a constant or a sinusoidal time function.

For a given port of a model, which of the two variables (effort or flow) can be computed from the model equations without use of computational differentiation is a function of the physical nature of the energy storage elements contained in the model. This association of the input/output variable specification for a given port of a model with the computational operations required to compute the designated output variable from the solution of the model equations is defined as the computational causality for that port of the model. When the designation of input and output variables for a port is such that the output variable can be computed without use of computational differentiation the causality for that port is referred to as integral causality. Conversely, if differentiation is required to compute the designated output variable the port is said to have derivative causality. For example, the electrical ports of the machine model have integration causality when the voltages are the designated input variables and the currents are the computed outputs. Conversely, when the currents are the designated inputs, the ports have derivative causality.

It should be emphasized that the association between computational causality and input/output variable designations for a model of a given

physical system is dependent only upon the physical nature of the energy storage elements embedded in the model, and cannot be altered by mathematical manipulation. The reason for this dependence of model causality upon the physical nature of the energy storage elements in the model is briefly described in the following.

There are basically two types of energy storage multiports; capacitative and inertive. The dynamical relations for each these two types of energy storage multiports may be expressed in terms of the generalized vector effort and flow variables, $\underline{e}$ and $\underline{f}$, and are given below. The n components of $\underline{e}$ and $\underline{f}$ are the effort and flow variables, respectively, at each of the n ports of the model.

Capacitative	Inertive
$\underline{f} = \overset{o}{\underline{q}}$	$\underline{e} = \overset{o}{\underline{p}}$
$\underline{q} = \underline{C}(\underline{e})$	$\underline{p} = \underline{I}(\underline{f})$

$\underline{C}(\underline{e})$ and $\underline{I}(\underline{f})$ are generally non-linear vector functions for capacitative and inertive multiports respectively. The above equations express the functional relations between $\underline{e}$ and $\underline{f}$ for the respective multiports. Note that for the capacitative multiport, when $\underline{e}$ is an independently specified input variable, computation of $\underline{f}$ will require computational differentiation. However, when $\underline{f}$ is an independently specified input, the computation of $\underline{e}$ requires only integration. First $\underline{f}$ is integrated to obtain $\underline{q}$ and then $\underline{e}$ is computed using the inverse of the C function. For the inertive multiport, the computational operations required to compute $\underline{e}$ when $\underline{f}$ is the specified input, or conversely, are exactly the opposite of those for the capacitative multiport. Specifically for the

inertive multiport, if computational differentiation is to be avoided, $\underline{e}$ must be specified as the independent "input" variable. Note that the computational causality for inertive multiports is the opposite of that for capacitative multiports.

The computational formulation for the evaluation of these multiport dynamical equations by integration is given below. The independent or "input" variables in this formulation are the integrands of the integrals on the right hand side.

Capacitative	Inertive
$\underline{e} = \underline{C}^{-1}\left[\int_{t_o}^{t} \underline{f}dt + \underline{C}(\underline{e}_o)\right]$	$\underline{f} = \underline{I}^{-1}\left[\int_{t_o}^{t} \underline{e}dt + \underline{I}(\underline{f}_o)\right]$
$\underline{f}$ specified as independent input	$\underline{e}$ specified as independent input

The dynamical equations of some common single port capacitative and inertive energy storage elements for conventional mechanical and electrical systems are given in Table I.

A summary of the input/out variable designations associated with integral and derivative computational causality for inertive and compliant energy storage elements is given in Table II. It should be emphasized that, although the relationships between computational causality and input/output designations for the individual ports of a model are given by Table II, not all ports of a multiport physical system model will necessarily have identical causalities.

TABLE I

System	Effort, e	Flow, f	Momentum, p	Displmt., q	Capacitance, C(e)	Inertance, I(f)
Electrical	Voltage, e	Current, i	Flux Linkage, λ	Charge, q	Capacitor, $q = C(e)$	Inductor, $\lambda = L(i)$
Mechanical (rotation)	Torque, τ	Speed, ω	Angular Momentum, h	Angle, θ	*Torsional Spring $\theta = k^{-1}(\tau)$	Inertia, $h = I\omega$
Mechanical (translation)	Force, f	Speed, v	Momentum, p	Distance, x	*Lineal Spring $x = k^{-1}(f)$	Mass, $p = mv$

*These functions are the inverse of the more common elastance functions for mechanical springs of the form $f = k(x)$.

TABLE II

Causality:	Integral		Derivative	
Energy Storage	Input	Output	Input	Output
Inertive	e	f	f	e
Compliant	f	e	e	f

From a physical point of view, the rotating electrical machine is an inertive multiport consisting of coupled electrical inductors and mechanical inertia. Consequently, the energy storage mechanism in the machine, from both the electrical and mechanical points of view, is inertive. The effort variables at the ports of the machine model are voltages and torque, and the corresponding flow variables are the terminal currents and shaft speed. Thus, in accordance with Table II, if the solution of the machine model equations is to be carried out using only computational integration, only the terminal currents and shaft speed may be designated as computed output variables at the ports of the model. If, on the other hand, it is desired to specify the electrical currents at the machine terminals as inputs to the machine model, evaluation of the resulting terminal voltages, during simulation can only be achieved by means of computational differentiation. It should be emphasized that when the terminal currents are the designated input variables, it is only the associated terminal voltages that cannot be computed without using differentiation. When the terminal currents and also the shaft torque are given as designated input variables, it is still possible to compute the mechanical motion of the machine, that is its shaft speed and displacement, without having to use computational

differentiation. Similarly, when the shaft speed is given as a designated input variable, the computation of the electrical performance of the machine for given terminal voltage inputs can also still be performed, without requiring differentiation, if the computation of the resulting shaft torque is not required. An example of this latter situation is the modelling of the performance of an automobile alternator. In this situation the car engine effectively acts as a speed source because its power rating is many times higher than that of the alternator. Consequently, although the rotor speed of the alternator is specified by the operating speed of the engine, because of the vast differences in power rating, the resultant torque produced by the alternator has only a negligible effect on the engine speed, so that computation of the alternator torque may be omitted.

In general the designation of input variables for derivative causality (for the case of the rotating electrical machine, terminal currents and shaft speed) effectively by-passes, or eliminates, the computation of the associated state variables in the model equations. For example, in Eq. (16) for the machine's mechanical motion, the mechanical state variables are θ and ω. Normally, with the shaft torque given as the designated input variable, this equation in conjunction with Eqs. (13-15), is solved for θ and ω. However when the shaft speed is given as a designated input variable, the evaluation of θ and ω by Eq. (16) is effectively by-passed. The situation is similar on the electrical side of the machine. Designation of the terminal currents as input variables yields the flux linkages directly via the algebraic transformation of Eq. (13), thus by-passing the state variable computation for the linkages via the voltage equations (15). Thus the number of

independent electrical state variables (the components of λ) is reduced by the number of winding terminal currents which are given as specified input variables. A specific example of such a situation in which winding currents are specified, and the corresponding reduction of the number of independent electrical state variables, is given by a four-winding machine having one or more non-existent or open-circuited windings (non-existent windings are represented as existing but open-circuited windings). When a winding is open-circuited, its current is effectively specified to be zero. Nevertheless, the simulation of a machine having one or more open-circuited windings may be carried out without resorting to computational differentiation. This does not violate the causality conditions because if the current is zero, the derivative of the current must also be zero, and is therefore implicitly known. Effectively, what is done is to use the condition of zero current in the open windings to form a constraint equation which is then combined with the voltage equations for the remaining windings. As a result, the total number of independent electrical state variables of the model is reduced by the number of open windings. This procedure for handling the simulation of machines having open-circuited windings without use of computational differentiation is described in detail in Appendix B.

It was mentioned earlier that the machine terminal voltages could not, in general, be computed as outputs from the solution of the machine model equations without using computational differentiation. However, consider the following <u>apparent</u> counter-example to this statement. On page 259 of [5] an anlog computer block diagram is described for simulation of a salient pole alternator in terms of dq variables. The significant feature of that simulation is its causality - the terminal currents

are the specified inputs and the corresponding voltages are the computed outputs, and yet the computation for the voltages does not involve differentiation! This apparent contradiction of the causality rules for electrical machinery can be explained as follows. When the model equations are expressed in terms of dq variables, the expressions for the dq coordinate voltages consist of the following three components: (1) the voltage drop across the machine winding resistance, (2) a "speed voltage" term given by the product of the d or q coordinate flux linkage and the machine rotor speed, and (3) a "transformer voltage" component given by the time derivative of the associated dq flux linkage. Thus, because the "transformer voltage" component is given in the form of a derivative, the computation of the dq coordinate voltages will, in general, also require the use of computational differentiation. However a commonly made simplifying assumption is that the magnitude of the "transformer voltage" component is negligible in comparison to that of the "speed voltage". Thus when this assumption is made, the "transformer voltage" component need not be computed, and the need for using computational differentiation is avoided. Since this assumption was made in the alternator simulation described above, the desired voltages can be computed without using computational differentiation and the apparent causality contradiction is explained. However, it should be emphasized that the simplifying assumption made in neglecting the "transformer voltages" was not just mathematical manipulation but effectively constituted an alteration of the physical nature of the machine model. Thus the previous statement that computational causality is a function of the physical nature of the model and is invariant under mathematical transformation remains unaltered.

In summary, one can say that if it is desired to compute either terminal voltages or shaft torque as the outputs of a rotating machine simulation (this implies that the corresponding flow variables, terminal currents and shaft speed are specified as inputs), then the computational evaluation of these output variables will necessarily require the use of computational differentiation. The use of computational differentiation in a simulation is generally considered to be undesirable, particularly on an analog computer. However, its use in digital computer simulations may be quite acceptable, although this does not seem to be widely appreciated. Indeed, in the digital simulation of systems involving electrically interconnected rotating machines, [1], the use of a computer simulation model for one of the machines in the interconnected system, which uses numerical differentiation, provides the necessary current input "voltage output" causality for resolving the causality dilemna posed by the interconnection between machines. A detailed discussion of the computation aspects of numerical differentiation vs integration on a digital computer, including step size criteria to ensure computational stability is given in [2].

However, methods of machine simulation which require the use of computational differentiation will not be used in this thesis. Although the computational implementation of the machine simulation developed in this thesis is carried out on a digital computer, the machine equations are expressed in state variable form and are solved by numerical integration using the method of Runge-Kutta.

The manipulation of the machine equations (13-16) into a state variable formulation proceeds as follows. As was mentioned earlier the selected state variables are the four winding flux linkages and the

speed and angular position of the rotor shaft. Equations (13-16) are combined by substituting Eq. (18b) for $\underline{i}$ as a function of $\underline{\lambda}$ into Eqs. (14-16), and then combining the torque Eq. (14) with the rotor dynamical Eq. (16). The result of this combination process is a system of six non-linear coupled differential equations in terms of the six state variables; the four components of $\underline{\lambda}$ and θ, ω. Four of these six equations are electrical equations relating the terminal voltages to the winding flux linkages. The remaining two are electromechanical equations relating the external shaft torque to the rotor dynamics. The input variables to this system of equations are, as described earlier, the four terminal voltages and the applied shaft torque. The four voltage equations are most compactly expressed in vector form. However, there is no convenient way of expressing the torque explicitly as a function of the vector $\underline{\lambda}$ (it can of course be done but the result is awkward). Consequently for reasons of notational convenience, the expression for the torque substituted into the rotor dynamical equation continues to appear, as in (14), in terms of both currents and flux linkages, rather than as an explicit function of $\underline{\lambda}$. However, it is understood that the current components in this equation are explicitly evaluated as a function $\underline{\lambda}$ and θ by Eq. (18b).

Vector Voltage Equation

$$\overset{o}{\underline{\lambda}}' = \underline{N}^{-1}\,\underline{V} - \underline{R}'\underline{\Gamma}(\theta)\underline{\lambda} \tag{19}$$

Rotor Dynamical Equations

$$\overset{o}{\theta} = \omega$$

$$\overset{o}{\omega} = \frac{1}{J}\left(\lambda_f' i_g' - \lambda_g' i_f' + \tau_s - \rho\omega\right) \tag{20}$$

The six differential equations represented by (19), (20) are nothing more than a condensation of Eq. (13-16) into a state variable formulation. These equations form the basis of the machine simulation of this thesis. The form of these equations will be slightly modified for the simulation of machines having open-circuited or asymmetric windings.

2.8 Computation of the Inverse Inductance Matrix

The state variable formulation of the machine dynamical equations in terms of $\underline{\lambda}$, given by (19), (20), requires the knowledge of the inverse inductance matrix $\underline{\Gamma}(\theta,F_p)$ which appears in (19).

The matrix $\underline{\Gamma}(\theta,F_p)$ is defined in (17) as the inverse of $\underline{L}(\theta,F_p)$. However, usually only the inductance matrix $L(\theta,F_p)$ for a machine is explicitly known, as its elements are directly measureable circuital constants - namely the winding leakage inductance and the chordal or "magnetizing" mutual inductance of the machine. Thus the inductance matrix $\underline{L}(\theta,F_p)$ is primitive, and its inverse $\underline{\Gamma}(\theta,F_p)$ is derived from it by computation. The $\underline{\Gamma}$ matrix can be evaluated either by direct numerical inversion of the $\underline{L}$ matrix or by obtaining an algebraic expression for the inverse of $\underline{L}$. Numerical matrix inversion is very time consuming, and in the interests of computational efficiency should be used only as a last resort. In principle an algebraic expression for the inverse of $\underline{L}$ can always be found; however, with the exception of one special case to be described, the resulting algebraic expression is usually so complex that its evaluation offers little or no computational advantage over a direct numerical matrix inversion. The one case for which the algebraic inverse of $\underline{L}$ matrix has a particularly simple form is that of the symmetric machine. A symmetric four winding machine is defined as one

having symmetrical pairs of windings on both rotor and stator structures. The two windings on a given structure of a machine are defined as symmetric if the referred values of their leakage inductances are equal. Thus a symmetric machine is characterized by windings on each structure which have equal referred values of leakage inductance. Note that the above definition of machine symmetry only makes reference to the machines inductance parameters, no mention of winding resistances is made in this definition. Consequently two windings which are symmetric, and thus have equal values of referred leakage inductance, do not necessarily need to have equal resistances. Thus the winding leakage inductances of a symmetric machine satisfy the following conditions.

$$\ell_s' \equiv \ell_a' = \ell_b' \qquad \text{stator leakage inductance}$$

$$\ell_r' \equiv \ell_f' = \ell_g' \qquad \text{rotor leakage inductance}$$

The inverse inductance matrix for the symmetric machine, $\underline{\Gamma}^*(\theta,F_p)$ is given below. The * signifies that this particular formulation for $\underline{\Gamma}$ is valid only for the symmetric machine.

$$\underline{\Gamma}^*(\theta,F_p) = \frac{1}{\Delta}\begin{bmatrix} L+\ell_r' & 0 & -L\cos\theta & -L\sin\theta \\ 0 & L+\ell_r' & -L\sin\theta & L\cos\theta \\ -L\cos\theta & -L\sin\theta & L+\ell_s' & 0 \\ -L\sin\theta & -L\cos\theta & 0 & L+\ell_s' \end{bmatrix} \qquad (21)$$

$$\Delta \equiv L(\ell_r' + \ell_s') + \ell_r'\ell_s'$$

Because of the particularly simple form of this inverse inductance matrix, its use in the model equations for a symmetric machine is computationally very efficient. Furthermore, it is also possible to take advantage of the computational simplicity provided by the use of Eq. (21) in the simulation of machines having asymmetric or open circuited windings. Consequently such unsymmetrical machines will be modelled in terms of the basic four-winding symmetric machine, with appropriate modifications. Such an approach to the computational simulation of unsymmetrical machinery is both more flexible and computationally efficient than a direct frontal attack on the problem, as the latter approach would involve computation of the actual $\underline{\Gamma}$ matrix either by numerical matrix inversion or by evaluating a very cumbersome algebraic expression for the inverse of the $\underline{L}$ matrix. This method of modelling machines having asymmetric or open circuited windings, in terms of a basic symmetric machine, is the subject of the next section.

2.9 Simulation of Machines Having Asymmetric and/or Open Circuited Windings

It is possible in the simulation of unsymmetric machines - that is machines having asymmetric and/or open circuited windings - to take advantage of the computational simplicity of the equations for the symmetric machine model (19-21), by appropriately modifying the flux linkage computations for the effected windings. Basically the flux linkage vector $\underline{\lambda}$ for any machine, symmetric or otherwise, can be obtained by integration of the voltage equation (19). However, when the special inverse inductance matrix Γ^* for the symmetric machines given by Eq. (21), is substituted into (19) only the flux linkages for existing symmetric windings may be computed from the resulting equation. The flux linkages of

asymmetric or open-circuited windings must then be computed by other means, as described below. The auxilliary flux linkage computations required for open circuited windings will be described first. In the following it should be noted that a non-existent winding may also be treated as a hypothetical existing, but open-circuited winding. Thus a machine having less than four windings, but which otherwise satisfies the conditions outlined in Section 2.2 may also be simulated using the technique to be described.

A four winding machine having one or more open-circuited windings cannot be directly simulated by Eq. (19) because the integration of (19) requires that impressed terminal voltages be specified as "inputs" on all four windings, whereas such an impressed voltage is undefined for an open-circuited winding. Indeed, the "input" condition for an open circuited winding is that its current be specified as equal to zero. The causality requirements for integration in general preclude the specification of current as an "input" function. However, the constraint of zero current in an open circuited winding may be used to determine the flux linkage of the open winding in terms of the flux linkage components of those remaining windings which are not open circuited. The current in each winding of a symmetric machine may be expressed as a function of the flux linkages of that winding and of the two windings on the opposite machine structure by means of Eq. (18b) and (21). Note that an open circuited winding may be considered to be symmetric with the other winding on the same structure. Thus the inverse inductance matrix (21) for the four-winding symmetric machine is directly applicable when a machine either has (1) open circuited windings on both rotor and stator, or (2) open circuited winding(s) on only one structure and symmetric

windings on the opposite structure. Consequently, for an otherwise symmetric machine, the flux linkage of an open-circuited winding is computed as follows. The inverse inductance matrix (21) for the symmetric machine is substituted into (18b). Each row of the resulting matrix equation: $\underline{L}' = \underline{\Gamma}^*(F_p,\theta)\underline{\lambda}'$ is the equation for the current in a given winding as a function of $\underline{\lambda}'$. In the row equation corresponding to the open winding, the value of current on the left hand side of the equation is set to zero and the resulting equation is then solved for the flux linkage of the open circuited winding in terms of the flux linkages of the other windings which remain connected to external voltage sources. This computation for the flux linkage of an open circuited winding replaces the flux linkage computation for that winding ordinarily performed by integration of the corresponding component of the voltage Eq. (19). Because the flux linkages of open circuited windings are thus uniquely determined in terms of the flux linkages of the remaining windings, they are no longer independent variables. Consequently the number of independent electrical state variables (flux linkages) of the machine is reduced by the number of open windings. The equations for the flux linkages of open circuited windings, for several different winding configurations, are derived in Appendix B.

The procedure for simulating machines with open circuited windings, using the basic equations for the symmetric machine (19-21), is briefly summarized. The flux linkages of those windings which have external voltage "inputs" impressed upon them are found by integrating the corresponding components of the voltage equation (19), in the normal manner. The flux linkages of the remaining open circuited windings are

then computed in terms of the former flux linkages by setting the components of current in (18b) corresponding to the open windings equal to zero and solving the resulting equations for the flux linkages of the open windings.

When simulating a machine with asymmetric windings in terms of the basic symmetric model, use is made of the fact that when the machine parameters are expressed on a referred basis the effect of asymmetry can be represented by unequal referred values of the winding leakage inductances. Furthermore, the leakage inductance of a winding may be represented as an external inductance attached to the machine terminals for that winding. Consequently, the asymmetric machine may be modelled as a symmetric machine whose windings are connected in series with unequal external inductances. Specifically, each pair of asymmetric windings is represented as two symmetric windings, one of which is connected to an external inductor whose value is equal to the difference between the unequal referred leakage inductances of the original asymmetric windings. At most, two such external inductances are required, one for each asymmetric winding pair. However, because machines having asymmetric windings on both machine structures are uncommon, the development of the asymmetric machine model in this thesis is carried out only for the case of asymmetric windings on the stator structure. The flux linkage differential equations for the symmetric machine component of this asymmetric model are given by voltage Eq. (19), using the symmetric machine inverse inductance matrix from (21). However, the component voltage equation for the stator winding connected to the external inductor representing the asymmetry must be modified to account for the voltage drop across that inductor. Note that the flux linkages computed by integration

of the voltage equations (19) are those of the symmetric machine component of the asymmetric model only, and do not include the flux linkage of the hypothetical external inductor. The details of this development for the asymmetric machine model and the derivation of the modified voltage equation for the stator winding connected to the external inductor are given in Appendix B.

2.10 Computational Considerations

The machine model equations (19-20) are solved numerically on a digital computer for arbitrarily specified "input" functions (terminal voltages and shaft torque) using the Runge-Rutta method of numerical integration. Because such a numerical solution is merely a discrete approximation to the true solution of these equations, questions of computational stability and accuracy of the numerical integration of these equations must be considered. The primary factor affecting the computational stability and accuracy of the solution is the integration step size, Δt, used in the numerical integration. For reasons of computational economy this step size should be made as large as possible consistent with the requirements posed by computational stability and solution accuracy. The larger the step size, the fewer the computations required to cover a given time span of the simulation. An upper limit on the permissible step size is imposed by the requirements of computational stability and solution accuracy. The two principal factors which determine this upper limit on step size are (1) the bandwidth of signal frequencies in the specified input functions that are to be accurately reproduced in the computed outputs of the simulation, and (2) the inherent physical time constants of the machine model which are refelected in the "eigenvalue" of the model's state variable coefficient matrix.

One of the most obvious factors limiting the permissible step size of the numerical integration is the maximum signal frequency which is to be accurately reproduced in the computed outputs of the simulation. Generally this frequency is related to the frequency content in the "input" functions applied to the model - the winding terminal voltages and the shaft torque. Reproduction of input frequency components in the computed output variables of the simulation with reasonable accuracy requires that the integration step size, Δt, be limited such that $\Delta t \leq T/20$, where T is the period of the highest frequency component of interest to be reproduced by the simulation.

As an aside, it should be mentioned that in ceratin special cases involving balanced sinusoidal input voltages, application of a dq transformation to the model equations and input voltages will result in a relaxation of the step size constraint imposed by the period of the electrical input frequency. This is due to the fact that use of the dq transformation usually results in a downward frequency shift of the transformed inputs by an amount equal to the rotational speed of the dq reference frame. An example of such a situation is given by the simulation, in dq coordinates, of a balanced polyphase synchronous machine, operating at near synchronous speed with balanced sinusoidal voltages applied to its armature terminals. In this example, transformation of the machine dynamical equations and applied terminal voltages to a dq reference frame which is either locked to the rotor or rotating at synchronous speed will result in a problem formulation in which the highest signal frequency component of interest is the rotor slip frequency rather than the line frequency of the applied terminal voltages. When the machine is operating near synchronous speed, the slip frequency will be only a small fraction of the line frequency, thus allowing a relaxation of the

constraint on integration step size due to frequency content of the "input" functions. However, since dq transformations are not used in the machine equations developed in this thesis, the above consideration is not applicable to the determination of integration step size in the present situation.

The step size constraint imposed by the frequency content of the input functions affects only the accuracy with which these input functions are simulated, and does not affect the computational stability of the numerical integration. A far more serious constraint on step size is that imposed by the dynamical nature of the model itself, as this constraint must be met in order to insure not only the accuracy, but also the computational stability of the numerical integration of the model equations. In very general terms, it may be said that a requirement for computational stability of the numerical integration is that the integration step size be limited to a value less than approximately one half the reciprocal magnitude of the largest eigenvalue of the system. Furthermore, if the largest eigenvalue is either real or if its damping ratio is at least 80%, an equivalent statement of the above criterion is that the step size be limited to less than one half the value of the shortest system time constant. Although reference to eigenvalues usually implies a linear system, in the present case the eigenvalues referred to are those of the non-linear state variable coefficient matrix whose value is "frozen" at the instant of each integration step.

Unfortunately, for a large physical system, it is usually either impossible or inconvenient to determine all the physical time constants of the system by inspection, nor is it convenient to compute the eigenvalues of the system from the model equations, particularly when the

system is non-linear. Consequently it would be desirable to have a simple stability criterion for directly determining the maximum permissible integration step size at each step of the solution.

A simple qualitative stability criterion for step size that is applicable for the special case of the machine model equations of this thesis is described in the following. It is based upon the following considerations: (1) the machine is basically a stable physical system, thus all of the "eigenvalues" of the state variable coefficient matrix for the model equations have negative real parts, (2) the "eigenvalues" associated with electrical state variables (due to L/R time constants of the machine windings) are real and are much larger than those associated with the mechanical state variables, (3) complex "eigenvalues" are associated with the effects of electromechanical coupling and are much smaller in magnitude than those associated with the electrical state variables only, (4) all of the diagonal elements of the state variable coefficient matrix are real and negative, and thus have the same sign as the real parts of the eigenvalues. It is a well known fact that the sum of the eigenvalues of any matrix is equal to the sum of its diagonal elements. Since as pointed out above all of these quantities are of the same sign, and since their sums are also equal, it is reasonable to expect that their values are likely to be distributed over nearly identical ranges. Furthermore, from the above considerations, it is also assumed that the largest eigenvalue is real, being associated with the electrical state variables (due to the L/R time constants of machine windings). Therefore, it is likely that the value of the largest eigenvalue will be on the same order as that of the largest diagonal element of the state variable coefficient matrix.

Thus the stability constraint on step size is chosen as equal to one half the reciprocal of the magnitude of the largest diagonal element of the state variable coefficient matrix:

$$\Delta t \leq \frac{1}{2 \max_i |\gamma_{ii}|}$$

Admittedly, the above justification for the use of this constraint has been very qualitative and is far from rigorous. Its primary justification is based upon some prior knowledge about the physical nature of the model - primarily that the largest "eigenvalues" of interest are real. The principal merit of this constraint however, is its simplicity. Extensive numerical experimentation and operating experience with the machine simulation being described have indicated that this bound on step size is fairly tight (the step size cannot be increased appreciably above this value without risking numerical instability), and furthermore that this value of step size results in acceptable accuracy of the solution when the model equations are integrated by a second order Runge-Kutta integration algorithm.

The state variable coefficient matrix for the model equations of the symmetric machine (19-21) consists of the coefficient matrix $R\Gamma^*(\theta)$ for the electrical state variables, $\underline{\lambda}$, (from Eq.19), augmented by the coefficients of the mechanical state variables θ, ω from Eq. (20) and is shown below.

$$\begin{bmatrix} -r_a\Gamma_a & 0 & -r_a\Gamma\cos\theta & -r_a\Gamma\cos\theta & 0 & 0 \\ 0 & -r_b\Gamma_a & -r_b\Gamma\sin\theta & r_b\Gamma\cos\theta & 0 & 0 \\ -r_f\Gamma\cos\theta & -r_f\Gamma\sin\theta & -r_f\Gamma_f & 0 & 0 & 0 \\ -r_g\Gamma\sin\theta & r_g\Gamma\cos\theta & 0 & -r_g\Gamma_f & 0 & 0 \\ 0 & 0 & 0 & 0 & 0 & 1 \\ 0 & 0 & \frac{i_f}{J} & -\frac{i_g}{J} & 0 & -\frac{\mathfrak{T}}{J} \end{bmatrix}$$

The above coefficient matrix is non-linear because its elements are functions of the state variables $\underline{\lambda}$ and θ (the current terms i_f, i_g in the last row are function of $\underline{\lambda}$). The diagonal elements are all non-positive and the largest element, in keeping with the previous discussion, will almost always be one of the $(r\Gamma)$ terms associated with the electrical time constants of the machine. Consequently the previous step size criterion may be reformulated as:

$$\Delta t \leq \frac{1}{2\max_i (r\Gamma)_i} = \frac{1}{2} \min_i \frac{1}{(r\Gamma)_i} \tag{22}$$

When the expression for Γ_i is expanded in terms of the machine inductance parameters, in accordance with (21), (22) becomes

$$\Delta t \leq \frac{1}{2} \min_i \frac{L(\ell_r' + \ell_s') + \ell_r'\ell_s'}{r_i'(L + \ell_i)} \quad \text{where } \ell_i = \ell_r, \ell_s \tag{23}$$

It should be noted that r_i' and ℓ_i' include not only the internal resistance and leakage reactance of each winding but also any external resistance or inductance which may be connected in series with the winding.

In many applications $L >> \ell_s', \ell_r'$, under these circumstances (23) reduces to:

$$\Delta t \leq \frac{1}{2} \min_i \frac{\ell_r' + \ell_s'}{r_i'} \tag{24}$$

The expression $(r\Gamma)$ as expanded in (23) has an interesting physical interpretation in terms of circuital time constants. For example, it is easily verifiable that the following expansion of the reciprocal of the term $(r_a\Gamma_a)$:

$$\frac{1}{\Gamma_a r_a} = \frac{L(\ell_r' + \ell_s') + \ell_r'\ell_s'}{r_a'(L + \ell_r')}$$

is simply the L/R time constant of the following circuit.

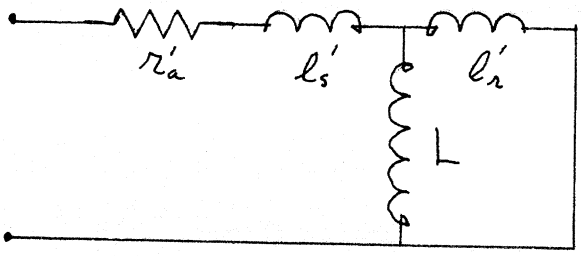

The above circuit clearly illustrates, as stated earlier, that when $L >> \ell_r'$, the effect of L may be neglected. The expansion for $(\Gamma_f r_f)$ has a similar interpretation viewed from the rotor side of the machine.

The practical consequence of the above development is that the principal constraint on the integration step size, posed by the requirement of computational stability, is due to the physical time constant

formed by the total machine leakage inductance and the largest winding circuit resistance of the machine. This criterion is conservative in the sense that the addition of external series inductance to the machine circuit configuration would tend to increase this time constant, thus raising the limit on the maximum allowable step size.

Because of the above considerations, the model of this thesis is ill-suited to the simulation of machine configurations in which one or more windings are connected such that the total circuit resistance for that winding (winding plus load) is large in comparison to the total circuit inductive reactance (winding leakage plus load reactance). Such a configuration would give rise to a very small value of L/R time constant, forcing the use of a correspondingly small integration step size and thus increasing the computation time and cost of the simulation. Fortunately, this problem occurs only infrequently in power system applications which typically involve a single machine connected to an "infinite" bus via a transmission network, because the resistance to reactance ratio of such a combined machine-transmission network is usually very low. However, this problem does become quite troublesome in the simulation of many stand-alone machine configurations such as an independently operating alternator connected to a resistive load, particularly when the per unit value of load resistance is equal or greater than the per-unit rating of the alternator. For example, consider an alternator having a total leakage reactance of 0.05 pu whose armature is connected to a 1.0 pu resistive load. In accordance with Eq. (24) the effective circuit time constant would be approximately $0.05/2\pi f$ secs, where f is the alternator frequency in hz, thus imposing an upper limit on step size of $0.05/4\pi f$ secs. This should be contrasted with the step size

constraint of 1/20f posed by the rotor electrical speed, or equivalently the frequency of the terminal voltages. Thus, in this case the circuit time constant limits the step size to approximately 1/12 of the value required to accurately reproduce the fundamental frequency sine wave in the computed output currents. The computation time required for the simulation of this machine configuration over a given time span will therefore be an order of magnitude greater than that required if the step size were not limited by physical time constants of the model. Obviously, the higher the load resistance, the more severe this problem becomes.

It should be pointed out, that unlike the limit on step size imposed by the frequency content to be reproduced in the computed output, because the step size constraint for computational stability is determined by the eigenvalues or time constants of the physical model, this constraint cannot be relaxed by application of a dq transformation. This is understandable as the latter constraint is associated with the physics of the model, and the model physics remain unchanged by application of the dq transformation. Techniques do of course exist for handling the digital simulation of physical models in which the presence of small time constants proves computationally burdensome. Such techniques involve reformulating the basic model equations such that the presence of the troublesome time constants may be neglected, and result in a corresponding reduction in the number of model state variables. However, such "model reduction" techniques will not be considered in this thesis.

In summary, the maximum allowable step size for the numerical integration of the machine model equations is limited by the smaller of the following two quantities: (1) one-twentieth of the period of the

highest frequency component to be accurately reproduced in the computed output, or (2) one half of the smallest electrical time constant formed by the total machine leakage inductance and the winding circuit resistances of the machine. This constraint on step size may be expressed as follows:

$$\Delta t \leq \min\left(\left(\frac{\tau_{min}}{2}\right), \frac{\tau}{20}\right)$$

τ_{min} smallest electrical time constant formed with total machine leakage inductance $(\ell_r' + \ell_s')$, (referred)

τ period of highest frequency component to be accurately reproduced in the computed output

In closing it should be stated that computational problems of this type do not arise at all when the machine equations are simulated on an analog computer, as on an analog computer the operation of integration is continuous rather than discrete. The step size problem may be viewed as a problem of achieving a wide frequency bandwidth in the simulation of the model equations. In effect, the analog computer can easily provide a very wide frequency bandwidth for simulation but because of component limitations it is extremely limited in dynamic range. On the other hand, although a digital computer can provide a very large dynamic range through the use of floating point arithmetic, the computation time required for a given simulation increases in direct proportion with the bandwidth of the system being simulated. This is perhaps the principal reason why most electrical machinery simulations have in the past been performed on analog rather than digital computers.

2.11 Simulation of Systems Composed of Two or More Electrically Interconnected Machines

In this section the problem of simulating a system of several electrically interconnected machines rather than just a single machine, is described. It will be seen that the simulation of multi-machine systems poses some unique and difficult problems that did not arise in the simulation of single machines.

A multi-machine system, in the context of the following discussion, consists of a group of two or more individual machines that are electrically interconnected by means of stationary networks. However, not all multi-machine system simulations can be realized merely by representing each individual machine in the system by the single machine computation model developed in the previous sections of this chapter, and then interconnecting these single machine models through a model of the system interconnection network. In particular, such a straightforward computational implementation of a multi-machine system simulation, in which each of the individual machines are represented by means of the previously developed single machine model, is possible only when the system interconnection network contains resistive or capacitative shunt admittance elements.

However, there are many practical multi-machine systems in which the machines are directly coupled (electrically) and no shunt admittance elements appear across the interconnection bus. Examples of such directly coupled systems are electro-motive drive systems for ships and trains and selsyn systems used for transmission of angular position information. In simulations of such directly coupled machine systems, not all of the individual machines can be represented using the previously developed single machine computation model.

Frequently, in the simulation of the direct-coupled multi-machine system, it is necessary to represent one or more of the individual machines in the system by computational models having derivative causality. In principal, it is possible to simulate directly coupled systems without resorting to models requiring computational differentiation; however, the algebraic manipulations required to combine all of the machine model equations in such a system into a state variable formulation, which can be solved using only computational integration, usually becomes prohibitively burdensome, except for some very limited special cases which are described later.

Nearly all practical multi-machine systems involve parallel interconnections between the windings of the different machines. Generally these interconnections are made through an electrical network which represents the combined transmission system and load impedances. Typical examples of such systems of interconnected machines are (1) a power system composed of a finite number of machines, and a transmission network which interconnects these machines to each other and to a load network, (2) a stand-alone generator-motor combination in which the motor power is produced by the generator, the latter being driven by an external mechanical power source, (3) a system of selsyns (synchros), consisting of a single transmitter and one or more receivers, for transmitting angular position data.

A "block diagram" type of sketch illustrating the manner of interconnection common to all such systems is illustrated below.

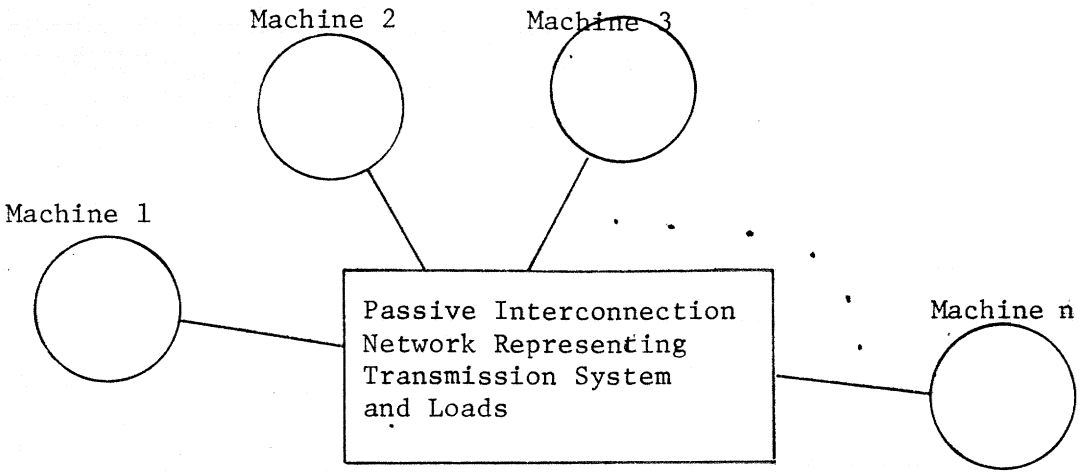

Fig. 2.6 Representation of an Electrically Coupled Multi-Machine System

The problem common to all multi-machine systems which are interconnected as shown above is that no "external" voltages are applied as inputs to the interconnection network. When the individual machines in such an interconnected system are modelled using a conventional single machine model with integration causality, such as the model developed in the earlier sections of this chapter, the integration causality of each machine model requires that the terminal voltages be specified as inputs to the model equations. Since in the present situation there are no externally specified (ie: bus) voltages, the voltages applied to the terminals of the machine models must be computable from the equations of the interconnecting network as functions of the machine currents, the latter in turn being computed as outputs from the solution of the machine model equations of the individual machines. In other words the machine terminal voltages are obtained by simultaneously solving the network equations and all of the machine model equations. This computation of

the machine terminal voltages in terms of the machine currents, using the equations of the interconnecting network, is only possible when that network contains shunt impedance elements. Furthermore, if this computation of terminal voltages using the network equations is to be done without use of computational differentiation, at least one of the shunt impedance elements of the network must be free of inductance (be composed entirely of resistors and capacitors). When no resistive or capacitative shunt impedances are present in the interconnection network, it becomes impossible to computationally solve the equations of the interconnected system model without resorting to computational differentiation, unless the redundant state variables in the interconnected system are eliminated by algebraically combining the machine equations with those of the interconnecting network. The latter task of algebraic combination of the machine and network equations appears to be prohibitive except in the simplest case of two directly coupled symmetric machines.

An obvious solution to the dilemna posed by the conflicting requirements of integration causality in a multi-machine system, when no shunt elements are present in the interconnecting network, is to simulate some of the machines by a model having derivative causality. Such a model would require the use of computational differentiation, but would have a reversed assignment of input/output variables, allowing the specification of currents as independent input variables and generating terminal voltages as computed outputs. The simplest example of such an application to a multi-machine simulation is a directly connected two-machine system. In the simulation of this system, one of the machines is represented by a conventional integration causality model requiring specified input voltages and producing currents as computed outputs;

the other machine is then represented by a derivative causality model having the reciprocal, and thus compatible, causality requirements of "current in-voltage out". Many of the past objections to the use of simulation models requiring computational differentiation can be overcome by implementing such simulations on digital computers. One example of such an application involving the start-up performance of generator-motor system consisting of two synchronous machines is described in (1). Furthermore a detailed discussion of the use of computational differentiation vs integration in the solution of dynamical equations on a digital computer is given in (2). A systematic procedure for describing the computational causality requirements posed by the interconnection of individual components in a multi-component system is provided by the bond-graph technique of modelling physical systems for computer simulation. This method is particularly appropriate for the determination of causality requirements and/or conflicts in a system composed of several rotating electrical machines which are interconnected by a stationary but arbitrary electrical network. A very brief introduction to bond-graphs and their application in the determination of causality requirements for systems of electrically interconnected rotating electrical machines is given in Appendix E.

The basic problem of multi-machine system simulation is that posed by the need to satisfy the computational causality requirements of the model equations for each machine in the system as well as for the interconnecting network. The simulation model for the single machine developed earlier can be extended to the multi-machine case only when resistive or capacitative shunt impedance elements are present in the interconnecting network. When such shunt elements are present in the

interconnecting network, the network equations can be used to satisfy the integration causality requirements of the machine model equations by computing the machine terminal voltages as functions of the machine currents. In other simultions of multi-machine systems, one must either use a machine model having a reversed causality of "current in-voltage out", thus requiring the use of computational differentiation, or one must algebraically eliminate redundant state variables in the combined system by analytically combining the machine model and network equations into a state variable formulation for the overall system which is numerically soluble by integration. The former course involving computational differentiation is suitable if the simulation is implemented on a digital computer. The latter course involving algebraic combination of machine equations appears to be only practical for the special case of two directly coupled symmetric machines. These three methods of simulating multi-machine systems are summarized below.

1. Conventional state variable formulation (integration causality) of model equations for each machine. Interconnection network includes resistive or capacitative shunt elements. Network equations are used to compute machine terminal voltages.
2. At least one machine in system is simulated using a derivative causality model. The computed output voltage of this machine is used to determine the input terminal voltages to the remaining machines simulated by the conventional integration causality model.
3. Model equations for two parallel connected symmetric equations are algebraically combined, thus eliminating

redundant state variables. Resulting two-machine model has integration causality.

In the remainder of this section some salient features of the multi-machine simulation techniques described earlier will be discussed in terms of a model for two electrically interconnected four-winding, uniform air gap machines. The two machine model is the simplest case of a multi-machine system, but it nevertheless serves to illustrate the computational difficulties generally encountered in the simulation of multi-machine systems. Only the following two simulation models will be discussed.

1. Extension of the single machine model developed earlier to the simulation of a two machine system having a resistive shunt load across the armature interconnection bus.
2. A model of a system of two symmetric machines whose stator windings are directly connected with no additional shunt load. This model is formed by algebraically combining the equations of two symmetric single machines using the interconnection constraint that the stator currents and terminal voltages of both machines must be identical.

Both of these two-machine simulation models have integration causality. Multi-machine simulations which use machine models having derivative causality will not be discussed further in this thesis; however, the practical importance of such models, particularly for digital computer simulation should not be underestimated.

The second model, formed by algebraic combination of the equations for two single machines, will be described first as it has a rather

limited practical application. This algebraic combination process appears to be practical only when both machines are symmetric and have no open windings. The algebraic combination of the machine equations results in the elimination of the two electrical stator state variables for one of the two machines, reflecting the fact that the stator currents in both machines must be identical and thus cannot be independent. Consequently the resulting two machine formulation has only six electrical state variables rather than eight. These six are composed of two rotor state variables (flux linkages) for each of the two machines and one pair of stator state variables (flux linkages) for the interconnected stator windings. The derivation of the dynamical equations for such a combined model of two interconnected symmetric machines is given in Appendix C. However, because of the complexity of the required algebraic manipulations, the extension of this technique to the simulation of a system of more than two machines appears to be impractical. The further restriction of the analysis described in Appendix C that both machines be symmetric and have no open windings also limits the applicability of this technique to a very restricted class of problems, thereby considerably reducing its practical importance.

The simulation model for the two machine system with resistive shunt load, which is based upon a direct extension of the single machine model developed earlier, is more general in its application. There are no restrictions as to symmetry or open-circuited windings in either machine, and theoretically this method of simulation may be extended to a system composed of an arbitrary number of machines which are interconnected to common shunt load. The integration causality requirements of the machine model equations are satisfied by the presence of a shunt load

impedance in the interconnection network; the shunt load resistance enabling the computation of machine terminal voltages as function of the machine currents.

An example of this method, applied to the simulation of a multi-machine power system, is given in [11]. However, in that reference, the load network is forced to have a "current in-voltage out" causality despite the inclusion of inductive impedance elements in the shunt load. This is done by neglecting transients effects due to the reactive components in the load network and is equivalent to assuming that the load and transmission impedances act as if they were subject to steady state sinusoidal excitation. As a result of this assumption the load network may be algebraically represented as a purely static AC impedance network, thus enabling an aribtrary choice of causality for the load network. The consequence of such an assumption is that the dynamic effects of the load and transmission impedances due to frequency swings in the interconnected system are neglected.

Despite the general applicability of this simulation method, rather serious computational problems may be encountered in the implementation of this method on a digital computer. The nature of this problem is, as discussed in Section 10, that in order to insure computational stability of the simulation, the integration step size used in the computation must be kept smaller than the smallest time constant of the interconnected system. Quite frequently, the smallest system time constant will be that formed by the ratio of the smallest value of total machine leakage inductance to the sum of the shunt load and winding resistances. In a situation where the per-unit value of the load resistance is on the same order as the machine rating, and the total machine

leakage inductance has a low per-unit value, the resulting time constant may be so small as to limit the value of integration step size used in the computations to the point where the numerical solution of the system model equations economically impractical. This problem can become quite severe for the case of two machines connected to a common resistive shunt load, when the per-unit value of the load resistance is on the same order as the power rating of the machines.

This computational problem is clearly illustrated when the equations for the two-machine system with shunt load resistance across the interconnection bus are expressed in state variable form. The equations for each of the two machines are given by Eq. (19-20). Because of the interconnection, the stator terminal voltages on both machines are identical.

$$v_{a1} = v_{a2}$$
$$v_{b1} = v_{b2} \tag{25}$$

Furthermore, these terminal voltages are equal to the voltage drops across the shunt load resistances; the currents flowing through these resistances are equal to the sum of the corresponding stator currents of both machines.

$$v_{a1} = v_{a2} = -R_a(i_{a1} + i_{a2})$$
$$v_{b1} = v_{b2} = -R_b(i_{b1} + i_{b2}) \tag{26}$$

R_a and R_b are the shunt resistances across the a and b phases of the interconnection bus.

When Eq. (26) is combined with the machine voltages equations

(19), the stator terminal voltages $v_{a1,2}$, $v_{b1,2}$ are eliminated from the resulting equation. The only remaining terminal voltages to be specified as inputs are the rotor winding voltages for each machine. Upon elimination of the terms $v_{a1,2}$, $v_{b1,2}$, the voltage equations for the stator flux linkages of each machine take the following form:

$$\overset{o}{\lambda}_{a1} = -(R_a + r_{a1})i_{a1} - R_a i_{a2}$$

When these equations are expressed soley in terms of the winding flux linkages, the above becomes:

$$\begin{aligned}\overset{o}{\lambda}_{a1} = &- (R_a + r_{a1})(\Gamma_{a1}\lambda_{a1} + \Gamma_1(\lambda_{f1}\cos\theta + \lambda_{g1}\sin\theta_1)) \\ &- R_a(\Gamma_{a2}\lambda_{a2} + \Gamma_2(\lambda_{f2}\cos\theta_2 + \lambda_{g2}\sin\theta_2))\end{aligned} \tag{27}$$

The equations for the stator winding flux linkages, as given by (27), give rise to terms on the main diagonal of the 12 x 12 state variable coefficient matrix for the two-machine system of the form:

$$\gamma_{11} = -(R_a + r_{a1})\,\Gamma_{a1}$$

As discussed in Section 10, these terms correspond to the reciprocals of the time constants formed by the ratio of the machine leakage inductance to the resistance given by the sum $(R_a + r_{a1})$. The larger the value of the shunt load resistance R_a, the smaller the resulting time constant and the corresponding limit on the maximum allowable computation step size.

A good indication of the computational efficiency of the simulation is the ratio of the step size limit imposed by the smallest system time constant to the period of fundamental system frequency;

the smaller this ratio the less efficient the simulation. As was pointed out in Section 10, the step size limit imposed by the frequency content of the computed output variables is approximately $\tau/20$, where τ is the period of the fundamental frequency component. Thus when the value of the smallest system time constant is less than $\tau/20$, the upper limit on integration step size is governed by magnitude of the system time constants, or reciprocal eigenvalues. The relative value of the system time constants with respect to the period of the fundamental system frequency is given directly when the machine and network impedances are expressed in terms of per-unit quantities. The resulting values of time constant are dimensionless and are expressed as radians of fundamental frequency. Consequently a system time constant, computed in terms of the per unit values of impedances, of less than 0.3 radian corresponds roughly to the time interval $\tau/20$. For systems having per-unit time constants of less than 0.3 radian, the digital computer simulation of this thesis becomes increasingly unattractive because of the long computation times required.

In this section several alternative methods of simulating multi-machine systems have been described. The basic problem of simulating such systems is to interconnect or combine the equations of the individual machine models in the system in a causally compatable manner. In Appendix E, bond-graphs are shown to be a useful way of indicating causality requirements when combining physical component models into an overall model of an interconnected system, and are also helpful in determining modifications required to resolve causal incompatabilities. There are three distinct modelling methods for simulating multi-machine systems.

1. Use of shunt load components in the interconnection network to satisfy the voltage input-current output integration causality requirements for the state variable models of each of the individual machines.
2. Use of a separate machine model having derivative causality for at least one of the machines in the system.
3. Algebraic combination of the individual machine model equations to eliminate redundant state variables in the interconnected system.

The first method is quite general and commonly used but is dependent upon the presence of resistive and/or capacitative shunt impedance elements in the interconnecting network. Furthermore, the numerical implimentation of this method on a digital computer is ofen inefficient or even impractical because of limitations on the integration step size used in the computations. The second method may be used for a large variety of problems and seems to be the only general method of simulating a multi-machine system when no static shunt loads are present in the interconnection network. The implimentation of this method requires the use of computational differentiation, and therefore, it has not been widely used. Nevertheless, although such derivative causality models are unconventional, it appears that their use may provide not only the most general but also the most computationally efficient means of simulating multi-machine systems. The last method of algebraically combining the model equations of the individual machines in the system appears to be of little practical consequence because of the complexity, in the general case, of the resulting equations for the model of the interconnected system. This method appears to have some practical merit

only in the special case of a two machine system where each machine is symmetric and has no open-circuited windings.

CHAPTER 3

APPLICATIONS

3.1 Outline of Application Examples

In this chapter some typical examples of single and two-machine simulations, which were conducted using a digital computer program based on the machine simulation models developed in Chapter II, are presented. The wide variety of machine configurations which are simulated in these examples illustrates the versatility of the generalized four-winding, cylindrical rotor machine computational model developed in the previous chapter.

The individual single machine simulations to be described consist of the following examples: (1) Free acceleration from rest of a symmetric two-phase induction motor connected to a balanced two-phase infinite bus. (2) Free acceleration from rest of an unsymmetric capacitor start induction motor connected to a single-phase infinite bus. (3) Electromechanical oscillations of a balanced synchronous motor, connected to a balanced two phase infinite bus, in response to sudden changes in mechanical load applied to the shaft. The single and two phase infinite busses from which these machines receive electrical power are ideal sinusoidal voltage sources. In addition, the two-phase sinusoidal voltage sources are in phase quadrature; phase a leads phase b by 90^{o}.

The simulation results observed for example (1) and (2) above are verified by comparison with results given in [7], [8] for analog computer simulations of the identical machine models. The observed simulation results of the third example are compared against analytical

results computed from expressions for rotor swing frequency and damping ratio of a synchronous machine, for small disturbances about an operating point. These analytical expressions for the small disturbance dynamic response of a synchronous machine are derived in Appendix D.

Two examples are given for simulations of two machine systems. Both of these cases are similar in that the machine models are connected back-to-back across a resistive shunt load. Specifically, the corresponding stator phase windings of both machines are interconnected, and identical load resistors are connected across each of the two phases of the interconnection bus. This particular two-machine configuration was chosen because it is representative of certain practical situations, and because the presence of shunt load resistors across the interconnection bus resolves the computational causality conflict posed by the direct interconnection of two individual machines (see Chapter II, Section 11).

In the first example of a two-machine system having the above configuration, machine 1 is a two phase alternator and machine 2 is a symmetric two phase induction motor. Thus the system is electrically balanced. The bus load resistors are 1.0 pu on the alternator base and the power rating of the motor is 10% that of the alternator (rated motor power is 0.1 pu). The alternator is driven by a speed governed prime mover and its field excitation is controlled by a voltage regular. The altenator speed governor and voltage regulator are both modeled as proportional controllers with first order time lag and are included in the simulation. The induction motor is initially disconnected from the system and is at rest. The alternator is initially operating at rated speed and supplying rated power at rated voltage to the load resistors.

The simulation describes the transient behavior of the system during start up and free acceleration of the induction motor to synchronous speed. The only load on the motor is its own mechanical shaft inertia.

The second example is similar to the first except that both machines and their common interconnection are now single-phase. Consequently there is only a single load resistor, having a value of 0.5 pu, across the single phase interconnection bus. The motor is an unsymmetrical capacitor-start induction motor similar to that described earlier in the single machine simulations, except that its power rating is again 10% of that of the alternator. The alternator speed governor and voltage regulator are identical to those used in the first example. The simulation of this second example is representative of a rather common application - the operation of a single phase portable emergency power plant, supplying a base incandescent lighting load, when a small motor load, such as a refrigerator compressor, is suddenly applied to the line.

3.2 Start-Up and Free Acceleration of a Symmetric Two-Phase Induction Motor

The per-unit parameters of the induction motor being simulated in this example are given below:

$r_a' = r_b' = r_s' = .0453$ $\qquad$ $\omega\ell_a' = \omega\ell_b' = x_s = .0775$

$r_f' = r_g' = r_r' = .0222$ $\qquad$ $\omega\ell_f' = \omega\ell_g' = x_r = .0322$

$\frac{J\omega_o^2}{2VA} = H = 1.0$ secs $\qquad$ $\omega L = x_m = 2.042$

$\omega_o = 377$ rad/sec (60 cps) $\qquad$ $v_f' = v_g' = 0$

$v_a' = v_b' = V = 1.0$

The only load on the motor shaft is its own mechanical inertia.

The motor parameters listed above were taken from Ref. [7] in which an analog computer simulation of the same motor is described. Consequently, the results of the analog computer simulation described in [7] are used as a bench mark for verification of the results obtained in the present simulation.

The results of the present simulation of motor performance during start-up and free acceleration to synchronous speed are described by the time histories of speed, torque, real and reactive power, and phase current illustrated in Figs. 3.1 through 3.5. Although the time axes in these figures are calibrated in terms of radians of line frequency phase, the time scale is easily converted to seconds using the conversion factor of 377 radians/sec at 60 cps. Comparison of the torque, speed, and phase current data with the corresponding results given in [7] indicates excellent agreement between the results of the two simulations.

Perhaps the most interesting aspect of the simulation results obtained in this example is the pulsating torque component associated with the initial transient. Examination of these torque pulsations indicates that their frequency is equal to the rotor slip frequency, unlike the double frequency torque pulsations inherent in the operation of unbalanced or single-phase machinery. These slip frequency torque pulsations are due to the decaying DC component of rotor current that was induced by the initial transient.

3.3 Start-Up and Acceleration of an Unsymmetric Capacitor-Start Single Phase Induction Motor

The connection diagram for the motor being simulated in this example is illustrated in Fig. 3.6. The motor parameters are given

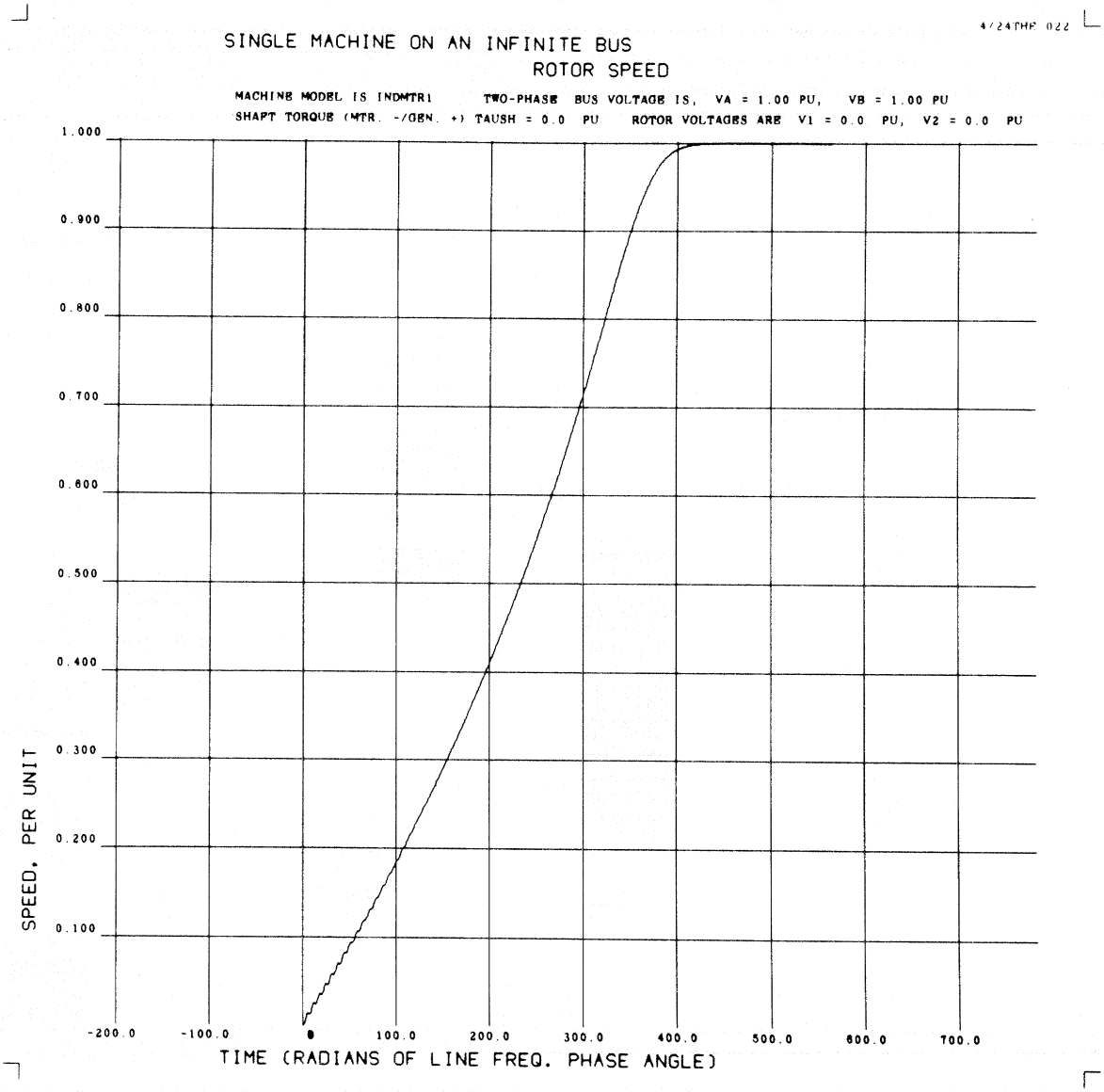
4/24THF 022
SINGLE MACHINE ON AN INFINITE BUS
ROTOR SPEED
MACHINE MODEL IS INDMTR1
TWO-PHASE BUS VOLTAGE IS, VA = 1.00 PU, VB = 1.00 PU
SHAFT TORQUE (MTR. -/GEN. +) TAUSH = 0.0 PU
ROTOR VOLTAGES ARE V1 = 0.0 PU, V2 = 0.0 PU
SPEED, PER UNIT
1.000
0.900
0.800
0.700
0.600
0.500
0.400
0.300
0.200
0.100
-200.0
-100.0
0
100.0
200.0
300.0
400.0
500.0
600.0
700.0
TIME (RADIANS OF LINE FREQ. PHASE ANGLE)

Fig 3.1

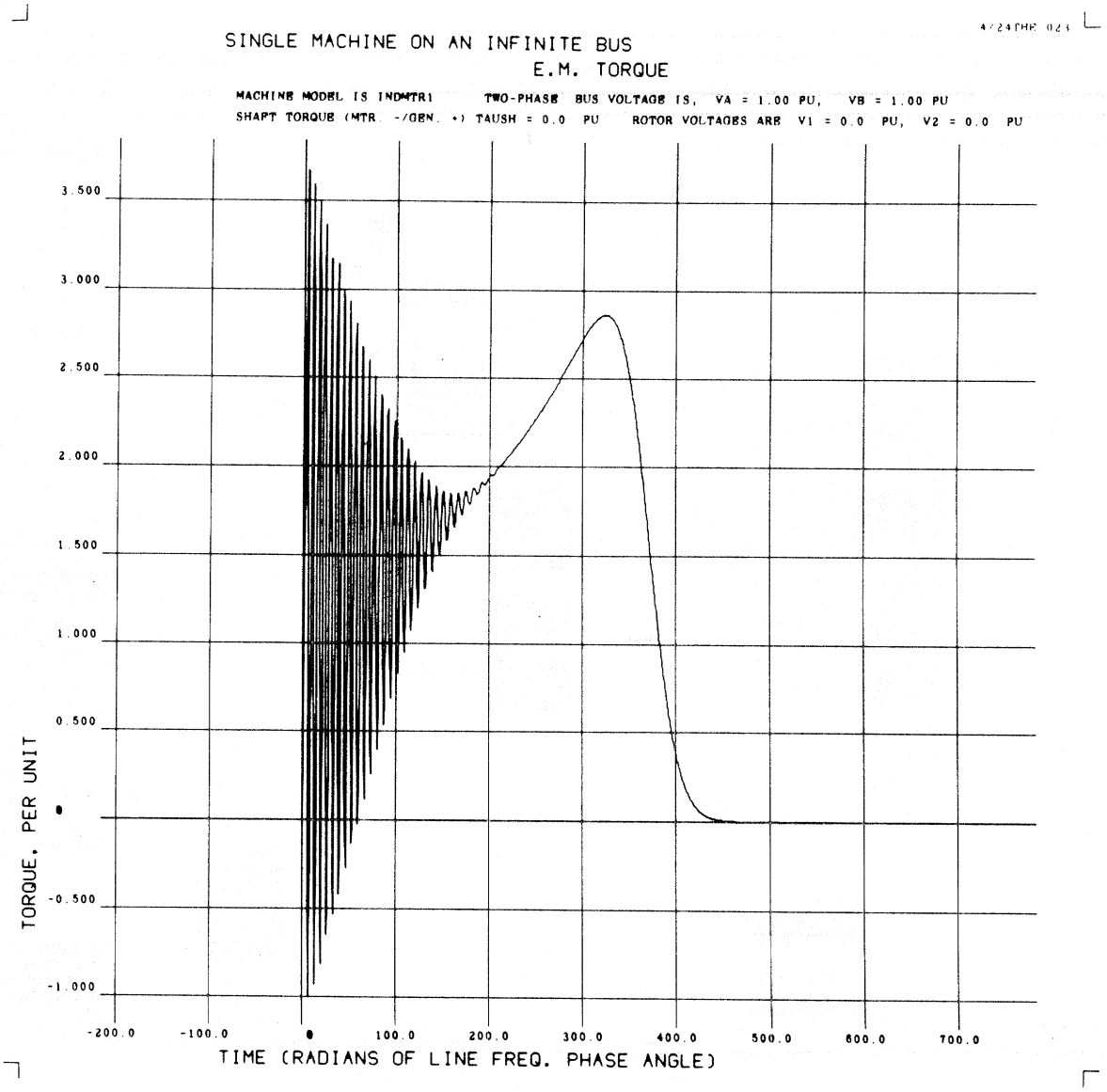
SINGLE MACHINE ON AN INFINITE BUS
E.M. TORQUE
MACHINE MODEL IS INDMTR1 TWO-PHASE BUS VOLTAGE IS, VA = 1.00 PU, VB = 1.00 PU
SHAFT TORQUE (MTR -/GEN +) TAUSH = 0.0 PU ROTOR VOLTAGES ARE V1 = 0.0 PU, V2 = 0.0 PU
3.500
3.000
2.500
2.000
1.500
1.000
0.500
-0.500
-1.000
TORQUE, PER UNIT
-200.0
-100.0
100.0
200.0
300.0
400.0
500.0
600.0
700.0
TIME (RADIANS OF LINE FREQ. PHASE ANGLE)

Fig 3.2

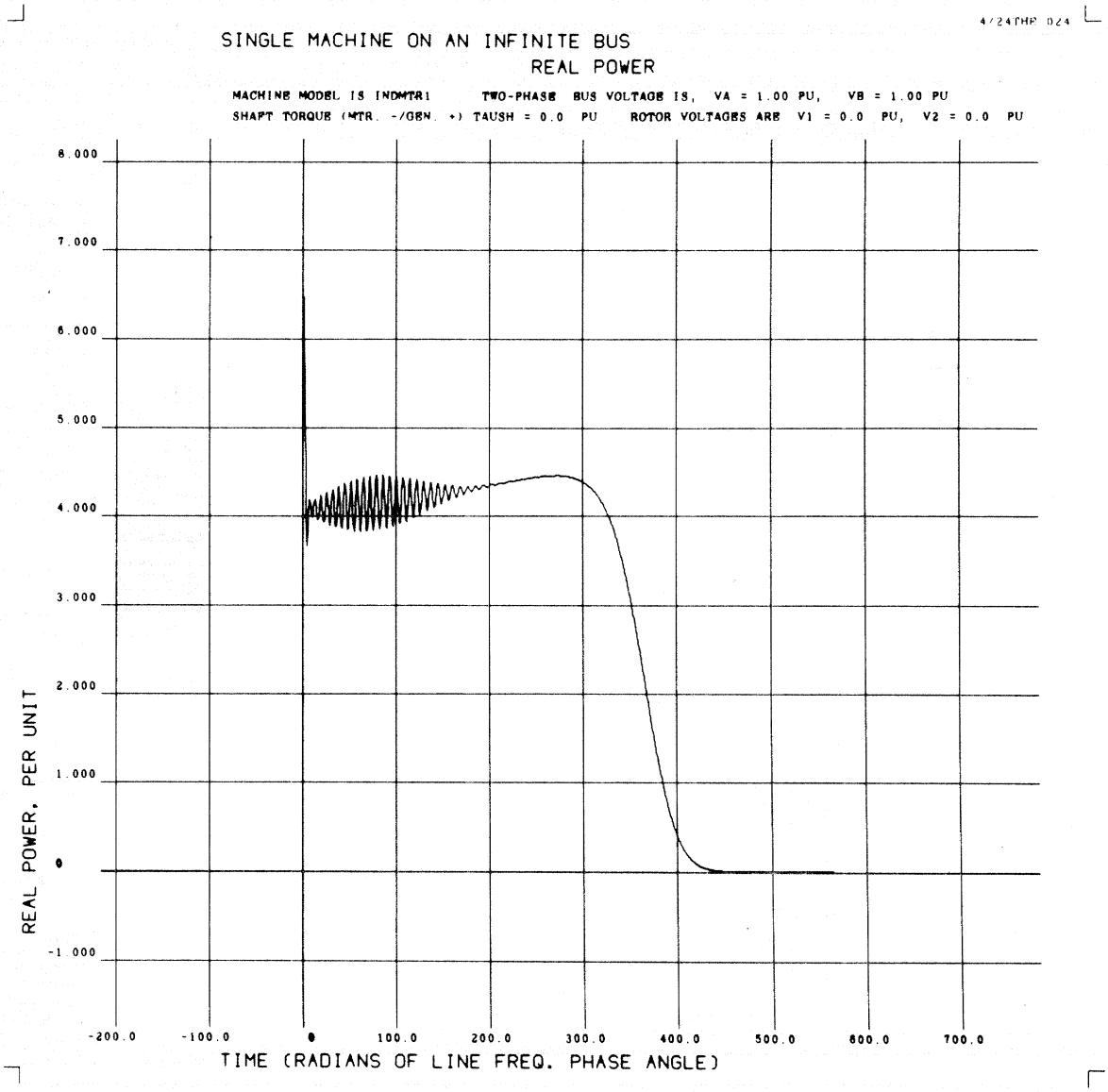
4/24THP 024
SINGLE MACHINE ON AN INFINITE BUS
REAL POWER
MACHINE MODEL IS INDMTR1 TWO-PHASE BUS VOLTAGE IS, VA = 1.00 PU, VB = 1.00 PU
SHAFT TORQUE (MTR. -/GEN. +) TAUSH = 0.0 PU ROTOR VOLTAGES ARE V1 = 0.0 PU, V2 = 0.0 PU
8.000
7.000
6.000
5.000
4.000
3.000
2.000
1.000
0
-1.000
REAL POWER, PER UNIT
-200.0
-100.0
0
100.0
200.0
300.0
400.0
500.0
600.0
700.0
TIME (RADIANS OF LINE FREQ. PHASE ANGLE)

Fig. 3.3

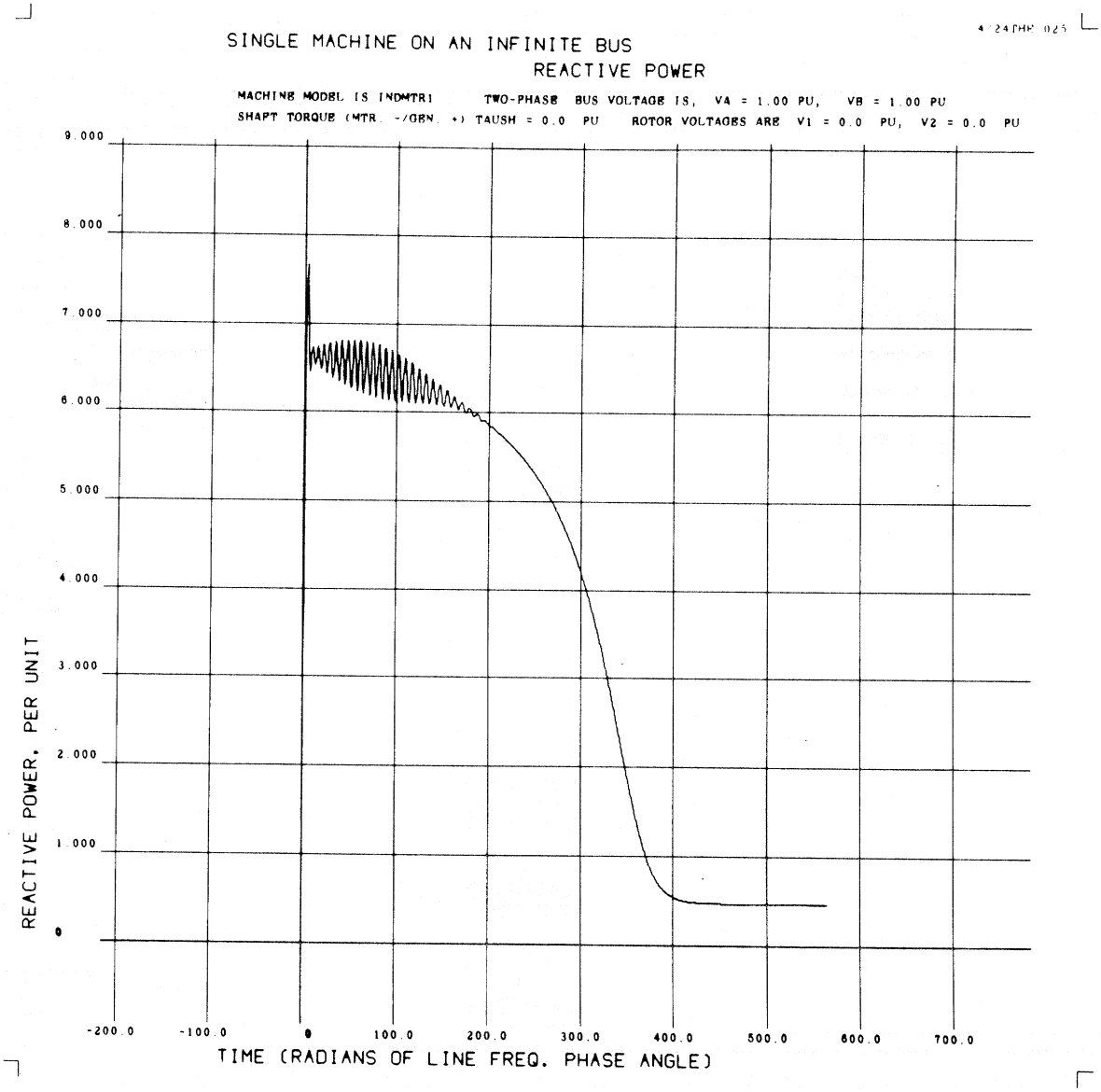
SINGLE MACHINE ON AN INFINITE BUS
REACTIVE POWER
MACHINE MODEL IS INDMTR1 TWO-PHASE BUS VOLTAGE IS, VA = 1.00 PU, VB = 1.00 PU
SHAFT TORQUE (MTR. -/GEN. +) TAUSH = 0.0 PU ROTOR VOLTAGES ARE V1 = 0.0 PU, V2 = 0.0 PU
REACTIVE POWER, PER UNIT
9.000
8.000
7.000
6.000
5.000
4.000
3.000
2.000
1.000
0
-200.0
-100.0
0
100.0
200.0
300.0
400.0
500.0
600.0
700.0
TIME (RADIANS OF LINE FREQ. PHASE ANGLE)

Fig. 3.4

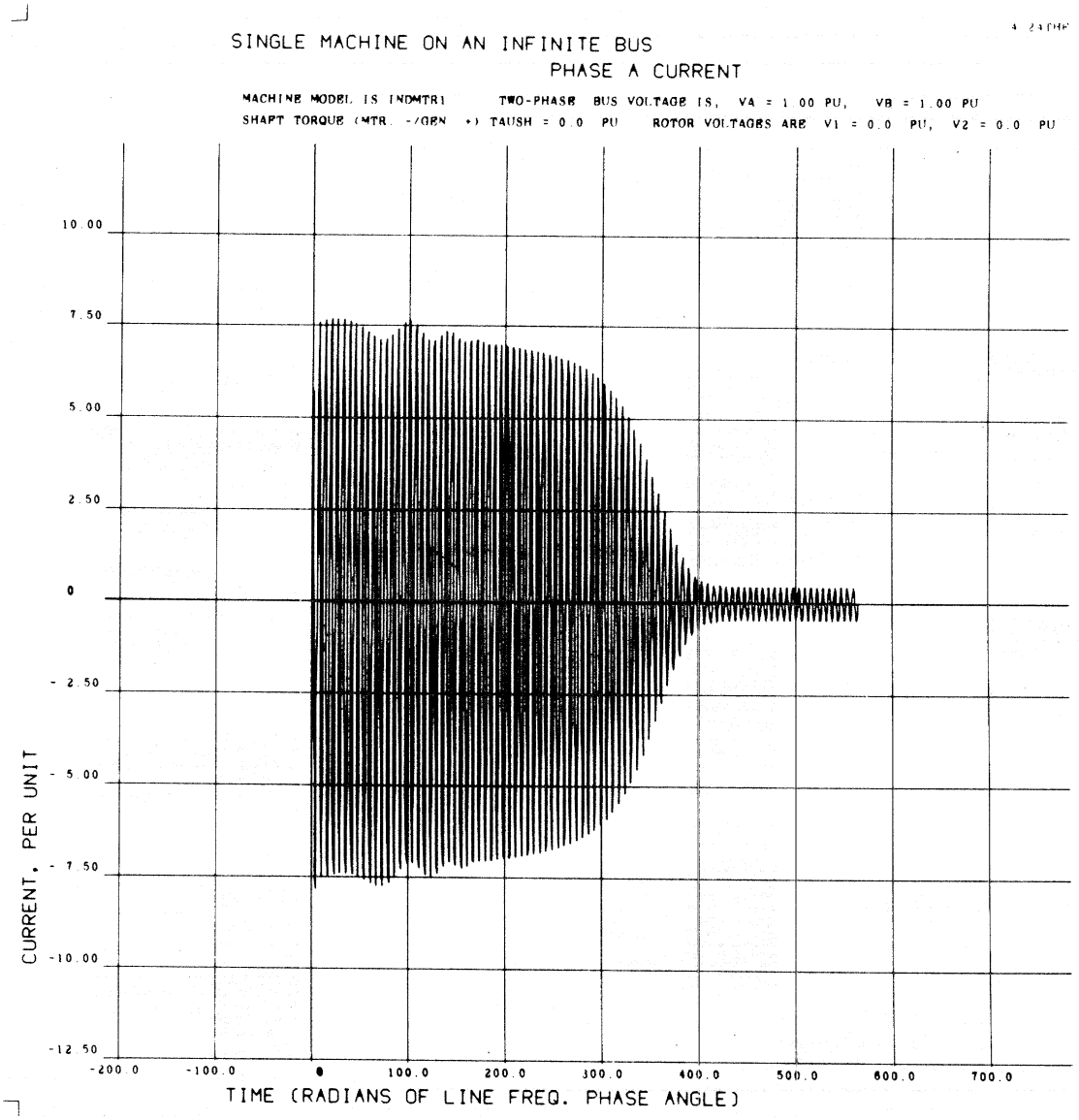
SINGLE MACHINE ON AN INFINITE BUS
PHASE A CURRENT
MACHINE MODEL IS INDMTR1 TWO-PHASE BUS VOLTAGE IS, VA = 1.00 PU, VB = 1.00 PU
SHAFT TORQUE (MTR. -/GEN +) TAUSH = 0.0 PU ROTOR VOLTAGES ARE V1 = 0.0 PU, V2 = 0.0 PU
10.00
7.50
5.00
2.50
0
- 2.50
- 5.00
- 7.50
-10.00
-12.50
CURRENT, PER UNIT
-200.0
-100.0
0
100.0
200.0
300.0
400.0
500.0
600.0
700.0
TIME (RADIANS OF LINE FREQ. PHASE ANGLE)

Fig. 3.5

below in terms of per-unit quantities: The parameters of both rotor windings and of the starting winding (stator b winding) are referred to the main winding (stator a winding).

$r_a' = .0184$ $\qquad$ $\omega\ell_a' = x_a' = .0254$

$r_b' = .0465$ $\qquad$ $\omega\ell_b' = x_b' = .0210$

$r_f' = r_g' = r_r' = .0374$ $\qquad$ $\omega\ell_f' = \omega\ell_g' = x_r' = .0193$

$x_c' = .095$ $\qquad$ $\omega L = X_m' = 0.607$

$r_c' = .0197$ $\qquad$ turns ratio: $n_b/n_a = 1.18$

$\omega_o = 377$ rad/sec $\qquad$ $\dfrac{J\omega_s^2}{2VA} = H = 1.18$

$N_p = 4$ poles

$\omega_s = \dfrac{2}{N_p}\omega_o = 1800$ rpm

$v_a' = -v_b' = 1.0$ $\qquad$ $v_f' = v_g' = 0$

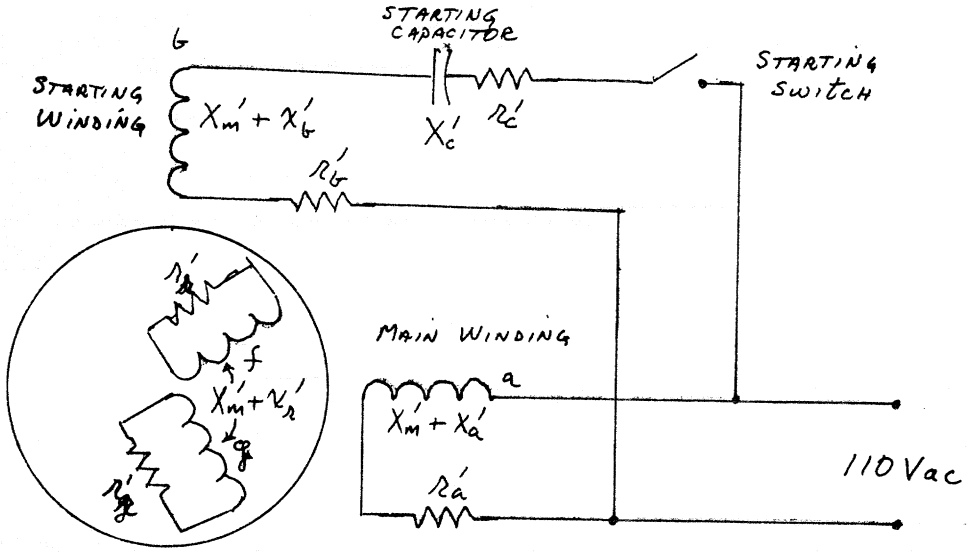

Fig. 3.6 Connection Diagram for Capacitor-Start Single-Phase Induction Motor

It should be noted that this machine is asymmetric, not because the two stator windings have an unequal number of turns, but because the referred values of their leakage inductances are unequal. Furthermore, it is noteworthy that despite the large difference between number of turns between the two stator windings (18%) the asymmetry is slight as indicated by the very small difference between the leakage reactances for the two windings.

The motor parameters listed above were taken from Ref. [8] in which an analog computer simulation of the same motor is described. Again, the results of the analog computer simulation described in [8] are used as a bench mark for validation of the results obtained in the present simulation.

The motor parameters and simulation results described in [8] are given in absolute (dimensional) form. For purposes of the present

simulation it was more convenient to convert these absolute parameters to per-unit quantities. In [8], the motor is described as having four poles, and a rating of 1/4 HP at 110 volts. Thus the per unit parameters listed earlier for this motor were obtained from the original dimensional parameters given in [8] by arbitrarily selecting the following base values: base rms voltage = 110 volts, base VA = 220 volt-amps, base speed = 1800 rpm. These same base quantities must of course also be used to convert the absolute results given in [8] to per-unit values of torque, speed and voltage for comparison with results obtained in the present simulation.

Although provisions for placing a capacitor in series with one of the windings of the machine model were not explicitly described in Chapter 2, the necessary modifications are quite simple. The inclusion of a capacitor in the simulation effectively adds an additional state variable, the capacitor voltage, to the model. For a capacitor placed in series with the stator b winding, the additional state variable equation for capacitor voltage is simply:

$$\overset{o}{v}_c = \frac{i_b}{c} \; ; \qquad i_b = i_b(\underline{\lambda}) \tag{28}$$

In addition, the b winding voltage equation is slightly modified and is now given by:

$$\overset{o}{\lambda}_b = v_b - i_b(r_b + r_c) - v_c \tag{29}$$

r_c is the resistance of the capacitor, v_c is the capacitor voltage, and v_b is the terminal voltage applied across the series combination of the capacitor with the stator b winding.

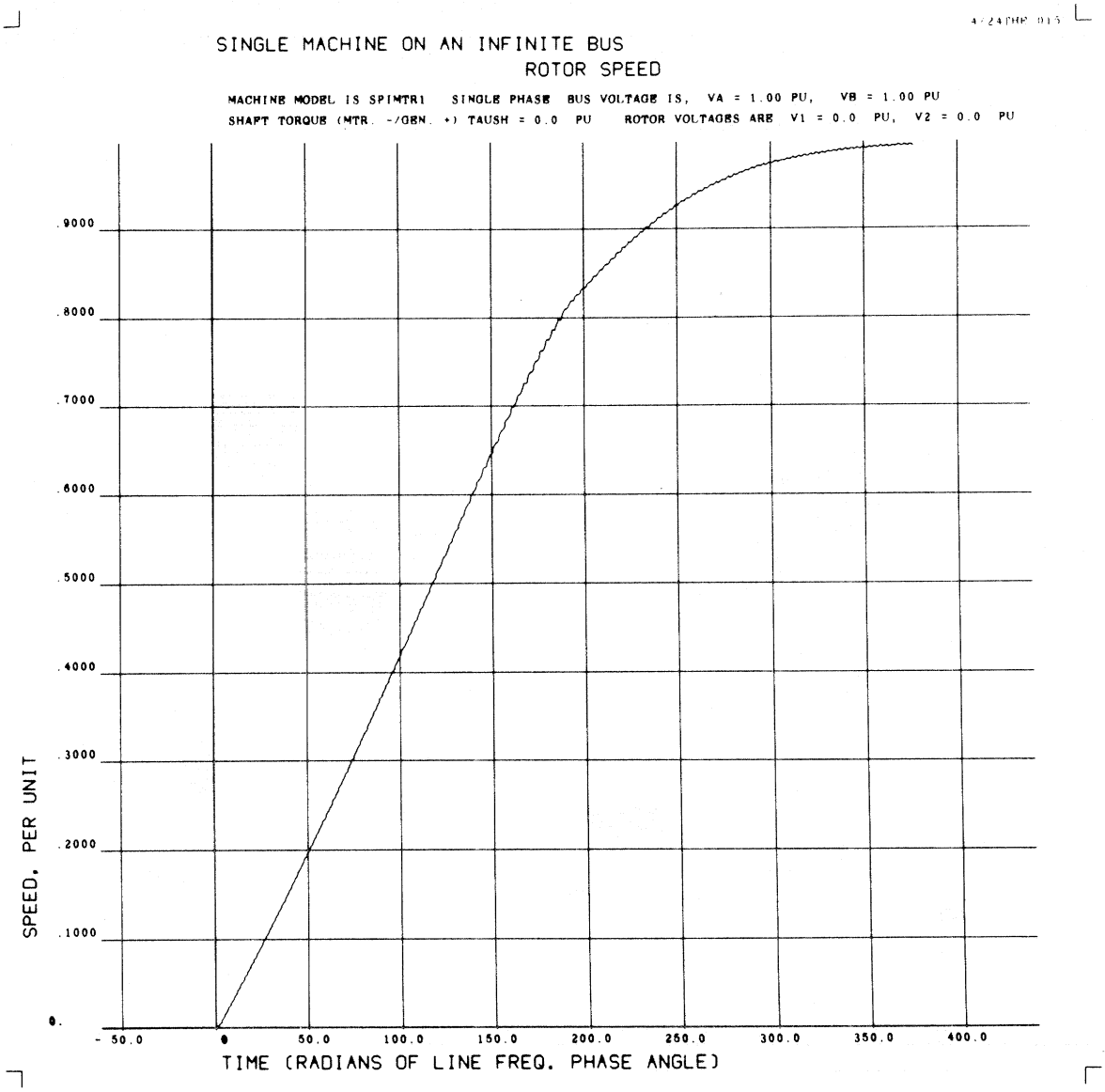
SINGLE MACHINE ON AN INFINITE BUS
ROTOR SPEED
MACHINE MODEL IS SPIMTR1 SINGLE PHASE BUS VOLTAGE IS, VA = 1.00 PU, VB = 1.00 PU
SHAFT TORQUE (MTR. -/GEN. +) TAUSH = 0.0 PU ROTOR VOLTAGES ARE V1 = 0.0 PU, V2 = 0.0 PU
.9000
.8000
.7000
.6000
.5000
.4000
.3000
.2000
.1000
0.
SPEED, PER UNIT
- 50.0
0
50.0
100.0
150.0
200.0
250.0
300.0
350.0
400.0
TIME (RADIANS OF LINE FREQ. PHASE ANGLE)

Fig. 3.7

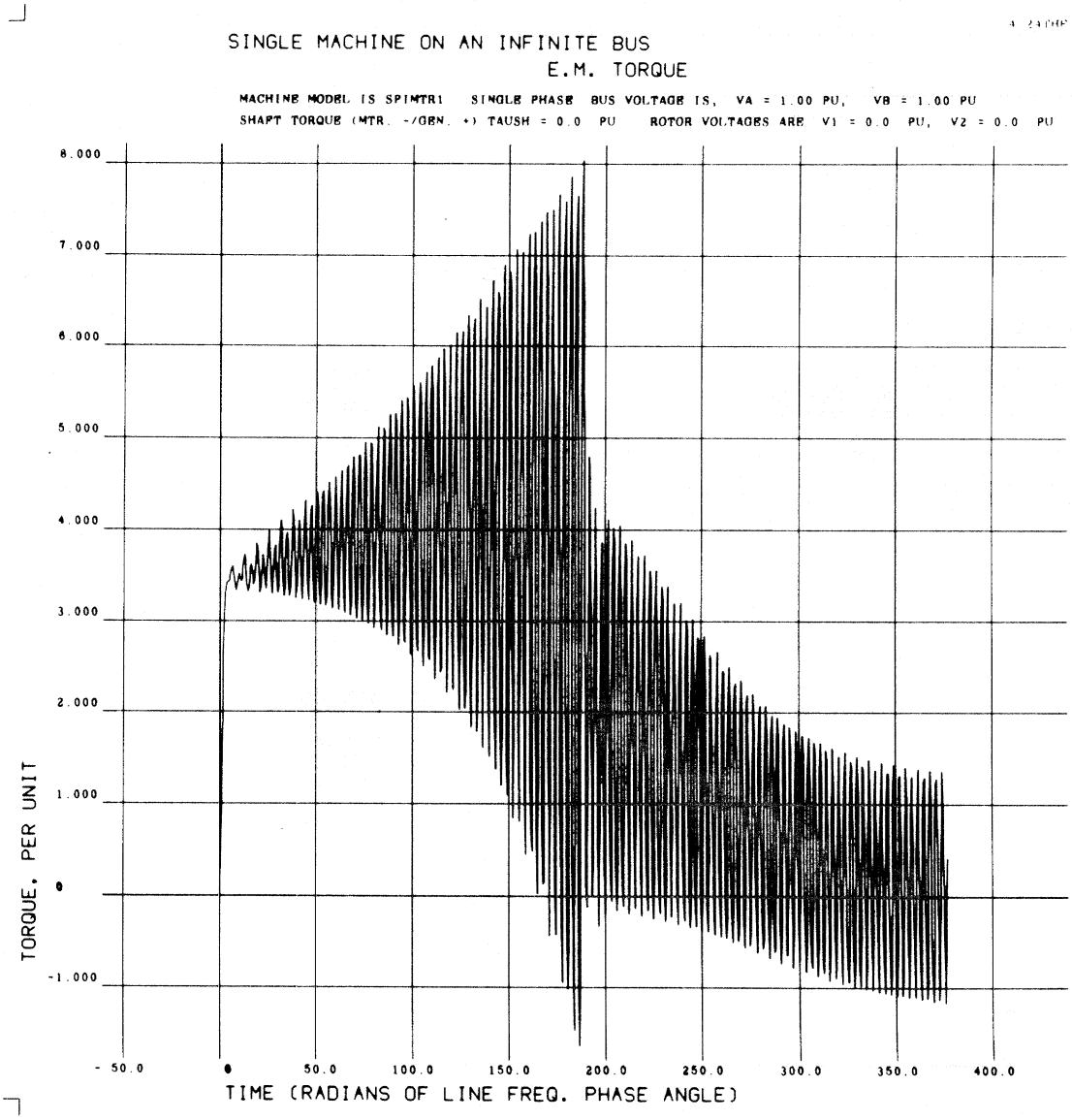
SINGLE MACHINE ON AN INFINITE BUS
E.M. TORQUE
MACHINE MODEL IS SPIMTR1 SINGLE PHASE BUS VOLTAGE IS, VA = 1.00 PU, VB = 1.00 PU
SHAFT TORQUE (MTR. -/GEN. +) TAUSH = 0.0 PU ROTOR VOLTAGES ARE V1 = 0.0 PU, V2 = 0.0 PU
8.000
7.000
6.000
5.000
4.000
3.000
2.000
1.000
0
-1.000
TORQUE, PER UNIT
- 50.0
0
50.0
100.0
150.0
200.0
250.0
300.0
350.0
400.0
TIME (RADIANS OF LINE FREQ. PHASE ANGLE)

Fig. 3.8

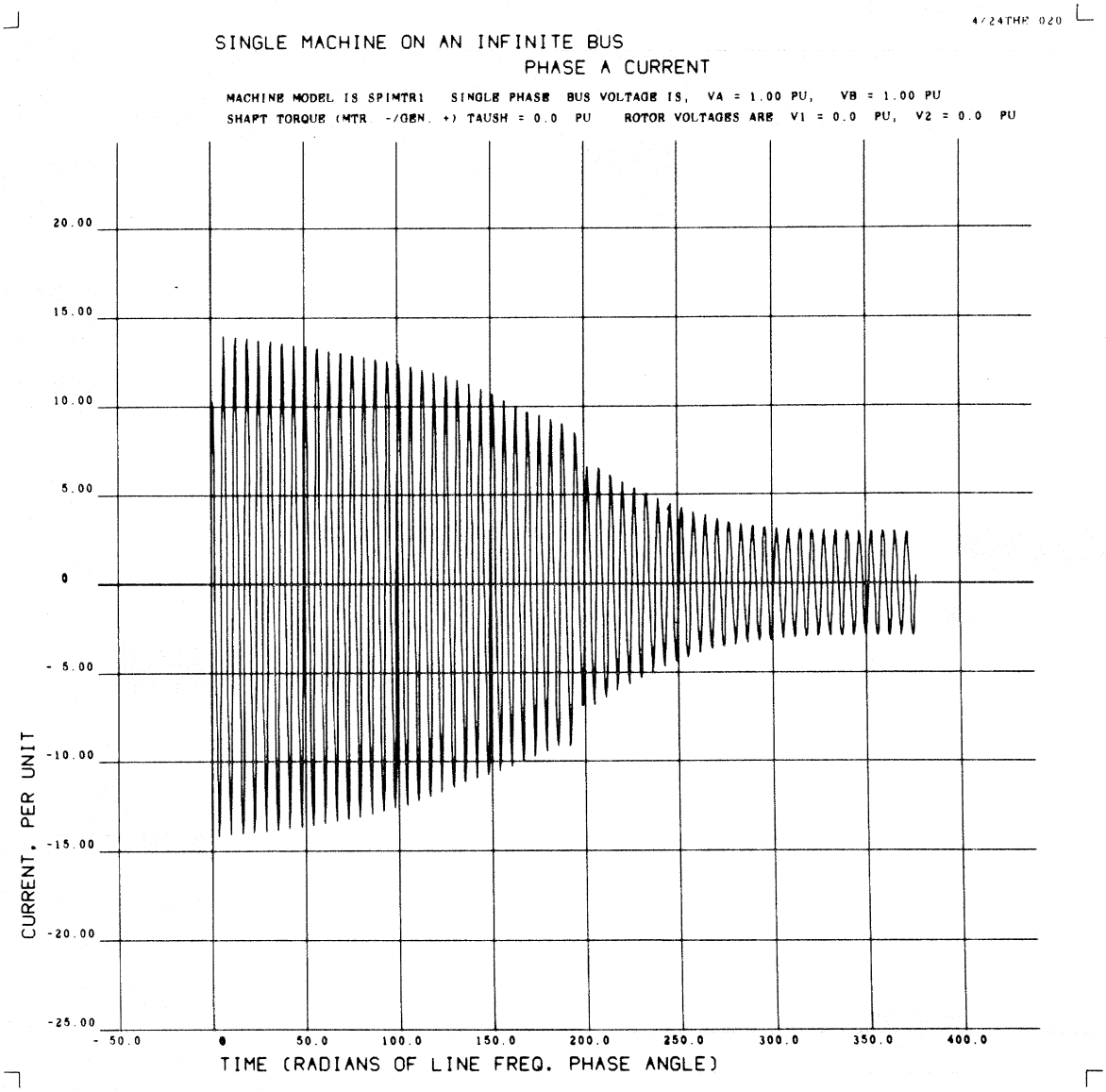
4/24THP 020
SINGLE MACHINE ON AN INFINITE BUS
PHASE A CURRENT
MACHINE MODEL IS SPIMTR1 SINGLE PHASE BUS VOLTAGE IS, VA = 1.00 PU, VB = 1.00 PU
SHAFT TORQUE (MTR -/GEN. +) TAUSH = 0.0 PU ROTOR VOLTAGES ARE V1 = 0.0 PU, V2 = 0.0 PU
20.00
15.00
10.00
5.00
0
- 5.00
-10.00
-15.00
-20.00
-25.00
CURRENT, PER UNIT
- 50.0
0
50.0
100.0
150.0
200.0
250.0
300.0
350.0
400.0
TIME (RADIANS OF LINE FREQ. PHASE ANGLE)

Fig. 3.9

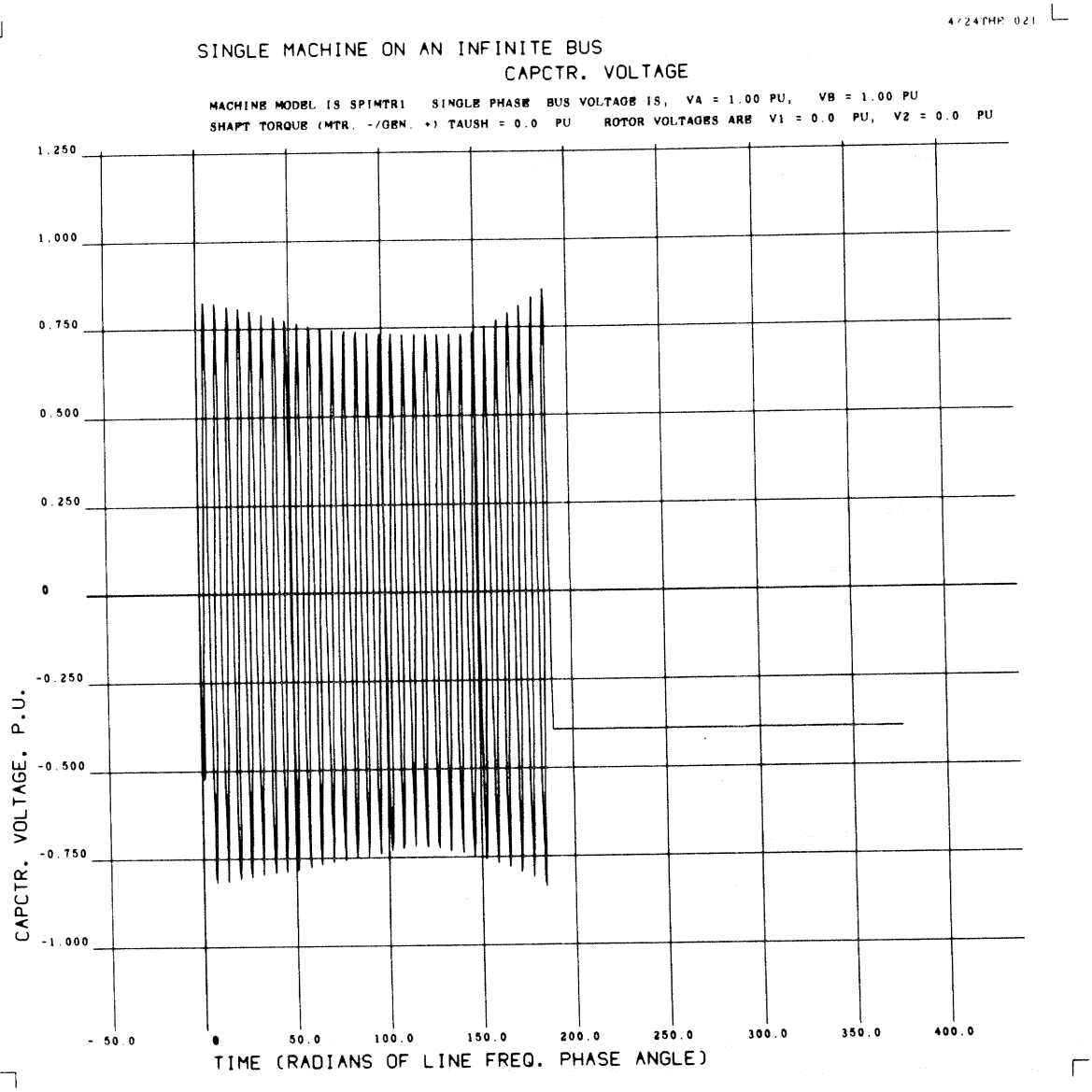
4/24THP 021
SINGLE MACHINE ON AN INFINITE BUS
CAPCTR. VOLTAGE
MACHINE MODEL IS SPIMTR1 SINGLE PHASE BUS VOLTAGE IS, VA = 1.00 PU, VB = 1.00 PU
SHAFT TORQUE (MTR. -/GEN. +) TAUSH = 0.0 PU ROTOR VOLTAGES ARE V1 = 0.0 PU, V2 = 0.0 PU
1.250
1.000
0.750
0.500
0.250
0
-0.250
-0.500
-0.750
-1.000
CAPCTR. VOLTAGE, P.U.
- 50.0
0
50.0
100.0
150.0
200.0
250.0
300.0
350.0
400.0
TIME (RADIANS OF LINE FREQ. PHASE ANGLE)

Fig. 3.10

The results obtained from the present simulation of motor performance during start-up and free acceleration to synchronous speed are described by time histories of rotor speed, torque, main winding current and capacitor voltage illustrated in Figs. 3.7 through 3.10. The time scale in these figures is again given in terms of radians of line frequency phase but this may be easily converted to seconds using the conversion factor of 377 radians/sec. In the analog computer simulation described in [8], the auxiliary starting winding, with which the capacitor is in series, was automatically disconnected when the rotor speed had reached 75% of the synchronous maximum. Because of the nature of the computer program used for the present simulation, it was inconvenient to disconnect the winding at precisely this value of rotor speed. Consequently, in the present simulation the starting windings were not disconnected until the rotor had reached 81% of synchronous speed. Notwithstanding this difference between the two simulations, comparison of the time histories for torque, speed, and capacitor voltages with the corresponding results given in [8] indicates excellent agreement. When converting the results for capacitor voltage given in [8] to per-unit for comparison with those obtained in the present simulation, it should be noted that the instantaneous values of capacitor voltage given in [8] should be divided by the peak value of base voltage, $110\sqrt{2}$, rather than just the rms value.

3.4 Electromechanical Oscillations of a Synchronous Motor for Sudden Load Changes

The parameters of the synchronous machine simulated in this example are the same as those of the symmetric induction machine described in section 3.2 except that now the rotor g winding is open circuited, and

the rotor f winding, in lieu of being short-circuited, is excited by a constant DC voltage source. The stator a and b windings are again connected to a balanced two-phase infinite bus whose voltage is 1.0 pu. The resultant machine configuration represents a model of a balanced two-phase synchronous machine having a single field winding and no damper windings. It should be noted that in order to represent a conventional round-rotor synchronous machine having a single field winding and no damper windings in terms of the four-winding machine model of this thesis, it is necessary that the rotor g winding of the model be open circuited in accordance with the methods given in Appendix B. If the g winding were left closed (short-circuited), that winding would appear as a quadrature axis damper winding in the simulation. Although the steady state performance of the machine would be the same in either case, the inclusion of the effects of a quadrature axis damper winding through closure of the g winding in the simulation, would significantly alter the dynamic performance of the resultant model.

The excitation voltage applied to the f winding is held constant at a value such that when the machine operates as a motor delivering rated power, the resultant value of power factor will be approximately unity. At this level of excitation, the machine will become over excited and deliver reactive power to the bus when the mechanical load applied to the shaft is reduced to a value less than 1.0 pu.

The simulation results illustrated in Figs. 3.11 through 3.20 describe the transient performance of the machine model in response to step changes in the mechanical load torque applied to the rotor shaft. Figure 3.11 through 3.15 describe the machine response for a sudden increase in load torque from 0.5 to 1.0 pu. The response of the machine is rather heavily damped. Figures 3.16 through 3.20 describe the machine

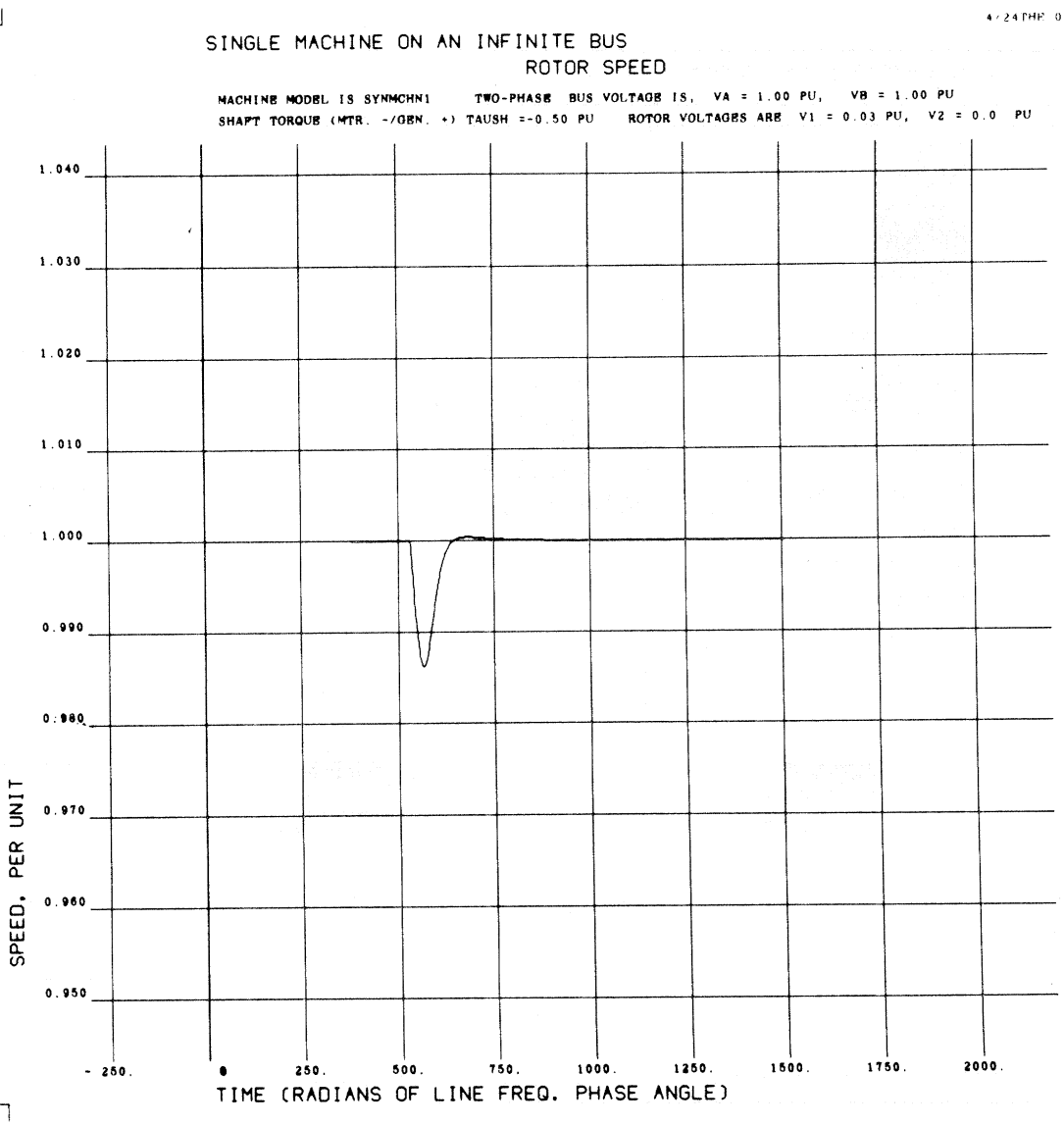
SINGLE MACHINE ON AN INFINITE BUS
ROTOR SPEED
MACHINE MODEL IS SYNMCHN1 TWO-PHASE BUS VOLTAGE IS, VA = 1.00 PU, VB = 1.00 PU
SHAFT TORQUE (MTR. -/GEN. +) TAUSH =-0.50 PU ROTOR VOLTAGES ARE V1 = 0.03 PU, V2 = 0.0 PU
1.040
1.030
1.020
1.010
1.000
0.990
0.980
0.970
0.960
0.950
SPEED, PER UNIT
- 250.
0
250.
500.
750.
1000.
1250.
1500.
1750.
2000.
TIME (RADIANS OF LINE FREQ. PHASE ANGLE)

Fig. 3.11

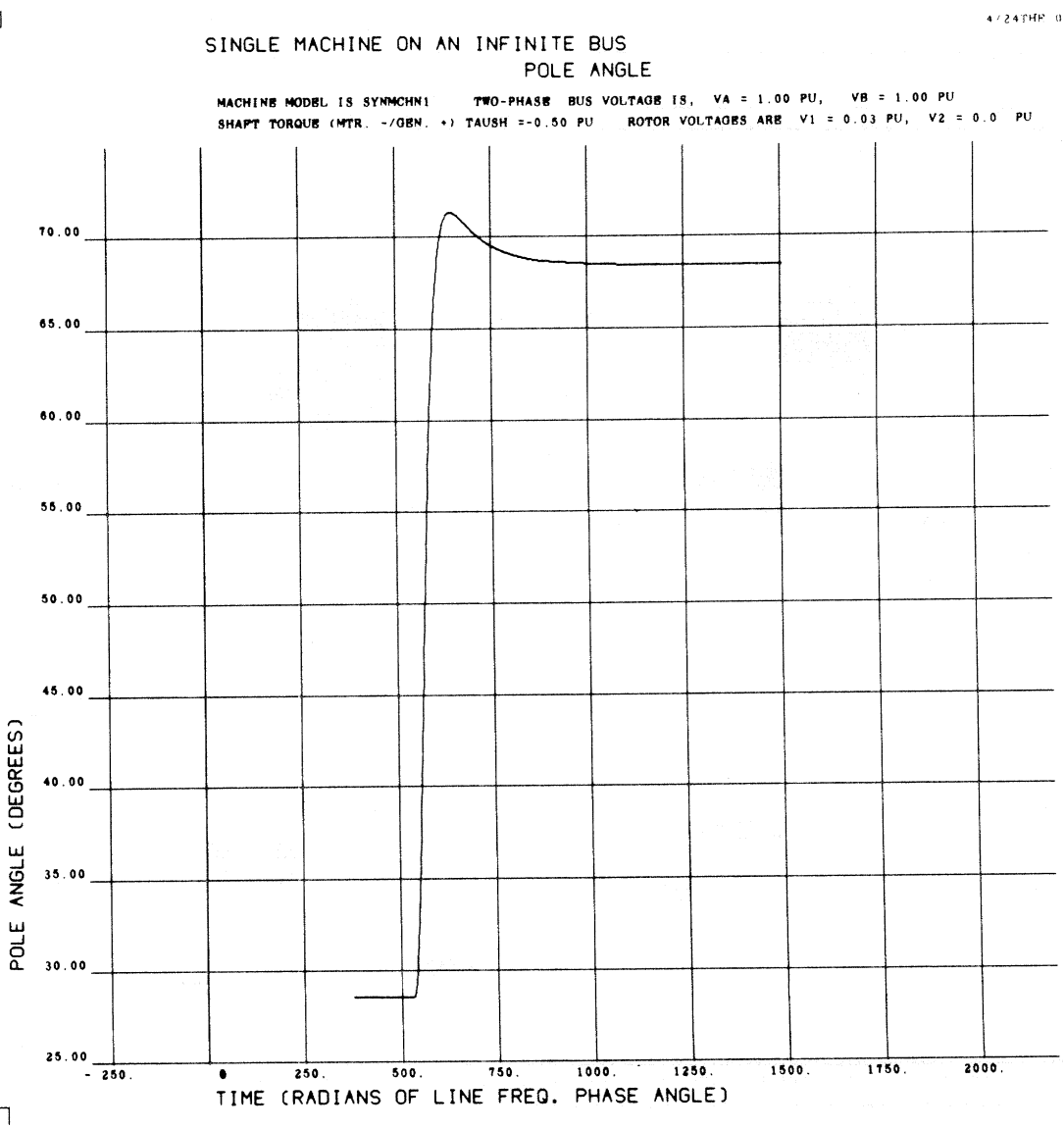
4/24THP 007
SINGLE MACHINE ON AN INFINITE BUS
POLE ANGLE
MACHINE MODEL IS SYNMCHN1 TWO-PHASE BUS VOLTAGE IS, VA = 1.00 PU, VB = 1.00 PU
SHAFT TORQUE (MTR. -/GEN. +) TAUSH =-0.50 PU ROTOR VOLTAGES ARE V1 = 0.03 PU, V2 = 0.0 PU
70.00
65.00
60.00
55.00
50.00
45.00
40.00
35.00
30.00
25.00
POLE ANGLE (DEGREES)
- 250.
0
250.
500.
750.
1000.
1250.
1500.
1750.
2000.
TIME (RADIANS OF LINE FREQ. PHASE ANGLE)

Fig. 3.12

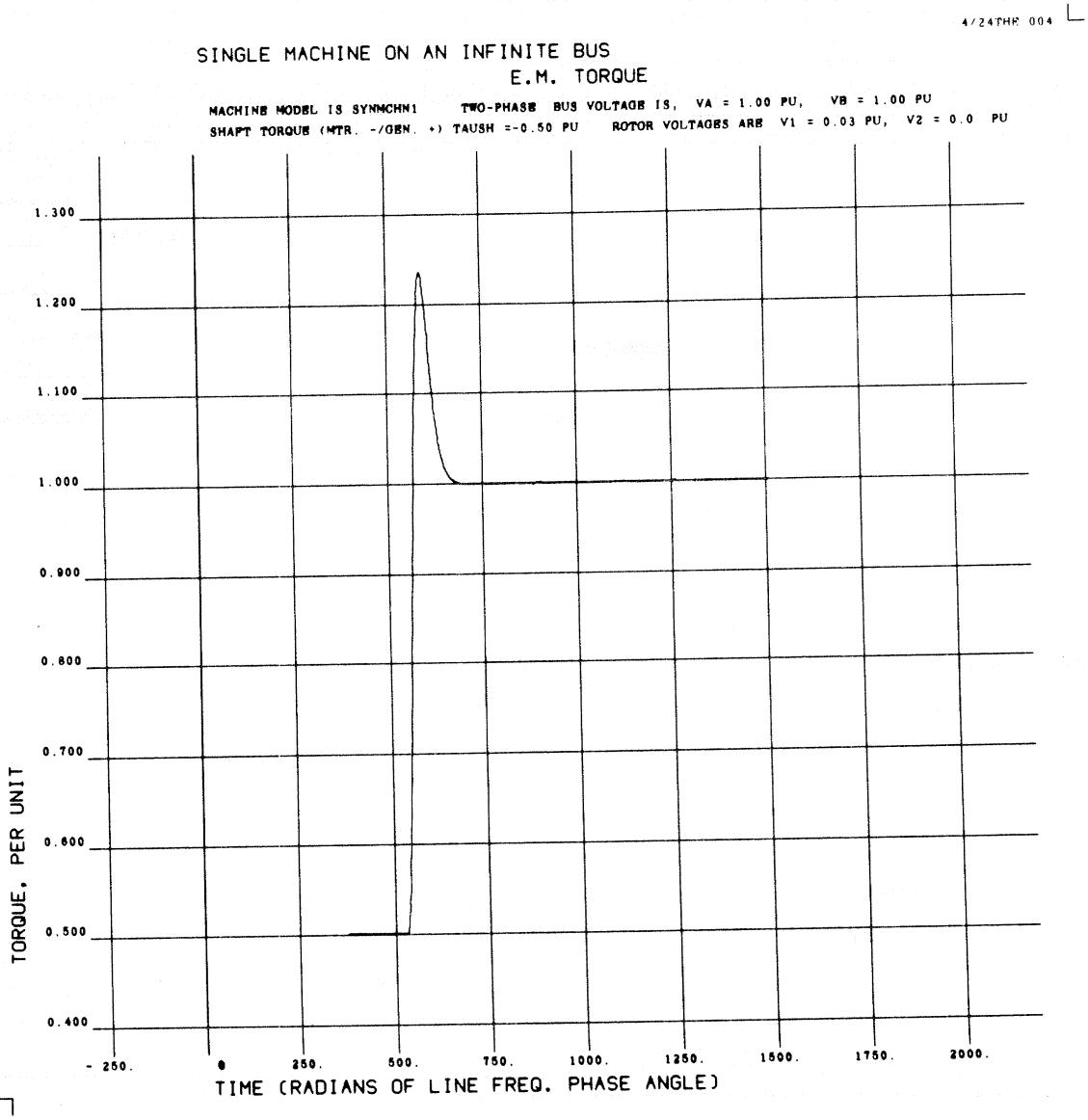
4/24THR 004
SINGLE MACHINE ON AN INFINITE BUS
E.M. TORQUE
MACHINE MODEL IS SYNMCHN1 TWO-PHASE BUS VOLTAGE IS, VA = 1.00 PU, VB = 1.00 PU
SHAFT TORQUE (MTR. -/GEN. +) TAUSH =-0.50 PU ROTOR VOLTAGES ARE V1 = 0.03 PU, V2 = 0.0 PU
1.300
1.200
1.100
1.000
0.900
0.800
0.700
0.600
0.500
0.400
TORQUE, PER UNIT
- 250.
0
250.
500.
750.
1000.
1250.
1500.
1750.
2000.
TIME (RADIANS OF LINE FREQ. PHASE ANGLE)

Fig. 3.13

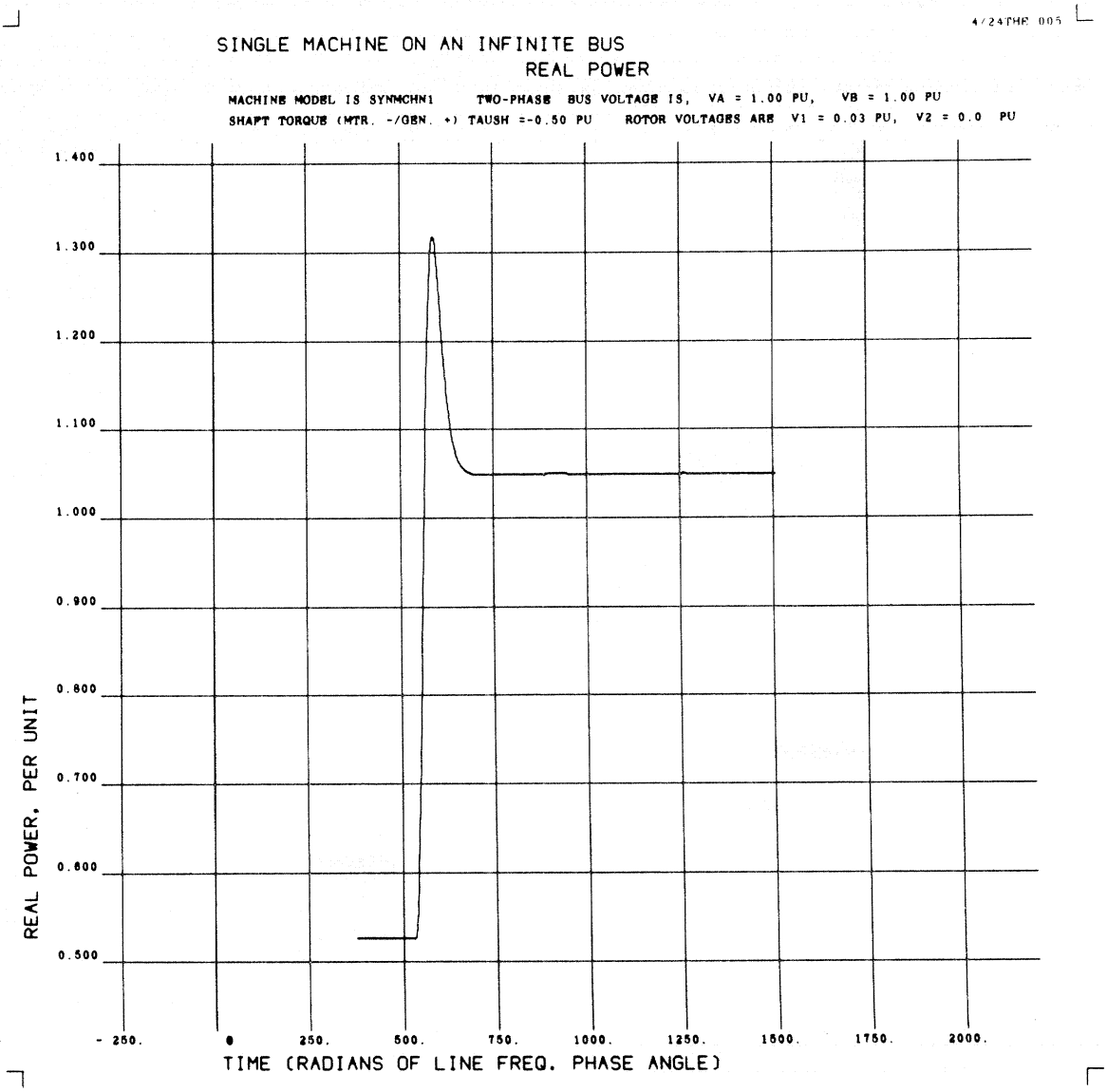
4/24THE 005
SINGLE MACHINE ON AN INFINITE BUS
REAL POWER
MACHINE MODEL IS SYNMCHN1 TWO-PHASE BUS VOLTAGE IS, VA = 1.00 PU, VB = 1.00 PU
SHAFT TORQUE (MTR. -/GEN. +) TAUSH =-0.50 PU ROTOR VOLTAGES ARE V1 = 0.03 PU, V2 = 0.0 PU
1.400
1.300
1.200
1.100
1.000
0.900
0.800
0.700
0.600
0.500
REAL POWER, PER UNIT
- 250.
0
250.
500.
750.
1000.
1250.
1500.
1750.
2000.
TIME (RADIANS OF LINE FREQ. PHASE ANGLE)

Fig. 3.14

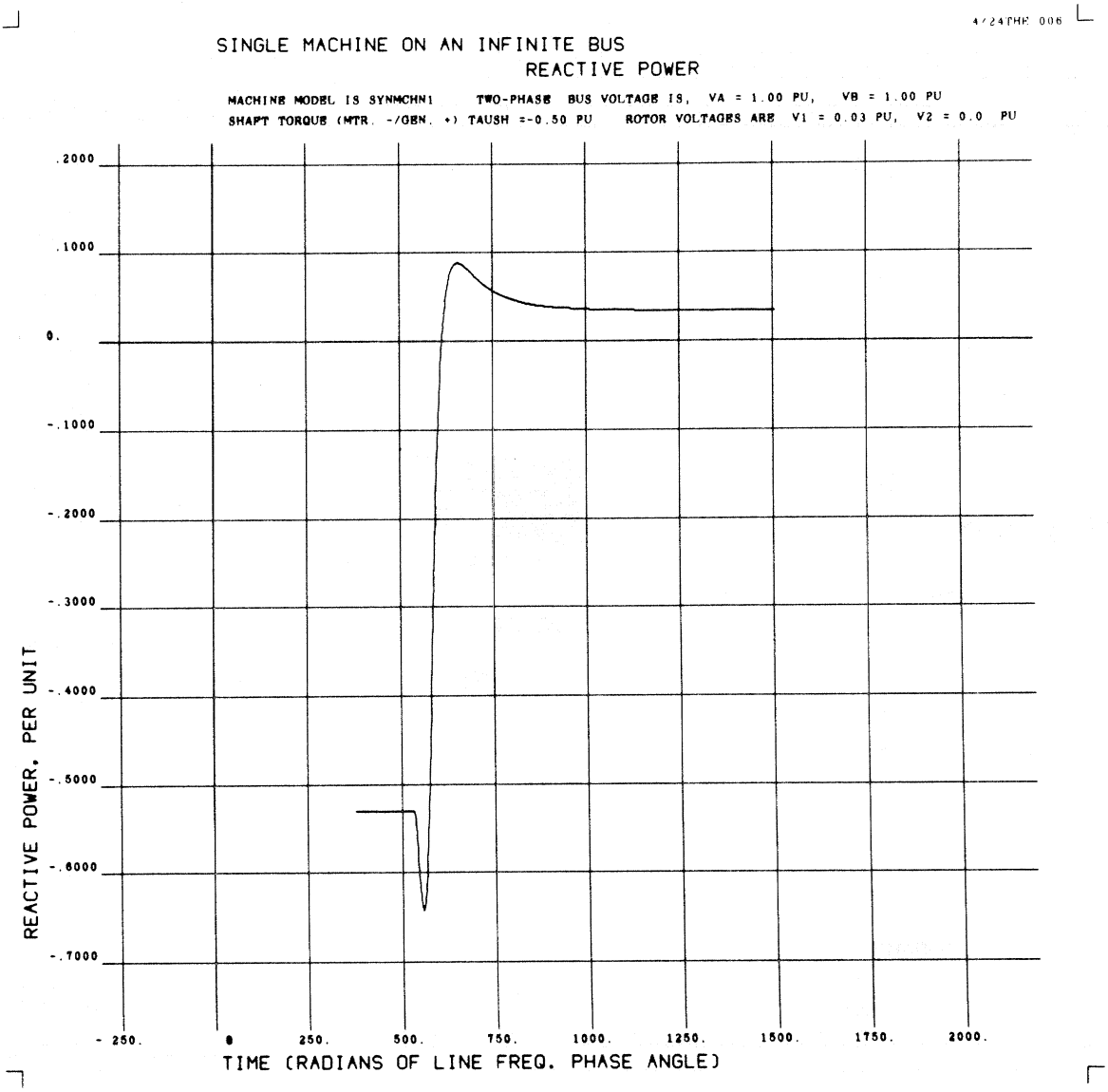
4/24THE 006
SINGLE MACHINE ON AN INFINITE BUS
REACTIVE POWER
MACHINE MODEL IS SYNMCHN1 TWO-PHASE BUS VOLTAGE IS, VA = 1.00 PU, VB = 1.00 PU
SHAFT TORQUE (MTR. -/GEN. +) TAUSH =-0.50 PU ROTOR VOLTAGES ARE V1 = 0.03 PU, V2 = 0.0 PU
.2000
.1000
0.
-.1000
-.2000
-.3000
-.4000
-.5000
-.6000
-.7000
REACTIVE POWER, PER UNIT
- 250.
0
250.
500.
750.
1000.
1250.
1500.
1750.
2000.
TIME (RADIANS OF LINE FREQ. PHASE ANGLE)

Fig. 3.15

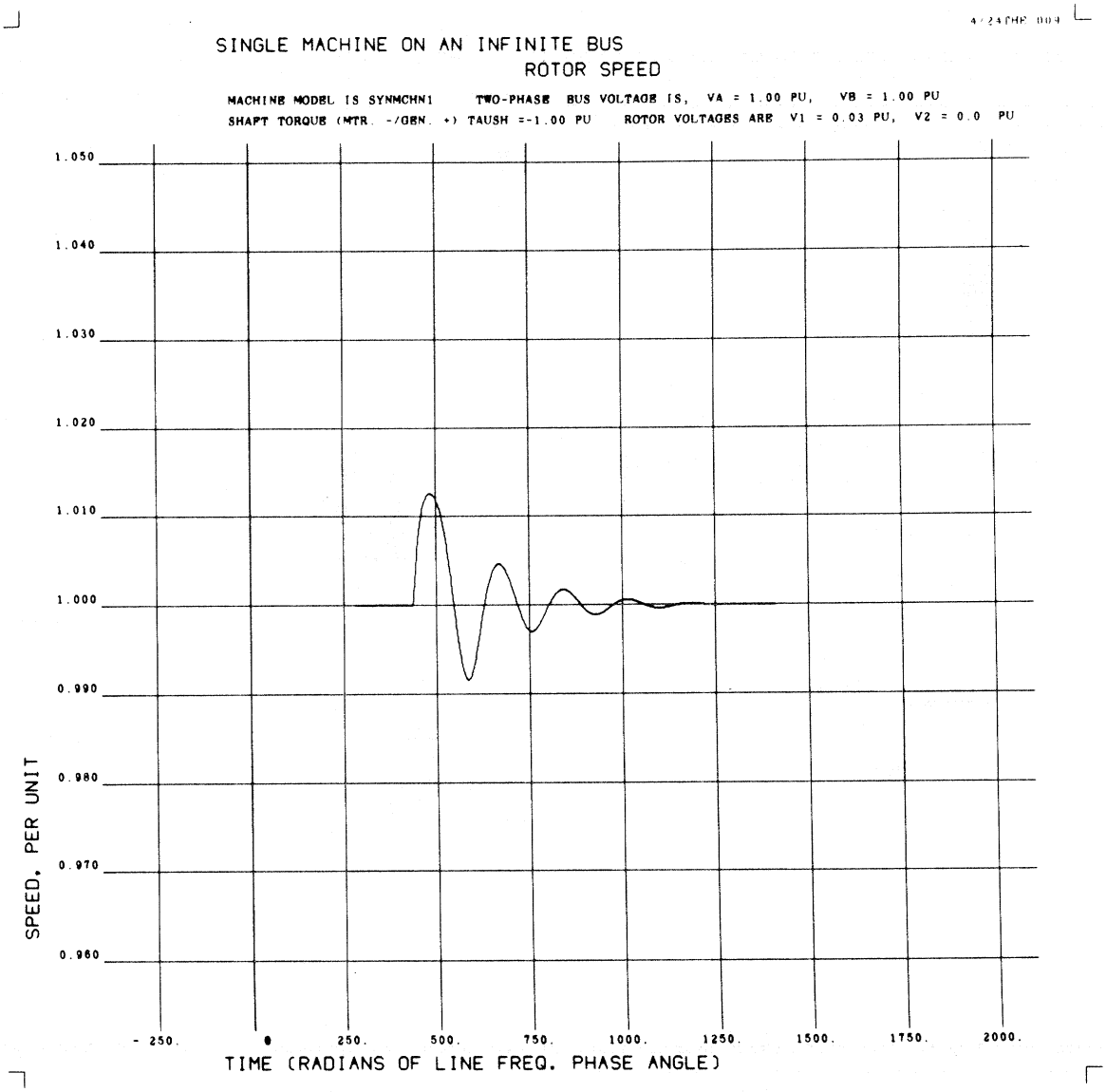
SINGLE MACHINE ON AN INFINITE BUS
ROTOR SPEED
MACHINE MODEL IS SYNMCHN1 TWO-PHASE BUS VOLTAGE IS, VA = 1.00 PU, VB = 1.00 PU
SHAFT TORQUE (MTR. -/GEN. +) TAUSH =-1.00 PU ROTOR VOLTAGES ARE V1 = 0.03 PU, V2 = 0.0 PU
1.050
1.040
1.030
1.020
1.010
1.000
0.990
0.980
0.970
0.960
SPEED, PER UNIT
- 250.
0
250.
500.
750.
1000.
1250.
1500.
1750.
2000.
TIME (RADIANS OF LINE FREQ. PHASE ANGLE)

Fig. 3.16

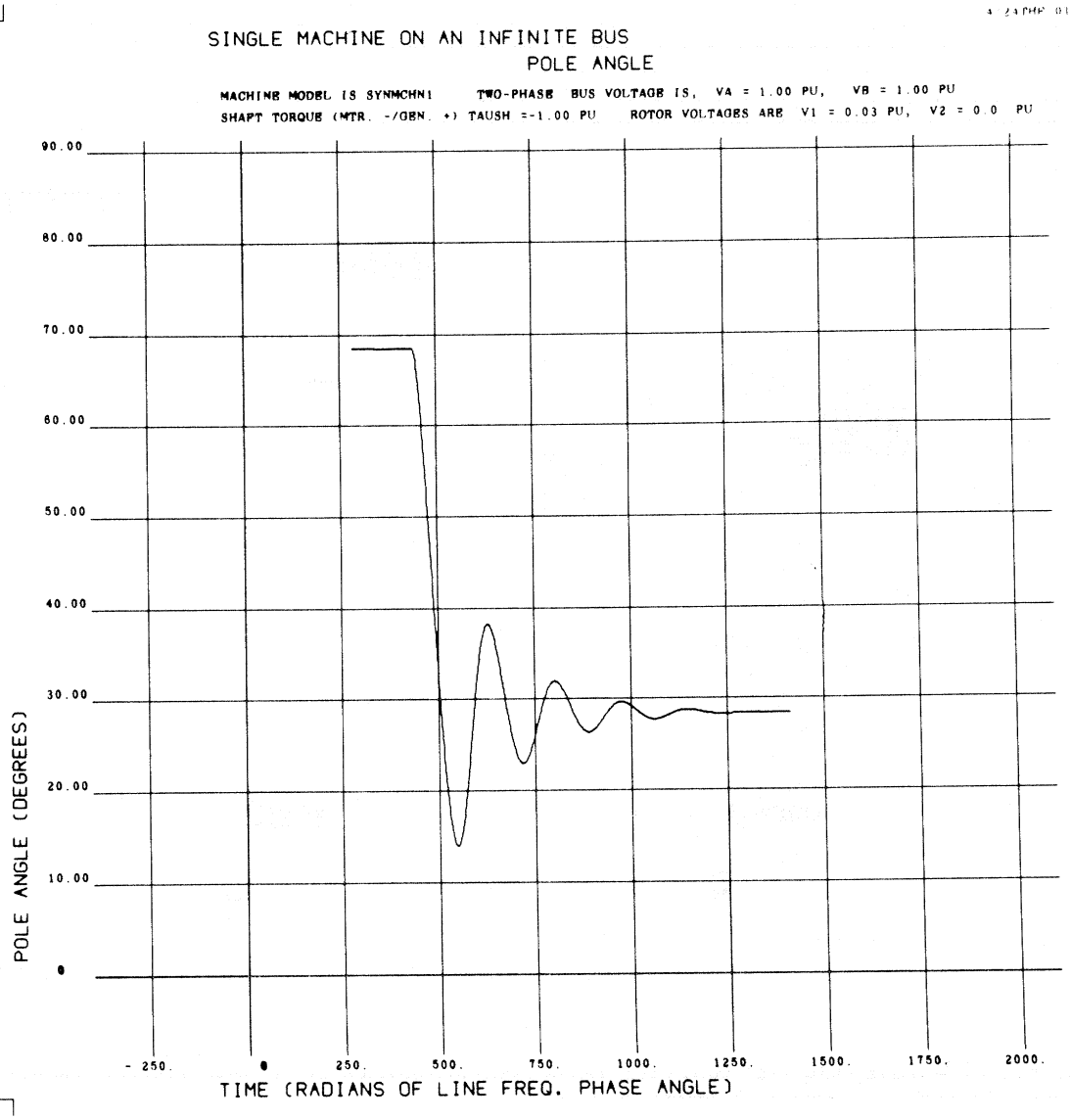
SINGLE MACHINE ON AN INFINITE BUS
POLE ANGLE
MACHINE MODEL IS SYNMCHN1 TWO-PHASE BUS VOLTAGE IS, VA = 1.00 PU, VB = 1.00 PU
SHAFT TORQUE (MTR. -/GEN. +) TAUSH =-1.00 PU ROTOR VOLTAGES ARE V1 = 0.03 PU, V2 = 0.0 PU
90.00
80.00
70.00
60.00
50.00
40.00
30.00
20.00
10.00
0
POLE ANGLE (DEGREES)
- 250.
0
250.
500.
750.
1000.
1250.
1500.
1750.
2000.
TIME (RADIANS OF LINE FREQ. PHASE ANGLE)

Fig. 3.17

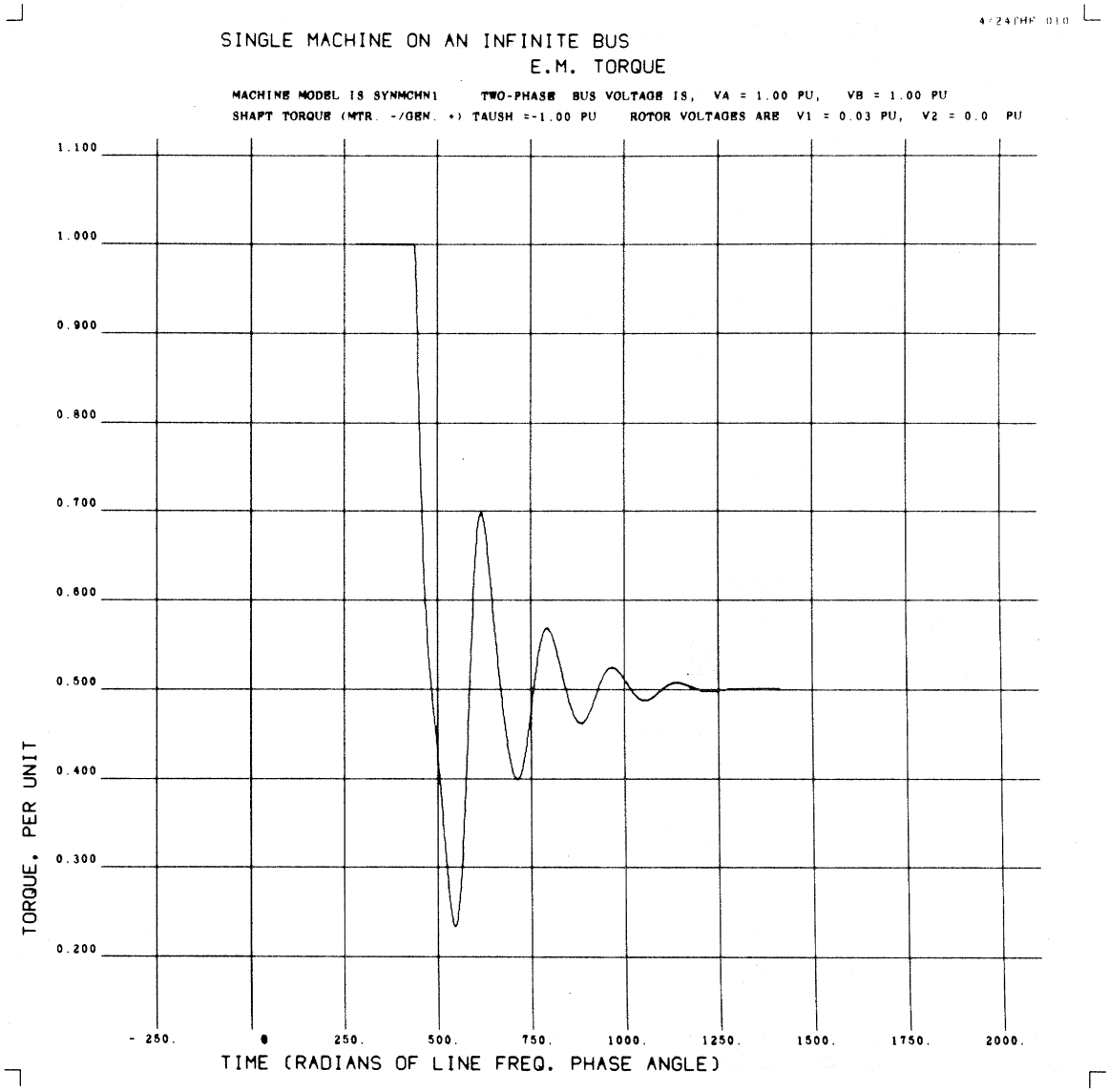
SINGLE MACHINE ON AN INFINITE BUS
E.M. TORQUE
MACHINE MODEL IS SYNMCHN1 TWO-PHASE BUS VOLTAGE IS, VA = 1.00 PU, VB = 1.00 PU
SHAFT TORQUE (MTR. -/GEN. +) TAUSH =-1.00 PU ROTOR VOLTAGES ARE V1 = 0.03 PU, V2 = 0.0 PU
1.100
1.000
0.900
0.800
0.700
0.600
0.500
0.400
0.300
0.200
TORQUE, PER UNIT
- 250.
0
250.
500.
750.
1000.
1250.
1500.
1750.
2000.
TIME (RADIANS OF LINE FREQ. PHASE ANGLE)

Fig. 3.18

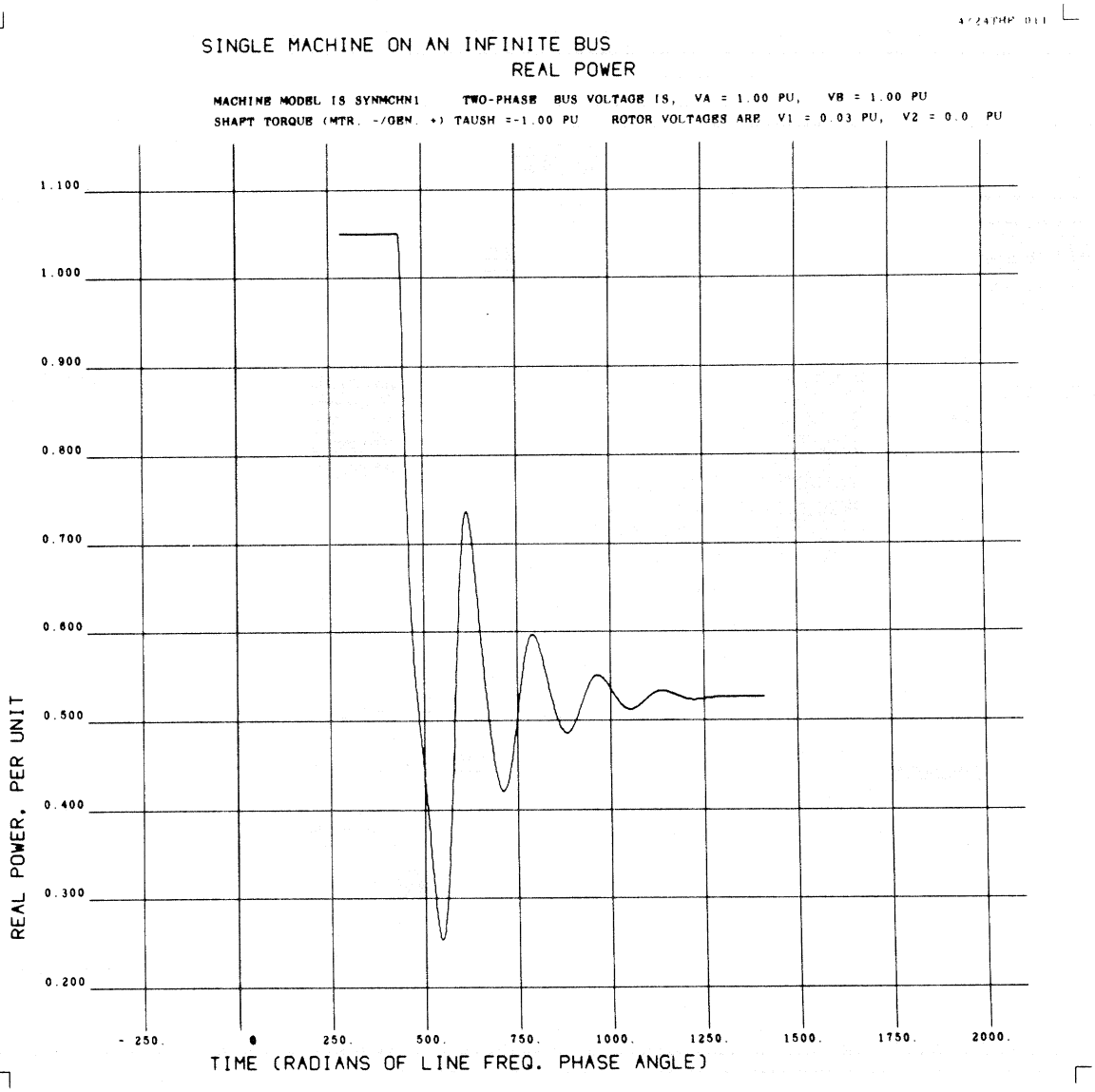
SINGLE MACHINE ON AN INFINITE BUS
REAL POWER
MACHINE MODEL IS SYNMCHN1 TWO-PHASE BUS VOLTAGE IS, VA = 1.00 PU, VB = 1.00 PU
SHAFT TORQUE (MTR. -/GEN. +) TAUSH =-1.00 PU ROTOR VOLTAGES ARE V1 = 0.03 PU, V2 = 0.0 PU
1.100
1.000
0.900
0.800
0.700
0.600
0.500
0.400
0.300
0.200
REAL POWER, PER UNIT
- 250.
0
250.
500.
750.
1000.
1250.
1500.
1750.
2000.
TIME (RADIANS OF LINE FREQ. PHASE ANGLE)

Fig. 3.19

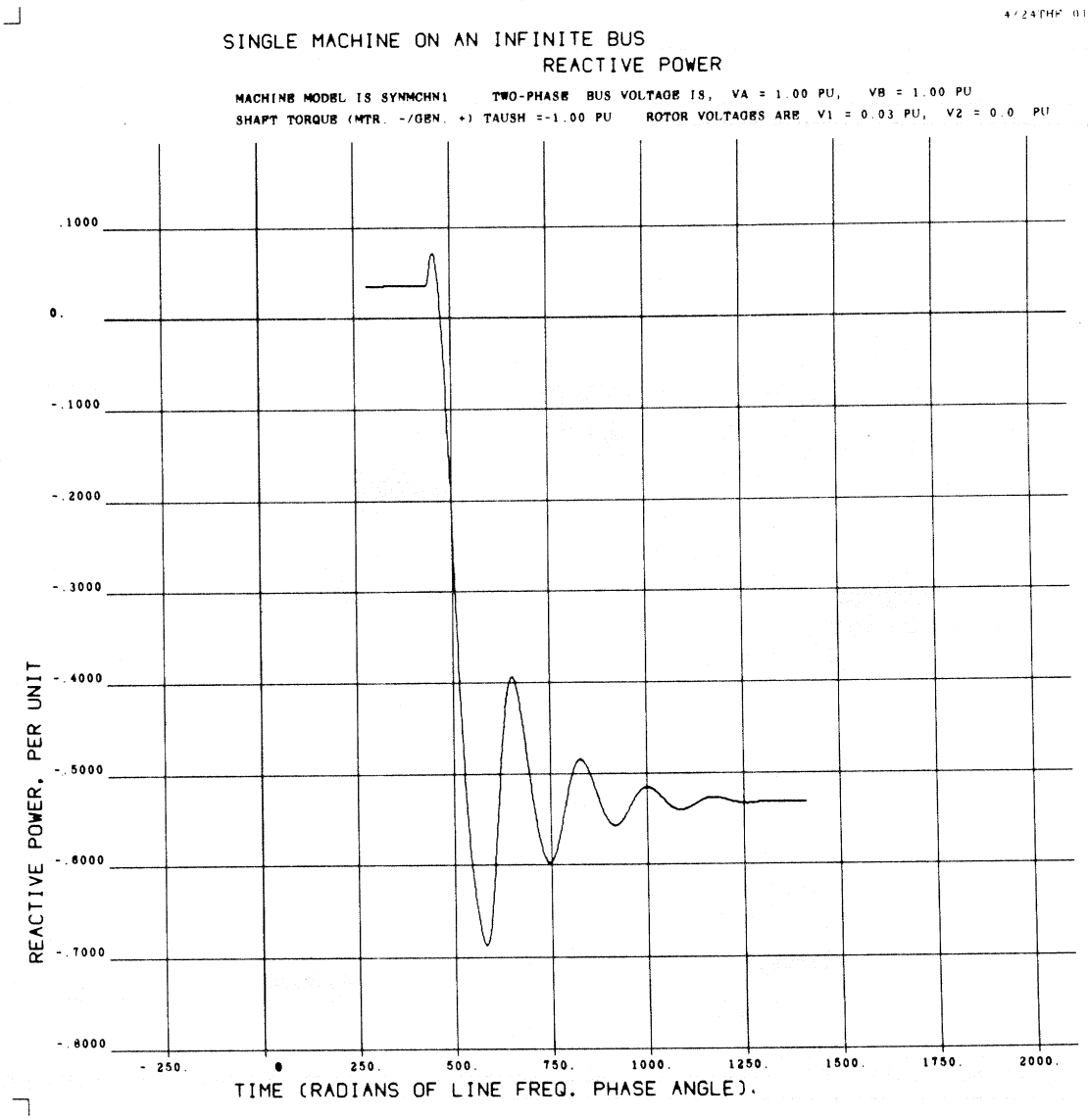
SINGLE MACHINE ON AN INFINITE BUS
REACTIVE POWER
MACHINE MODEL IS SYNMCHN1 TWO-PHASE BUS VOLTAGE IS, VA = 1.00 PU, VB = 1.00 PU
SHAFT TORQUE (MTR. -/GEN. +) TAUSH =-1.00 PU ROTOR VOLTAGES ARE V1 = 0.03 PU, V2 = 0.0 PU
.1000
0.
-.1000
-.2000
-.3000
-.4000
-.5000
-.6000
-.7000
-.8000
REACTIVE POWER, PER UNIT
- 250.
0
250.
500.
750.
1000.
1250.
1500.
1750.
2000.
TIME (RADIANS OF LINE FREQ. PHASE ANGLE).

Fig. 3.20

response for a corresponding decrease in load torque from 1.0 to 0.5 pu. The response of the machine is now much more lightly damped than during the previous transient, as evidenced by the mechanical oscillations of the rotor about synchronous speed. The steady state operating conditions (following decay of the transients) illustrated in Figs. 3.11 through 3.20 are easily verified by comparison against results obtained from a standard phasor analysis of the machine equations at the corresponding steady state operating points. It should be noted that the magnitude of the real electrical power drawn by the machines, as given in Figs. 3.14 and 3.19, is always slightly larger, on a per-unit basis, than the electromagnetic torque delivered by the machine to its rotor structure. The difference between these two values is attributable to the I^2R losses in the stator windings.

The simulation results for the transient portion of the machine response may be independently verified by comparing observed values of rotor swing frequency and damping ratio, computed from the response data illustrated in Figs. 3.16 through 3.20, with corresponding values of these parameters obtained from a linearized analysis of the machine dynamical equations for small disturbances which is described in Appendix D. Theoretical values of rotor swing frequency and damping ratio are plotted in Figs. D3, D4 of Appendix D as functions of the following derived machine parameters: (1) the dimensionless product of the undamped natural swing frequency ω_n, and the machines direct axis short circuit time constant τ_d', (2) the machine damping parameter ξ_o.

The relations for these derived parameters in terms of the per-unit values of the basic machine parameters are given below:

Short circuit field time constant:

$$\tau_d' = \frac{(X_m + x_a)(X_m + x_f) - x_m^2}{\omega_o (X_m + x_a) r_f} \tag{30a}$$

Undamped natural swing frequency:

$$\omega_n = \sqrt{\frac{e_f \, v \, \omega_o}{2H \, X_m} \cos \delta_o} \tag{30b}$$

Damping Parameter

$$\xi_o = \left(\frac{X_m}{X_m + x_a}\right)^2 \left(\frac{v^2 \sin^2 \delta_o}{4H\omega_n r_f}\right) \tag{30c}$$

All variables in Eq. (30) above are in per unit, except the bus frequency ω_o and the machine pole angle δ_o.

The transient response components of the simulation results described in Figs. 3.11 through 3.20 are now compared against the theoretical results given in Figs. D3 and D4 of Appendix D. First of all, the fact that the transient about the rated value of torque (τ = 1.0; $\delta_o = 68^{\circ}$) illustrated in Figs. 3.11 through 3.15 is much more heavily damped than that about the operating point (τ_o = 0.5; $\delta = 28.5^{\circ}$), described in Figs. 3.16 through 3.20, is qualitatively in agreement with Eq. (30c) and Fig. D4; the damping ratio from Fig. D4 is nearly equal to the damping parameter ξ_o, except at large values of (ω_n ξ) and Eq. (30c) indicates that the damping parameter ξ_o is proportional to sin δ_o.

A more quantitative comparison of the simulation transient results with the theoretical results of Appendix D can be made between the frequency and decay of the rotor oscillations illustrated in Fig. 3.16, 3.17, in response to the load decrease, and the corresponding theoretical values of swing frequency and damping ratio obtained from Fig. D4. The value of rotor swing frequency, ω_s, is:

$$\omega_s^* = 13.9 \text{ radians/sec} \qquad \text{(from simulation)}$$

The determination of the damping ratio of the observed transient response illustrated in Fig. 3.16 requires somewhat more effort. The values of the alternate positive and negative peak deviations of speed or rotor angle about their final values are plotted vs time on semi-log paper in Fig. 3.21. The slope of the straight line drawn through these points is the logarithmic decrement of the damped response and is equal to $-\ln(\xi\omega_n)$, the negative of the natural logarithm of the product of the damping ratio ξ and the undamped natural frequency ω_n. The derived value of $\xi\omega_n$ obtained from Fig. 3.21 is:

$$(\xi\omega_n)^* = 2.2 \qquad \text{(from simulation)}$$

In comparison with the above values of ω_s and $\xi\omega_n$ derived from the simulated transient response data in Fig. 3.16, 3.17 the corresponding values of these parameters derived from the analysis of Appendix D are obtained by evaluating Eq. (30) for the parameters $(\omega_n\tau_d)$ and ξ_o, and then using these parameters to determine the rotor swing frequency

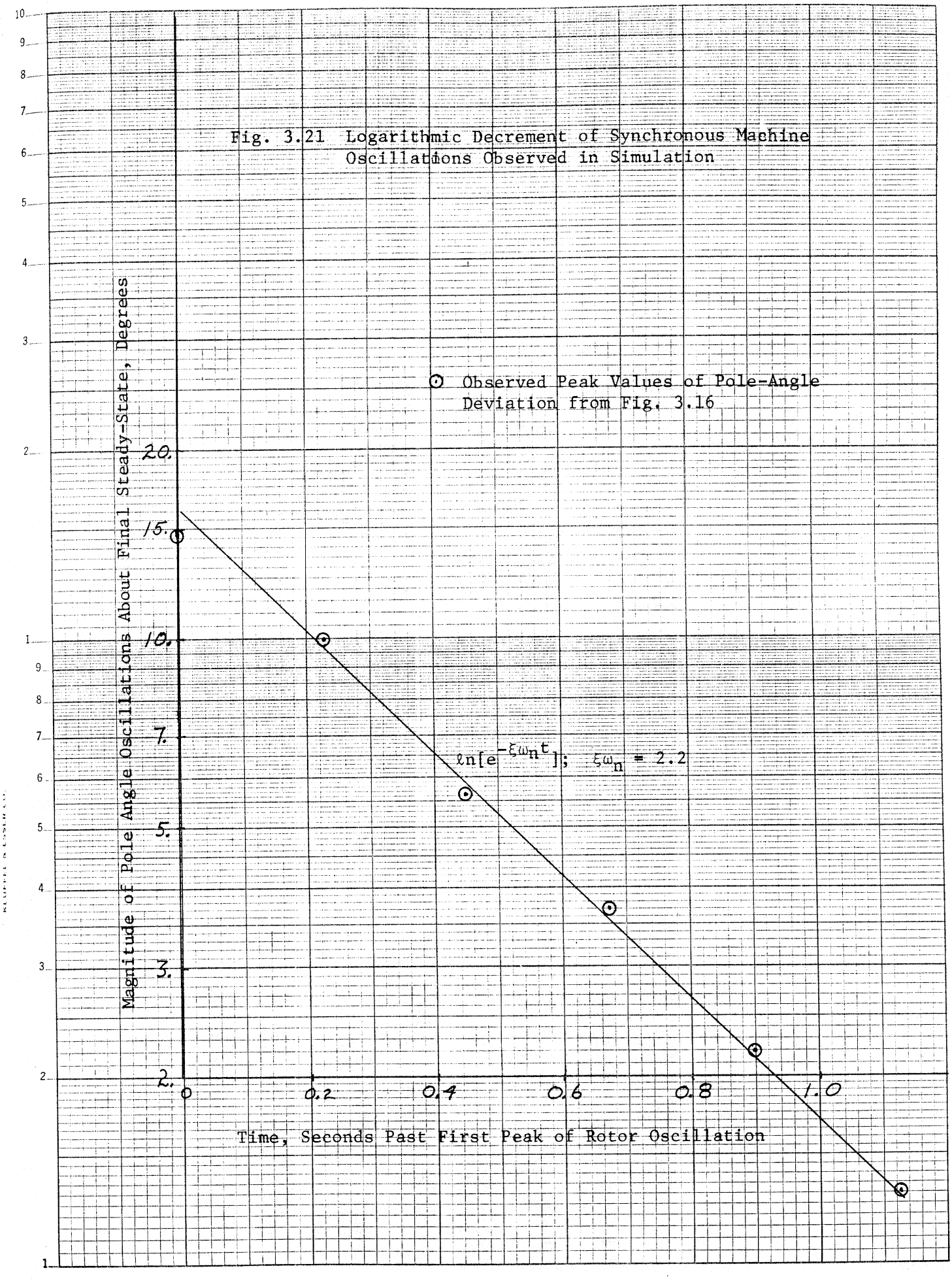

Fig. 3.21 Logarithmic Decrement of Synchronous Machine Oscillations Observed in Simulation

and damping ratio from Fig. D3, D4. A list of the pertinent machine parameters and operating variables at the steady-state operating point for $\tau = 0.5$, which are required to evaluate Eq. (30) are given below.

Machine Parameters	Operating Variables
$r_f = .0222$ pu	$\delta_o = 28.5^o$
$x_m = 2.042$ pu	$v = 1.0$ pu
$x_a = .0775$ pu	$e_f = \frac{v_f}{r_f} X_m = 2.4$ pu
$x_f = .0322$ pu	$\omega_o = 377$/sec
$H = 1.0$ secs	

Substituting these values into Eq. (30) gives the following results:

$\tau_d' = .0128$ secs	$\omega_n = 13.95$ rad/sec
$\omega_n \tau_d' = 0.178$	$\xi_o = 0.171$

The corresponding values of rotor swing frequency and damping ratio obtained from Fig. D3, D4 are:

$\xi = 0.171$	$\omega_s = 14.2$

and $\xi\omega_n = 2.38$

Comparison of these values of $\xi\omega_n$ and ω_s, which are based upon a small disturbance, linearized analysis of the machine dynamics, with the actual observed value of $(\xi\omega_n)^*$ and ω_s^* from the simulation data, indicates good agreement between the simulation and the theoretical analysis of Appendix D.

3.5 Two Machine Simulation: Start-Up and Free Acceleration of a Symmetric Two-Phase Induction Motor From a Balanced Bus Supplied by a Two-Phase Alternator With Automatic Voltage and Speed Control

A diagram illustrating the two-machine system to be simulated is shown in Fig. 3.22. Machine 1 is identical to the synchronous machine described in section 3.4, except that it now functions as an alternator rather than as a motor. In addition the field excitation and shaft torque applied to this synchronous machine are no longer constant but are regulated by the corresponding alternator voltage and frequency (speed) controllers. Machine 2 is a balanced two-phase induction motor similar to that described in section 3.2 except that its parameters are scaled such that its power rating is only 10% that of the alternator. The per unit parameters of all components in this system are based upon the power rating of the alternator. Therefore, given that the induction motor rating is 10% that of the alternator, the per-unit parameters of the motor are obtained by multiplying the per-unit impedances of the motor described in section 3.2 by a factor of 10, and dividing the inertia constant of that machine by the same factor.

Both the voltage and the speed governor are proportional controllers having first-order time lags. Thus the equations for these controllers are:

$$v_t = \sqrt{v_a^2 + v_b^2}$$

$$\Delta v_f = \left(\frac{r_f}{X_m}\right) \frac{Kv}{T_v s + 1} (v_o - v_t); \quad v_o = 1.0$$

$$v_f = v_{fo} + \Delta v_f$$

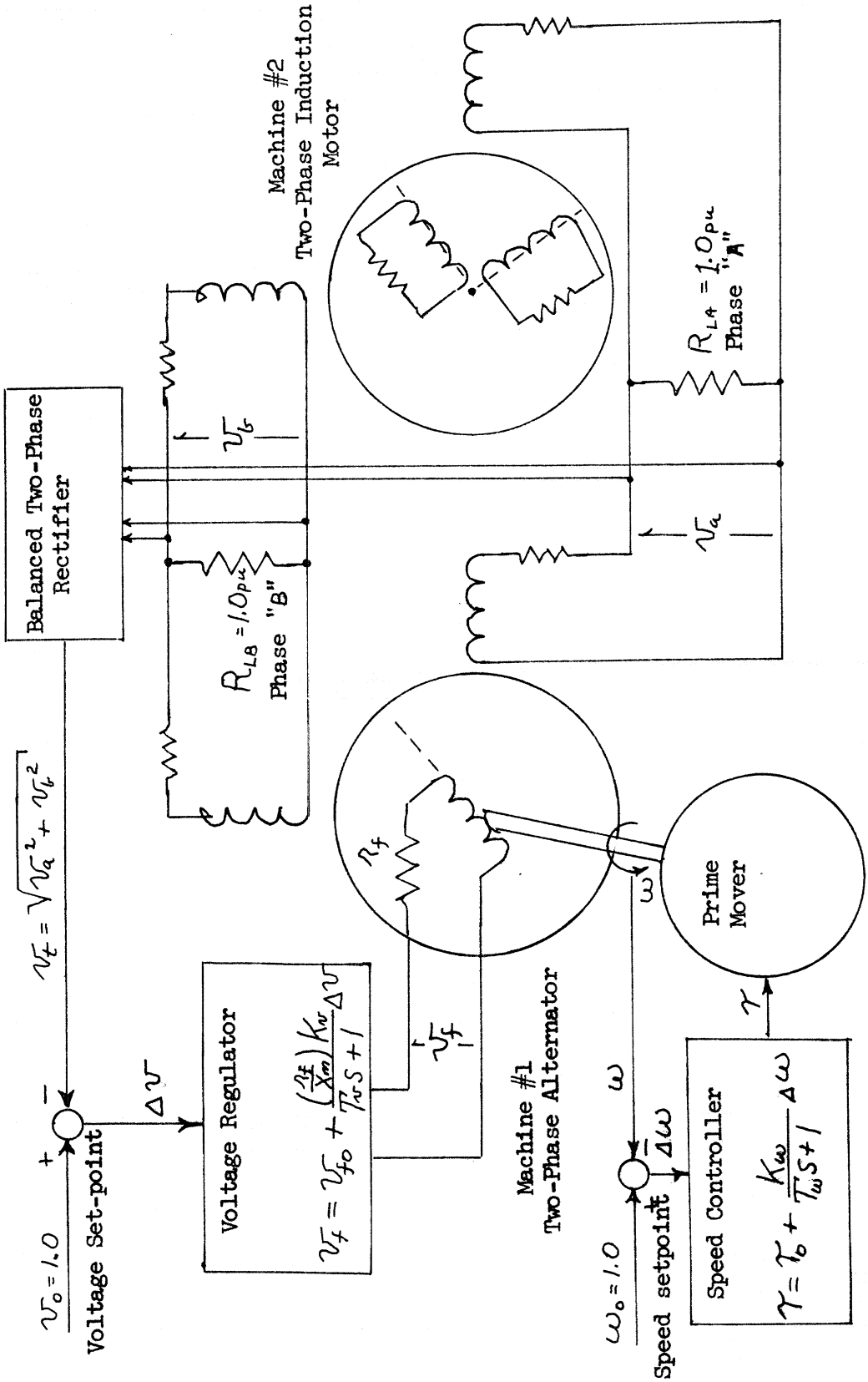

Fig. 3.22 Circuit Diagram of a Two-Machine System Consisting of a Balanced Two-Phase Alternator, Induction Motor, and Resistive Shunt Load

$$\Delta\tau = \frac{K_\omega}{\mathcal{T}_\omega s + 1} (\omega_o - \omega); \quad \omega = 1.0$$

$$\tau = \tau_o + \Delta\tau$$

s Laplace transform operator for $\frac{d}{dt}$

v_f voltage applied to field winding

τ prime mover torque

K_v voltage regulator gain

K_ω speed governor gain

$\mathcal{T}_v$ voltage regulator time constant

$\mathcal{T}_\omega$ speed governor time constant

v_{fo} field voltage set point

τ_o prime mover torque set point

The factor $(\frac{r_f}{x_m})$ in the voltage regulator equation relates the applied field voltage v_f to the internal excitation voltage E_f, or "voltage behind synchronous reactance" of the machine:

$$v_f = (\frac{r_f}{x_m}) E_f$$

The values of the field excitation and torque set points, v_{fo} and τ_o, are specified such that the alternator will supply rated power to the 1.0 pu balanced resistive load, at rated voltage and frequency, when the induction motor is disconnected from the system bus. The required values of v_{fo} and τ_o are easily obtained from a steady-state phasor analysis of the machine for conditions of rated voltage, frequency, and power, at unity power factor, and are given below:

$v_{fo} = .026$ pu

$\tau_o = 1.0453$ pu

The value of the torque set point, τ_o, is 1.0453 rather than 1.0 at rated electrical power, to compensate for the copper losses in the machine armature windings.

The values of controller parameters were arbitrarily assigned as follows:

$K_v = 10.0$

$K_\omega = 10.0$

$\mathcal{T}_v = 0.1$ sec

$\mathcal{T}_\omega = 0.25$ sec

It should be noted that the controller gain factors represent incremental and not absolute gains. This distinction is particularly significant for the case of the voltage regulator. Thus $K_v = 10.$ does not result in the absolute value of excitation voltage being increased by 100% in response to a 10% decrease in terminal voltage. Rather, it means that for a 0.1 pu change in v_t the corresponding change in E_f will be 1.0 pu. Therefore since the value of the field excitation set point, $v_{fo} = .026$, corresponds to $E_f \cong 2.4$, the internal excitation voltage E_f is only increased by 1.0 pu to $E_f = 3.4$ in response to a 0.1 pu decrease in v_t to 0.9 pu.

The simulation results presented in Figs. 3.23 through 3.28 describe the transient response of the system during start-up and free acceleration of the induction motor to synchronous speed. The

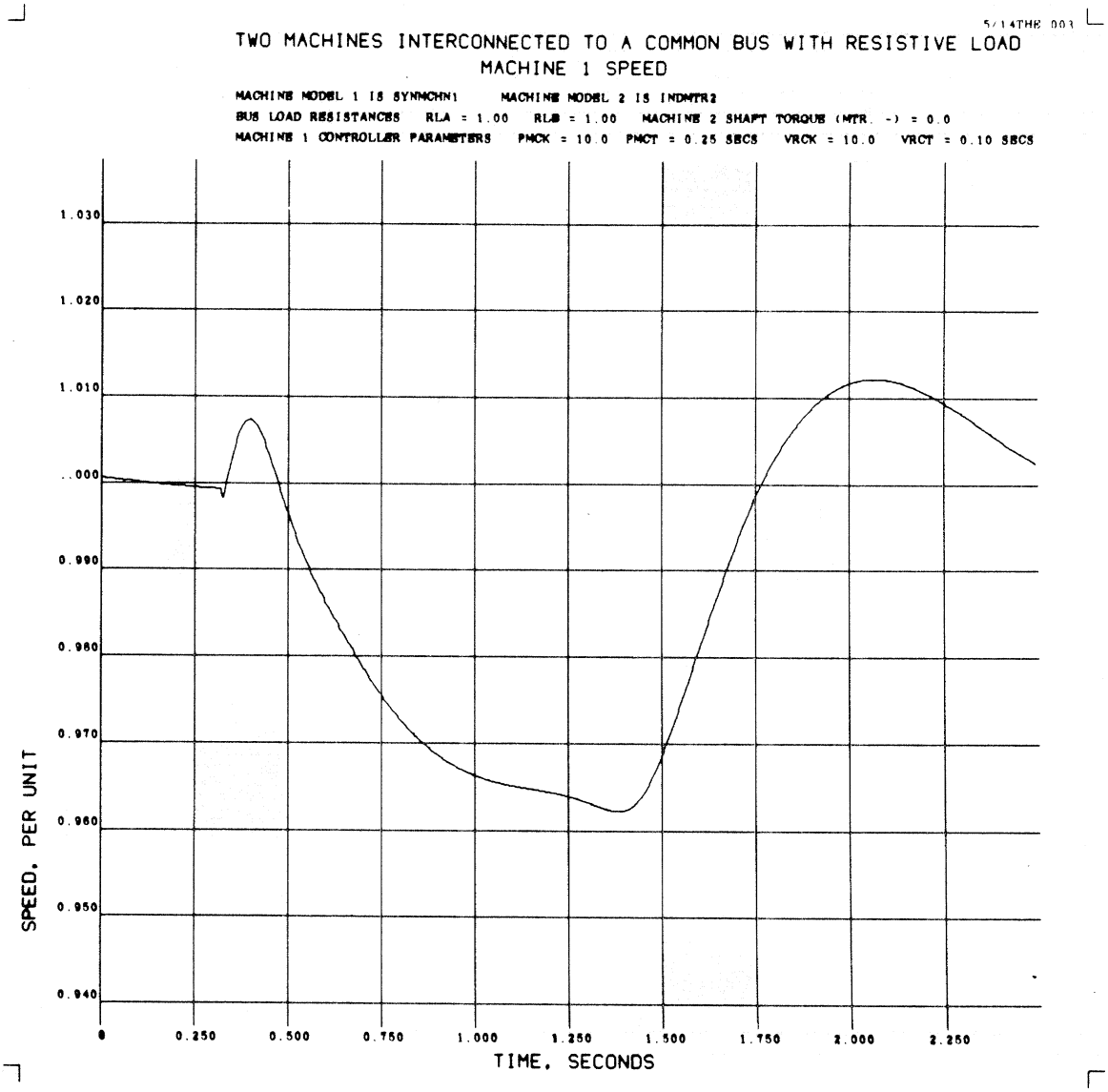
5/14THR 003
TWO MACHINES INTERCONNECTED TO A COMMON BUS WITH RESISTIVE LOAD
MACHINE 1 SPEED
MACHINE MODEL 1 IS SYNMCHN1 MACHINE MODEL 2 IS INDMTR2
BUS LOAD RESISTANCES RLA = 1.00 RLB = 1.00 MACHINE 2 SHAFT TORQUE (MTR. -) = 0.0
MACHINE 1 CONTROLLER PARAMETERS PMCK = 10.0 PMCT = 0.25 SECS VRCK = 10.0 VRCT = 0.10 SECS
1.030
1.020
1.010
1.000
0.990
0.980
0.970
0.960
0.950
0.940
SPEED, PER UNIT
0
0.250
0.500
0.750
1.000
1.250
1.500
1.750
2.000
2.250
TIME, SECONDS

Fig. 3.23

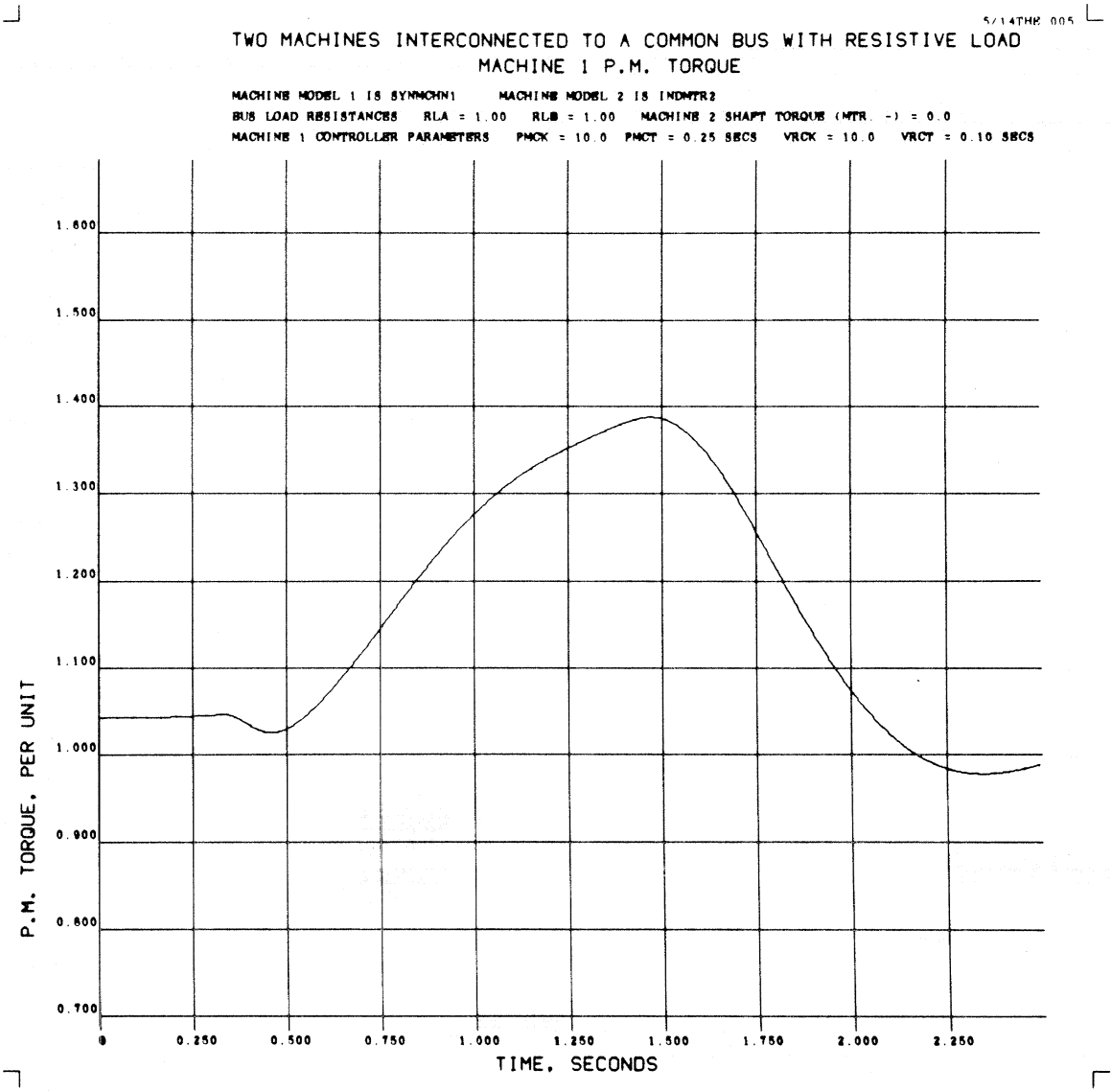
5/14THR 005
TWO MACHINES INTERCONNECTED TO A COMMON BUS WITH RESISTIVE LOAD
MACHINE 1 P.M. TORQUE
MACHINE MODEL 1 IS SYNMCHN1 MACHINE MODEL 2 IS INDMTR2
BUS LOAD RESISTANCES RLA = 1.00 RLB = 1.00 MACHINE 2 SHAFT TORQUE (MTR. -) = 0.0
MACHINE 1 CONTROLLER PARAMETERS PMCK = 10.0 PMCT = 0.25 SECS VRCK = 10.0 VRCT = 0.10 SECS
P.M. TORQUE, PER UNIT
1.600
1.500
1.400
1.300
1.200
1.100
1.000
0.900
0.800
0.700
0
0.250
0.500
0.750
1.000
1.250
1.500
1.750
2.000
2.250
TIME, SECONDS

Fig. 3.24

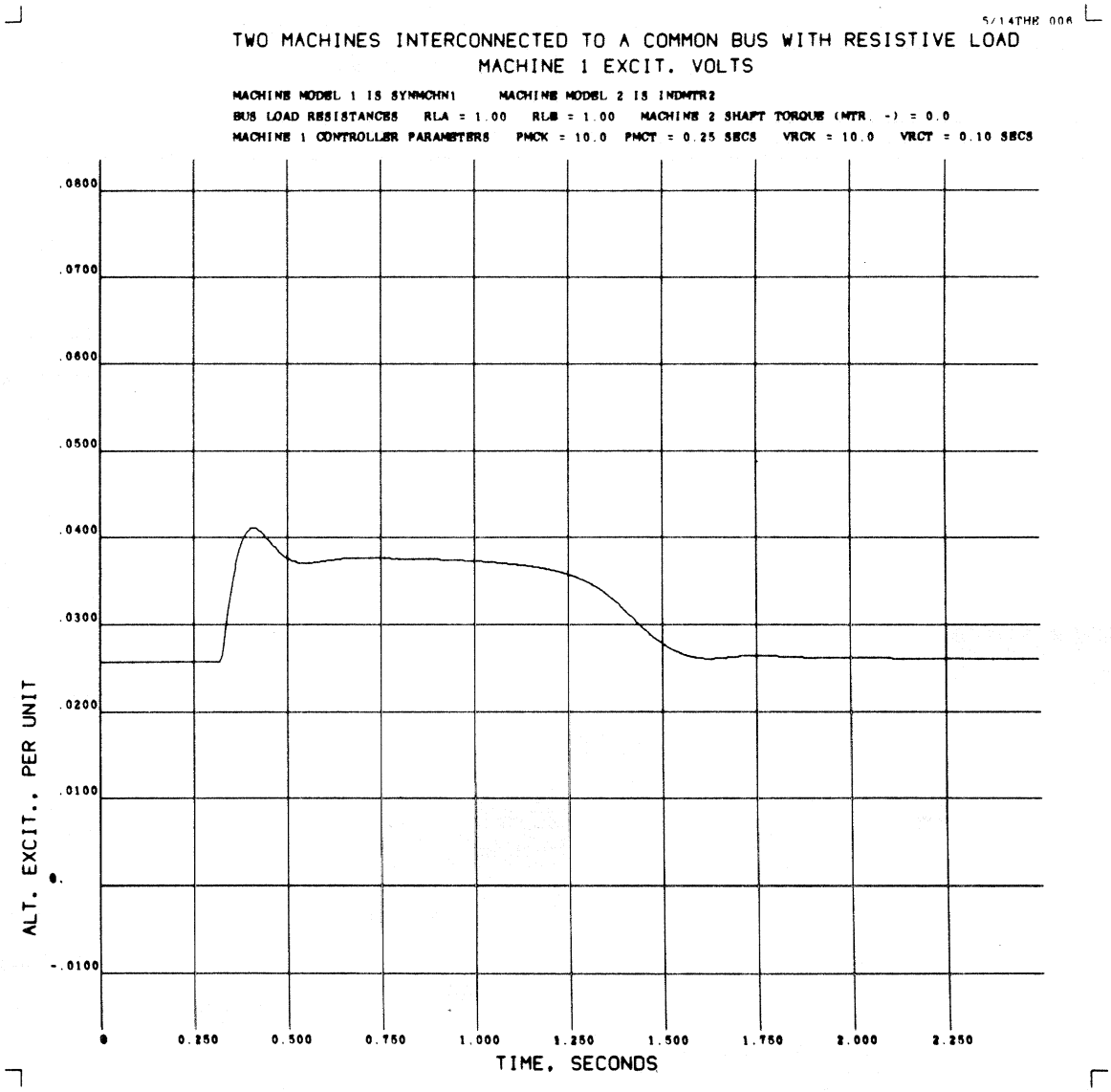
5/14THR 008
TWO MACHINES INTERCONNECTED TO A COMMON BUS WITH RESISTIVE LOAD
MACHINE 1 EXCIT. VOLTS
MACHINE MODEL 1 IS SYNMCHN1 MACHINE MODEL 2 IS INDMTR2
BUS LOAD RESISTANCES RLA = 1.00 RLB = 1.00 MACHINE 2 SHAFT TORQUE (MTR. -) = 0.0
MACHINE 1 CONTROLLER PARAMETERS PMCK = 10.0 PMCT = 0.25 SECS VRCK = 10.0 VRCT = 0.10 SECS
.0800
.0700
.0600
.0500
.0400
.0300
.0200
.0100
0.
-.0100
ALT. EXCIT., PER UNIT
0
0.250
0.500
0.750
1.000
1.250
1.500
1.750
2.000
2.250
TIME, SECONDS

Fig. 3.25

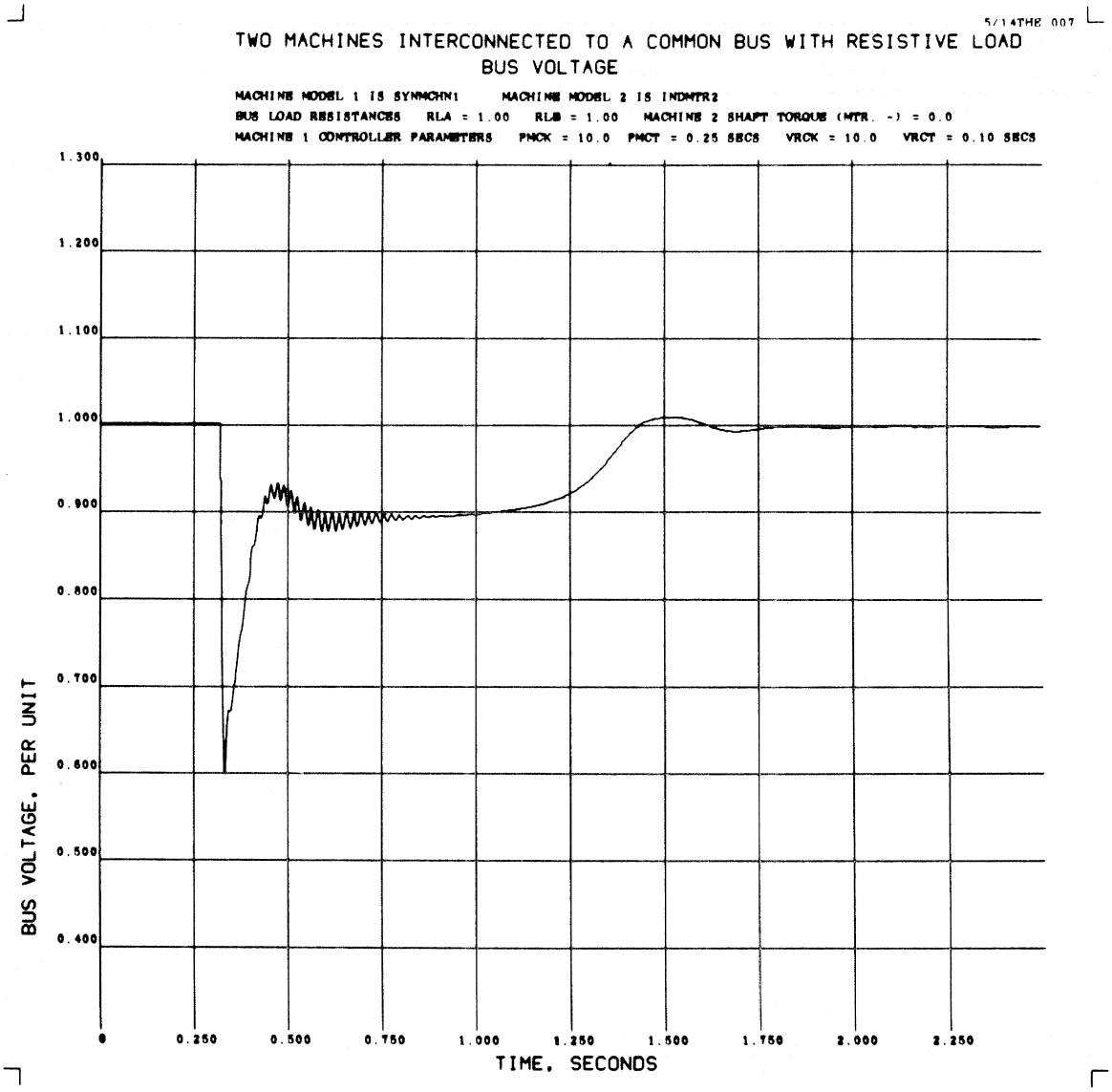
5/14THR 007
TWO MACHINES INTERCONNECTED TO A COMMON BUS WITH RESISTIVE LOAD
BUS VOLTAGE
MACHINE MODEL 1 IS SYNMCHN1 MACHINE MODEL 2 IS INDMTR2
BUS LOAD RESISTANCES RLA = 1.00 RLB = 1.00 MACHINE 2 SHAFT TORQUE (MTR. -) = 0.0
MACHINE 1 CONTROLLER PARAMETERS PMCK = 10.0 PMCT = 0.25 SECS VRCK = 10.0 VRCT = 0.10 SECS
BUS VOLTAGE, PER UNIT
1.300
1.200
1.100
1.000
0.900
0.800
0.700
0.600
0.500
0.400
0
0.250
0.500
0.750
1.000
1.250
1.500
1.750
2.000
2.250
TIME, SECONDS

Fig. 3.26 -

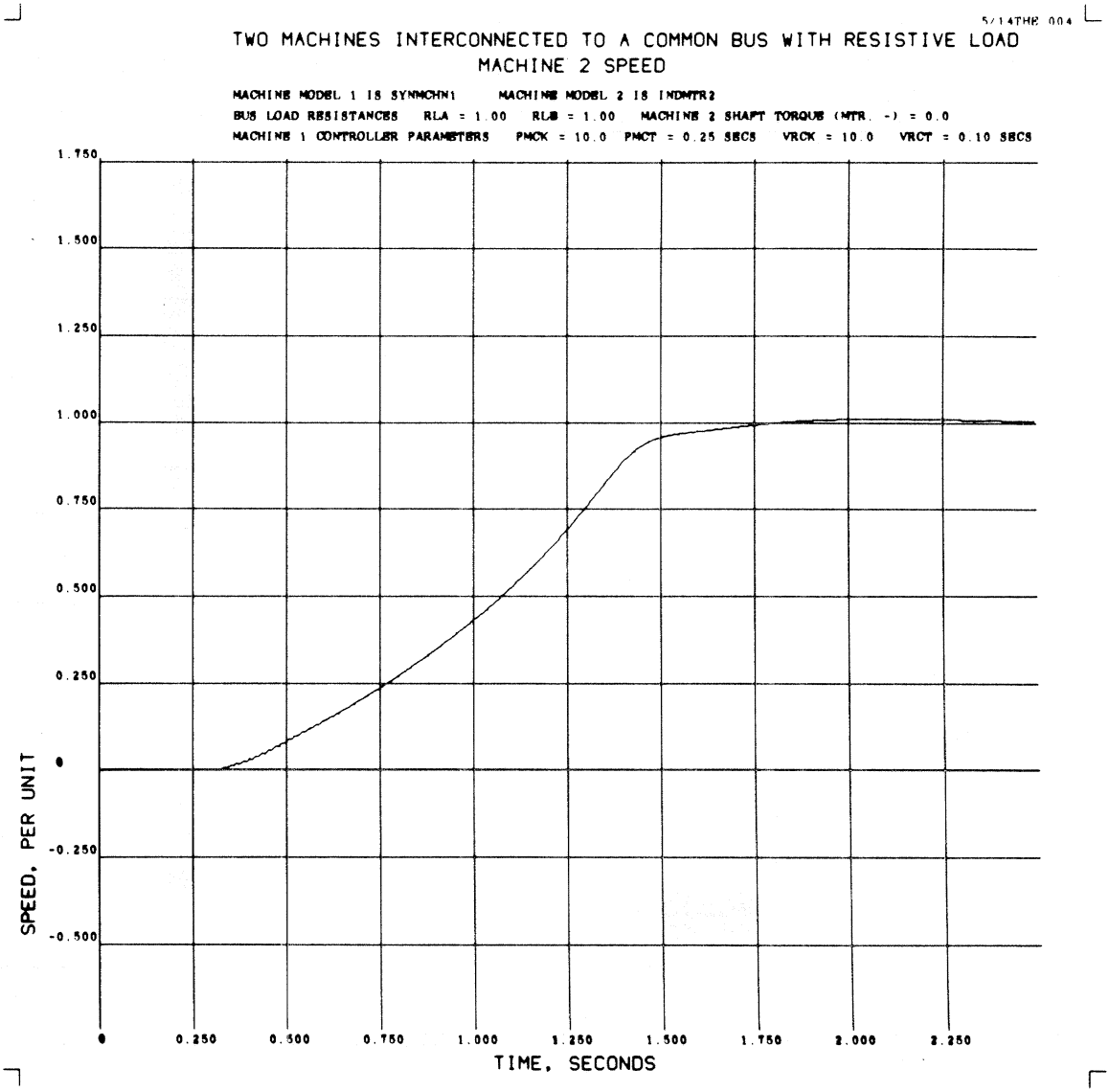
5/14THR 004
TWO MACHINES INTERCONNECTED TO A COMMON BUS WITH RESISTIVE LOAD
MACHINE 2 SPEED
MACHINE MODEL 1 IS SYNMCHN1 MACHINE MODEL 2 IS INDMTR2
BUS LOAD RESISTANCES RLA = 1.00 RLB = 1.00 MACHINE 2 SHAFT TORQUE (MTR. -) = 0.0
MACHINE 1 CONTROLLER PARAMETERS PMCK = 10.0 PMCT = 0.25 SECS VRCK = 10.0 VRCT = 0.10 SECS
1.750
1.500
1.250
1.000
0.750
0.500
0.250
0
-0.250
-0.500
SPEED, PER UNIT
0
0.250
0.500
0.750
1.000
1.250
1.500
1.750
2.000
2.250
TIME, SECONDS

Fig. 3.27

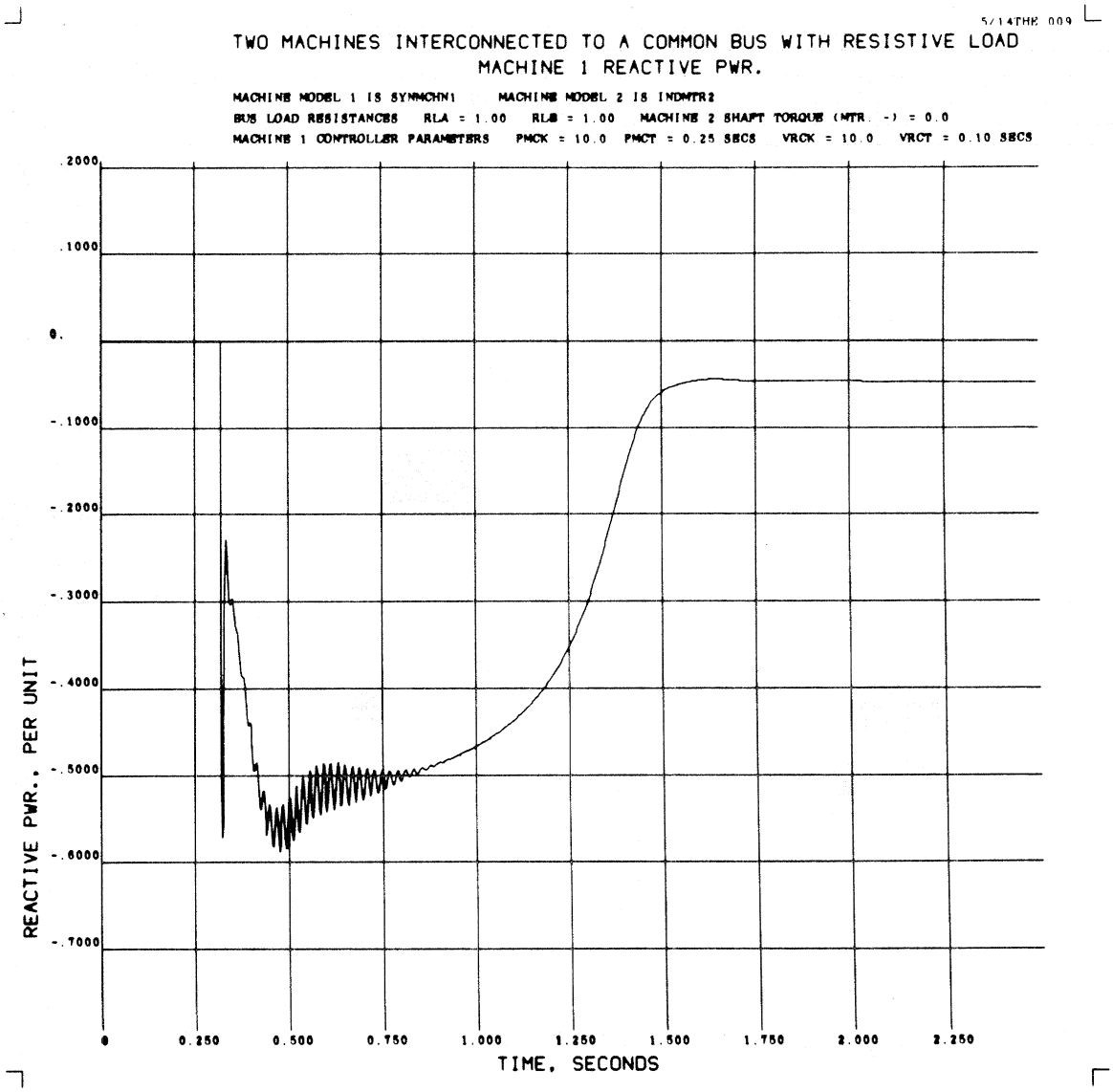
5/14THR 009
TWO MACHINES INTERCONNECTED TO A COMMON BUS WITH RESISTIVE LOAD
MACHINE 1 REACTIVE PWR.
MACHINE MODEL 1 IS SYNMCHN1 MACHINE MODEL 2 IS INDMTR2
BUS LOAD RESISTANCES RLA = 1.00 RLB = 1.00 MACHINE 2 SHAFT TORQUE (MTR. -) = 0.0
MACHINE 1 CONTROLLER PARAMETERS PMCK = 10.0 PMCT = 0.25 SECS VRCK = 10.0 VRCT = 0.10 SECS
.2000
.1000
0.
-.1000
-.2000
-.3000
-.4000
-.5000
-.6000
-.7000
REACTIVE PWR., PER UNIT
0
0.250
0.500
0.750
1.000
1.250
1.500
1.750
2.000
2.250
TIME, SECONDS

Fig. 3.28

induction motor is initially at rest and disconnected from the system; the only load on the induction motor is the mechanical inertia of its rotor shaft. Prior to starting of the motor the alternator is operating at steady state delivering rated power to the resistive load on the bus, at rated voltage and frequency.

The results of this simulation exhibit some interesting characteristics of the system response to the start-up of a relatively small (10% of rated power) motor. As illustrated in Fig. 3.26, as soon as the switch to the induction motor is closed, the bus voltage drops abruptly to a value of about 0.6 pu. Although a voltage drop is to be expected, at first glance the magnitude of observed drop may seem surprisingly large, especially in consideration of the fact that the motor rating is only 10% that of the generator. However, with its rotor initially at standstill, the induction motor appears as a short-circuited transformer whose total effective impedance is quite low, composed merely of the sum of its leakage reactances and winding resistances. The rapid partial recovery of the bus voltage from 0.6 pu to 0.9 pu, illustrated in Fig. 3.26, is due only to the fast action of the voltage regulator, as indicated by the behavior of the field excitation voltage illustrated in Fig. 3.25.

Another interesting aspect of the system behavior illustrated in Fig. 3.23 is the initial tendency of the alternator to briefly accelerate before losing speed in response to the additional load presented by the motor. This initial tendency of the alternator to accelerate is due to momentary decrease in total electrical power absorbed from the bus which results from the sharp drop in bus voltage when the induction motor is initially turned on. In effect, because of this voltage drop, the

decrease in power absorbed by the system load resistors exceeds the additional power initially drawn by the motor. Because of this net decrease in electrical power absorbed from the bus, the corresponding momentary excess of power supplied by the prime mover is channeled into acceleration of the alternator inertia. Again the day is saved by the rapid response of the voltage regulator in partially restoring the bus voltage to its rated value. As the voltage recovers from the initial drop, the net electrical power absorption, due to the combination of load resistors and induction motor, increases more rapidly than the power supplied from the prime mover, resulting in a drop of alternator speed and thus system frequency.

Finally, because of the fact that the power drawn by the accelerating induction motor falls off very rapidly after the motor attains 80% of synchronous speed (see Fig. 3.3), this rapid decrease in electrical power absorbtion again results in acceleration of the alternator by the excess prime-mover power, causing a slight overshoot in system frequency before the system finally settles down at nearly the same values of voltage and frequency as before connection of the induction motor.

3.6 Two Machine Simulation: Start-up and Free Acceleration of an Unsymmetric, Capacitor-Start Single Phase Induction Motor Connected to a Power Line Supplied by a Single-Phase Alternator with Automatic Speed and Voltage Regulation

A diagram of the two-machine system being simulated in this example is given in Fig. 3.29. The present example is similar to that of the two-machine system described in the previous section except that now both machines are single rather than polyphase.

The model for the single phase alternator in Fig. 3.29 is a modified version of the two-phase synchronous machine previously described

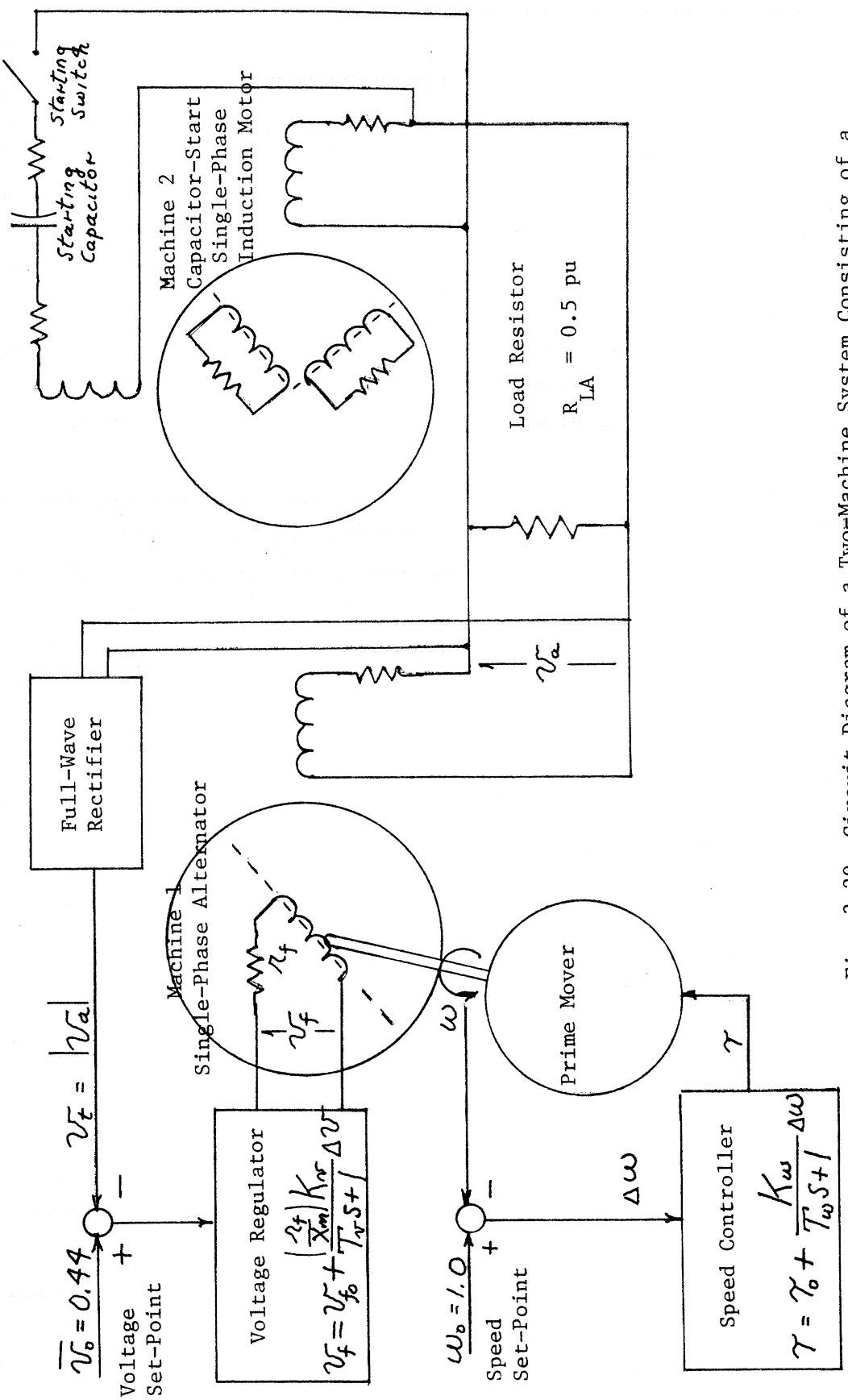

Fig. 3.29 Circuit Diagram of a Two-Machine System Consisting of a Single-Phase Alternator, Capacitor-Start Induction Motor, and Resistive Shunt Load

in Sections 3.4 and 3.5. In addition to the fact that, for single phase operation, the stator "b" winding is now non-existent or open-circuited, all per-unit values of machine impedances described in Section 3.4, except the field winding resistance, have been divided by 2. This reduction in machine impedances was necessary so that the machine could deliver all of its rated power, at rated voltage, through only a single phase, rather than two phases as before. In addition, in order to supply a somewhat stiffer source of field excitation voltage, the value of field terminal voltage was doubled while the value of field winding resistance remained unchanged. Although the average steady state value of field current was thus doubled, this was counterbalanced by the previously described factor of two reduction in the machine magnetizing reactance. Consequently the resultant values of field flux and associated internal excitation voltage remained unchanged from the values in the balanced two-phase case. The stiffer (more nearly constant current) field excitation system was desired in order to counteract the tendency of the unbalanced armature reaction flux in a single-phase machine to distort the sinusoidal waveform of the generated output voltage. Unfortunately, it turned out that the increase in excitation stiffness which resulted from doubling the relative value of field resistance fell far short of that required for maintenance of undistorted sinusoidal output waveforms, when operating at rated load.

Again, because the rated power generated by the alternator at rated terminal voltage had to be transmitted and absorbed over a single phase rather than two, the per unit value of the shunt load resistor across the single phase power line was also reduced by a factor of two from 1.0 to 0.5 pu.

The capacitor-start single phase induction motor in Fig. 3.29 is similar to that described in Section 3.3 except that its power rating is only 10% that of the alternator. Again the per-unit values of all the motor parameters are based upon the power rating of the alternator. Consequently, the per-unit impedances of the induction motor are obtained by multiplying the corresponding impedance values for the motor described in Section 3.3 by a factor of 10., and similarly, the motor's inertia constant is obtained by dividing the corresponding value given in Section 3.3 by the same factor.

The alternator voltage and speed controllers are identical to those described in Section 3.5, except that the set point on the voltage regulator must be lowered to a value equal to the integrated average of the full-wave rectified value of the desired line voltage. This modification is also a consequence of the change from balanced two-phase to single-phase operation. Consequently, if the single phase line voltage were sinusoidal and had a peak value of 1.0 pu, as in the previous case of balanced two-phase operation, the value of the voltage regulator setpoint, v_o, which appears in the voltage regulator equations of Section 3.5, would have to be reduced from 1.0 to $2/\pi = 0.637$, the integrated average value of the full-wave-rectified sinusoidal line voltage. Unfortunately, because of the unbalanced nature of single-phase operation, the actual waveform of the generated voltage will be very badly distorted, as seen by the resistive load current waveform illustrated in Fig. 3.30. Consequently, the factor of 0.637 for the voltage regulator set-point, based upon the assumption of sinusoidal voltage waveform, does not apply in the present situation. The actual value of voltage regulator set-point used in the simulation was

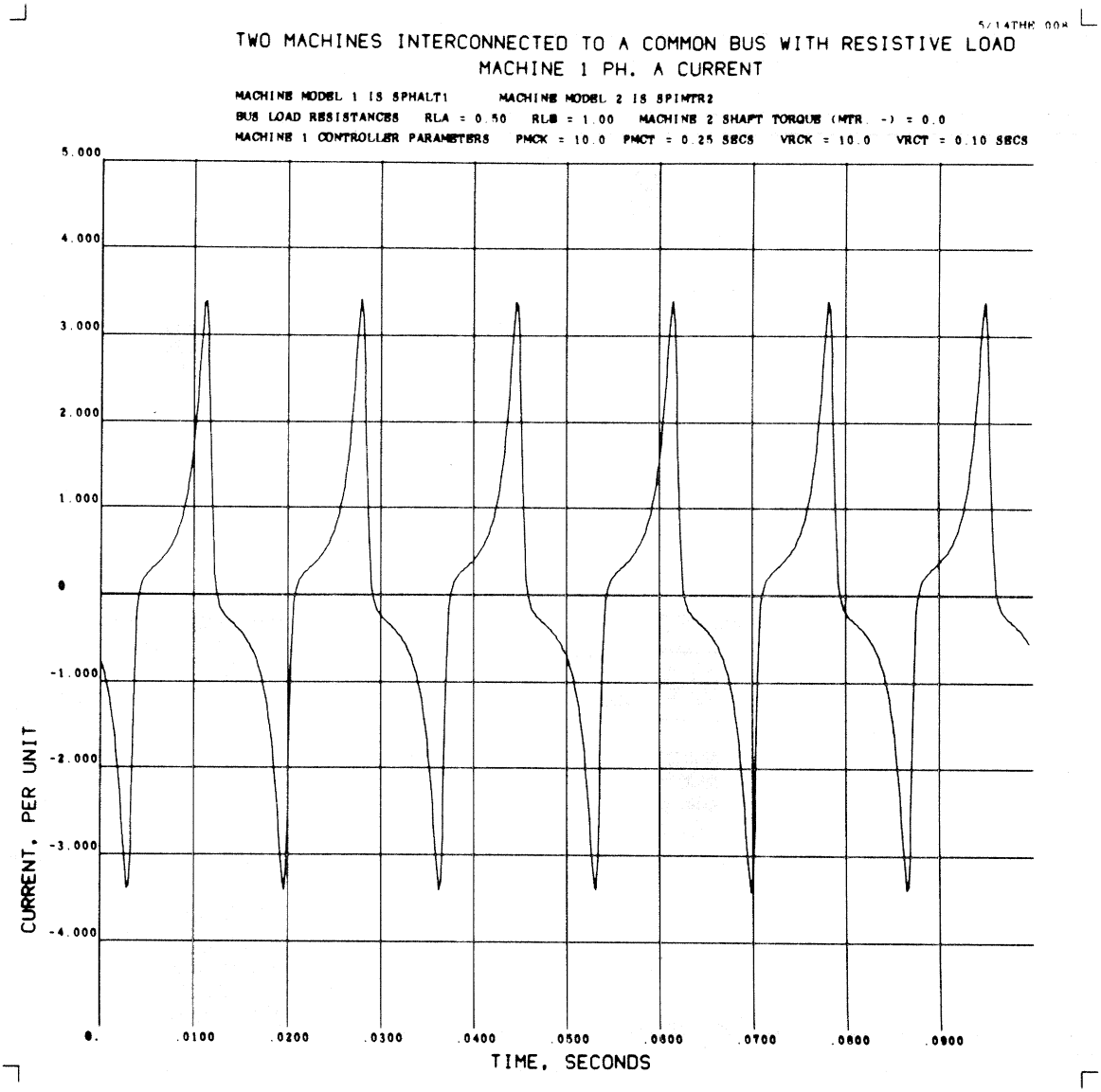
TWO MACHINES INTERCONNECTED TO A COMMON BUS WITH RESISTIVE LOAD
MACHINE 1 PH. A CURRENT
MACHINE MODEL 1 IS SPHALT1 MACHINE MODEL 2 IS SPIMTR2
BUS LOAD RESISTANCES RLA = 0.50 RLB = 1.00 MACHINE 2 SHAFT TORQUE (MTR. -) = 0.0
MACHINE 1 CONTROLLER PARAMETERS PMCK = 10.0 PMCT = 0.25 SECS VRCK = 10.0 VRCT = 0.10 SECS
5.000
4.000
3.000
2.000
1.000
0
-1.000
-2.000
-3.000
-4.000
CURRENT, PER UNIT
0.
.0100
.0200
.0300
.0400
.0500
.0600
.0700
.0800
.0900
TIME, SECONDS

Fig. 3.30

determined by an indirect method. With the induction motor disconnected from the system, it is known that with the given value of load resistance connected to the armature terminals, the application of rated torque to the rotor shaft should result in operation of the alternator at rated speed. Under these conditions the terminal voltage will be such as to cause rated power to be delivered to the load resistance. Consequently, the required value of the voltage regulator set-point, v_o, was found as follows. With rated torque applied to the rotor shaft, the value of the voltage regulator set-point, v_o, was adjusted, by trial and error, until the alternator operated at rated speed and therefore rated power. The resulting value of v_o obtained by this method was 0.44, substantially less than that of 0.637 which would have been necessary had the waveform of the output voltage been sinusoidal. The large difference between these two values is not surprising considering the amount of distortion in the actual voltage waveform as illustrated in Fig. 3.30. As in the case of the balanced two-phase example given in Section 3.5, the value of the torque set-point for the alternator speed regulator was $\tau_o = 1.0453$.

The simulation results for this example are illustrated in Figs. 3.31 through 3.35. The induction motor is initially at rest and disconnected from the system; prior to starting of the motor, the alternator is operating at rated torque and speed, and delivering rated power to the resistive load on the line. Figure 3.30 is a plot of the alternator line current under these conditions, over a period of 0.1 secs. As mentioned earlier the waveforms are anything but sinusoidal. Figure 3.31 through 3.34 illustrate the transient response of the system during start-up and free acceleration of the induction motor. Again the only

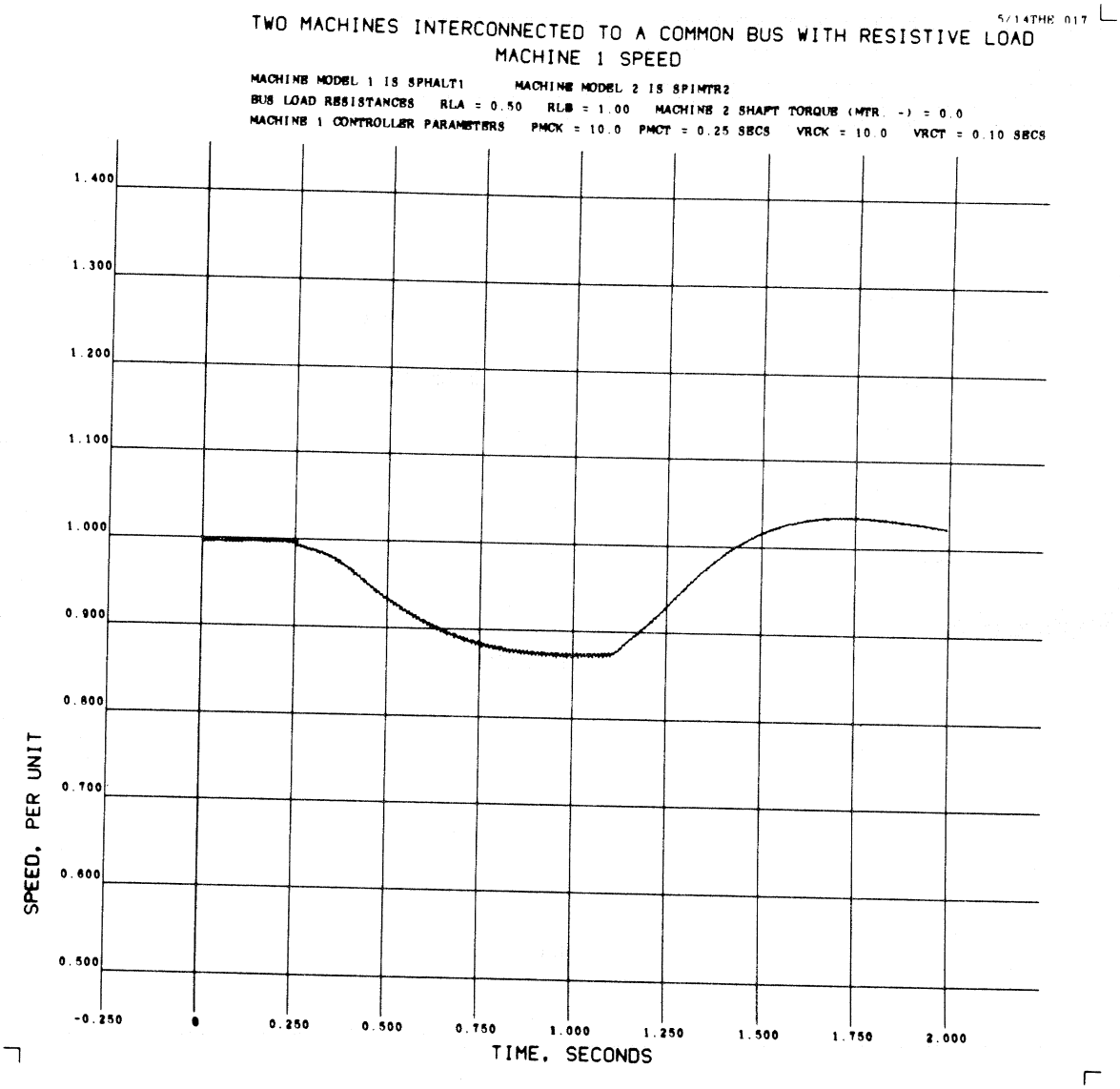
TWO MACHINES INTERCONNECTED TO A COMMON BUS WITH RESISTIVE LOAD
5/14THR 017
MACHINE 1 SPEED
MACHINE MODEL 1 IS SPHALT1
MACHINE MODEL 2 IS SPIMTR2
BUS LOAD RESISTANCES RLA = 0.50 RLB = 1.00 MACHINE 2 SHAFT TORQUE (MTR. -) = 0.0
MACHINE 1 CONTROLLER PARAMETERS PMCK = 10.0 PMCT = 0.25 SECS VRCK = 10.0 VRCT = 0.10 SECS
1.400
1.300
1.200
1.100
1.000
0.900
0.800
0.700
0.600
0.500
SPEED, PER UNIT
-0.250
0
0.250
0.500
0.750
1.000
1.250
1.500
1.750
2.000
TIME, SECONDS

Fig. 3.31

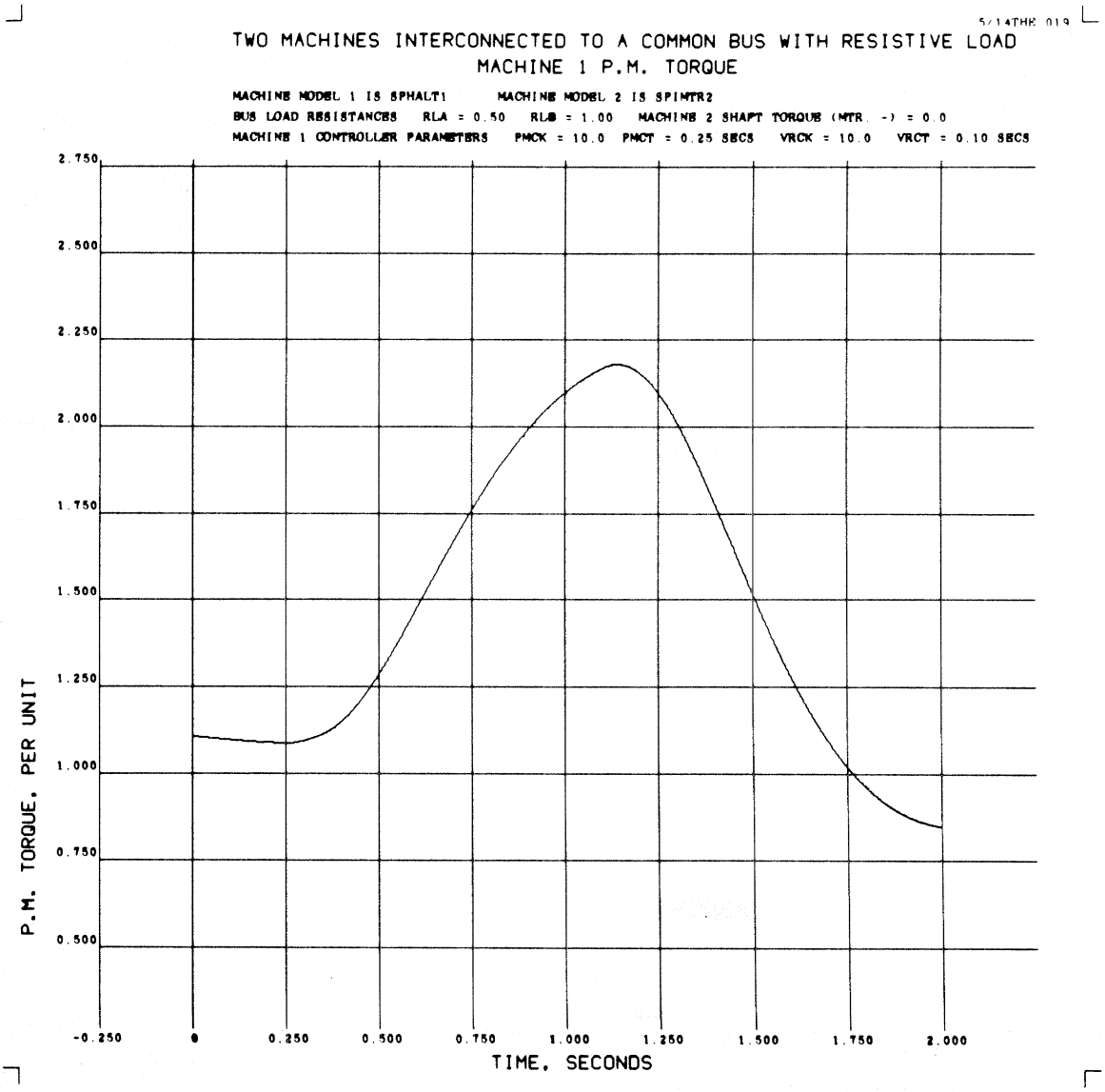
5/14THR 019
TWO MACHINES INTERCONNECTED TO A COMMON BUS WITH RESISTIVE LOAD
MACHINE 1 P.M. TORQUE
MACHINE MODEL 1 IS SPHALT1 MACHINE MODEL 2 IS SPIMTR2
BUS LOAD RESISTANCES RLA = 0.50 RLB = 1.00 MACHINE 2 SHAFT TORQUE (MTR. -) = 0.0
MACHINE 1 CONTROLLER PARAMETERS PMCK = 10.0 PMCT = 0.25 SECS VRCK = 10.0 VRCT = 0.10 SECS
P.M. TORQUE, PER UNIT
2.750
2.500
2.250
2.000
1.750
1.500
1.250
1.000
0.750
0.500
-0.250
0
0.250
0.500
0.750
1.000
1.250
1.500
1.750
2.000
TIME, SECONDS

Fig. 3.32

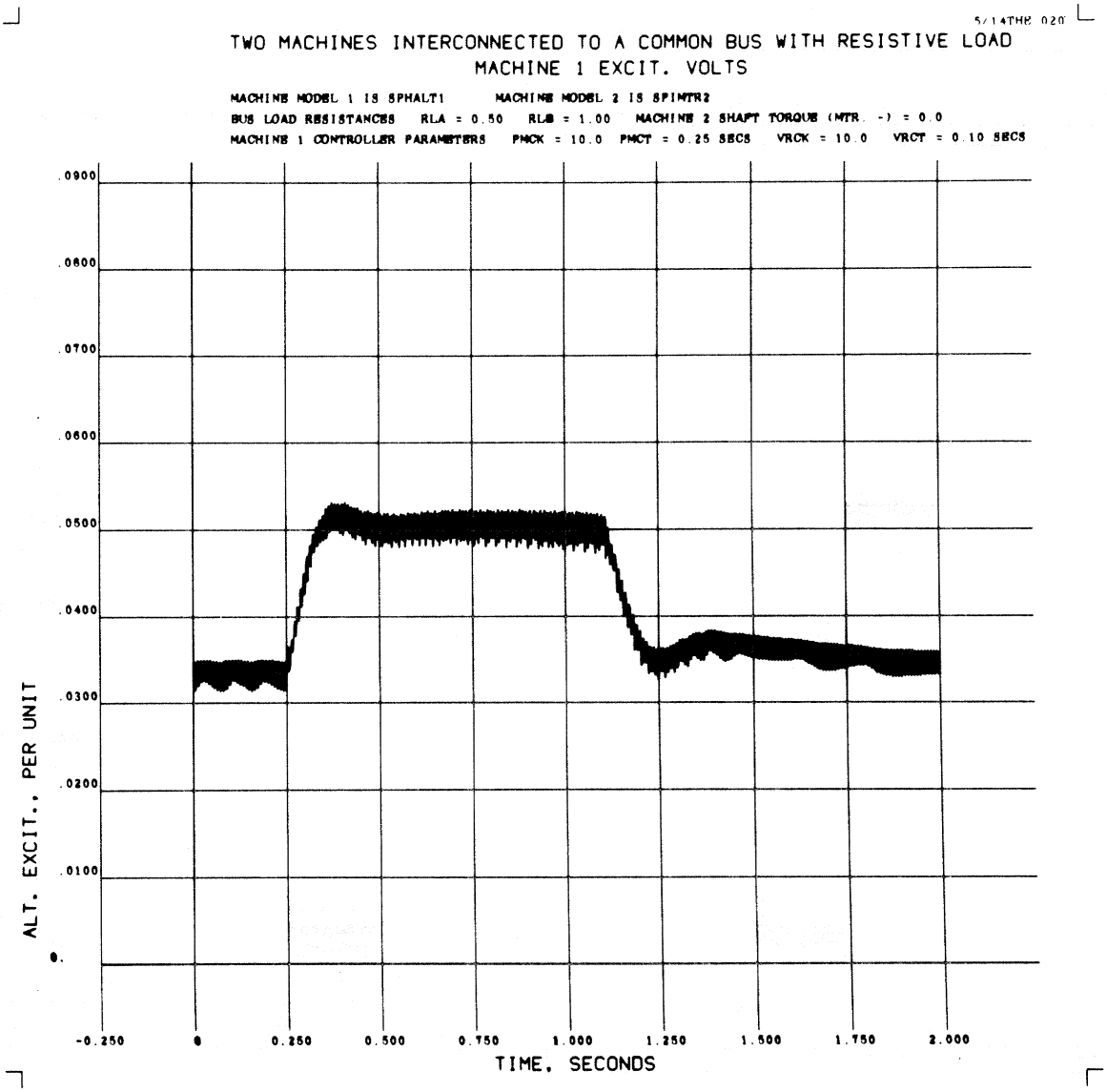
5/14THR 020
TWO MACHINES INTERCONNECTED TO A COMMON BUS WITH RESISTIVE LOAD
MACHINE 1 EXCIT. VOLTS
MACHINE MODEL 1 IS SPHALT1
MACHINE MODEL 2 IS SPIMTR2
BUS LOAD RESISTANCES RLA = 0.50 RLB = 1.00 MACHINE 2 SHAFT TORQUE (MTR. -) = 0.0
MACHINE 1 CONTROLLER PARAMETERS PMCK = 10.0 PMCT = 0.25 SECS VRCK = 10.0 VRCT = 0.10 SECS
.0900
.0800
.0700
.0600
.0500
.0400
.0300
.0200
.0100
0.
ALT. EXCIT., PER UNIT
-0.250
0
0.250
0.500
0.750
1.000
1.250
1.500
1.750
2.000
TIME, SECONDS

Fig. 3.33

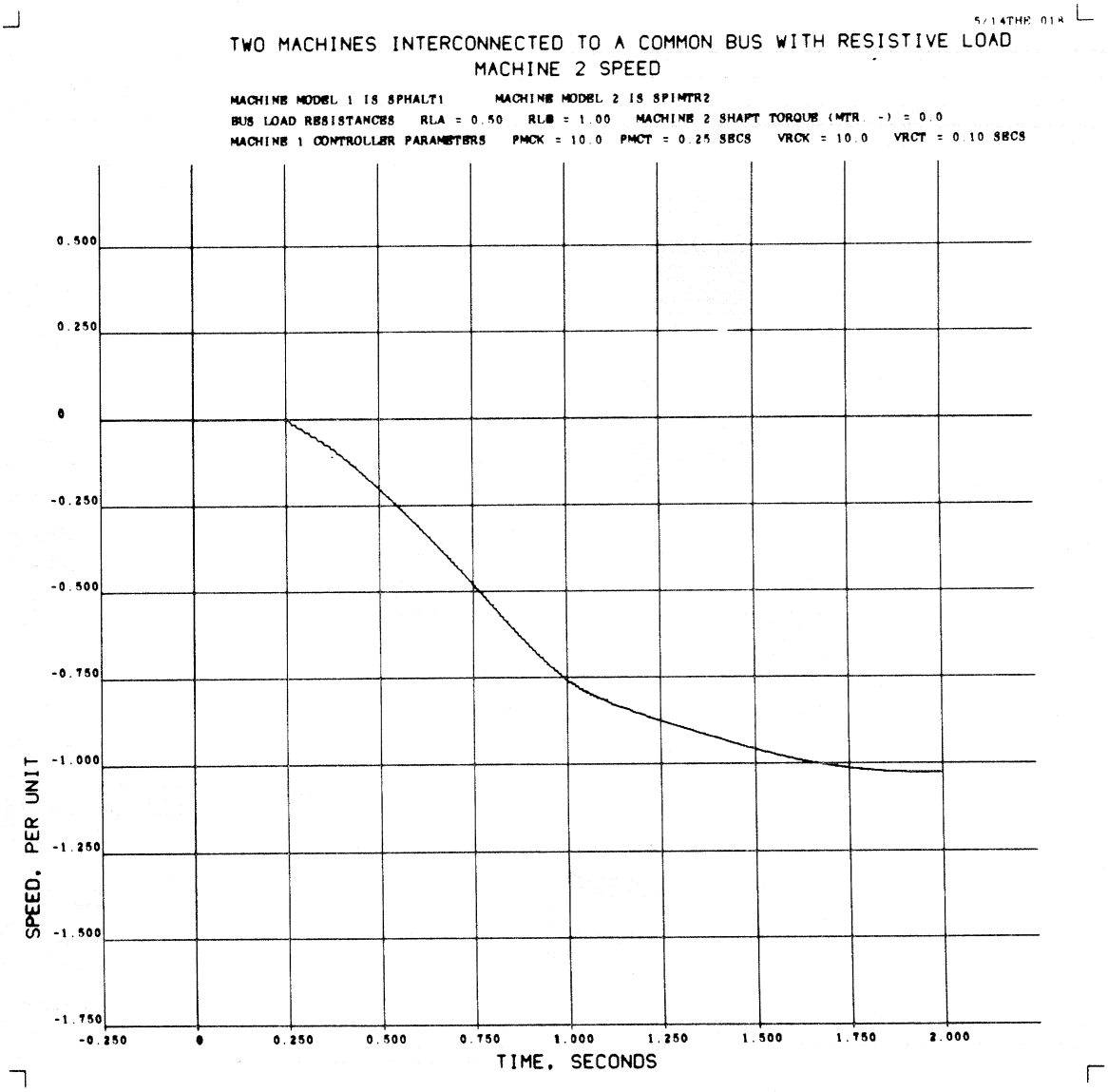
5/14THE 018
TWO MACHINES INTERCONNECTED TO A COMMON BUS WITH RESISTIVE LOAD
MACHINE 2 SPEED
MACHINE MODEL 1 IS SPHALT1 MACHINE MODEL 2 IS SPIMTR2
BUS LOAD RESISTANCES RLA = 0.50 RLB = 1.00 MACHINE 2 SHAFT TORQUE (MTR. -) = 0.0
MACHINE 1 CONTROLLER PARAMETERS PMCK = 10.0 PMCT = 0.25 SECS VRCK = 10.0 VRCT = 0.10 SECS
0.500
0.250
0
-0.250
-0.500
-0.750
-1.000
-1.250
-1.500
-1.750
SPEED, PER UNIT
-0.250
0
0.250
0.500
0.750
1.000
1.250
1.500
1.750
2.000
TIME, SECONDS

Fig. 3.34

load on the induction motor is its own mechanical inertia. Also, as in the example of Section 3.3, the motor starting winding is disconnected when the motor reaches about 80% of its rated speed.

The results illustrated in Fig. 3.31 through 3.34 are generally similar to those given in the previous section for the balanced two-phase case. The one noticeable difference is that in the present example the speed deviations during the transient, and resultant controller action are more than twice as large as in the balanced two-phase case described in the previous section. This is probably due to the lower overall conversion efficiency of single phase machinery, particularly in view of the badly distorted voltage waveforms obtained during operation of the present system. Similarly, a comparison of the induction motor speed response in the present system, illustrated in Fig. 3.34, with the response of a similar machine connected to an ideal single-phase sinusoidal voltage source, illustrated in Fig. 3.7, shows that the acceleration of the motor in the present system is about twice as sluggish as when the motor is connected to an ideal sinusoidal voltage source.

As mentioned earlier, the starting winding of the motor is disconnected when the motor reaches 80% of synchronous speed. The effects on the system response of the opening of the starting winding are particularly evident in Figs. 3.31 and 3.33 for the speed and excitation voltage of the alternator. When the starting winding is opened at 80% of maximum motor speed, the electrical load on the system is decreased, resulting in acceleration of the alternator and a drop in the output of the voltage regulator. The voltage regulator output decreases because of the recovery of line voltage which results from the decrease in

electrical load. The ripple in the output of the voltage regulator, which can be seen in Fig. 3.33, results from full wave rectification of the line voltage. However, the magnitude of the ripple shown in Fig. 3.33 is relatively small because of the filtering effect produced by the 0.1 second time constant of the voltage regulator. Unfortunately, because of the heavy harmonic content of the line voltage, and the fact that the minimum time interval between digital data samples taken for plotting is rather large relative to the periods of the line voltage harmonics, a satisfactory plot of line voltage over a 2 second time span could not be produced by the present computer program. Consequently, no plot of line voltage response is given in this example.

CHAPTER 4

SUMMARY AND CONCLUSIONS

4.1 Basic Machine Model

In this thesis a mathematical model has been developed for digital computer simulation of a four-winding, uniform air-gap rotating AC electrical machine. The four coil windings of the machine are sinusoidally distributed in space around the circumference of the air gap, such as to produce a net sinusoidal space distribution of mmf in the machine, and consist of two magnetically orthogonal rotor windings and a similar pair of magnetically orthogonal stator windings.

The machine simulation developed in this thesis differs from most other conventional simulations of rotating electrical machinery in that the machine is modelled directly in terms of the physical winding currents, flux linkages, and voltages, rather than in terms of transformed fluxes, currents and voltages defined on a suitably rotating "dq" reference frame. The principal advantage of simulating the machine model in terms of physical coil variables, rather than "dq" variables, is the increased flexibility provided for simulating machine configurations which involve asymmetric winding and/or unbalanced environmental conditions. Typical examples of such situations are:

(1) machines having asymmetric windings

(2) machines connected to unbalanced or non-linear external networks - for example solid state voltage or frequency changing devices used for speed control

(3) machines connected to an unbalanced source of supply voltage, the most common example being fractional horsepower machines

for single-phase application

On the other hand, a machine simulation in terms of coil variables will be more complex and less computationally efficient than a simulation in terms of dq variables in those cases where the machine being simulated is either symmetric or is connected to balanced polyphase electrical networks and/or voltage sources. This is, in effect, the price paid for the greater generality of machine simulation in terms of coil variables. The widespread use of "dq" variable representations of machine models for simulation purposes is largely due to the fact that the majority of industrial high-power rotating electrical machinery applications involve symmetric polyphase machines connected to balanced polyphase electrical networks or voltage sources.

The simulation presented here is unique in two respects. First of all the problem of magnetic saturation in the machine is treated at a very fundamental level in the development of the machine model equations. The non-linearity of the magnetic energy storage in the machine, due to saturation, may be represented in terms of a magnetic coenergy function. In turn, the expressions for electromagnetic torque and flux linkages in a machine can be obtained directly as derivatives of this coenergy function. Consequently, in the development for the model of this thesis, the effects of magnetic saturation were incorporated in the derivation of the basic equations for electromagnetic torque and flux linkage in the machine.

Generally, the non-linear effects of magnetic saturation in a machine will also result in distortion of the basic sinusoidal shape of the spatial flux distribution around the air-gap circumference of the

machine. However, it was shown that for the special case of the uniform air-gap machine with sinusoidally distributed windings, the harmonic content of the distorted space flux distribution, arising from the non-linear effects of magnetic saturation, does not effect the torque, winding currents, or voltages in the machine. The performance of the actual machine, subject to magnetic saturation, is the same as if the actual distorted flux space distribution were replaced by a purely sinusoidal distribution whose magnitude is equal to the fundamental sinusoidal space component of the actual distribution in the saturated machine. Consequently, the performance of a magnetically saturated uniform air-gap machine with sinusoidally distributed windings can be represented by an equivalent magnetically linear machine. One aspect of this representation by an equivalent magnetically linear machine is the fact that the effective magnetizing inductance of the saturated machine can be represented as the slope of the chord from the origin to the operating point on the open-circuit magnetization curve of the actual machine. This representation of the effects of magnetic saturation by a chordal inductance, in terms of an equivalent magnetically linear machine, considerably simplifies the treatment of saturation for the machine model of this thesis.

The second unique feature of the present simulation is its generality in terms of its ability to model machines having asymmetric and/or an arbitrary number of open-circuited windings. This feature is a direct consequence of the fact that the machine model was developed directly in terms of physical coil variables. Consequently, the machine model of this thesis may be used to simulate single-phase machinery, unbalanced faults, or opening and reclosing of circuit breakers in

polyphase machinery, etc. Furthermore, it should be emphasized that machines having less than four windings may also be simulated by the machine model of this thesis, as long as the existing windings satisfy the basic conditions of sinusoidal distribution and orthogonality. This representation of machines having less than four windings by the model of this thesis is possible because any non-existent winding may be considered as an existing, but open circuited, winding in the basic four-winding model. The simulation of machines having open-circuited or asymmetric winding in terms of the physical coil-variable machine model of this thesis is particularly appropriate because the computational advantages of a simulation in terms of dq variables are often lost or greatly diminished whenever the machine is asymmetric or its environment is unbalanced.

A particularly vexing problem associated with the digital simulation of rotating electrical machinery is that of the upper limit on computational step size imposed by the value of the smallest electrical time constant in the system consisting of the machine and its external environment. In effect, the maximum allowable value of integration step size used in digital simulation must be limited to less than approximately 1/2 of the smallest electrical time constant in the system being simulated, in order to insure computational stability of the simulation. As a result of this limitation, the computation time required for digital simulation of the machine's dynamic behavior over a given time span can become excessively large, and thus correspondingly expensive, in situations where the electrical time constants formed by the machine and its environment are very small relative to the desired time span of the simulation. Generally, the most critical time constant, in this regard,

is that formed by a combination of the total machine leakage inductance and the largest value of stator or rotor winding circuit resistance. It is noteworthy that this problem does not exist when the machine simulation is implemented on an analog computer, because computational integration on an analog computer is a continuous rather than a discrete process. The existence of this problem is perhaps the principal reason for the traditional implementation, at least until recently, of most dynamical simulations of rotating electrical machinery on analog rather than digital computers.

4.2 Simulation of Multi-Machine Systems

Several methods of simulating systems consisting of two or more electrically interconnected machines were described in Section 2.11, and the relative advantages and difficulties associated with each method were discussed. The basic problem of multi-machine system simulation is to organize the equations of the individual machine models and of the interconnection network in such a way as to enable a computationally efficient implementation of the simulation.

From another point of view, the problem is to choose and combine the mathematical models of the individual machines and network components in the system such that the input/output computational causality requirements of each component model in the overall system are satisfied. The conventional simulation model for a rotating electrical machine has integral causality (voltage input/current output). Furthermore a direct interconnection between two or more machine models having the same causality requirements is causally inconsistent. Consequently, the computational causality requirements of all component models in an interconnected multi-machine system can almost always be satisfied if

some of the machines in the system are allowed to be represented by computational models having derivative causality (current in/voltage out). However the use of machine models having derivative causality entails the use of computational differentiation in the simulation, and this is frequently considered undesirable, particularly when the simulation is to be implemented on an analog computer. If the use of computational differentiation is to be avoided, the problem of simulating a system of interconnected electrical machines becomes particularly difficult in situations where the machine interconnection network does not include resistive or capacitative shunt impedances. In principle, such a system of directly interconnected machines (in which the interconnection network does not include shunt impedance elements) can always be simulated without resorting to the use of computational differentiation in the simulation. However, the complexity of the mathematical operations required to combine the model equations of the individual machines in the system with those of the interconnection network, such that the simultaneous solution of the resulting system of equations can be obtained without resorting to the use of computational differentiation often becomes prohibitively burdensome. Consequently, in many simulations of directly interconnected machine systems, the use of computational differentiation appears as the lesser of two evils.

Basically, notwithstanding techniques in which the causality requirements of machine models are inverted through the use of simplifying assumptions about the nature of the model (ie., a model representation in terms of voltage behind a single machine reactance), there are three distinct methods of modelling a system composed of two or more interconnected rotating electrical machines. The first of these is

applicable only to situations where the interconnection work includes resistive or capacitative shunt impedance elements. The applicability of the latter two methods is more general in scope; however, their application is of interest primarily in situations where the interconnection between machines is direct and does not include stationary shunt impedance elements.

1. The machine interconnection network contains resistive or capacitative shunt impedance elements. The individual machines in the system are represented by single machine models which have integration causality (voltage in/current out), such as the basic machine model of this thesis. Because of the presence of resistive or capacitative shunt elements in the interconnection network, the required input voltages to individual machine models can be computed from the equations of the interconnection network as a function of the machine currents. When this simulation method is implemented in a digital computer, the physical time constants of the system, arising from the interaction of the machine leakage inductances with the network impedances, may restrict the maximum allowable integration step size to the point where the simulation becomes computationally rather inefficient, or in extreme cases, even uneconomic.

2. At least one machine in the system is simulated by a model having derivative causality (current in/voltage out). The computed output voltage of this machine is then used to determine the input voltages to the remaining machines in the system which are simulated by conventional models having integral causality. The use of a machine model having derivative causality entails the use of computational differentiation in the simulation, which may be undesirable.

3. The equations of the individual machine models are analytically combined with those of the interconnection network in order to eliminate redundant state variables created by the constraints of the interconnection. In other words, the equations of all machine models and components of the interconnection network are combined into a single system of equations for the overall system whose solution can be obtained without the use of computational differentiation. In the case where the interconnection network includes resistive or capacitative shunt impedance elements, this method is equivalent to method 1 described above. When the interconnection network does not include these shunt impedance elements, the situation becomes much more difficult. A preliminary investigation has indicated that, because of its complexity, the application of this method appears to be generally impractical except for the special case of two directly interconnected symmetric machines. An example of the application of this method to the simulation of a system of two directly interconnected four winding symmetric machines was given in Appendix C.

The above discussion of the various methods of implementing simulations of systems of two or more electrically interconnected machines is applicable to both analog and digital computer implementations of such simulations.

4.3 Representative Applications

Several application examples of the machine simulations developed in this thesis were described in Chapter 3 for a variety of single and two-machine systems.

The following three examples were given for simulation of single machines; the individual machines were connected to an infinite bus

(ideal voltage source): (1) start-up and free acceleration of a balanced two phase induction motor, (2) start-up and free acceleration of a capacitor-start, unsymmetric single phase induction motor, (3) transient response of a synchronous motor to step changes in shaft load torque.

Two examples of two-machine simulations were also described. In both of these examples, the systems consisted of an induction motor being started from a power line which was connected to a basic resistive load, such as incandescent lighting, and supplied by a single alternator having voltage and frequency regulation. In the first of these two examples, the machines, the power lines, and the resistive load were represented as balanced two-phase components. In the second example, the machines, power line, and resistive load were modeled as single phase components. In both of these simulations, because of the presence of the resistive load on the power line, the system was modeled using the first method of multi-machine simulation described in the previous section. The individual machines were represented by the basic round-rotor single machine model developed in this thesis.

4.4 Conclusions

The following appear to be the most significant problem areas in the digital simulation of rotating electrical machinery.

4.4.1 Computational Constraints Imposed by Value of Physical Time Constants on the Allowable Magnitude of Integration Step Size

This problem is generally encountered in digital simulations of all dynamic systems whose eigenvalues (or natural frequencies) encompass a wide bandwidth. In effect, the value of integration step sized used

in the computations must be kept smaller than the magnitude of the shortest time constant, or period of the highest natural frequency, in the system being simulated, in order to insure computational stability of the simulation. For the case of rotating electrical machinery, the bandwidth of interest ranges from the low frequencies associated with the relative long electromechanical time constants (seconds) to high frequencies associated with the reciprocals of the relatively short electrical circuit time constants (milliseconds) of the machine. In order to simulate the dynamic response of the machine over this entire frequency range, the time duration of the simulation must be greater than the longest system time constant, or period of the lowest natural frequency of interest. However, since the maximum allowable step size is limited by the value of the shortest system time constant, the number of integration steps, and thus computation time, increases in direct proportion with the bandwidth of the simulation.

Development of methods for "spectral decomposition" of the machine dynamical equations, so that machine variables directly associated with the fast electrical time constants could either be neglected or computed separately from those associated with the slower electromechanical dynamical response of the machine, would greatly increase the computational efficiency for digital computer simulations of rotating electrical machinery. It appears that one of the principal reasons for the widespread use of analog computers in the simulation of rotating electrical machinery is the fact that, because computational integration on an analog computer is a continuous process, the computational efficiency of analog computer simulations is generally not degraded by increased bandwidth of simulation.

4.4.2 Computational Representation of Models for Multi-Machine System Simulation

Several alternative methods of modelling multi-machine systems were described, however there are significant problems associated with the application of each of these methods. In the first method, the presence of resistive or capacitative shunt impedances in the interconnection network permitted each of the individual machines in the system to be represented by conventional computational models having integration causality. However, this method is particularly prone to computational difficulties, such as described in Section 4.4.1 above, arising from the presence of relatively short time constants in the interconnected system, due to the interaction between the leakage inductances of individual machines and the network impedances.

The second method entails the use of computational differentiation, which may be undesirable, particularly if the simulation is implemented on an analog computer.

The third method of analytically combining the equations of the individual machine models with those of the interconnection network appears to be impractical, because of the complexity of the resulting equations, in all but the very simplest case of two direct-coupled symmetric machines.

However, it appears that use of either the second or the third method is required in the simulation of directly coupled machine systems situations in which no shunt impedance elements are present in the interconnection network), unless the computational causality for one or more machine models in such a system is inverted through the use of a simplified model such as "voltage behind a fixed machine reactance", or

a dq representation in which the "transformer voltages" are neglected.

Unlike the problem of computational constraints posed by the physical time constants of the system, the problem of modelling multi-machine systems for simulation, particularly those which are direct coupled, must be faced regardless of whether the simulation is implemented on an analog or a digital computer.

Despite the additional computational difficulties encountered in digital simulation of rotating electrical machinery, in comparison with analog simulation, the principal advantages of digital simulation are its much greater flexibility, reliability, and reproducibility. In addition, digital simultion also has another important advantage with respect to the simulation of multi-machine systems. The implementation on an analog computer of a simulation for a system composed of more than two interconnected rotating machines, in which each machine is modelled in detail, usually becomes extremely cumbersome. The representation of such a system for simulation on a digital computer, on the other hand, presents no special problems. However, the computation time required for digital simulation of a multi-machine system usually increases at least linearly with the size of the system and may, under certain conditions, become so large as to make the simulation uneconomic.

REFERENCES

1. Concordia, C., Brown, P. G., Miller, W. J., and Wuosmaa, L. "Synchronous Starting of Motor from Generator of Small Capacity", IEEE Trans. PAS, Vol 86, pp 1215-1227, October 1967.

2. Ewart, D. N. and DeMello, F. P. "FACE, A Digital Dynamical Analysis Program", presented at Power Industry Computer Applications Conference, May 15-17, 1967.

3. Fitzgerald, A. E. and Kingsley, C., Jr. "Electric Machinery", Second Edition, McGraw Hill, 1961.

4. Jordan, H. E. "Digital Computer Analysis of Induction Machines in Dynamic Systems", IEEE Trans. PAS, Vol 86, pp 722-728, June 1967.

5. Karnopp, D. C. and Rosenberg, R. C. "Analysis and Simulation of Multiport Systems", MIT Press, 1968.

6. Koopman, R. J. W. and Trutt, F. C. "Direct Simulation of AC Machinery Including Third Harmonic Effects" presented at IEEE Summer Power Meeting, Chicago, Illinois, June 23-28, 1968.

7. Krause, P. C. and Thomas, C. H. "Simulation of Symmetrical Induction Machinery", IEEE Trans. PAS, Vol 84, pp 1038-1053, November 1965.

8. Krause, P. C. "Simulation of Unsymmetrical Two-Phase Induction Machines", IEEE Trans. PAS, Vol 84, pp 1025-1037, November 1965.

9. Krause, P. C. "Method of Multiple Reference Frames Applied to the Analysis of Symmetrical Induction Machinery", IEEE Trans. PAS, Vol 87, pp 218-227, January 1968.

10. Kron, G. "Equivalent Circuits of Electric Machinery", Dover Publications, Inc., 1967.

11. Prabhashankar, K. and Janischewskj, W. "Digital Simulation of Multi-Machine Power Systems for Stability Studies", IEEE Trans. PAS, Vol 87, pp 73-80, January 1968.

12. Rosenberg, R. C. "Computer-Aided Teaching of Dynamic System Behavior" PhD Thesis, Department of Mechanical Engineering, Massachusetts Institute of Technology, September 1965.

13. Schultz, D. G. and Melsa, J. L. "State Functions and Linear Control Systems", McGraw Hill, 1967.

14. Undrill, J. M. "Power System Stability Studies by the Method of Liapunov: I-State Space Approach to Synchronous Machine Modelling" IEEE Trans. PAS, Vol 86, pp 791-80, July 1967.

15. Undrill, J. M."Dynamic Stability Calculations for an Arbitrary Number of Interconnected Synchronous Machines", IEEE Trans. PAS Vol 87, pp 835-844, March 1968.

16. White, D. C. and Woodson, H. H. Electromechanical Energy Conversion, John Wiley & Sons, 1959.

APPENDIX A

DERIVATION OF THE ELECTRO-MECHANICAL EQUATIONS OF MOTION FOR A MAGNETICALLY NON-LINEAR, SMOOTH AIR GAP ROTATING MACHINE

A.1 Description of Machine Model

In this Appendix the dynamical equations of motion for the conventional, four-winding, smooth air-gap, rotating electrical machine will be derived. A schematic sketch of this machine, illustrating the arrangement of windings follows:

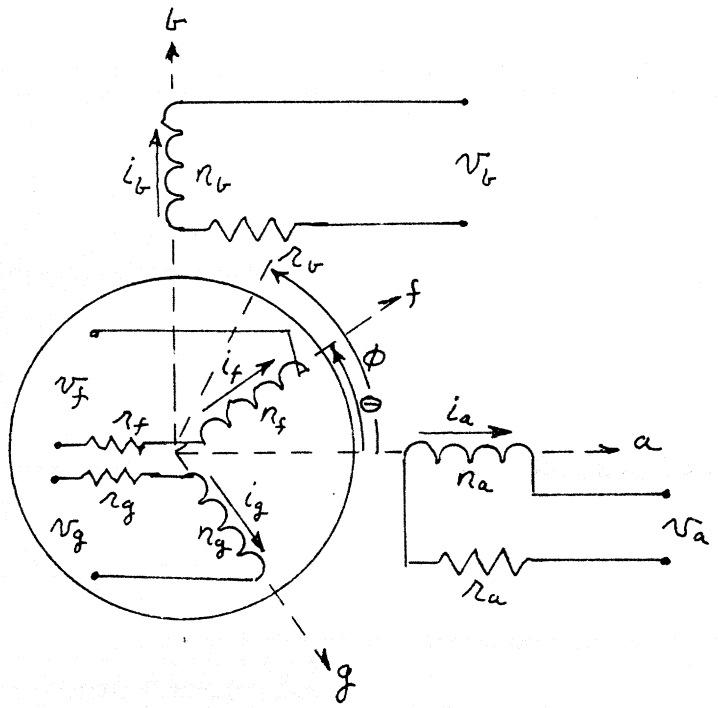

Fig. A1. Schematic Diagram of Four-Winding Machine Model

θ angle measured from stator "a" axis to rotor "f" axis

ϕ angle measured from stator "a" axis to an arbitrary angular position of the air-gap periphery

The orthogonal set of axes (a,b) is fixed to the stator and is coincident with the axes of the two stator windings; and similarly the set of axes (f,g) is fixed to the rotor and is coincident with the two orthogonal rotor winding axes.

In the analysis which follows, no restrictions of magnetic linearity are imposed, thus enabling the effects of saturation to be rigorously treated; however, hysteretic effects will not be considered. In addition, no assumption of winding symmetry will be made in this analysis. Consequently the analytical model to be developed may be used to simulate machines having arbitrary numbers of turns on each winding.

However, the class of machines which are analyzed herein will be restricted to those having a smooth rotor and a uniform, coencentric air-gap between stator and rotor, such that the path for magnetic flux across the air-gap and through the iron of the two machine structures (rotor, stator) will be independent of their relative position.

Aside from the geometrical restriction of a smooth air gap, discussed above, the following additional assumptions regarding the machines electromechanical characteristics are made in order to simplify the analysis.

1. Sinusoidal Distribution of MMF in the Air Gap

All coil windings on both machine structures are assumed to be so distributed as to produce sinusoidal space waves of mmf around the periphery of the air gap. This is a very reasonable assumption for a large class of machinery, since the actual winding distributions, particularly in polyphase AC machinery, are generally designed to provide as

close an approximation to a sinusoidal space distribution of mmf in the air-gap as is economically feasible. Note however, that this assumption does not necessarily also imply a sinusoidal space distribution of air gap flux, since the basic sinusoidal shape of the flux wave will generally be distorted by the effects of magnetic saturation.

2. Orthogonality of Windings

The winding axes on each of the two machine structures are assumed to be electrically orthogonal to each other. However, the windings themselves are not restricted to being symmetrical and may have arbitrary numbers of turns. The implication of electrical orthogonality is that there is no mutual magnetic coupling between orthogonal windings - thus for example in Fig. A1 there is no mutual coupling between the two stator windings or between the two rotor windings. For a two-pole machine, as described in Fig. A1, electrical orthogonality also implies physical or mechanical orthogonality between the winding axes. The analytical model to be developed is for a two pole machine. However, the extension of the results obtained from this model to a 2n pole machine is straightforward, the effect of the n pole pairs being simulated simply by a gear ratio on the mechanical shaft in proportion to the number of electrical pole pairs. The assumption of electrical orthogonality between windings precludes the simulation of machines having non-orthogonal windings such as shaded-pole motors.

3. Single Layers of Winding on Each Machine Structure

It is assumed that there is only a single winding on each axis of each machine structure (stator, rotor). Thus the basic machine to be analyzed has at most four independent windings, one orthogonal pair on

each structure as shown in Fig. A1. Because of this restriction, machinery problems in which the effects of multi-layered windings such as direct axis armostisseur windings in synchronous machines, double-squirrel cage windings in induction machine, or in which the distributed inductance effects due to eddy currents in solid iron structures become important, cannot be treated by the analytical model to be developed here.

4. Leakage Inductances

It is assumed that the leakage flux paths for all windings are mostly in air and thus remain unsaturated. On the basis of this assumption, the leakage fluxes for each winding are considered to be linear functions of the respective winding currents, and therefore the effect of winding leakage fluxes are modeled by constant linear inductances which are appended externally to each winding.

A.2 Derivation of Magnetic Coenergy Function for the Machine Model

Since it is desired to take the effects of magnetic saturation into account in a more or less rigorous manner, no assumptions regarding electromagnetic linearity are made. A very general method of obtaining the constitutive relations for a non-linear electromechanical system is to derive these relations from the magnetic energy and co-energy functions which describe the nature of the magnetic energy stored in the machine iron structures and the air gap.[16] In the present machine model, the space density of magnetic energy storage will vary around the periphery of the air-gap because of the space sinusoidal distribution of mmf created by currents flowing in the coil windings. However, since the air-gap and iron structure of the machine have been assumed to be axi-symmetric, a single magnetization curve for the local

variation of flux density with mmf around the air gap will represent the magnetic characteristics at all points along the air-gap periphery. Such a magnetization curve of the radial flux per unit length along the periphery of the air gap as a function of the local value of mmf is illustrated in Fig. A2. The local value of mmf at a point along the air gap periphery is defined as the instantaneous mmf produced by all windings enclosed by the semi-circular path which crosses the air gap at that point.

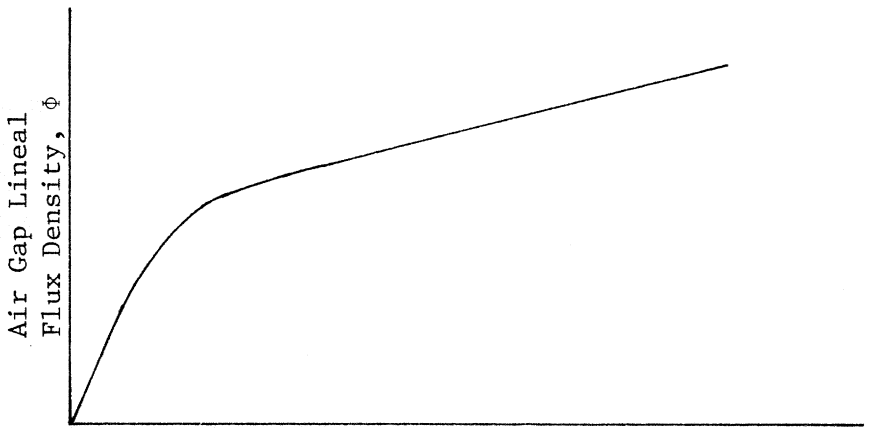

Fig. A2. Localized Magnetization Curve for Any Point Along Air Gap Periphery

Given the local magnetization characteristics in terms of a curve such as Fig. A2, the magnetic stored energy and coenergy may be computed per unit peripheral length as

$$\text{energy} \qquad W_m = \int_0^{\Phi} F \, d\Phi' \qquad \text{(A1)}$$

$$\text{co-energy} \qquad W_m^* = \int_0^F \Phi d\, F' \tag{A2}$$

where the primes signify dummy variables of integration.

It is shown in most modern electromechanics texts[3], [16] that the mechanical torque and the winding flux leakages can be obtained from A2 by differentiation of the coenergy of the electromechanical system:

$$\tau = -\frac{\partial W_m^*}{\partial \theta}\ ; \qquad \lambda_i = \frac{\partial W_m^*}{\partial i_i} \tag{A3}$$

Equation A3 implies that W_m^* is a function of the rotor angle θ, and the currents flowing in all four windings (i_a, i_b, i_f, i_g). This is indeed the case since, as will be shown in the following, the upper limit of integration in Eq. A2 for W_m^* is a function of those five variables.

Equations A3 are the cornerstones upon which the following analysis is constructed. We next examine the relationship for the air gap mmf $F(\theta, \phi, i_a, i_b, i_f, i_g)$ which is the upper limit of integration of (A2). For brevity this mmf will be written as $F(\theta, \phi, \underline{i})$, the four coil currents being represented as a vector.

The winding of each coil was assumed to be sinusoidally distributed, consequently each winding produces an mmf, proportional to the current through it, that is sinusoidally distributed in space along the circumference of the air-gap periphery. The definition of air-gap mmf is the net sum of currents flowing through the interior of a closed contour which encloses the coil turns of all the windings and which

crosses the air-gap circumference at two diametrically opposite points (in a multipole machine this closed contour crosses the air gap at two points which are 180° electrically apart). The value of the mmf at a particular angular position along the air-gap circumference is then defined as the mmf value associated with the integration contour crossing the air gap at that point. This interpretation of air-gap mmf corresponds to that developed in Chapter 3 of [3]. Since the mmf distributions produced by each of the windings are additive, and because the sum of several sinusoids of equal period is also a sinusoid, the combined mmf of all the windings will also be sinusoidally distributed in space around the air-gap circumference.

A developed view of the air gap, illustrating the distribution of all four windings, the reference contour for computation of mmf, and the resultant sinusoidal mmf space distribution is shown in Fig. A3. In correspondence with Fig. A1, all angles are measured from the stator "a" axis; θ is the rotor angle, and ϕ is the angle to some arbitrary point on the air-gap periphery. In addition, the following quantities which describe the sinusoidal mmf wave are also defined. F_p is the peak magnitude of the resultant mmf distribution, and ϕ_p is the angular location of the peak mmf on the air-gap circumference. It can be seen that the parameters ϕ_p, F_p uniquely define the instantaneous mmf distribution in the air-gap; both ϕ_p and F_p are functions of the four coil currents and the rotor angle.

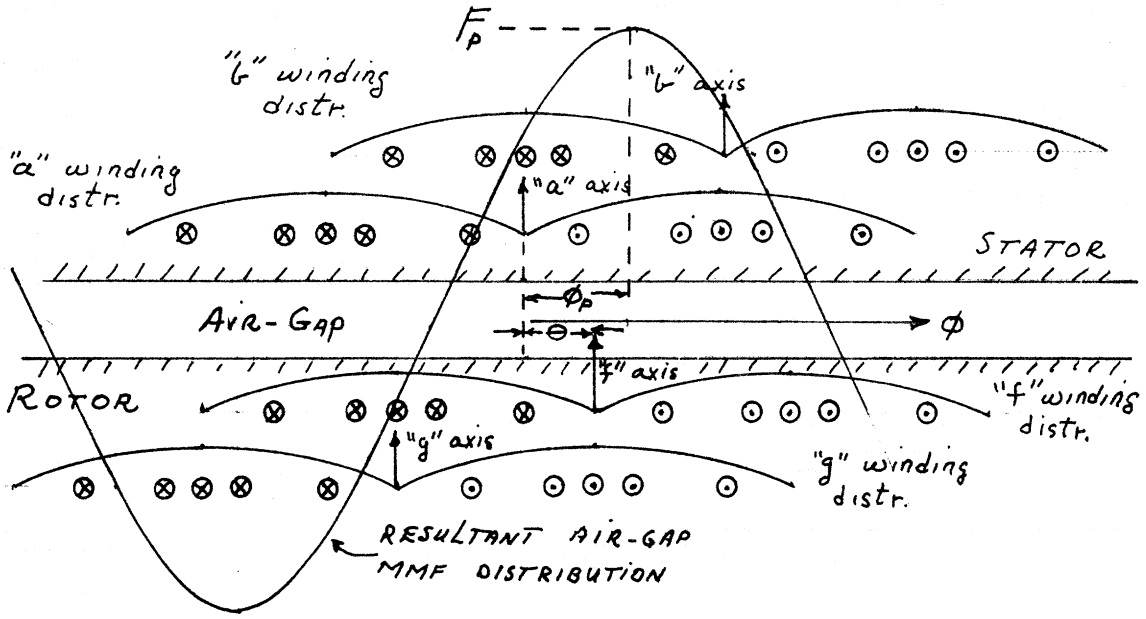

Fig. A3. Developed View of Winding and MMF Space Distributions Along Air Gap Periphery

The relation for the mmf distribution illustrated in Fig. A3 can be obtained in terms of the coil currents and rotor angle, by adding the mmf contributions of each of the four windings at the air gap position, defined by the angle, ϕ, at which the mmf is to be computed. With reference to Fig. A1, this conbination of winding mmf's can also be performed vectorially as follows. Since the mmf distributions due to the individual windings are all space sinusoids, the contribution of each winding may also be represented as a space phasor directed along the winding axis. The net mmf at location ϕ is then equal to the sum of the projections of the space phasors for each winding in the ϕ direction. By either method, the resultant expression of the net mmf distribution is found to be:

$$F(\theta,\phi,\underline{i}) = n_a i_a \cos\phi + n_b i_b \sin\phi + n_f i_f \cos(\phi-\theta) - n_g i_g \sin(\phi-\theta) \quad \text{(A4)}$$

Note that the mmf computed by Eq. A4 creates a magnetic field intensity distribution around the entire contour, passing through both the air gap and the iron structure, and no assumption is made that the resultant magnetic field intensity is concentrated entirely in the air gap and is thus zero in the iron structure, as in the case analyses in which magnetic saturation is neglected. However, the specific distribution of H in the iron and air along the contour does not need to be explicitly determined. The effect of this distribution on the resultant flux is taken into account empirically by use of the magnetization curve, Fig. A2, which is an empirical relationship between the local flux and mmf along the air gap circumference.

From Eq. A4 the values of mmf in the air gap at the locations of the coil axes for the stator "a" and "b" windings ($\phi = 0, \pi/2$) can be obtained directly as follows:

$$F_a(\theta,\underline{i}) = F(\theta,0,\underline{i}) = (n_a i_a + n_f i_f \cos\theta + n_g i_g \sin\theta) \quad \text{(A5a)}$$

$$F_b(\theta,\underline{i}) = F(\theta,\pi/2,\underline{i}) = (n_b i_b + n_f i_f \sin\theta + n_g i_g \cos\theta) \quad \text{(A5b)}$$

One can then compute the magnitude and position along the air gap periphery of the peak mmf in terms of the orthogonal components given by A5, as follows.

$$F_p(\theta,\underline{i}) = (F_a^2(\theta,\underline{i}) + F_b^2(\theta,\underline{i}))^{1/2}$$

$$\phi_p(\theta,\underline{i}) = \tan^{-1}\frac{F_b(\theta,\underline{i})}{F_a(\theta,\underline{i})} \quad \text{(A6)}$$

Using the definitions given by (A6), the expression (A4) for mmf at any location ϕ along the air gap may also be written as:

$$F(\theta,\phi,\underline{i}) = F_p(\theta,\underline{i}) \cos(\phi - \phi_p(\theta,\underline{i})).$$

Having established expressions for the mmf $F(\theta,\phi,\underline{i})$ at any angle ϕ in the air-gap, we can now proceed to compute an expression for the total magnetic co-energy in the air-gap from which the electromagnetic torque and winding flux linkages may then be computed using Eq. (A3). Because of the assumed uniform smoothness of the air-gap, the magnetization curve Fig. A2, gives the functional relationship between flux and mmf at every point along the air-gap periphery. It can be seen from Fig. A2 that the flux per unit length of air gap periphery may be expressed as a non-linear single-valued function of the mmf, F. $\Phi = \Phi(F)$. Using this substitution, the expression (A2) for co-energy per unit peripherial length at angle ϕ along the air gap becomes:

$$w_m^*(\theta,\phi,\underline{i}) = \int_0^{F(\theta,\phi,\underline{i})} \Phi'(F')dF'$$

Here the upper limit of the integral is the local value of mmf given by (A4). Thus w_m^* is an implicit function of the variables, $\theta,\phi,\underline{i}$ which determine F.

The total magnetic co-energy of the air gap may then be obtained by integrating the above expression for co-energy per unit length around the air-gap periphery to obtain:

$$W_m^*(\theta,\underline{i}) = R \int_0^{\pi} \int_0^{(\theta,\phi,\underline{i})} \Phi(F')\, dF'\, d\phi \qquad \text{(A7)}$$

where R is the air-gap radius. The integration limits in Eq. (A7) are 0 to π rather than 0 to 2π, because the both flux and mmf are symmetrically distributed and the same flux crosses the air gap twice, thus all the flux crossing the air-gap is taken into consideration when integrating from 0 to π.

The total magnetic co-energy of the machine may be obtained by adding the co-energy of the constant external winding leakage inductances to the magnetic co-energy of the air gap given by (A7) to obtain

$$W_m^*(\theta,\underline{i}) = R \int_0^{\pi} \int_0^{F(\theta,\phi,\underline{i})} \Phi(F')\, dF' d\phi + \frac{1}{2} \sum_{j=1}^{4} \ell_j\, i_j^2 \qquad \text{(A8)}$$

A.3 Derivation of Electromagnetic Torque from Machine Co-Energy

We can now proceed to obtain direct expressions for the electromagnetic torque and the winding flux linkages by differentiating (A8) as per Eq. (A3).

We begin by finding the expression for the torque by differentiating $W_m^*(\theta,\underline{i})$ with respect to the mechanical displacement variable θ.

$$\tau = -\frac{\partial W_m^*(\theta,\underline{i})}{\partial \theta} = -R \int_0^{\pi} \Phi[F(\theta,\phi,\underline{i})]\, \frac{\partial F(\theta,\phi,i)}{\partial \theta}\, d\phi \qquad \text{(A9)}$$

where the differentiation has been performed inside the ϕ integral. The expression for $\frac{\partial F}{\partial \theta}$ can be readily found by differentiating (A4).

$$\frac{\partial F(\theta,\phi,\underline{i})}{\partial \theta} = (n_f i_f \sin(\phi - \theta) + n_g i_g \cos(\phi - \theta)) \qquad \text{(A10)}$$

In order to carry out the ϕ integration it is still necessary to obtain an expression for the flux $\Phi[F(\theta,\phi,\underline{i})]$ as an explicit function of the variables θ, ϕ, and $\underline{i}$. The easiest way to proceed is to note that because Φ is a single valued function of F, as shown for example in Fig. A2, and because magnetic hysteretic effects are neglected, the space distribution of flux Φ will merely be a symmetrical distortion of the sinusoidal space distribution of mmf shown in Fig. A3. The distortion of the shape of the space flux distribution from that of a sinusoid is due soley to the non-linearity in the relationship between Φ and F. If Φ were a strictly linear function of F, the Φ space distribution would also be sinusoidal and differ from the sinusoidal F distribution by only a scale factor. A sketch of the space distribution of flux, distorted because of magnetic saturation, is shown below in comparison with the sinusoidal mmf distribution.

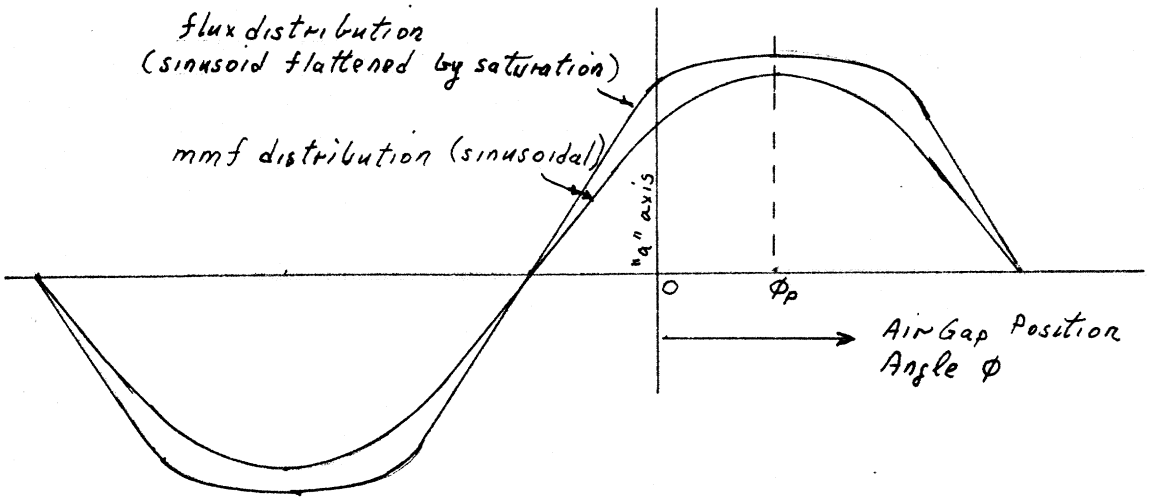

Fig. A4. Space Distributions of MMF and Flux Along Air Gap Periphery of Machine

From the symmetry of Fig. A4 it should be evident that the flux distribution in the air-gap can be represented as a Fourier cosine series about ϕ_p, the position in the air gap of the peak value of F, F_p. Thus,

$$\Phi(\phi,\phi_p) = \sum_{k=1}^{\infty} \psi_k \cos k(\phi - \phi_p) \qquad \text{(A11)}$$

Note that because the zero crossings of flux always coincide with those of mmf, the cosine series in (A11) contains odd harmonics only, that is: all $\psi_k = 0$, for k even. The ψ_k, in (A11) above, are the magnitudes of the harmonic components of the flux - ψ_1 is the magnitude of the fundamental component of Φ, etc.; the ψ_k are functions of the magnitude of the mmf distribution F_p and of the shape of the Φ vs F magnetization curve shown in Fig. A2. Thus in the following, ψ_k will be written as $\psi_k(F_p)$ to indicate that these coefficients are not necessarily absolute

constants.

Upon substituting (A10) and (A11) into (A9) the expression for the torque becomes:

$$\tau = - R \int_0^{\pi} \sum_{k=1}^{\infty} \psi_k(F_p) \cos k(\phi' - \phi_p) \left(n_f i_f \cos(\phi' - \theta) + n_g i_g \cos(\phi' - \theta) \right) d\phi' \qquad \text{(A12)}$$

Now if we make a substitution of variables and rearrange terms, the above may be written as:

$$\tau = - R\, n_f i_f \sum_{k=1}^{\infty} \psi_k(F_p) \int_{-\theta}^{\pi-\theta} \cos k(\phi' + \theta - \phi_p) \sin \phi'\, d\phi'$$

$$- R\, n_g i_g \sum_{k=1}^{\infty} \psi_k(F_p) \int_{-\theta}^{\pi-\theta} \cos k(\phi' + \theta - \phi_p) \cos\phi'\, d\phi'$$

and upon evaluating the indicated integrals, one obtains:

$$\int_{-\theta}^{\pi-\theta} \cos k(\phi' + \theta - \phi_p) \sin \phi'\, d\phi' = \begin{cases} 0; & k \text{ odd and } \neq 1 \\ \frac{\pi}{2} \sin(\theta - \phi_p); & k = 1 \end{cases}$$

$$\int_{-\theta}^{\pi-\theta} \cos k(\phi' + \theta - \phi_p) \cos \phi'\, d\phi' = \begin{cases} 0; & k \text{ odd and } \neq 1 \\ \frac{\pi}{2} \cos(\theta - \phi_p); & k = 1 \end{cases}$$

And so the expression for the torque reduces to:

$$\tau = -\frac{\pi R}{2} \psi_1 (F_p) \quad n_f i_f \sin(\theta - \phi_p) + n_g i_g \cos(\theta - \phi_p) \qquad (A12)$$

Now consider that $\psi_1(F_p)$ is the peak magnitude of the fundamental component of the space distribution of flux in the air gap, in terms of flux per unit length along the periphery of the gap. We can then express (A12) in terms of λ_{fm}, λ_{gm}, the fundamental components of the f and g winding mutual, or air-gap, flux-linkages, in lieu of in terms of ψ_1, ϕ_p, and θ. It will be shown subsequently that indeed:

$$\lambda_{gm} = \frac{-\pi R \psi_1 n_g}{2} \sin(\theta - \phi_p)$$

and

$$\lambda_{fm} = \frac{\pi R \psi_1 n_f}{2} \cos(\theta - \phi_p)$$

and that thus Eq. (A12) may be written in the following familiar form, the primes signifying referral of variables by the respective turns in each winding:

$$\tau = \lambda'_{gm} i'_f - \lambda'_{fm} i'_g \qquad (A13)$$

Consider the flux linkage of one turn of any machine winding by the fundamental component of air gap flux, the two sides of the turn being located at angles of α and $\alpha+\pi$. Then as seen in Fig. A5, the flux linkage of this single turn is given by:

$$\lambda_\alpha = R\psi_1 \int_{\alpha}^{\pi+\alpha} \cos(\phi - \phi_p)\, d\phi \qquad \text{(A14)}$$

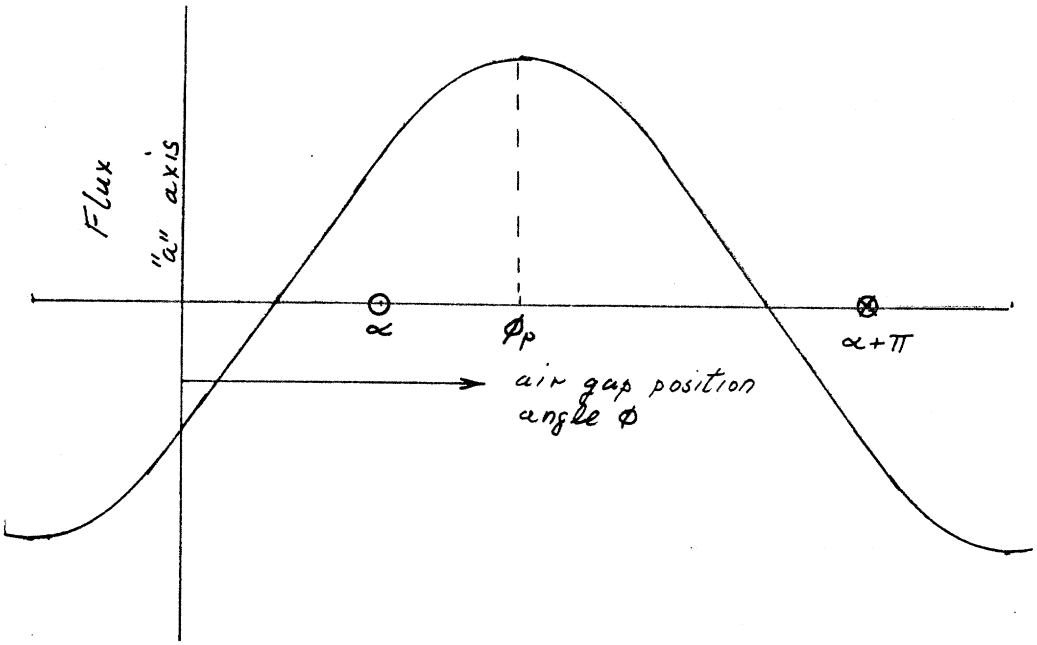

Fig. A5. Fundamental Component of Flux Distribution Relative to a Single Turn

Integration of Eq. (A14) gives the air-gap flux linkage of a single turn whose sides are located at α and $\pi+\alpha$ as:

$$\lambda_\alpha = -2R\psi_1 \sin(\alpha - \phi_p) \qquad \text{(A15)}$$

We now proceed to use Eq. (A15) to compute the total flux linkage for a given winding. As an example, the computation will be carried out for the "f" winding. The computations of total linkage for the other windings is completely analogous. Since the windings are assumed to be sinusoidally distributed in space, the number of turns of "f" winding per differential increment of air gap space angle is:

$$dn_f' = \frac{n_f}{2} \sin(\alpha - \theta)\, d\alpha \qquad \text{(A16)}$$

for $\theta - \pi \leq \alpha \leq \theta$

In the above θ is the angle of the "f" winding axis, α is the angular position of the first coil side of a particular turn, and n_f is the total number of turns in the "f" winding. When Eq. (A16) is integrated from $\theta - \pi$ to θ the result obtained is n_f turns as expected.

The total air-gap flux linkage for the f winding is obtained by integrating the product of the linkage per turn given by Eq. (A15) and the turns density given by (A16) over the extent of the turns in the winding, from θ to $\theta + \pi$.

$$\lambda_{fm} = \int_{\theta}^{\theta+\pi} \lambda_{\alpha}\, dn_f' = +R\, \psi_1\, n_f \int_{\theta}^{\theta+\pi} \sin(\alpha - \phi_p) \sin(\alpha - \theta)\, d\alpha \qquad \text{(A17)}$$

Thus, λ_{fm} is the total linkage of the f winding by the flux crossing the air gap. Upon change of variable and expansion this becomes:

$$\lambda_{fm} = R\, \psi_1\, n_f \int_{o}^{\pi} [\sin^2\alpha' \cos(\theta - \phi_p) + \sin\alpha'\, \cos\alpha'\, \sin(\theta - \phi_p)]d\alpha'$$

Integration gives:

$$\lambda_{fm} = R\, \psi_1\, n_f\, (\tfrac{\pi}{2})\, \cos(\theta - \phi_p) \qquad \text{(18a)}$$

When the above procedure is repeated for the "g" winding, the result obtained is:

$$\lambda_{gm} = -R\ \psi_1\ n_g(\tfrac{\pi}{2})\ \sin(\theta - \phi_p) \qquad \text{(A18b)}$$

When (A18a,b) are substituted into (A12) the following expression for torque is obtained:

$$\tau = \frac{\lambda_{gm}}{n_g}\, n_f i_f - \frac{\lambda_{fm}}{n_f}\, n_g i_g \qquad \text{(A19)}$$

Since in the formulation of Eq. (A3) $\tau d\theta > 0$ represents positive work input into the electromechanical system, the value of τ given in (A19) represents the external torque applied by the machine shaft to the magnetic field and is positive in the direction of increasing θ. Thus the magnetic field applies an equal and opposite torque to the rotor mechanical structure. When the flux linkages and currents appearing in (A19) are "referred" to the number of turns in the corresponding windings, (A19) reduces to (A13).

A.4 Derivation of Winding Flux Linkages

Although a method for determining the mutual component of the winding flux linkages by integrating the air-gap flux linkages of individual turns over the entire winding was developed in the previous section, in the course of the derivation of the torque Eq. (A19), the equations for linkages can also be directly determined from the magnetic co-energy by applying Eq. (A3). Thus upon differentiating Eq. (A8) as per (A3)

$$\lambda_i = \frac{\partial w_m^*(\theta,\underline{i})}{\partial i_i} = R \int_0^{\pi} \Phi[F(\theta,\phi,\underline{i})]\, \frac{\partial F}{\partial i_i}\,(\theta,\phi,\underline{i})\, d\phi + \ell_i i_i \qquad \text{(A20)}$$

The computation will now proceed explicitly for the case of the "f" winding; as before the computation of the flux linkages for the other windings is analogous. The expression for the space distribution of flux around the air gap was previously derived and is given by Eq. (A11). The derivative of $F(\theta,\phi,\underline{i})$ with respect to i_f is obtained from (A4) and is simply:

$$\frac{\partial F}{\partial i_f} = n_f \cos(\phi - \theta) \tag{A21}$$

Substitution of Eq. (A11) and Eq. (A21) into Eq. (A20) yields:

$$\lambda_f = Rn_f \int_0^{\pi} \sum_{k=1} \psi_k(F_p) \cos k(\phi - \phi_p) \cos(\phi - \theta) d\phi + \ell_f i_f$$

As before, the integrals of all terms in the summation over k vanish except when k = 1, and the result reduces to:

$$\lambda_f = \frac{\pi}{2} R\psi_1(F_p) n_f \cos(\theta - \phi_p) + \ell_f i_f \tag{A22}$$

Note that except for the additional term, $\ell_f i_f$, representing the flux linkage due to the winding's leakage inductance, Eq. (A22) gives exactly the same result as the previously derived expression for the air gap flux linkage λ_{fm} given in Eq. (A18a). The effect of leakage flux did not appear in Eq. (A18a) because that relation was solely derived on the basis of the mutual flux crossing the air gap between stator and rotor.

We now desire to express the flux linkages in terms of the winding currents. We proceed as follows. Recall that, in lieu of Eq. (A4), the expression for the mmf distribution could also be written as:

$$F(\theta,\phi,\underline{i}) = F_p(\theta,\underline{i}) \cos(\phi - \phi_p(\theta,\underline{i})) \tag{A7}$$

Then, according to Eq. (A7), the mmf along the "f" axis $\phi = \theta$, is given by:

$$F_f(\theta,\underline{i}) \equiv F(\theta,\theta,\underline{i}) = F_p(\theta,\underline{i}) \cos(\theta - \phi_p) \tag{A23}$$

Now use Eq. (A23) to eliminate $\cos(\theta - \phi_p)$ in (A22). The resulting expression for λ_f is:

$$\lambda_f = \frac{\pi R}{2} n_f \frac{\psi_1(F_p)}{F_p} F_f(\theta,i) + \ell_f i_f \tag{A24}$$

Similar expressions can be obtained for the flux linkages of the other windings. It will be recalled that ψ_1 is the magnitude of the fundamental component of the space harmonic expansion of the actual flux density distribution, and is a function only of the magnitude of the mmf distribution F_p, and of the magnetization curve for the machine. Thus given the local magnetization curve for the machine, such as illustrated in Fig. A2, and assuming a sinusoidal mmf distribution of the magnitude F_p, the relationship between ψ_1 and F_p can be computed from a harmonic analysis of the resultant space flux distribution. Indeed, when a saturation curve for a particular machine is actually obtained from experimental measurements, the resulting curve corresponds to this ψ vs F_p curve rather than the localized air-gap magnetization curve shown in Fig. A2. We now define the air-gap base inductance of the machine as

$$L(F_p) \equiv \frac{(\pi R)}{2} \frac{\psi_1(F_p)}{F_p} \tag{A25}$$

If $\psi_1(F_p)$ is plotted as a function of F_p, the value given by (A25) can be considered as the "chordal inductance" of the machine since its value is proportional to the slope of the chord to the operating point on the machine magnetization curve. Recall that the dimensions of $\psi_1(F_p)$ are flux per unit length, since in the localized magnetization curve (Fig. A2) $\phi(F_p)$ was defined as a flux density per unit length along the air-gap circumference. Consequently, the dimensions of (A25) are those of inductance, flux/mmf.

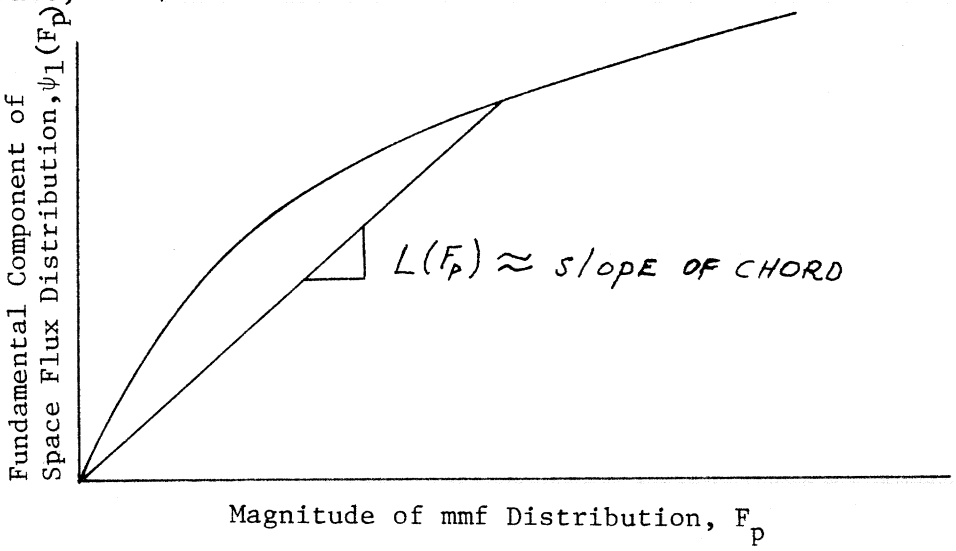

Fig. A6 Effective Machine Magnetization Curve

Fig. A6 is the effective machine magnetization curve because the fundametnal component, ψ_1, of the actual machine flux distribution is the effective value of magnetic flux with regard to the computation of torque and terminal voltage. Although Fig. A6 appears very similar to Fig. A2, the two magnetization characterisitcs are not the same. Fig. A2 is the local magnetization curve which relates local values of flux and mmf at any position along the air-gap. In contrast, Fig. A6 relates the fundamental component of the actual flux space distribution to the magnitude of the mmf space distribution in the machine.

Curves corresponding to Fig. A6 are normally obtained for generators in terms of open circuit voltage vs field excitation. For open circuit (no load) operation at constant speed the armature voltage is proportional to the air-gap flux magnitude, and in turn the magnitude of the mmf distribution is directly proportional to the applied field current. The value of chordal air-gap inductance can then be directly derived from such an open circuit magnetization curve.

Now we can substitute the defintion of Eq. (A25) into (A24), thus expressing the "f" winding linkage as

$$\lambda_f = L(F_p)\, n_f\, F_f(\theta,\underline{i}) + \ell_f i_f$$

Furthermore, if the expression for $F_f(\theta,\underline{i})$ is expanded using Eq. (A4) the result gives an explicit relation between the "f" winding flux linkage and the currents in all windings:

$$\lambda_f = (n_f^2\, L(F_p) + \ell_f) i_f + n_f n_a\, L(F_p)\, i_a \cos\theta + n_f n_b\, L(F_p)\, i_b \sin\theta \qquad \text{(A26)}$$

The flux linkage expressions for the remaining windings are obtained analogously. The results for all four windings are most compactly expressed in matrix notation as illustrated by Eq. (A27). For simplicity the chordal inductance $L(F_p)$ is written as L, though it is understood that it is not constant.

$$\begin{bmatrix} \lambda_a \\ \lambda_b \\ \lambda_f \\ \lambda_g \end{bmatrix} = \begin{bmatrix} n_a^2 L + \ell_a & 0 & n_a n_f L \cos\theta & n_a n_g L \sin\theta \\ 0 & n_b^2 L + \ell_b & n_b n_f L \sin\theta & -n_b n_g L \cos\theta \\ n_a n_f L \cos\theta & n_b n_f L \sin\theta & n_f^2 L + \ell_f & 0 \\ n_a n_g L \sin\theta & -n_b n_g L \cos\theta & 0 & n_g^2 L + \ell_g \end{bmatrix} \begin{bmatrix} i_a \\ i_b \\ i_f \\ i_g \end{bmatrix} \qquad \text{(A27)}$$

A.5 Effects of Magnetic Non-Linearity (Saturation)

The torque equation for the machine Eq. (A19) and the equations for the flux linkages of all four windings (A27), were derived in the previous section. Thus, having obtained the constitutive relations between the flux linkages, the currents, and the electromagnetic torque of the machine, we can proceed to develop the dynamical equations of motion for the machine in terms of applied winding terminal voltages and applied shaft torque. Before doing so, however, it is appropriate to pause briefly in order to spot-light some of the interesting and salient points of the previous analysis. First of all, although the mmf space distribution in the machine is, by definition, purely sinusoidal, the resultant space flux distribution will, because of magnetic saturation, generally appear as a distorted or squashed sinusoid, as shown in Fig. A4. This distorted flux distribution may be represented by a space harmonic expansion in terms of a Fourier series. The distortion of the fundamental space sinusoidal flux distribution by the effects of magnetic saturation therefore gives rise to the presence of harmonic components in the space flux distribution. It is therefore significant that only the fundamental component of the flux distribution, ψ_1, carried through into the final expressions for torque and winding flux linkages. Under

the assumptions of a uniform air-gap, and a sinusoidal mmf distribution, the effects of space harmonics in the flux distribution cancelled and in no way affected the final results. Thus since the final results depend only upon the fundamental component of the actual flux distribution, the final equations are greatly simplified and reduce to those of a magnetically linear machine having a flux distribution equal to the fundamental component of the non-sinusoidal flux distribution in the saturated machine. From the development leading to Eq. (A12) it is seen that the effect of the flux harmonics cancels only because the mmf distribution was assumed to be purely sinusoidal and thus free of harmonics. Had the mmf distribution also contained harmonics, there would have been interaction between the flux and mmf harmonics and the integrals leading to Eq. (A12) would not have vanished for $k \neq 1$. As a result, both the flux and torque expressions would have depended not only on the fundamental but also on the harmonic content of the space flux distribution. The same comments apply to a machine with a non-uniform air-gap. It can be shown that in a machine having a non-uniform air-gap, even when the mmf distribution is sinusoidal, any harmonics in the space flux distribution will, because of saliency, effect the expressions for torque and flux linkages of such a machine. It thus seems indeed fortuitous that for the case of a uniform air-gap machine with sinusoidally distributed windings, the effect of flux harmonics due to magnetic non-linearity cancel. Consequently the dynamical equations of this machine, in the event of magnetic non-linearity due to saturation, are identical to the equations of an equivalent magnetically linear machine whose sinusoidal space flux distribution has a magnitude equal to that of the fundamental space component of flux in the saturated machine.

The second point of interst has been well established in machinery practice for many years, but is not always satisfactorily justified on a fundamental basis. This is the fact that the mutual or "air-gap" inductance of a machine $L(F_p)$ which appears in the machine linkage equations is the chordal inductance of the machine magnetization curve as shown in Fig. A5. It should be noted that the "chordal inductance" $L(F_p)$ appearing in (A27) is not a linearizing approximation, it represents the exact relation between linkage and current as shown in Eq. (A27). Nonetheless care should be used in interpretating the meaning of the chordal inductance $L(F_p)$. Because it is not a constant, but a function of the air-gap mmf, F_p, expressions of the form:

$$e = \overset{o}{\lambda} = \frac{d}{dt}[Li] = L\frac{di}{dt}$$

are not valid, the problem being in the last equality since now:

$$\frac{d}{dt}[Li] = \left(\frac{dL}{di} + L\right)\frac{di}{dt}$$

Problems that could arise because of such a misinterpretation of the meaning of this chordal inductance parameter are avoided in the subsequent analysis by choosing the flux linkages, $\underline{\lambda}$, rather than the winding currents $\underline{i}$, as the state variables of the model.

A.6 Machine Dynamical Equations

Using motor reference conventions (current flow into machine) the voltage dynamical equations are:

$$
\begin{aligned}
v_a &= \overset{o}{\lambda}_a + r_a i_a \\
v_b &= \overset{o}{\lambda}_b + r_b i_b \\
v_f &= \overset{o}{\lambda}_f + r_f i_f \\
v_g &= \overset{o}{\lambda}_g + r_g i_g
\end{aligned}
\tag{A28}
$$

The quantities v_a, v_b, v_f, v_g are the terminal voltages applied to the four windings of the machine. The remaining dynamical equation is the torque balance equation for the rotor of the machine. Since the convention used in the derivation of the torque Eq. (A19) was that externally applied torques to the magnetic field of the machine are positive in the direction of increasing rotor angle θ, and since motor load torques (in keeping with the motor convention for the voltage equations above) oppose the direction of rotation, the torque balance equations become

$$
\tau_e = \tau_s - \rho\overset{o}{\theta} - J\overset{oo}{\theta} \tag{A29}
$$

In Eq. (A29) τ_e is the electromechanical torque given by Eq. (A19), τ_s is the externally applied mechanical torque (position for generator being driven by a prime mover, negative for a motor load), ρ is the mechanical bearing friction coefficient, and J is the moment of inertia of the rotor and shaft load. The dynamical Eqs. (A28) and (A29) together with the constitutive relations between linkages, currents and torque given by Eqs. (A19), (A27) serve to completely describe the electromechanical dynamics of the machine.

Before proceeding with the combination of these dynamical and constitutive relations into a single consistent set of differential

equations which describe the dynamical motion of the machine, it is desirable to simplify the constitutive relationships (A19), (A27) by a set of transformations which eliminate the appearance of the number of turns of each winding. This is the well known procedure of "referring" the parameters and variables for each winding to a common base. Thus we define the referred currents and linkages for each winding as follows:

$$\lambda_j' = \frac{\lambda_j}{n_j} \qquad i_j' = n_j i_j \tag{A30}$$

The unprimed quantities are the actual variables and the primed quantities are the referred variables.

Substituting these definitions into Eq. (A27) gives:

$$\begin{bmatrix} \lambda_a' \\ \lambda_b' \\ \lambda_f' \\ \lambda_g' \end{bmatrix} = \begin{bmatrix} L + \frac{\ell_a}{n_a^2} & 0 & L\cos\theta & L\sin\theta \\ 0 & L + \frac{\ell_b}{n_b^2} & L\sin\theta & -L\cos\theta \\ L\cos\theta & L\sin\theta & L + \frac{\ell_f}{n_f^2} & 0 \\ L\sin\theta & -L\cos\theta & 0 & L + \frac{\ell_g}{n_g^2} \end{bmatrix} \begin{bmatrix} i_a' \\ i_b' \\ i_f' \\ i_g' \end{bmatrix} \tag{A31}$$

When Eq. (A30) is substituted into the torque Eq. (A19) together with the following relations between the air-gap and the total (including leakage) winding flux linkages:

$$\lambda_{fm} = \lambda_f - \ell_f i_f \qquad \lambda_{gm} = \lambda_g - \ell_g i_g$$

(λ_f, λ_g are the total flux linkages and λ_{fm}, λ_{gm} are the air gap or mutual flux linkages of the f and g windings repectively.) The result is:

$$\tau_e = (\lambda_g' - \frac{\ell_g}{n_g^2} i_g') i_f' - (\lambda_f' - \frac{\ell_f'}{n_f^2} i_f') i_g'$$

OR:

$$\tau_e = \lambda_g' i_f' - \lambda_f' i_g' + (\frac{\ell_f}{n_f^2} - \frac{\ell_g}{n_g^2}) i_f' i_g' \qquad \text{(A32)}$$

Because the magnetic flux paths around each of two windings on a given structure of a uniform air-gap machine are usually equivalent, the ratio between the leakage inductances of the two windings is generally equal to the square of their turns ratio. When the leakage inductances of the two windings on a given structure satisfy the above proportionality condition, the windings are said to be symmetric. Consequently, for a uniform air-gap machine with symmetric windings, the last term in (A32) vanishes, and the resulting torque equations for a <u>symmetric</u> machine reduces to:

$$\tau = \lambda_g' i_f' - \lambda_f' i_g' \qquad \text{(A32a)}$$

In both Eq. (A32) and (A32a) the λ's are the total flux linkage for each winding, including the linkage due to the leakage fluxes.

Furthermore, in combining (A31) and (A32) with (A28) and (A29) it will also be convenient to define the leakage inductance and resistance of each winding on a referred basis:

$$r_k' \equiv \frac{r_k}{n_k^2} \qquad \ell_k' \equiv \frac{\ell_k}{n_k^2} \qquad \text{(A33)}$$

We are now in a position to combine Eq. (A28) through (A33) to obtain the differential equations of motion for the machine. There is still, however, one more choice to be made. We may use as state variables either the winding linkages λ_j or the winding currents i_j. That is, the differential equations may be written in either terms of λ_j or i_j. We choose to use the linkages λ_j as state variables in preference to the currents for the i_j for the following reasons. The first reason is associated with the physics of the machine. This is that the internal mutual flux linkages across the air gap of a machine are always continuous time functions despite the occurrence of discontinuities in the time behavior of winding currents or in the external environment to which the machine is connected. This is a manifestation of the well known "constant flux linkage theorem" that is often used in deriving the simplified equations for the response of the machine to electrical transients such as a sudden short circuit at the armature terminals of a machine. Thus if the machine flux linkages λ_i are used as state variables, it becomes unnecessary to recompute a new set of initial conditions when the machine environment undergoes a sudden change, as for example, when a winding current suddenly is forced to vanish because of the opening of a circuit breaker. The second reason for preferring the flux linkages as state variables over the currents is one of mathematics, in that magnetic non-linearity of the machine poses no special analytical problems when the λ's are the state variables. If, however, the currents were used as state variables, the expressions for voltages induced in the windings by the changing flux linkages would, in the case of the magnetically non-linear machine, involve derivatives of the chordal inductance function $L(F_p)$, thus greatly increasing the complexity of the resultant

differential equations.

Having decided to formulate the state differential equations of the machine in terms of the flux linkages, the currents may be eliminated from the voltage Eqs. (A28) by solving (A31) for the currents in terms of linkages. Equation (A31) may be written in vector-matrix form as:

$$\underline{\lambda}' = \underline{L}(F_p,\theta)\ \underline{i}' \tag{A34a}$$

where $\underline{L}(F_p,\theta)$ is the inductance matrix in Eq. (A31). Solving Eq. (A34a) for $\underline{i}$ gives:

$$\underline{i}' = \underline{\Gamma}(F_p,\theta)\underline{\lambda}' \tag{A34b}$$

where $\underline{\Gamma}(F_p,\theta) \equiv \underline{L}^{-1}(F_p,\theta)$ the inverse inductance matrix. Note by referring to Fig. A6 that $\underline{\Gamma}$ may also be equivalently expressed as a function of the magnitude of the fundamental space component of air gap flux in the machine, ψ_1, rather than the peak mmf, F_p. When Eq. (A34b) is substituted into (A28) the result in terms of referred variables, and in matrix notation is:

$$\underline{N}^{-1}\ \underline{V} = \overset{o}{\underline{\lambda}}' + \underline{R}'\ \underline{\Gamma}(\psi_1,\theta)\underline{\lambda}' \tag{A35}$$

The vectors and matrices used in Eq. (A35) are defined as follows:

Linkage Vector: λ

$$\underline{\lambda}' \equiv \begin{bmatrix} \lambda_a' \\ \lambda_b' \\ \lambda_f' \\ \lambda_g' \end{bmatrix}$$

Terminal Voltage Vector: V

$$\underline{V} \equiv \begin{bmatrix} v_a \\ v_b \\ v_f \\ v_g \end{bmatrix}$$

Coil Turns Referral Matrix: $\underline{N}$

$$\underline{N} \equiv \begin{bmatrix} n_a & 0 & 0 & 0 \\ 0 & n_b & 0 & 0 \\ 0 & 0 & n_f & 0 \\ 0 & 0 & 0 & n_g \end{bmatrix}$$

Referred Resistance Matrix

$$\underline{R}' \equiv \begin{bmatrix} r_a' & 0 & 0 & 0 \\ 0 & r_b' & 0 & 0 \\ 0 & 0 & r_f' & 0 \\ 0 & 0 & 0 & r_g' \end{bmatrix}$$

Inverse Inductance Matrix: $\underline{\Gamma}(\psi_1,\theta)$

$$\underline{\Gamma}(\psi_1,\theta) \equiv \underline{L}^{-1}(F_p,\theta)$$

$\underline{L}(F_p,\theta)$ defined by (A31)

ψ_1 is the fundamental component of the air gap flux distribution and is related to F_p by (A25). ψ_1 may be directly computed from the air-gap mutual components of the total coil flux linkages. $\underline{\Gamma}$ may be computed either as a function of ψ_1 or F_p which ever happens to be more computationally convenient.

The torque balance equation, which results from the combination of Eq. (A32) and (A29) may also be written in state variable form. For compactness, however, we do not eliminate the appearance of the currents in the torque equation, although it is understood that the currents appearing there are computed as a function of the flux linkages by Eq. (A34b). Thus the second order torque balance equation (A29), in combination with the expression for the electromagnetic torque Eq. (A32), can be written as two first order equations in the two mechanical state variables θ, ω.

$$\dot{\theta} = \omega$$

$$\dot{\omega} = \frac{1}{J} [\lambda_f' \, i_g' - \lambda_g' \, i_f' + (\ell_g' - \ell_f') \, i_f' \, i_g' - \rho\omega + \tau_s] \tag{A36}$$

The voltage equations for the four windings (A35) together with the shaft torque balanced Eqs. (A36) constitute a set of six simultaneous non-linear differential equations in the six machine state variables - the four winding flux linkages λ_a, λ_b, λ_f, λ_g, the rotor angular position θ, and the rotor speed ω. Usually the four winding terminal voltages v_a, v_b, v_f, v_g and the applied shaft torque τ_s are considered as the forcing functions or "input" variables to this system of equations. The equations are non-linear because of the dependence of $\underline{\Gamma}$ in Eq. (A35) upon both the shaft position θ and the magnitude or either the magnetizing mmf or the flux, and because of the appearance of λi products in the torque equation.

The machine equations (A35) and (A36) are integrated on a step-by-step basis by the method of Runge-Kutta, the step size being limited by the highest frequency components of interest in the applied terminal

voltages, and by the smallest significant electrical time constant of the machine. Usually, only the inductance matrix of the machine $\underline{L}(F_p,\theta)$ is given explicitly, and in general this matrix would have to be computationally inverted at each step to obtain $\underline{\Gamma}(\psi_1,\theta)$. The value of F_p or ψ_1 is computed at each step in the integration in order to determine the air-gap mutual inductance coefficient $L(F_p)$ which appears in the $\underline{L}$ matrix. A great increase in computational efficiency would be realized if a simple inverse of $\underline{L}$, that is a simple form of $\Gamma(\psi_1,\theta)$ could be obtained algebraically. This is indeed possible, as shown below, if the referred leakage inductances on each machine structure are symmetrical, that is if $\ell_a' = \ell_b'$ and $\ell_f' = \ell_g'$. Thus for the case of symmetrical leakage case if we define:

$$\ell_s' \equiv \ell_a' = \ell_b'; \qquad \ell_a' \equiv \ell_f' = \ell_g' \tag{A37}$$

The matrix $\underline{\Gamma}(F_p,\theta) = L^{-1}(F_p,\theta)$ for the symmetric machine is designated as $\underline{\Gamma}^*(F_p,\theta)$ and is given by:

$$\underline{\Gamma}^*(F_p,\theta) = \frac{1}{\Delta}\begin{bmatrix} L+\ell_r' & 0 & -L\cos\theta & -L\sin\theta \\ 0 & L+\ell_r' & -L\sin\theta & L\cos\theta \\ -L\cos\theta & -L\sin\theta & L+\ell_s' & 0 \\ -L\sin\theta & L\cos\theta & 0 & L+\ell_s' \end{bmatrix} \tag{A38}$$

$$\Delta \equiv (L+\ell_r')(L+\ell_s') - L^2$$

$$= L(\ell_r' + \ell_s') + \ell_r'\ell_s'$$

and where $L(F_p)$ has been written as L for compactness.

Because of the simplicity of the $\underline{\Gamma}$ matrix for the symmetric machine, as given by Eq. (A38), and because a large number of practical machines do indeed satisfy the symmetry condition Eq. (A37), we will assume that our basic machine model is a symmetric one. Note also that for the symmetric machine because the leakage inductances on each structure are equal (Eq. (A38)), the torque equation (A32) assumes the simpler form given by Eq. (A32a).

We now turn to the problem of modeling the more general machine with asymmetric and/or open circuited windings in terms of the analytically simpler symmetric machine. The principal motivation for using the symmetric machine as the basis for constructing a model of the asymmetric machine is that the Γ matrix for the symmetric machine can be computed merely by evaluating Eq. (A38), whereas a direct computation of the Γ matrix for the asymmetric machine would require a numerical matrix inversion of its inductance matrix for each value of θ and F_p. Indeed for the smooth air-gap four-winding machine which is being considered here, only two types of asymmetry are possible. Either there are open circuited (or non-existent) windings on one or both machine structures, or the windings on one or both structures have asymmetrical leakage inductances. It should be clear that a non-existent winding may be viewed as an existing open circuited winding. As will be seen in Appendix B, the modification of the basic symmetrical machine for one or more open-circuited windings is quite simple and straightforward. The machine with asymmetrical stator winding leakage inductances can be represented by connecting an external inductor, whose value is equal to the differential leakage inductance, of the two stator windings, in series with one of the stator windings of a symmetric machine model. The treatment

of open-circuited and/or asymmetric windings as adjuncts to the basic symmetric machine model is the subject of Appendix B. Thus, it can be seen that the mathematical model of a symmetric four winding smooth-air gap machine can be readily modified to represent a general asymmetric smooth air-gap machine.

To recapitulate, our basic symmetric machine can be represented by the following equations.

$$\left.\begin{aligned} \underline{\lambda}^{o\prime} &= \underline{N}^{-1}\,\underline{V} - R'\underline{\Gamma}^*(F_p,\theta)\lambda' \\ \overset{o}{\theta} &= \omega \\ \overset{o}{\omega} &= \frac{1}{J}\left[\lambda_f' i_g' - \lambda_g' i_f' - \rho\omega + \tau_s\right] \end{aligned}\right\} \qquad \text{(A39)}$$

where $\underline{\Gamma}^*(F_p,\theta)$ is given by (A38). F_p may be computed from (A5), (A6). It is only used to determine $L(F_p)$ from the air-gap magnetization curve, Fig. A6. The resulting value of $L(F_p)$ is used in Eq. (A38) to compute $\underline{\Gamma}$. The methods of modifying Eq. (A39) to represent the various types of machine asymmetry are the subject of Appendix B.

A.7 Summary

In this Appendix we have derived the dynamical equations for the basic four-winding smooth-air gap rotating electrical machinery with sinusoidally distributed windings, starting from an expression for the magnetic co-energy of the magnetic fields in the iron and air gap of the machine. Magnetic linearity was not assumed, thus making the analysis applicable to regions of operation where the machine iron is saturated. Despite the appearance of space harmonics in the space flux distribution due to saturation, the effects of such harmonics cancelled for a uniform

air-gap machine when the windings were sinusoidally distributed. Thus the equations for the saturated machine were shown to be equivalent to those of an unsaturated (magnetically linear) machine having a sinusoidal space distribution of flux equivalent to the fundamental component of the actual flux distribution in the saturated machine. For the saturated machine, the fundamental component of the flux space distribution could be represented in terms of the "chordal inductance" of the machine magnetization curve. The torque and flux linkage relations, which were derived from the field co-energy expressions, were then combined with the torque balance and voltage equations to obtain the six differential equations describing the machine dynamics. The state variables of this sixth order system of equations are the four winding flux linkages (λ_a, λ_b, λ_f, λ_g), the rotor position angle θ, and the rotor velocity ω.

It was then demonstrated that when the leakage inductances of the machine were symmetric, the inverse inductance matrix $\underline{\Gamma}$ could be found in a simple straightforward manner by algebraically inverting the inductance matrix $\underline{L}$. Symmetry of the leakage inductances also resulted in a simplification of the expression for the electromagnetic torque. Because of the analytical simplifications which result from symmetry of the leakage inductances, the symmetric machine was taken as the basic machine model for the purposes of developing the simulation.

A model of the general asymmetric uniform air-gap machine with sinusoidally distributed windings can then be constructed from the basic symmetric model as follows. Non-existent windings are modeled as open-circuited windings (windings connected to infinite impedance external loads), and windings with asymmetrical leakage inductances are modeled by appending external inductances to the corresponding windings of the

basic symmetric model. The methods of modifying the simplified equations for the symmetric machine to represent the effects of open and/or asymmetrical windings is the subject of Appendix B.

APPENDIX B

REPRESENTATION OF ASYMMETRIC MACHINES BY MODIFICATION OF THE BASIC SYMMETRIC MACHINE MODEL

B.1 Introduction

The basic equations derived in Appendix A for the dynamic performance of smooth air-gap machines with sinusoidally distributed windings (Eqs. A35, A36) are general in the sense that no assumptions of winding symmetry were made in their derivation. However, it was shown that if the referred leakage inductances of the machine windings on both structures were symmetric, the computational solution of the machine equations could be simplified considerably. The principal reason for the resulting simplification was that, for the symmetric machine, the inductance matrix $\underline{L}(F_p,\theta)$ could be algebraically inverted to obtain the $\underline{\Gamma}$ matrix, and that the resulting $\underline{\Gamma}$ matrix appeared in a form no more complex than the original $\underline{L}$ matrix. Thus the need for time-consuming numerical inversion of the $\underline{L}$ matrix at each integration step could be avoided if the machine were symmetric. Although it was not explicitly stated in Appendix A, in the general asymmetric case there does not appear to be any comparably simple expression for the inverse inductance matrix $\underline{\Gamma}(F_p,\theta)$. Thus a direct approach to the solution of the equations for the asymmetric machine would either require numerical inversion of the inductance matrix $\underline{L}(F_p,\theta)$ or evaluation of a very complex expression for the algebraic inverse of $\underline{L}(F_p,\theta)$ at each integration step. Neither of these alternatives is desirable from the standpoint of computational efficiency.

However, since the intent of the simulation being developed in this thesis is generality, the devevelopment of a computationally efficient method for modelling the asymmetric machine is of great interest. In

particular, the need for performing time consuming numerical matrix inversions should be avoided, if at all possible. A concept of modelling asymmetric machinery, which would retain much of the computational simplicity of the specialized equations for the symmetric machine (Eqs. A38, A39), was introduced in Appendix A. It was pointed out that asymmetry of a uniform air-gap four-winding machine with sinusoidally distributed windings could be classified as falling into either or both of the following categories.

(1) Non-existent or open circuited windings.

(2) Unequal (asymmetric) referred leakage inductances on either or both machine structures.

The modelling concept introduced in Appendix A consisted of decomposing an actual asymmetric machine into a basic symmetric model, for which the simplified equations A38, A39 are applicable, and the following asymmetric representations. Non-existent windings are treated as existing symmetrical but open circuited windings, and asymmetrical referred leakage inductances are modelled by connecting external inductors to the winding terminals of the basic symmetric machine. The value of these external inductors is equal to the differential leakage inductance of the asymmetric windings.

Examples of asymmetrical machines of the first category described above, are most synchronous machines, both poly- and single-phase, which are excited on only single field winding, the orthogonal winding on the field structure being non-existent. Examples of the machines in the second category - that is those having asymmetrical leakage inductances - are split-phase induction motors such as are commonly used for single

phase applications.

The purpose of this Appendix is then to formulate the effects of open windings and/or asymmetric leakages in terms of constraint or conditional equations. A mathematical model of the general asymmetric machine is then formed by a combination of these constraint equations with the basic equations for the symmetric machine, given by Eqs. A38, A39. This method of formulating a mathematical model of the asymmetric machine should be contrasted with the direct method of representing the asymmetric machine in terms of the general equations A35 and A36. However, in this direct method an algebraic inversion of the asymmetric inductance matrix would be at least as cumbersome as a numberical inversion at each integration step, and thus would offer no significant advantages.

Nevertheless, it should be pointed out that the difference between the present method of representing the asymmetric machines and the direct method is one more of concept and computational organization rather than one of physics. The two approaches must of course be physically equivalent. From a stand point of computational organization, the present method seems preferable to the direct one. In the present method, as will be seen, only the linkage expressions for those windings which are actually open or asymmetric are modified by the constraint equations to be developed; the linkages of the remaining windings are obtained by integrating the voltage equations of the basic symmetric machine. Furthermore, the same basic inverse inductance matrix $\underline{\Gamma}^*(F_p,\theta)$ is used for all machines. In contrast, the direct method would either require the use of a different $\underline{\Gamma}$ matrix for every possible machine configuration, or would require that the $\underline{\Gamma}$ matrix be obtained

by numerical inversion of the generalized inductance matrix $L(F_p,\theta)$.

The present approach to the modelling of an asymmetric machine seems particularly appropriate for the simulation of machine performance in situations where the configuration of machine winding connections changes during operation. A specific example of such a situation is the opening and reclosing of either or both armature phases of a polyphase machine.

In such a case it is certainly preferable to continue to use the same basic set of equations, regardless of the current state of the winding connections, changing only the equations for those windings which are being opened or reclosed; rather than having to change machine models or call in a new form of the inverse inductance matrix $\underline{\Gamma}$ to continue the computations when an opening or reclosure of a winding changes the machine configuration.

As will be seen, a separate set of constraint or conditional equations must be developed for every possible asymmetric machine configuration. However, the number of such equations developed in each case is limited to the number of effected windings, and this is clearly preferable to having to modify the entire $\Gamma(\theta)$ matrix anew for each possible configuration.

In the following, the asymmetric constraint equations will first be developed for a machine with symmetrical leakage inductances, but having one or more open circuited (or non-existent) windings. The conditional equations for a machine with unsymmetrical leakage inductances on the stator, and with or without an open rotor winding are developed later. It should be pointed out that in order for a machine structure to have windings with unsymmetrical leakage inductances, both windings

on that structure must by definition be closed (not open). If one of the windings on that structure is open, the open winding may be considered as being symmetrical with the other winding on that structure, and the situation may be viewed simply as one open circuited winding in an otherwise symmetric machine. Thus a machine having windings with unsymmetrical leakages on both structures, can by definition have no open windings. This latter case of a machine with unsymmetrical leakages on both structures will not be considered in this thesis, as such a configuration is of little practical interest.

B.2 Open Windings

The simplest form of machine asymmetry is an open winding(s) on either or both machine structures. Note that a machine with only a single winding on a given machine structure (rotor or stator) is considered to have an orthogonal winding on that structure which is open-circuited. Thus a nonexistent winding is treated as an existing, but open circuited winding. A conventional alternator excited on only a single axis, and without cross-axis damper windings, is an example of a machine with an open winding on the field structure. Similarly, the single-phase alternator without dampers is an example of a machine with open windings on both machine structures.

There are three separate cases of open winding configurations which will be considered in the following; these cases are listed in the order of their complexity.

(a) Either or both windings on the same machine structure are open, but both windings on the opposite structure are closed and are symmetric.

(b) Both windings on one machine structure and one of the windings on the other structure are open.

(c) One winding on each structure is open, the remaining two windings are closed.

The basis of the development which follows is that the linkage of an open winding must be such that the current through that winding is forced to be zero. Thus, the linkage of an open winding is determined as a function of the linkages of the remaining closed windings such that the current in the open winding is zero, and not by integration of the voltage equation for that winding. Indeed, for an open winding the value of λ_j computed from the associated component of the voltage Eq. (A39) is meaningless - as is the concept of an applied terminal voltage for an open winding. Consequently, the number of independent state variables (linkages) of the machine, which are integrated using (A39), is reduced by the number of open windings. Nevertheless, the inverse inductance matrix $\underline{\Gamma}^*(F,\theta)$ given by Eq. (A38) for the symmetric machine still describes the relations between flux linkages and winding currents in an otherwise symmetric machine having one or more open windings. Therefore, the open winding cases described by (a), (b), (c) above may be represented by Eqs. (A38), (A39) for the symmetric machine with the additional constraint that the linkages of the open winding(s) be determined in such a way that the current(s) in the open winding(s) vanish.

We proceed by writing the relation between the flux linkages and the winding currents in a symmetric machine, using the inverse inductance matrix given by Eq. (A38).

$$\begin{bmatrix} i_a' \\ i_b' \\ i_f' \\ i_g' \end{bmatrix} = \left[\begin{array}{c|c|c|c} \Gamma_a & 0 & -\Gamma\cos\theta & -\Gamma\sin\theta \\ \hline 0 & \Gamma_b & -\Gamma\sin\theta & \Gamma\cos\theta \\ \hline -\Gamma\cos\theta & -\Gamma\sin\theta & \Gamma_f & 0 \\ \hline -\Gamma\sin\theta & \Gamma\cos\theta & 0 & \Gamma_f \end{array}\right] \begin{bmatrix} \lambda_a' \\ \lambda_b' \\ \lambda_f' \\ \lambda_g' \end{bmatrix} \qquad \text{(B1)}$$

where

$$\Gamma_a \equiv \frac{L + \ell_r'}{L(\ell_r' + \ell_s') + \ell_r'\ell_s'}$$

$$\Gamma_f \equiv \frac{L + \ell_s'}{L(\ell_r' + \ell_s') + \ell_r'\ell_s'}$$

$$\Gamma \equiv \frac{L}{L(\ell_r' + \ell_s') + \ell_r'\ell_s'}$$

Using Eq. (B1), one can easily compute, for cases (a), (b), (c) outlined earlier, the constraint equations for the linkages of the open windings such that the currents in those windings vanish.

Case (a): Either or both windings on the same machine structure are open, but both windings on the opposite structure are symmetric and closed.

1. If winding a is open; $i_a = 0$

Thus: $\lambda_a' = \frac{\Gamma}{\Gamma_a}(\lambda_f' \cos\theta + \lambda_g' \sin\theta)$ (B2)

2. And/or if winding b is open; $i_b = 0$

$$\text{Thus } \lambda_b' = \frac{\Gamma}{\Gamma_a} (\lambda_f' \sin\theta - \lambda_g' \cos\theta) \tag{B3}$$

In the derivation of (B2) and (B3) it was assumed that the f and g windings are symmetric and both closed.

Similarly, if windings a and b are symmetric and both closed but:

3. Winding f is open; $i_f = 0$

$$\text{Thus: } \lambda_f' = \frac{\Gamma}{\Gamma_f} (\lambda_a' \cos\theta + \lambda_b' \sin\theta) \tag{B4}$$

4. And/or winding g is open; $i_g = 0$

$$\text{Thus: } \lambda_g' = \frac{\Gamma}{\Gamma_f} (\lambda_a' \sin\theta - \lambda_b' \cos\theta) \tag{B5}$$

Case (b): Both windings on one machine structure, and one winding on the other structure are open: For the open winding (winding j) of that structure on which the remaining winding is closed:

$$\lambda_j = 0 \tag{B6}$$

The linkages of the two open windings on the opposite structure are as given in Case (a) above.

Example: Let windings a, b, g be open so that $i_a = i_b = i_g = 0$.

Then: $\lambda_g' = 0$

$$\lambda_a' = \frac{\Gamma}{\Gamma_a} (\lambda_f' \cos\theta + \lambda_g' \sin\theta) = \frac{\Gamma}{\Gamma_a} \lambda_f' \cos\theta$$

$$\lambda_b' = \frac{\Gamma}{\Gamma_a} (\lambda_f' \sin\theta - \lambda_g' \cos\theta) = \frac{\Gamma}{\Gamma_a} \lambda_f' \sin\theta$$

The linkages for other combinations of these sets of open windings are found similarly.

Case (c): One winding on each structure is open, the remaining two windings are closed.

Only two winding combinations for this case are considered; $i_a = 0$, $i_f = 0$ and $i_b = 0$, $i_f = 0$. The results for the combinations in which $i_g = 0$ follow similarly:

1. Windings a and f are open:

$$i_a = i_f = 0$$

The following two equations have to be solved simultaneously.

$$\lambda_a' = \frac{\Gamma}{\Gamma_a} (\lambda_f' \cos\theta + \lambda_g' \sin\theta)$$

$$\lambda_f' = \frac{\Gamma}{\Gamma_f} (\lambda_a' \cos\theta + \lambda_b' \sin\theta)$$

It is sufficient to solve the above explicity for λ_f' in terms of λ_b' and λ_g. λ_f' is then computed in terms of λ_b' and λ_g'. λ_a' is then evaluated by substituting the resultant value for λ_f' into the expression for λ_a'.

$$\lambda_f' = \frac{(\frac{\Gamma}{\Gamma_f}) \sin\theta}{1 - \frac{\Gamma^2}{\Gamma_a \Gamma_f} \cos^2\theta} (\frac{\Gamma}{\Gamma_a} \lambda_g' \cos\theta + \lambda_b') \qquad \text{(B7)}$$

Similarly:

2. Windings b and f are open:

$$i_b = i_f = 0$$

The following equations are solved simultaneously:

$$\lambda_b' = \frac{\Gamma}{\Gamma_a} (\lambda_f' \sin\theta - \lambda_g' \cos\theta)$$

$$\lambda_f' = \frac{\Gamma}{\Gamma_f} (\lambda_a' \cos\theta + \lambda_b' \sin\theta)$$

The result is:

$$\lambda_f' = \frac{-(\frac{\Gamma}{\Gamma_f}) \cos\theta}{1 - \frac{\Gamma^2}{\Gamma_a \Gamma_f} \sin^2\theta} (\frac{\Gamma}{\Gamma_a} \lambda_g' \sin\theta + \lambda_a') \qquad \text{(B8)}$$

Again, once λ_f' is computed in terms of the linkages of the closed windings λ_a, λ_g, the value of λ_f' is substituted into the expression for λ_b', and λ_b' is computed.

The constraint equations for the flux linkages of the open circuited windings, given by Eqs. (B2) to (B8) for the various winding configurations of cases (a), (b), (c), are combined with the equations of motion for the symmetric machine (A38), (A39) as follows. Only the linkages of those closed windings to which external voltages (including zero) are applied are integrated using the matrix differential equation (A39). This integration, along with that for the mechanical variables θ and ω, is performed numerically on a step by step basis. At each integration step, the flux linkages of the open-circuited windings are computed in terms of the integrated linkages of the closed windings by

using the appropriate open winding leakage equations given in the set (B2) to (B8), in accordance with the particular configuration of the open windings (cases a, b, or c).

Simulation of the operation of a machine in which the winding configuration changes, as caused for example by opening and reclosing of circuits, presents no special problems. At any given time in the simulation, the applicable winding constraint equations in the set (B2) to (B8) are chosen in accordance with which machine windings, if any, are open-circuited at the time.

We now turn to the development of the conditional equations for integrating the flux linkages of ~~those~~ windings ~~having~~ which have unsymmetrical leakage inductances.

B.3 Representation of the Effects of Unsymmetrical Leakage Inductance

Because the formulation of the conditional equations for windings having asymmetrical leakage inductances is much more complex than for the case of open-circuited windings, the following development will only apply to the situation of greatest practical interest - the case of asymmetrical stator windings. Furthermore, the development for asymmetrical stator windings is subdivided into two parts - one for the situation in which both rotor windings are symmetric and closed, the other for the case in which one rotor winding is open circuited. The development for the analogous situation in which the rotor windings are assymmetric but the stator windings are either symmetric or open circuited, is exactly the same; however, because that situation is of little practical interest, the details are not given here. The situation in which all four windings are asymmetrical is rather complex, and again

because it is of little practical interest, its development here is omitted.

Before proceeding, an important point must be made to clarify the definition, in the context of this thesis, of asymmetric windings. Two windings on the same machine structure of a smooth air gap machine are defined as asymmetric, if their referred leakage inductances, as defined by Eq. (A33) are unequal.

$$\ell_k' \equiv \frac{\ell_k}{n_k^2} \quad \text{referred leakage inductance of winding k} \qquad \text{(A33)}$$

Thus a pair of stator windings are defined as being asymmetric if and only if:

$$\ell_a' \equiv \frac{\ell_a}{n_k^2} \neq \ell_b' \equiv \frac{\ell_b}{n_b^2}$$

Note that according to the above definition, it is perfectly possible for two stator windings with different numbers of turns, and thus having different physical inductances, to be symmetric. Asymmmetry requires that the referred winding inductances, as defined by Eq. (A33), rather than the actual physical inductances be unequal. Thus two unequal stator windings will be symmetrical if the ratio of their individual inductances is the same as that of the square of their turns ratio.

Consider the schematic diagram sketched below for a machine with stator windings which are asymmetric in the sense of the above definition. All parameter values are given on a referred basis.

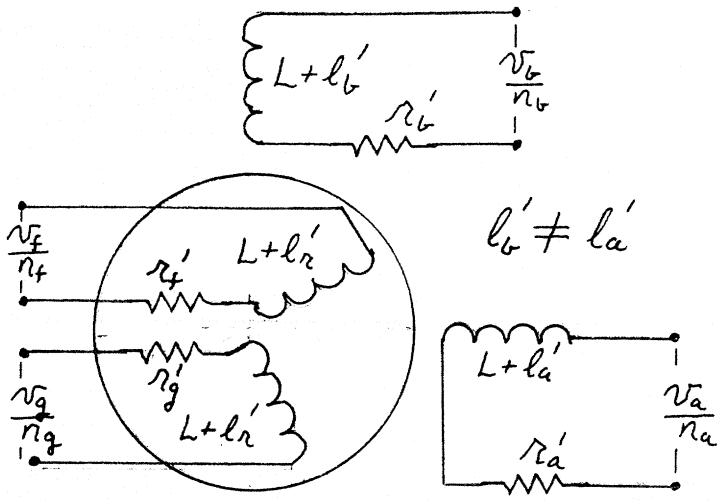

Fig. B1. Schematic Representation of Machine With Asymmetric Stator Winding

As is evident from the analysis of the uniform air-gap machine given in Appendix A and from the above definition of winding asymmetry, asymmetry of the windings on a given structure is reflected only in the referred leakage inductances of those windings. In addition, it makes no difference whether the leakage inductance is taken as being internal or external to the machine proper. Thus the above asymmetric machine may be represented as a combination of a symmetric machine and an external series leakage inductance whose value is equal to the difference of the referred leakage inductances of the two asymmetric windings, as shown in the diagram below:

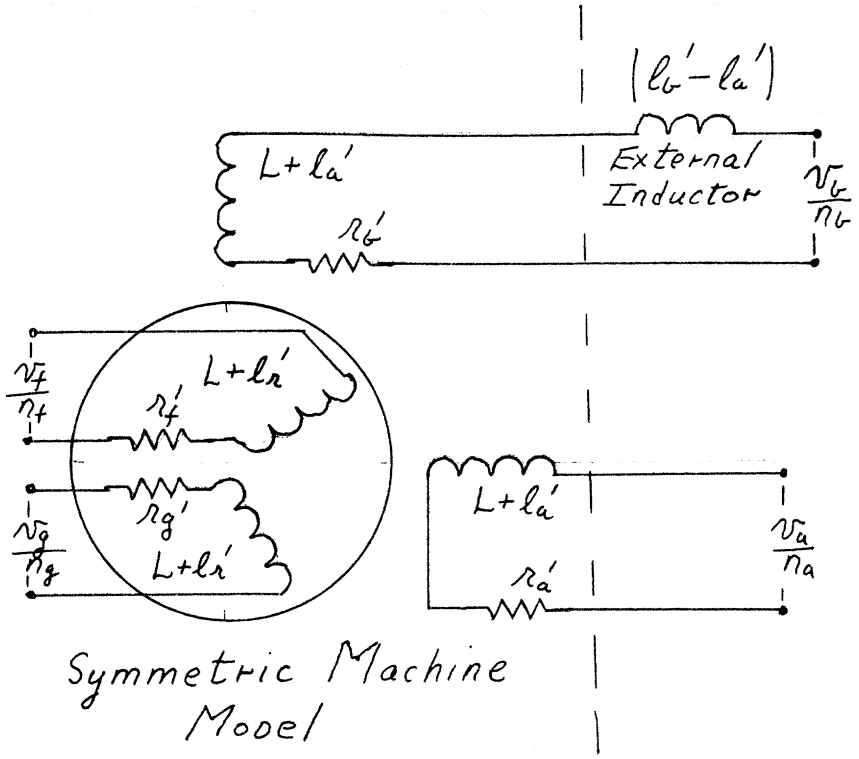

Fig. B2. Equivalent Symmetric Machine With External Induction Connected to Stator B Winding

As shown in Fig. B2 we have arbitrarily chosen to place the external inductance associated with the stator asymmetry in series with the stator "b" winding. It does not matter which of the two stator leakage inductances ℓ_a' or ℓ_b' is greater. In the event that $\ell_a' > \ell_b'$, the external inductance $(\ell_b' - \ell_a')$ in series with the "b" winding will be negative.

Thus the asymmetric machine has been decomposed into a symmetric machine, having referred stator leakage inductances equal to ℓ_a', in combination with an external inductance of $(\ell_b' - \ell_a')$ in series with the stator "b" winding. Because of the simplicity of the current-linkage relations for the symmetric machine, described by the $\underline{\Gamma}(F_p,\theta)$ matrix of Eq. (A38), we choose in the following, to define the machine

winding linkages as those of the component symmetric machine of Fig. B2. Thus in the following, the referred flux linkage λ_b' will only correspond to the linkage of the b winding of the component symmetric machine, and therefore does not include the additional physical flux linkage associated with the external inductance $(\ell_b' - \ell_a')$.

Since we are now dealing with a symmetric machine, the voltage equations for all windings, except the "b" winding, are as given by Eq. (A39). The voltage equation for the b winding may be written by inspection of Fig. B2 as:

$$\overset{o}{\lambda}_b' = \frac{v_b}{n_b} - r_b' i_b' - (\ell_b' - \ell_a') \frac{di_b'}{dt} \tag{B9}$$

In Eq. (B9) the voltage drop across the differential leakage inductance may be written as $(\ell_b' - \ell_a') \frac{di_b'}{dt}$ because the leakage inductances were assumed to remain unsaturated and therefore linear. Now i_b' may be computed as a function of the winding linkages of the symmetric machine, using Eq. (B1).

$$i_b' = \Gamma_a \lambda_b' - \Gamma(\lambda_f' \sin\theta - \lambda_g' \cos\theta) \tag{B10}$$

Then differentiating Eq. (B10) gives $\frac{di_b'}{dt}$ in terms of the winding linkages and their derivatives:

$$\frac{di_b'}{dt} = \Gamma_a \overset{o}{\lambda}_b' - \Gamma(\overset{o}{\lambda}_f' \sin\theta - \overset{\sigma}{\lambda}_g' \cos\theta) - \Gamma(\lambda_f' \cos\theta + \lambda_g' \sin\theta)\omega \tag{B11}$$

Now substitute (B11) into (B9) to eliminate $\frac{di_b'}{dt}$, and solve for $\overset{o}{\lambda}_b'$:

$$(1 + \ell_x\Gamma_a)\overset{o}{\lambda}_b = \frac{v_b}{n_b} - r_b'i_b' + \ell_x\Gamma[(\lambda_f' \cos\theta + \lambda_g' \sin\theta)\omega + (\overset{o}{\lambda}_f' \sin\theta - \overset{o}{\lambda}_g' \cos\theta)] \qquad \text{(B12)}$$

where $\ell_x \equiv (\ell_b' - \ell_a')$

Equation (B12 may be simplified slightly by noting from Eq. (B1) that:

$$\Gamma(\lambda_f' \cos\theta + \lambda_g' \sin\theta) = -(i_a' - \Gamma_a\lambda_a')$$

and by making the following definition:

$$e_b^* \equiv \frac{v_b}{n_b} - r_b'i_b' - \ell_x(i_a' - \Gamma_a\lambda_a')\omega + \ell_x\Gamma\overset{o}{\lambda}_f' \sin\theta \qquad \text{(B13)}$$

Then upon substituting Eq. (B13) into (B12), $\overset{o}{\lambda}_b$ may be expressed as:

$$\overset{o}{\lambda}_b' = \frac{e_b^* - \ell_x\Gamma\overset{o}{\lambda}_g'\cos\theta}{1 + \ell_x\Gamma_a} \qquad \text{(B14)}$$

Thus equation (B14), together with (B13), gives $\overset{o}{\lambda}_b$ as a function of the terminal voltage v_b and the values of the other winding linkages in the machine and their derivatives, when an external inductance ℓ_x is placed between the external voltage v_b, and the "b" winding of the symmetric machine model. Note that (B14) reduces to the conventional expression for $\overset{o}{\lambda}_b = v_b - r_bi_b$ when $\ell_x = 0$, as it should.

The computational procedure for combining the expression for $\overset{o}{\lambda}_b$ given by Eq. (B14) with the basic equations for the symmetric machine

in Eq. (A39) is as follows. Assuming that the rotor windings (f,g) are closed, the linkage derivatives for windings a, f, g are computed, as for any symmetric machine, from the voltage equations of (A39). After the quantities $\overset{o}{\lambda}_f'$, $\overset{o}{\lambda}_g'$ have been computed by Eq. (A39), these quantities are substituted into Eqs. (B13) and (B14) and $\overset{o}{\lambda}_b'$ is computed. The linkages for all four windings are then integrated as before. Again, the currents i_a' and i_b' appear as such in (B13) only for the sake of compactness - they are actually computed as functions of the winding linkages using Eq. (B1). The reason for defining e_b^* in (B13) as a separate entity will become evident in the following development for the case in which one of the rotor windings is open circuited.

The computation of $\overset{o}{\lambda}_b'$ from Eqs. (B13) and (B14) depended upon the availability of the derivatives of the rotor flux linkages $\overset{o}{\lambda}_f'$ and $\overset{o}{\lambda}_g'$. In the event that both rotor windings are closed, this presents no problem as the values of $\overset{o}{\lambda}_f'$ and $\overset{o}{\lambda}_g'$ may be computed from the voltage equations for the rotor windings in Eq. (A39). If, however, one of the rotor windings is open circuited, the derivative of the linkage for that winding is not directly available and therefore must be obtained from the constraint equations for an open rotor winding; Eqs. (B4) or (B5). The situation for an open "g" winding will be worked out below; the equations for $\overset{o}{\lambda}_b$ when the "f" winding is open are developed similarly and thus will not be explicitly derived here.

In general, when the "g" winding is open circuited:

$$\overset{o}{\lambda}_g' = \frac{\Gamma}{\Gamma_f} (\lambda_a' \sin\theta - \lambda_b' \cos\theta) \qquad \text{(B5)}$$

Differentiating this expression for λ_g' gives

$$\overset{o}{\lambda}_g' = \frac{\Gamma}{\Gamma_f}(\overset{o}{\lambda}_a' \sin\theta - \overset{o}{\lambda}_b' \cos\theta) + \frac{\Gamma}{\Gamma_f}(\lambda_a' \cos\theta + \lambda_b' \sin\theta)\omega$$

$$= \frac{\Gamma}{\Gamma_f}(\overset{o}{\lambda}_a' \sin\theta - \overset{o}{\lambda}_b' \cos\theta) + \frac{\omega}{\Gamma_f}(i_f' - \Gamma_f\lambda_f') \qquad \text{(B15)}$$

Upon substituting Eq. (B15) into (B14) and resolving for $\overset{o}{\lambda}_b'$ one obtains:

$$\overset{o}{\lambda}_b' = \frac{e_b^* - \ell_x \frac{\Gamma}{\Gamma_f}(\Gamma\overset{o}{\lambda}_a' \sin\theta + \omega(i_f' - \Gamma_f\lambda_f')) \cos\theta}{[1 + \ell_x(\Gamma_a - \frac{\Gamma^2}{\Gamma_f}\cos^2\theta)]} \qquad \text{(B16)}$$

Note that the quantity e_b^*, given by Eq. (B13), is common to both equations (B14) and (B16). Equation (B16) gives the derivative of the symmetric component of the stator "b" winding flux linkage when the "g" winding of the rotor is open circuited. The computational procedure for combining this expression for $\overset{o}{\lambda}_b$ with the remaining equations of the symmetric machine in (A39) is similar to that given previously. The linkage derivatives for the "a" and "d" windings are computed as before from the voltage equations of (A39). When $\overset{o}{\lambda}_a'$ and $\overset{o}{\lambda}_f'$ have been thus computed, their values are substituted into Eqs. (B13) and (B16) and the value of $\overset{o}{\lambda}_b'$ is evaluated. The linkages λ_a, λ_b, and λ_f can then be integrated once their derivatives are known. Since the "g" winding is open-circuited, its linkage is algebraically determined in terms of the other linkages by the open circuit constraint equation (B5).

APPENDIX C

DYNAMIC EQUATIONS FOR A PAIR OF ELECTRICALLY DIRECT COUPLED, UNIFORM AIR GAP, FOUR-WINDING SYMMETRIC MACHINES

The purpose of this Appendix is to derive the dynamical equations of a system composed of two, electrically direct coupled, four winding, symmetric machines, by algebraically combining the dynamical equations of the two individual machines using the interconnection constraint. The resulting system of differential and algebraic equations enable the numerical solution of these equations to be computed without resorting to iteration, numerical differentiation or matrix inversion, thus providing a simulation of this system which is very efficient from a computational standpoint. Unfortunately, the method of solution to be presented is restricted to machines which are symmetric, balanced and magnetically linear. This restriction is due to the fact that the dynamical equations of this system become exceedingly complex if any imbalances or asymmetries, such as open and/or asymmetric windings are present in either machine. However, when both machines are balanced and symmetric, the resulting symmetry leads to a significant simplification in the formulation of the dynamic equations. Although the resulting equations are considerably more complex than the corresponding differential equations describing the dynamic behavior of a single machine, their solution by numerical quadrature methods on a digital computer involves only slightly more effort than for the case of a single machine.

Consider the following direct interconnection of two four-winding, symmetrical electrical rotating machines:

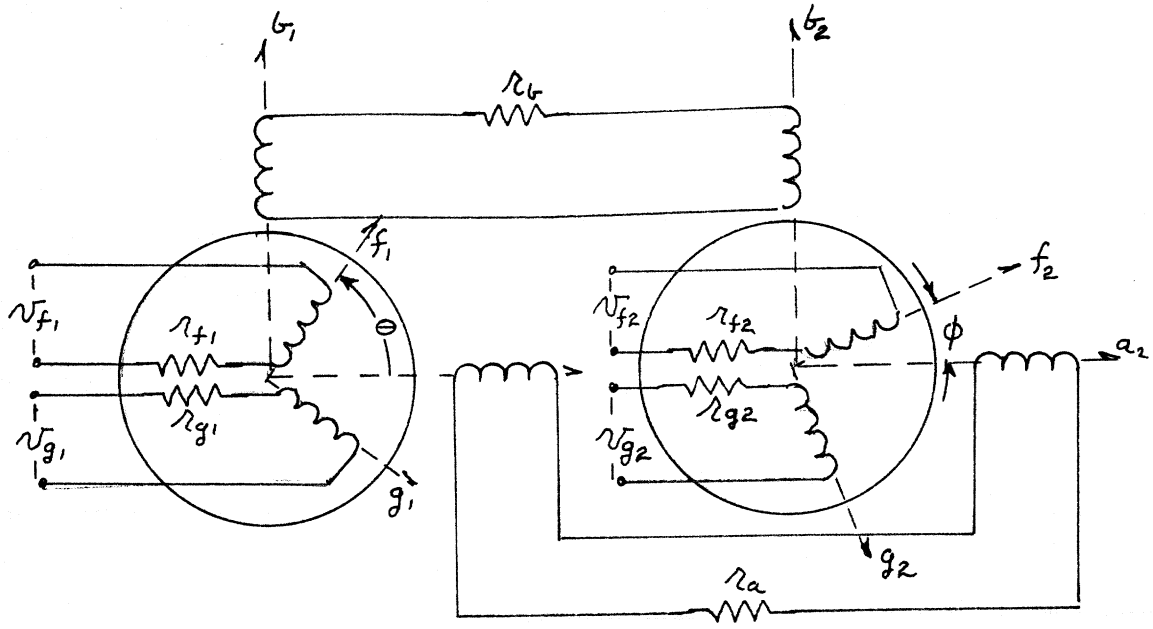

Fig. C1. Interconnection Diagram for Two Four-Winding, Direct Coupled, Symmetric Machines

The stator circuits of the two machines are connected back-to-back directly, there are no shunt loads across the two busses connecting the stator windings.

Because the stator windings of the two machines are directly connected, as shown in Fig. C1, the individual stator winding resistances of the two machines are lumped into single series resistances for each phase of the interconnection, as indicated by r_a and r_b in Fig. C1.

In order to proceed with the formulation of the system equations, we define the following terms:

θ rotor angle of machine 1

ϕ rotor angle of machine 2

$\Gamma(\theta)$ inverse inductance matrix machine 1

$Q(\phi)$ inverse inductance matrix machine 2

$$\underline{i}_{js} \equiv \begin{bmatrix} i_{ja} \\ i_{jb} \end{bmatrix} \quad \text{stator current vector for machine j}$$

$$\underline{i}_{jr} \equiv \begin{bmatrix} i_{jf} \\ i_{jg} \end{bmatrix} \quad \text{rotor current vector for machine j}$$

The rotor and stator linkage and voltage vectors for the two machines, $\underline{v}_{js}$, $\underline{v}_{jr}$, $\underline{\lambda}_{js}$, $\underline{\lambda}_{jr}$ are then defined similarly to $\underline{i}_{js}$, $\underline{i}_{jr}$ above. Since both of the machines are symmetric, Eq. (A38), (A39) apply directly to each machine. In the following we shall find it convenient to write Eq. (A38) and the vector voltage equation (A39) in terms of the partitioned vectors and matrices. Thus the voltage equations for the two machines are:

$$\begin{bmatrix} \underline{\lambda}_{1s}^{o} \\ \underline{\lambda}_{1r}^{o} \end{bmatrix} = \begin{bmatrix} \underline{v}_{1s} \\ \underline{v}_{1r} \end{bmatrix} - \left[\begin{array}{c|c} R_{1s} & \underline{O} \\ \hline \underline{O} & \underline{R}_{1r} \end{array}\right] \begin{bmatrix} \underline{i}_{1s} \\ \underline{i}_{1r} \end{bmatrix} \tag{C1a}$$

$$\begin{bmatrix} \underline{\lambda}_{2s}^{o} \\ \underline{\lambda}_{2r}^{o} \end{bmatrix} = \begin{bmatrix} \underline{v}_{2s} \\ \underline{v}_{2r} \end{bmatrix} - \left[\begin{array}{c|c} R_{2s} & \underline{O} \\ \hline \underline{O} & \underline{R}_{2r} \end{array}\right] \begin{bmatrix} \underline{i}_{2s} \\ \underline{i}_{2r} \end{bmatrix} \tag{C1b}$$

The relations between currents and linkages in each of the two machines are:

$$\begin{bmatrix} \underline{i}_{1s} \\ \underline{i}_{1r} \end{bmatrix} = \left[\begin{array}{c|c} \Gamma_{ss}(\theta) & \Gamma_{sr}(\theta) \\ \hline \Gamma_{sr}(\theta) & \Gamma_{rr}(\theta) \end{array}\right] \begin{bmatrix} \lambda_{1s} \\ \lambda_{1r} \end{bmatrix} \tag{C2a}$$

$$\begin{bmatrix} \underline{i}_{2s} \\ \underline{i}_{2r} \end{bmatrix} = \left[\begin{array}{c|c} Q_{ss}(\phi) & Q_{sr}(\phi) \\ \hline Q_{sr}(\phi) & Q_{rr}(\phi) \end{array}\right] \begin{bmatrix} \lambda_{2s} \\ \lambda_{2r} \end{bmatrix} \tag{C2b}$$

In keeping with Eq. (A38) the inverse inductance submatrices in Eq. (C2) are defined as follows.

For machine 1:

$$\underline{\Gamma_{ss}}(\theta) \equiv \left[\begin{array}{c|c} \Gamma_a & 0 \\ \hline 0 & \Gamma_a \end{array}\right] = \Gamma_a \underline{I}$$

$$\underline{\Gamma_{sr}}(\theta) \equiv \left[\begin{array}{c|c} -\Gamma\cos\theta & \Gamma\sin\theta \\ \hline -\Gamma\sin\theta & \Gamma\cos\theta \end{array}\right] = -\Gamma \left[\begin{array}{c|c} \cos\theta & \sin\theta \\ \hline \sin\theta & -\cos\theta \end{array}\right]$$

$$\underline{\Gamma_{rr}}(\theta) \equiv \left[\begin{array}{c|c} \Gamma_f & 0 \\ \hline 0 & \Gamma_f \end{array}\right] = \Gamma_f \underline{I}$$

Similarly for machine 2:

$$Q_{ss}(\phi) \equiv Q_a \underline{I}$$

$$Q_{sr}(\phi) \equiv -Q \left[\begin{array}{c|c} \cos\phi & \sin\phi \\ \hline \sin\phi & -\cos\phi \end{array}\right]$$

$$Q_{rr}(\phi) \equiv Q_f \underline{I}$$

The parameters Γ_a, Γ, Γ_f are defined in Eq. (B1). The corresponding parameters for machine 2, Q_a, Q, Q_f, are similarly defined. The resistance sub-matrices for each of the two machines are defined as:

$$\underline{R_{1s}} \equiv \left[\begin{array}{c|c} r_{a1} & 0 \\ \hline 0 & r_{b1} \end{array}\right], \qquad \underline{R_{1r}} \equiv \left[\begin{array}{c|c} r_{f1} & 0 \\ \hline 0 & r_{g1} \end{array}\right]$$

$$\underline{R_{2s}} \equiv \begin{bmatrix} r_{a2} & 0 \\ 0 & r_{b2} \end{bmatrix} \quad , \quad \underline{R_{2r}} \equiv \begin{bmatrix} r_{f2} & 0 \\ 0 & r_{g2} \end{bmatrix}$$

In accordance with Fig. C1; $r_a = r_{a1} + r_{a2}$, $r_b = r_{b1} + r_{b2}$.

Now the voltage equations for each machine separately have been given by Eqs. (C1a), (C1b). However, because of the interconnection, we also have the following relations between the stator variables of the two machines.

$$\underline{v_{1s}} = \underline{v_{2s}} \tag{C3}$$

$$\underline{i_{1s}} = - \underline{i_{2s}} \tag{C4}$$

The minus sign in Eq. (C4) is due to the fact that in the derivation of Eq. (C1) the direction of current flow was assumed positive into each machine.

Also by previous definition, the stator resistance of the two machines may be lumped into the two series resistances r_a, r_b of Fig. C1 as follows:

$$\begin{bmatrix} r_a & 0 \\ 0 & r_b \end{bmatrix} = \underline{R_{1s}} + \underline{R_{2s}} \tag{C5}$$

The stator terminal voltages, $\underline{v_{1s}}$, $\underline{v_{2s}}$ in eq (C1a,b) may be eliminated by combining equations (C3) thru (C5) with the stator components of (C1). The resulting constraint equations representing the stator interconnection is:

$$\underline{\overset{o}{\lambda}_{1s}} = \underline{\overset{o}{\lambda}_{2s}} + \begin{bmatrix} r_a & 0 \\ 0 & r_b \end{bmatrix} \underline{i_{2s}} \tag{C6}$$

Another relation between the stator linkages of the two machines may be obtained by substituting the stator current components of Eq. (C2) into Eq. (C4):

$$\underline{i_{1s}} = \underline{\Gamma_{ss}}^{-1}(\theta)\ \underline{\lambda_{1s}} + \underline{\Gamma_{sr}}(\theta)\ \underline{\lambda_{1r}} = -\left(\underline{Q_{ss}}(\phi)\ \underline{\lambda_{2s}} + \underline{Q_{sr}}(\phi)\ \underline{\lambda_{2r}}\right)$$

Solving for $\underline{\lambda_{1s}}$ gives:

$$\underline{\lambda_{1s}} = -\underline{\Gamma_{ss}}^{-1}(\theta)\left[\underline{\Gamma_{sr}}(\theta)\ \underline{\lambda_{1r}} + \underline{Q_{ss}}(\phi)\ \underline{\lambda_{2s}} + \underline{Q_{sr}}(\phi)\ \underline{\lambda_{2r}}\right] \qquad (C7)$$

As seen previously, for the symmetric and magnetically linear machine, the submatrices $\underline{\Gamma_{ss}}(\theta)$ and $\underline{Q_{ss}}(\phi)$ are constant matrices which are simply given by:

$$\Gamma_{ss}(\theta) = \Gamma_a\ \underline{I} \qquad\qquad Q_{ss}(\phi) = Q_a\ \underline{I}$$

When these expressions are substituted into Eq. (C7), the expression for $\underline{\lambda_{1s}}$ simplifies to:

$$\underline{\lambda_{1s}} = -\frac{1}{\Gamma_a}\left[Q_a\ \underline{\lambda_{2s}} + \underline{\Gamma_{sr}}(\theta)\ \underline{\lambda_{1r}} + \underline{Q_{sr}}(\phi)\ \underline{\lambda_{2r}}\right] \qquad (C8)$$

If we now differentiate Eq. (C8) and substitute into (C6) to eliminate $\overset{o}{\underline{\lambda}}_{1s}$, the resulting expression for $\overset{o}{\underline{\lambda}}_{2s}$ becomes:

$$\overset{o}{\underline{\lambda}}_{2s} = -\frac{1}{\Gamma_a + Q_a}\left[\underline{\Gamma_{sr}}(\theta)\ \overset{o}{\underline{\lambda}}_{1r} + \underline{Q_{sr}}(\phi)\ \overset{o}{\underline{\lambda}}_{2r} + \overset{o}{\underline{\Gamma}}_{sr}(\theta)\ \underline{\lambda_{1r}}\right.$$
$$\left. + \overset{o}{\underline{Q}}_{sr}(\phi)\ \underline{\lambda_{2r}} + \Gamma_a \left[\begin{array}{c|c} r_a & 0 \\ \hline 0 & r_b \end{array}\right] \underline{i_{2s}}\right] \qquad (C9)$$

In the differentiation of Eq. (C8) we have assumed magnetic linearity by treating Γ_a and Q_a as constant parameters.

Note that Eq. (C9) is completely free of terms in $\underline{\lambda_{1s}}$ or $\underline{\overset{o}{\lambda}_{1s}}$. The values of $\underline{\lambda_{2R}}$ and $\underline{\overset{o}{\lambda}_{2R}}$ appearing in Eq. (C9) are obtained from the rotor component of the voltage equation for machine 2, Eq. (C1b). Similarly $\underline{\lambda_{1R}}$ and $\underline{\overset{o}{\lambda}_{1R}}$ are obtained from the corresponding rotor voltage equations for machine 1. However, the rotor current for machine 1, $\underline{i_{1R}}$, which is required to evaluate $\underline{\overset{o}{\lambda}_{1R}}$, is expressed in terms of $\underline{\lambda_{1s}}$ by Eq. (C2a). Since we desire to eliminate $\underline{\lambda_{1s}}$ from the equations being developed, it is therefore necessary to reformulate the expression for $\underline{i_{1R}}$ in terms of $\underline{\lambda_{1R}}$, $\underline{\lambda_{2s}}$, and $\underline{\lambda_{2r}}$ only. This is done as follows: From Eq. (C2a) the expression for $\underline{i_{1R}}$ is:

$$\underline{i_{1R}} = \underline{\Gamma_{sr}}(\theta)\ \underline{\lambda_{1s}} + \underline{\Gamma_{rr}}(\theta)\ \underline{\lambda_{1R}}$$

Substitute (C8) into the above to eliminate $\underline{\lambda_{1s}}$, and express $\underline{\Gamma_{rr}}(\theta)$ in terms of its simplified equivalent for the symmetric machine, $\underline{\Gamma_{rr}}(\theta) = \Gamma_f\ \underline{I}$ to obtain:

$$\underline{i_{1R}} = \left[\Gamma_f \underline{I} - \frac{1}{\Gamma_a}\ \underline{\Gamma_{sr}}^2\ (\theta)\right]\ \underline{\lambda_{1R}} - \frac{\underline{\Gamma_{sr}}(\theta)}{\Gamma_a}\left[Q_a\ \underline{\lambda_{2s}} + \underline{Q_{sr}}(\phi)\ \underline{\lambda_{2r}}\right]$$

The above may be further simplified by referring to the definition of $\underline{\Gamma_{sr}}(\theta)$ and noting that:

$$\underline{\Gamma_{sr}}^2(\theta) = \Gamma^2\ \underline{I}$$

and substituting the following from Eq. (C2b) in the last term.

$$\underline{i_{2s}} = Q_a \underline{\lambda_{2s}} + \underline{Q_{sr}}(\phi)\, \underline{\lambda_{2r}}$$

The final expression for i_{1R} then reduces to:

$$\underline{i_{1R}} = (\Gamma_f - \frac{\Gamma^2}{\Gamma_a})\, \underline{\lambda_{iR}} - \frac{\underline{\Gamma_{sr}}(\theta)}{\Gamma_a}\, \underline{i_{2s}} \qquad \text{(C10)}$$

Equations (C9) and (C10) together with the rotor components of the voltage equations (C1a) and (C1b), and equation (C2b), constitute a complete set of electrical equations for the two-machine system in terms of all the currents and linkages of machine 2, the rotor linkages of machine 1, and the rotor terminal voltages of both machines. To summarize, all the equations necessary for evaluating $\overset{o}{\lambda}_{1R}$, $\overset{o}{\lambda}_{2s}$, $\overset{o}{\lambda}_{2R}$ to permit numerical integration of these linkages are given below.

Machine 1 Rotor Voltage Equation:

$$\underline{\overset{o}{\lambda}_{1R}} = \underline{v_{1R}} - \underline{R_{1R}}\, \underline{i_{1R}} \qquad \text{(C11)}$$

Machine 2 Rotor Voltage Equation:

$$\underline{\overset{o}{\lambda}_{2R}} = \underline{v_{2R}} - \underline{R_{2R}}\, \underline{i_{2R}} \qquad \text{(C12)}$$

Machine 2 Stator Voltage Equation:

$$\underline{\overset{o}{\lambda}_{2s}} = -\frac{1}{\Gamma_a + Q_a}\left[\underline{\Gamma_{sr}}(\theta)\underline{\overset{o}{\lambda}_{1R}} + \underline{Q_{sr}}(\phi)\underline{\overset{o}{\lambda}_{2R}} + \underline{\overset{o}{\Gamma}_{sr}}(\theta)\underline{\lambda_{1R}} + \underline{\overset{o}{Q}_{sr}}(\phi)\underline{\lambda_{2R}} + \Gamma_a \underline{R_s}\, \underline{i_{2s}}\right] \qquad \text{(C13)}$$

Machine 2 Stator Current Equation:

$$\underline{i_{2s}} = Q_a \underline{\lambda_{2s}} + \underline{Q_{sr}}(\phi)\ \underline{\lambda_{2r}} \tag{C14}$$

Machine 2 Rotor Current Equation:

$$\underline{i_{2R}} = \underline{Q_{sr}}(\phi)\ \underline{\lambda_{2s}} + Q_f \underline{\lambda_{2R}} \tag{C15}$$

Machine 1 Rotor Current Equation:

$$\underline{i_{1R}} = \left(\Gamma_f - \frac{\Gamma^2}{\Gamma_a}\right) \underline{\lambda_{1R}} - \frac{\underline{\Gamma_{sr}}(\theta)}{\Gamma_a}\ \underline{i_{2s}} \tag{C16}$$

The angle dependent coefficient matrices in the above equations are:

$$\underline{\Gamma_{sr}}(\theta) = -\Gamma \begin{bmatrix} \cos\theta & \sin\theta \\ \sin\theta & -\cos\theta \end{bmatrix} \tag{C17a}$$

$$\overset{o}{\underline{\Gamma_{sr}}}(\theta) = -\Gamma\, \omega_1 \begin{bmatrix} -\sin\theta & \cos\theta \\ \cos\theta & \sin\theta \end{bmatrix} \quad ; \quad \omega_1 = \overset{o}{\theta} \tag{C17b}$$

$$\underline{Q_{sr}}(\phi) = -Q \begin{bmatrix} \cos\phi & \sin\phi \\ \sin\phi & -\cos\phi \end{bmatrix} \tag{C17c}$$

$$\overset{o}{\underline{Q_{sr}}}(\phi) = -Q\,\omega_2 \begin{bmatrix} -\sin\phi & \cos\phi \\ \cos\phi & \sin\phi \end{bmatrix} \quad ; \quad \omega_2 = \overset{o}{\phi} \tag{C17d}$$

The procedure for using Eqs. (C11) through (C16) to evalutate the vector linkage derivatives $\overset{o}{\underline{\lambda_{1R}}}$, $\overset{o}{\underline{\lambda_{2s}}}$, $\overset{o}{\underline{\lambda_{2R}}}$ at each step, preparatory to numerical integration to obtain $\underline{\lambda_{1R}}$, $\underline{\lambda_{2s}}$, $\underline{\lambda_{2R}}$ for the next step is as follows:

At each step values of $\underline{\lambda_{1R}}$, $\underline{\lambda_{2s}}$, $\underline{\lambda_{2R}}$ are known from the results of the

previous integration step; values of $\underline{v_{1R}}$ and $\underline{v_{2R}}$ are also known, since they are externally specified rotor terminal voltages. First $\underline{i_{2s}}$ and $\underline{i_{2R}}$ are computed from the known values of $\underline{\lambda_{2s}}$ and $\underline{\lambda_{2R}}$ by Eqs. (C14), (C15). $\underline{i_{1R}}$ is then computed by Eq. (C16) from the known value of $\underline{\lambda_{1R}}$ and the value of $\underline{i_{2s}}$ is computed by Eq. (C14). Values of $\underline{\overset{o}{\lambda}_{1R}}$, $\underline{\overset{o}{\lambda}_{2R}}$ are then computed by Eqs. (C11), (C12) from the specified values of $\underline{v_{1R}}$, $\underline{v_{2R}}$, and the values of $\underline{i_{1R}}$, $\underline{i_{2R}}$ which were obtained from Eqs. (C15), (C16). Finally $\underline{\overset{o}{\lambda}_{2s}}$ is computed by Eq. (C13) from the known values of $\underline{\lambda_{1R}}$, $\underline{\lambda_{2R}}$, the values of $\underline{\overset{o}{\lambda}_{1R}}$, $\underline{\overset{o}{\lambda}_{2R}}$ obtained from Eq. (C11), (C12) and the value of $\underline{i_{2s}}$ obtained from (C14). The derivatives $\underline{\overset{o}{\lambda}_{1R}}$, $\underline{\overset{o}{\lambda}_{2s}}$, $\underline{\overset{o}{\lambda}_{2R}}$ having been computed, the linkages are integrated for the next step, and the procedure is repeated.

The electromechanical torque equation for each machine is exactly the same as that for the single symmetric machine given in Eq. (A32a). The electromagnetic torque is computed from the rotor currents and linkages of each machine, and these variables are available as results of computations described above. Once the electromagnetic torque is computed, the rotor angles of the two machines are obtained by integrating the electromechanical equations of (A39).

It should also be re-emphasized that all rotor terminal voltages must be specified in this simulation. Some of the rotor terminal voltages may of course be specified as zero; however, the above technique makes no provision for the simulation of any open-circuited windings in either or both machines. Unfortunately, no computationally simple method for simulation open windings in the case of the coupled machine pair could be found, as was the case for the single machine (see Appendix B).

As before, although the linkages are the independent state variables, the equations are written in terms of both linkages and currents

for simplicity and compactness. It is interesting to note that though the equations of the single machine had four independent electrical state variables (the four winding flux linkages), there are only six independent electrical state variables in the equations for the electrically coupled two machine system (the four winding flux linkages of machine 2 and the two rotor winding flux linkages of machine 1), rather than eight. Two of the state variables (the stator linkages of machine 1) were eliminated because of the direct stator interconnection. These variables are no longer independent because the interconnection forces the same currents to flow through the stator windings of both machines.

Finally it should be emphasized that although this problem has been formulated in terms of the winding flux linkages, the results developed in this Appendix, unlike those in Appendix A for the single machine, are strictly correct only for a magnetically linear machine. This assumption of magnetic linearity was invoked by considering the inverse inductance parameters Q_a, and Γ_a as constants during the differentiation of Eq. (C8).

APPENDIX D

APPROXIMATE RELATIONS FOR DESCRIBING THE ELECTROMECHANICAL OSCILLATIONS OF A BALANCED ROUND-ROTOR SYNCHRONOUS MACHINE HAVING A SINGLE FIELD WINDING AND NEGLIGIBLE ARMATURE RESISTANCE

Consider the balanced two-phase round-rotor synchronous machine illustrated in Fig. D1.

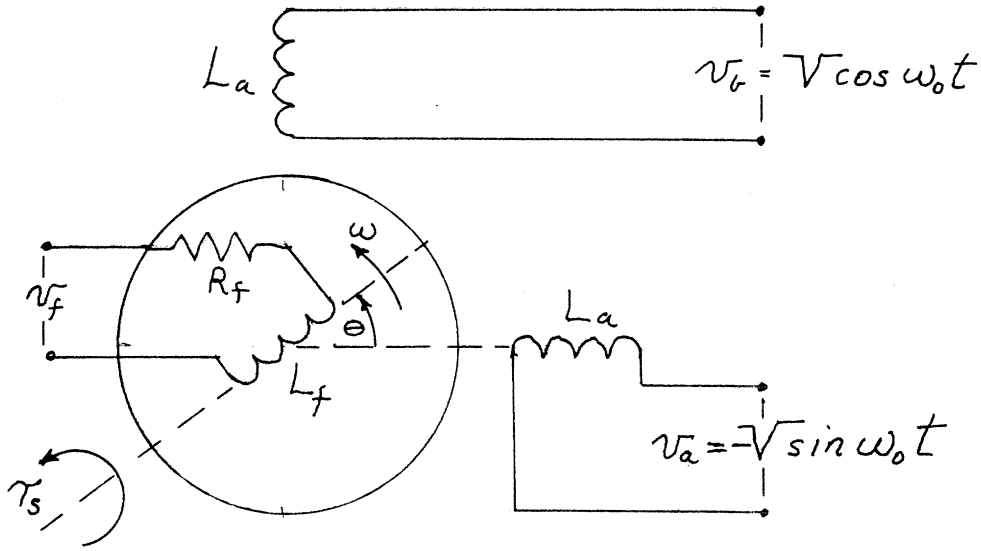

Fig. D1. The Round-Rotor Synchronous Machine With Single Field Winding and Negligible Armature Resistance

The armature (stator) windings are connected to a balanced two-phase infinite bus voltage source. The peak magnitude of the bus voltage is V. Thus the phase voltages applied to the two stator windings are:

$$v_a = -V\sin\omega_o t \qquad v_b = V\cos\omega_o t \tag{D1}$$

The resistance of the stator windings is assumed negligible. Consequently the time derivatives of the winding flux linkages are directly equal to the terminal voltages.

$$\dot{\lambda}_a = v_a \qquad \dot{\lambda}_b = v_b \tag{D1a}$$

Consequently the stator winding flux linkages are obtained directly by integrating D1a.

Integrating the above gives:

$$\lambda_a = \frac{v}{\omega_o} \cos \omega_o t$$

$$\lambda_b = \frac{v}{\omega_o} \sin \omega_o t \qquad \text{(D2)}$$

The relation between the winding flux linkages and currents of the machine illustrated in Fig. D1 is:

$$\begin{bmatrix} \lambda_a \\ \lambda_b \\ \lambda_f \end{bmatrix} = \begin{bmatrix} L_a & 0 & L\cos\theta \\ 0 & L_b & L\sin\theta \\ L\cos\theta & L\sin\theta & L_f \end{bmatrix} \begin{bmatrix} i_a \\ i_b \\ i_f \end{bmatrix} \qquad \text{(D3)}$$

$L_a \equiv L + \ell_a$

$L_f \equiv L + \ell_f$

L is the machines magnetizing inductance; ℓ_a, ℓ_f are the leakage inductances of the armature and field windings respectively. All machine parameters, voltages, currents, and flux linkages are expressed as referred to the stator windings.

The electromagnetic torque may be found as the derivative of the machine's magnetic coenergy. The machine coenergy is given by:

$$\omega_m^* = \frac{1}{2} \begin{bmatrix} i_a & i_b & i_f \end{bmatrix} \begin{bmatrix} L_a & 0 & L\cos\theta \\ 0 & L_a & L\sin\theta \\ L\cos\theta & L\sin\theta & L_f \end{bmatrix} \begin{bmatrix} i_a \\ i_b \\ i_f \end{bmatrix}$$

Thus the expression for the torque is found from

$$\tau_m = -\frac{\partial \omega_m^*}{\partial \theta} = -\frac{1}{2}\,[i_a\ i_b\ i_f]\begin{bmatrix} 0 & 0 & -L\sin\theta \\ 0 & 0 & L\cos\theta \\ -L\sin\theta & L\cos\theta & 0 \end{bmatrix}\begin{bmatrix} i_a \\ i_b \\ i_f \end{bmatrix}$$

This reduces to

$$\tau_m = L\ i_f(i_a \sin\theta - i_b \cos\theta) \qquad \text{(D4)}$$

The torque given by Eq. (D4) is the torque applied <u>to</u> the machines magnetic field storage <u>by</u> the rotor structure and is positive in the direction of increasing θ. Thus an equal and <u>opposite</u> torque is applied <u>by</u> the magnetic field of the machine <u>to</u> the mechanical rotor structure.

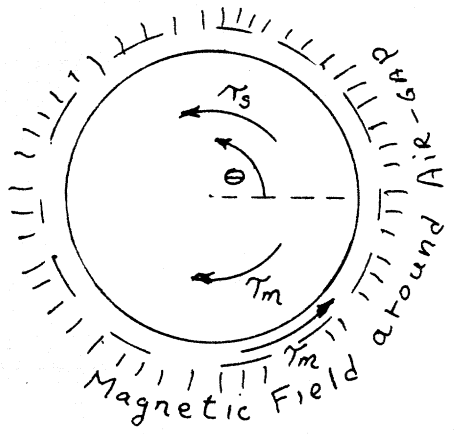

Thus the torque balance equation on the mechanical rotor structure of the machine is:

$$\tau_s - \tau_m = J\ddot{\theta} + \rho\dot{\theta} \tag{D5}$$

τ_s is externally applied shaft torque in direction of increasing θ

J is rotor moment of inertia

ρ is mechanical damping coefficient for rotor

Finally the voltage equation for the field winding is simply

$$v_f = \dot{\lambda}_f + R_f i_f \tag{D6}$$

where R_f is the value of field winding resistance referred to the stator winding.

Equations (D2) to (D6) completely describe the performance of the machine illustrated in Fig. D1. The approximate transient behavior of the machine for small disturbances may be determined by linearizing the machine equations about a fixed operating point. Because the machine and the applied armature voltages are balanced, it becomes much easier to work with the machine equations expressed in terms of a rotating dq coordinate system fixed to the rotor.

The dq coordinate flux linkages and currents are defined by the following transformations.

$$\begin{bmatrix} \lambda_d \\ - \\ \lambda_q \end{bmatrix} \equiv \left[\begin{array}{c|c} \cos\theta & \sin\theta \\ - - & - - \\ \sin\theta & -\cos\theta \end{array}\right] \begin{bmatrix} \lambda_a \\ - \\ \lambda_b \end{bmatrix}; \quad \begin{bmatrix} i_d \\ - \\ i_q \end{bmatrix} \equiv \left[\begin{array}{c|c} \cos\theta & \sin\theta \\ - - & - - \\ \sin\theta & -\cos\theta \end{array}\right] \begin{bmatrix} i_a \\ - \\ i_b \end{bmatrix} \tag{D7}$$

It is interesting to note that the matrix of this transformation is also equal to its inverse. Thus the inverse transformations are:

$$\begin{bmatrix} \lambda_a \\ \hline \lambda_b \end{bmatrix} = \left[\begin{array}{c|c} \cos\theta & \sin\theta \\ \hline \sin\theta & -\cos\theta \end{array}\right] \begin{bmatrix} \lambda_d \\ \hline \lambda_q \end{bmatrix}; \quad \begin{bmatrix} i_a \\ \hline i_b \end{bmatrix} = \left[\begin{array}{c|c} \cos\theta & \sin\theta \\ \hline \sin\theta & -\cos\theta \end{array}\right] \begin{bmatrix} i_d \\ \hline i_q \end{bmatrix} \tag{D8}$$

The relations between the linkages and currents in dq coordinates may be obtained by combining (D7) and (D8) with (D3)

$$\begin{bmatrix} \lambda_d \\ \hline \lambda_q \\ \hline \lambda_f \end{bmatrix} = \left[\begin{array}{c|c|c} \cos\theta & \sin\theta & 0 \\ \hline \sin\theta & -\cos\theta & 0 \\ \hline 0 & 0 & 1 \end{array}\right] \left[\begin{array}{c|c|c} L_a & 0 & L\cos\theta \\ \hline 0 & L_a & L\sin\theta \\ \hline L\cos\theta & L\sin\theta & L_f \end{array}\right] \left[\begin{array}{c|c|c} \cos\theta & \sin\theta & 0 \\ \hline \sin\theta & -\cos\theta & 0 \\ \hline 0 & 0 & 1 \end{array}\right] \begin{bmatrix} i_d \\ \hline i_q \\ \hline i_f \end{bmatrix}$$

which reduces to

$$\begin{bmatrix} \lambda_d \\ \hline \lambda_q \\ \hline \lambda_f \end{bmatrix} = \left[\begin{array}{c|c|c} L_a & 0 & L \\ \hline 0 & L_a & 0 \\ \hline L & 0 & L_f \end{array}\right] \begin{bmatrix} i_d \\ \hline i_q \\ \hline i_f \end{bmatrix} \tag{D9}$$

When the armature voltage equations (D2) are substituted into the transformation equations (D7) the result is

$$\lambda_d = \frac{v}{\omega_o} (\cos \omega_o t \cos\theta + \sin \omega_o t \sin\theta)$$

This may be simplified by expressing the rotor angle θ in terms of a synchronously rotating reference as:

$$\theta = \omega_o t + \delta \tag{D10}$$

Thus δ is the angle between the rotor field axis and the synchronously rotating stator flux linkage space phasor.

Upon substituting (D10) in the previous expression for λ_d, one obtains

$$\lambda_d = \frac{v}{\omega_o} \cos \delta \tag{D11a}$$

Similarly

$$\lambda_q = \frac{v}{\omega_o} \sin \delta \tag{D11b}$$

Furthermore, it is seen from Eq. (D7) that:

$$i_q = i_a \sin\theta - i_b \cos\theta$$

Substituting this relation into Eq. (D4) eliminates the appearance of phase quantities in the expression for the torque:

$$\tau_m = L\, i_f\, i_q \tag{D12}$$

The machine performance equations are now given by (D5), (D6), (D9), (D11), (D12). We wish further to eliminate $\overset{o}{\lambda}_f$ from (D6) and i_q from (D11). This may be done by inverting (D9) and combining the result with (D11) to eliminate the dq variables. The inverse of (D9) is given by

$$\begin{bmatrix} i_d \\ - \\ i_q \\ - \\ i_f \end{bmatrix} = \left(\frac{1}{L_a L_f - L^2}\right) \left[\begin{array}{c|c|c} L_f & 0 & -L \\ - & - & - \\ 0 & \dfrac{L_a L_f - L^2}{L_a} & 0 \\ - & - & - \\ -L & 0 & L_a \end{array}\right] \begin{bmatrix} \lambda_d \\ - \\ \lambda_q \\ - \\ \lambda_f \end{bmatrix} \tag{D13}$$

Expand the second and third rows of (D13) to obtain

$$i_q = \frac{\lambda_q}{L_a} \tag{D14}$$

$$i_f = -\left(\frac{L}{L_a L_f - L^2}\right) \lambda_d + \left(\frac{L_a}{L_a L_f - L^2}\right) \lambda_f \tag{D15}$$

For convenience define

$$\Gamma_f \equiv \frac{L_a}{L_a L_f - L^2} \tag{D16}$$

then solve (D15) for λ_f to obtain

$$\lambda_f = \frac{i_f}{\Gamma_f} + \frac{L}{L_a} \lambda_d \tag{D17}$$

Now substitute (D14) and (D11b) into (D12) to obtain

$$\tau_m = \frac{L}{L_a} i_f \frac{V}{\omega_o} \sin \delta \tag{D18}$$

Similarly substitute (D17) and (D11a) into (D6) to obtain

$$v_f = \frac{1}{\Gamma_f} \frac{d}{dt} (i_f) + R_f i_f - \frac{L}{L_a} \frac{V}{\omega_o} \sin\delta \frac{d}{dt} (\delta) \tag{D19}$$

Finally substitute (D18) and (D10) into (D5)

$$\tau_s - \frac{L}{L_a} i_f \frac{V}{\omega_o} \sin\delta = J \overset{oo}{\delta} + \rho (\omega_o + \overset{o}{\delta}) \tag{D20}$$

Equations (D19) and (D20) are a set of non-linear differential equations in the variables i_f and δ which describe the dynamic performance of the machine illustrated in Fig. D1. An approximate solution to these equations may be determined by linearizing them about a steady state operating point defined by

$$i_f = i_{fo}$$

$$\delta = \delta_o \qquad \text{(D21)}$$

$$\overset{o}{\delta}_o = 0$$

The perturbation relations for (D19) and (D20) about this operating point are

$$\Delta v_f = \frac{1}{\Gamma_f} \overset{o}{\Delta i_f} + R_f \Delta i_f - \frac{L}{L_a} \frac{V}{\omega_o} \sin\delta_o \overset{o}{\Delta\delta} \qquad \text{(D22)}$$

$$\Delta\tau_s = \frac{L}{L_a} \frac{V}{\omega_o} \sin\delta_o \Delta i_f + \frac{L}{L_a} \frac{V}{\omega_o} i_{f_o} \cos\delta_o \Delta\delta + \rho\Delta\overset{o}{\delta} + J\Delta\overset{oo}{\delta} \qquad \text{(D23)}$$

By defining $\omega_s = \overset{o}{\Delta\delta}$, Eqs. (D22), (D23) are most effectively written in the following state variable matrix formulation

$$\begin{bmatrix} \overset{o}{\Delta i_f} \\ \overset{o}{\Delta\delta} \\ \overset{o}{\omega_s} \end{bmatrix} = \begin{bmatrix} -\Gamma_f R_f & 0 & 0 & \frac{L}{L_a} \Gamma_f \frac{V}{\omega_o} \sin\delta_o \\ 0 & 0 & 0 & 1 \\ -\frac{L}{L_a} \frac{V}{J\omega_o} \sin\delta_o & -\frac{L}{L_a} \frac{V}{J\omega_o} i_{f_o} \cos\delta_o & -\frac{\rho}{J} & \end{bmatrix} \begin{bmatrix} \Delta i_f \\ \Delta\delta \\ \omega_s \end{bmatrix} + \begin{bmatrix} \Gamma_f & 0 \\ 0 & 0 \\ 0 & \frac{1}{J} \end{bmatrix} \begin{bmatrix} \Delta v_f \\ \Delta\tau_s \end{bmatrix}$$

(D24)

Equation (D24) represents the dynamical behavior of the machine for small disturbances about a steady operating point defined by (D21). Of particular importance in determining the machines dynamical behavior during small disturbances are the characteristic roots of (D24). Thus the remainder of this Appendix will be devoted to developing simple and approximate analytical relations for these roots when the roots include a complex pair - that is when the dynamical response of the machine to a disturbance is oscillatory. The characteristic equation for the system described by (D24) is given by the expansion of the following determinant.

$$\begin{vmatrix} s + R_f\Gamma_f & 0 & -\Gamma_f \frac{L}{L_a}\frac{V}{\omega_o}\sin\delta_o \\ 0 & s & -1 \\ \frac{1}{J}\frac{L}{L_a}\frac{V}{\omega_o}\sin\delta_o & \frac{1}{J}\frac{L}{L_a}\frac{V}{\omega_o} i_{f_o}\cos\delta_o & s + \rho/J \end{vmatrix}$$

To simplify the formulation of the characteristic equation for (D24) define the following quantities.

$$\begin{aligned} \omega_f &\equiv R_f\Gamma_f \quad \text{(it is easy to show that } \omega_f \text{ is the reciprocal of the direct axis short-circuit time constant)} \\ \mathcal{S}_o &\equiv \frac{L}{L_a}\frac{V}{\omega_o}\sin\delta_o \\ C_o &\equiv \frac{L}{L_a}\frac{V}{\omega_o}\cos\delta_o \\ \alpha &\equiv \rho/J \end{aligned} \qquad \text{(D25)}$$

Using the definitions of (D25), the resulting characterisitic equation may be written as

$$(s + \omega_f)(s^2 + \alpha s + \frac{C_o}{J} i_{f_o}) + \frac{\Gamma_f}{J} S_o^2 s = 0 \qquad \text{(D26)}$$

One of the simplest and direct methods of finding the roots of the above third order equation is to use the root locus method. A description of this use of the root locus for solving polynomial equations may be found in [13]. In preparation for plotting the root locus, (D26) is rewritten as follows.

$$1 + \frac{\frac{\Gamma_f}{J} S_o^2 s}{(s + \omega_f)(s^2 + \alpha s + \frac{C_o}{J} i_{f_o})} = 0 \qquad \text{(D27)}$$

The "open-loop" function of (D27) is characterized by a zero at the origin, a real pole at $s = -\omega_f$ and a pair of complex poles at $s = -\frac{\alpha}{2} \pm j\sqrt{\frac{C_o}{J} i_{f_o} - \frac{\alpha^2}{4}}$. The latter poles will almost always be complex, as shown, because the normalized mechanical damping coefficient $\alpha = \rho/J$ is generally very small. Furthermore, it is easily seen that this pair of complex poles will be located on a semicircle in the left-hand plane whose radius is equal to $\sqrt{\frac{C_o}{J} i_{f_o}}$. Their exact location on this semicircle is determined by the value of the $\alpha/2$. Typical locations of these poles and zeros and the corresponding approximate root locus for (D27) are sketched in Fig. D2 below.

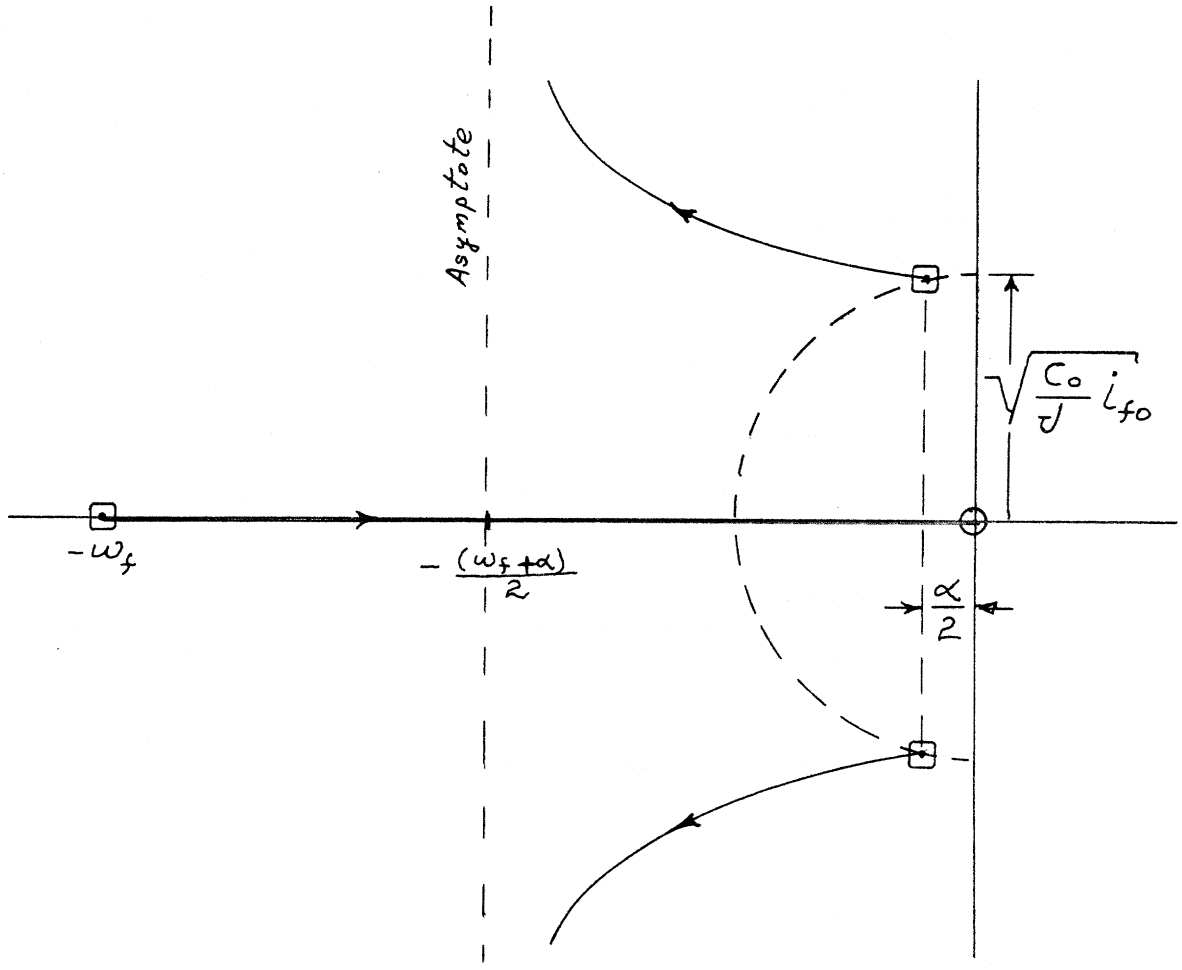

Fig. D2. Typical Root Locus for Eq. (28).

As seen from Fig. D2 the locus consists of three branches, each branch corresponding to one of the three roots of the cubic Eq. (D26). Two of these branches are the loci for the pair of complex conjugate roots, the third branch is the locus of the real root. As will be shown shortly, the value of α is usually so small as to be negligible in comparison to $\sqrt{\frac{C_o}{J} i_{f_o}}$. Consequantly, in most applications of practical interest the complex pole pair $s = -\frac{\alpha}{2} \pm \sqrt{\frac{C_o}{J} i_{f_o} - \frac{\alpha^2}{4}}$ may be taken as being located on the imaginary axis ($\alpha \to 0$). On the basis of this

assumption, the only remaining factor which determines the shape of the locus is the ratio of ω_f to the parameter $\sqrt{\frac{C_o}{J} i_{f_o}}$. A new root locus must be drawn for each value of $(\omega_f \sqrt{\frac{C_o}{J} i_{f_o}})$. To facilitate the construction of a generalized root locus diagram, it will be convenient to define the following additional parameters.

$$\omega_n \equiv \sqrt{\frac{C_o}{J} i_{f_o}} = \sqrt{\frac{L}{L_a} \frac{V}{J\omega_o} i_{f_o} \cos\delta_o} \qquad \text{(D28a)}$$

$$\tau_d' \equiv \frac{1}{\omega_f} \quad \text{(direct axis short circuit time constant)} \qquad \text{(D28b)}$$

$$\xi_o \equiv \frac{\tau_d'}{2\omega_n} \frac{\Gamma_f}{J} S_o^2 = \frac{\tau_d'}{2\omega_n} \frac{\Gamma_f}{J\omega_o^2} \left(\frac{L}{L_a}\right) V^2 \sin^2\delta_o \qquad \text{(D28c)}$$

The relations for ω_n and ξ_o given by (D28a), (D28c) become more convenient when expressed in terms of per-unit values of the machine parameters, and the machine's inertia constant, H. Furthermore, the dimensionality of these parameters is then also more easily established. As should be expected, it will be shown that ω_n has the dimensions of sec^{-1} and that ξ_o is dimensionless. The per-unit representation of machine parameters requires an arbitrary specification of base voltage V_b and base current A_b for the machine. Normally these values are chosen as the voltage and current drawn when the machine is operating at rated load and power factor. Having chosen these variables, the following parameters are defined:

$$Z_b \equiv \frac{V_b}{A_b} \qquad \text{base impedance, ohms} \qquad \text{(D29a)}$$

$$H \equiv \frac{J\omega_o^2}{2VA} \qquad \text{machine inertia constant, secs} \qquad \text{(D29b)}$$

$$e_f \equiv \frac{L\omega_o i_{f_o}}{V_b} \qquad \text{per-unit excitation voltage} \qquad \text{(D29c)}$$

$$v \equiv \frac{V}{V_b} \qquad \text{per-unit applied terminal voltage} \qquad \text{(D29d)}$$

$$r_f \equiv \frac{R_f}{z_b} \qquad \text{per-unit value of referred field resistance} \qquad \text{(D29e)}$$

$$X_s \equiv \frac{L_a\omega_o}{Z_b} \qquad \text{per-unit value of machine synchronous reactance} \qquad \text{(D29f)}$$

All per-unit parameters are of course dimensionless.

In terms of these parameters the definitions of ω_n and ξ_o may be rewritten as follows.

$$\omega_n = \sqrt{\frac{e_f v\omega_o}{2Hx_s}\cos\delta_o} \qquad \text{(D30a)}$$

$$\xi_o = \left(\frac{L}{L_a}\right)^2 \frac{v^2}{4H\omega_n r_f}\sin^2\delta_o \qquad \text{(D30b)}$$

All parameters on the right of (D30a) are dimensionless except ω_o and H, consequently, the dimension of ω_n is sec^{-1} as expected. Similarly it can be seen from (D30b) that ξ_o is dimensionless.

It is now convenient to rewrite the characteristic equation for the machines dynamic response, Eq. (D26), in terms of the parameters ω_n, τ_d', ξ_o defined above.

$$\left[\left(\frac{S}{\omega_n}\right) + \frac{1}{\left(\omega_n \tau_d'\right)}\right]\left[\left(\frac{S}{\omega_n}\right)^2 + \left(\frac{\alpha}{\omega_n}\right)\left(\frac{S}{\omega_n}\right) + 1\right] + \frac{2\xi_o}{\left(\tau_d' \omega_n\right)}\left(\frac{S}{\omega_n}\right) = 0 \qquad \text{(D31)}$$

Note that this equation is now in dimensionless form and its roots are a function of the dimensionless parameters $(\omega_n \tau_d')$, (α/ω_n), and ξ_o. It will now be shown that in most cases the effect of mechanical damping is negligible and, that therefore the term $(\alpha/\omega_n)\ (S/\omega_n)$ may be neglected. α was defined by Eq. (D25) as

$$\alpha = \frac{\rho}{J} \qquad \text{(D25)}$$

Furthermore, the base torque of the machine is defined as

$$T_b = \frac{VA}{\omega_o}$$

As was mentioned previously, this value of T_b is usually the torque of the machine when operating at rated load. Using this defintion of T_b, (D25) may be rewritten as follows

$$\alpha = \frac{\rho\omega_o}{J\omega_o}\frac{VA}{\omega_o T_b} = \frac{1}{2H}\left(\frac{\rho\omega_o}{T_b}\right)$$

$(\rho\omega_o)$ is merely the steady-state value of the torque required to overcome mechanical friction (bearing friction, windage, etc.). Thus the dimensionless group $\left(\frac{\rho\omega_o}{T_b}\right)$ is the fraction of rated torque, and thus power at rated speed, required to overcome the mechanical losses of the machine. Therefore, for most well designed machines the term $\left(\frac{\rho\omega_o}{T_b}\right)$ is rarely greater than 1%, unless the machine is connected to a highly dissipative mechanical load or prime mover. Consequently, the term $\left(\frac{\alpha}{\omega_n}\right)$ in (D31) may be written as

$$\frac{\alpha}{\omega_n} = \frac{1}{2H\omega_n}\left(\frac{\rho\omega_o}{T_b}\right)$$

For most machines $5 \leq H\omega_n \leq 50$. Then assuming a typical value of $\frac{\rho\omega_o}{T_b} = 0.01$, it is seen that generally: $\left(\frac{\alpha}{\omega_n}\right) < 0.001$, and thus is negligible as stated earlier.

Thus, when the effects of mechanical damping are neglected, the characteristic Eq. (D31) reduces to:

$$\left[\left(\frac{s}{\omega_n}\right) + \left(\frac{1}{\omega_n\tau_d'}\right)\right]\left[\left(\frac{s}{\omega_n}\right)^2 + 1\right] + \frac{2\xi_o}{\left(\omega_n\tau_d'\right)}\left(\frac{s}{\omega_n}\right) = 0 \qquad \text{(D32)}$$

The roots of this equation, in terms of the dimensionless complex frequency $\left(\frac{s}{\omega_n}\right)$ are now a function only of the parameters $(\omega_n\tau_d')$ and ξ_o. Root loci of Eq. (D32) are plotted in Fig. D3 for a range of values of the dimensionless parameter $(\omega_n\tau_d')$.

Also plotted in Fig. D3, are cross-loci for constant values of ξ_o ranging from 0.1 to 0.8. Consequently the root locations of Eq. (D32), for given values of the parameters $(\omega_n\tau_d')$ and ξ_o, may be easily determined from Fig. D3 by inspection. The information portrayed in Fig. D3 is replotted in Fig. D4 in terms of the rotor swing frequency and damping ratio which result for various combinations of the parameters $(\omega_n\tau_d')$ and ξ_o. The rotor swing frequency is equal to the imaginary part of the complex root, and the damping ratio is equal to the cosine of the angle in Fig. D3 between the negative real axis and the vector from the origin to the complex root location. Note that ω_n is equal to the undamped natural frequency of the rotor swings. Because $\xi_o = 0$ when the machine is unloaded ($\xi_o = 0$ when $\delta = 0$, See Eq. (D30b)), ω_n is also the swing frequency of the unloaded machine and is independent of

τ_d'. Furthermore, the parameter ξ_o is the damping ratio of the machine in the limit as $\tau_d' = 0$. Also note that as $\tau_d' \to 0$ the root-locus of Eq. (D32) approaches a circular arc of radius ω_n about the origin, as shown in Fig. D3.

The procedure for finding the characteristic response of the machine from Figs. D3, D4 is as follows. Values of ω_n and ξ_o are computed from Eq. (D30) in terms of the per unit machine parameters and the power angle δ_o at the operating point of interest. τ_d' is assumed to be a known machine parameter. The product $(\omega_n \tau_d')$ is then computed, and this parameter, together with ξ_o, are used as arguments to determine the characteristic root locations from Fig. D3, or the corresponding values of rotor swing frequency and damping ratio from Fig. D4. It should be pointed out that Figs. D3 and D4 only describe the loci of the two complex conjugate roots of Eq. (D32), and do not give the location of the third characteristic root. This remaining root is real and its magnitude lies between 0 and $1/\tau_d'$. However, because the response characteristic associated with this real root is merely that of an exponentially decaying bias, it is only of secondary interest relative to the oscillatory response associated with the complex roots, and thus the details of its locus have been omitted.

Finally it should be emphasized that a change in one of the machine parameters or in steady state operating condition of the machine will generally effect <u>both</u> $(\omega_n \tau_d')$ and ξ_o. Thus the effect of such changes on the machine's characteristic response is not always directly obvious from a cursory glance at Figs. D3, D4. For example, increasing the value of field resistance, r_f, decreases both ξ_o and $(\omega_n \tau_d')$. However, the effect of this increase in r_f on the response, as indicated

by the rotor swing frequency ω and damping ratio ξ, depends upon the initial values of ξ_o and $(\omega_n \tau_d')$, and the amount of the change in r_f. It is interesting to note that as $r_f \to \infty$, $(\omega_n \tau_d') \to 0$ and $\xi_o \to 0$; therefore $\omega \to \omega_n$ and $\xi \to 0$ which is not unexpected as $r_f \to \infty$ implies that the field is being excited by a current source. Finally, it should be noted that since most practical machines operate at values of δ of less than 30^o, the corresponding value of ξ_o is generally rather small, usually $\xi_o < 0.3$. As can be seen from Fig. D4, when $\xi_o < 0.3$, the rotor swing frequency $\omega \cong \omega_n$, and both ω and ξ are relatively insensitive to changes in τ_d'.

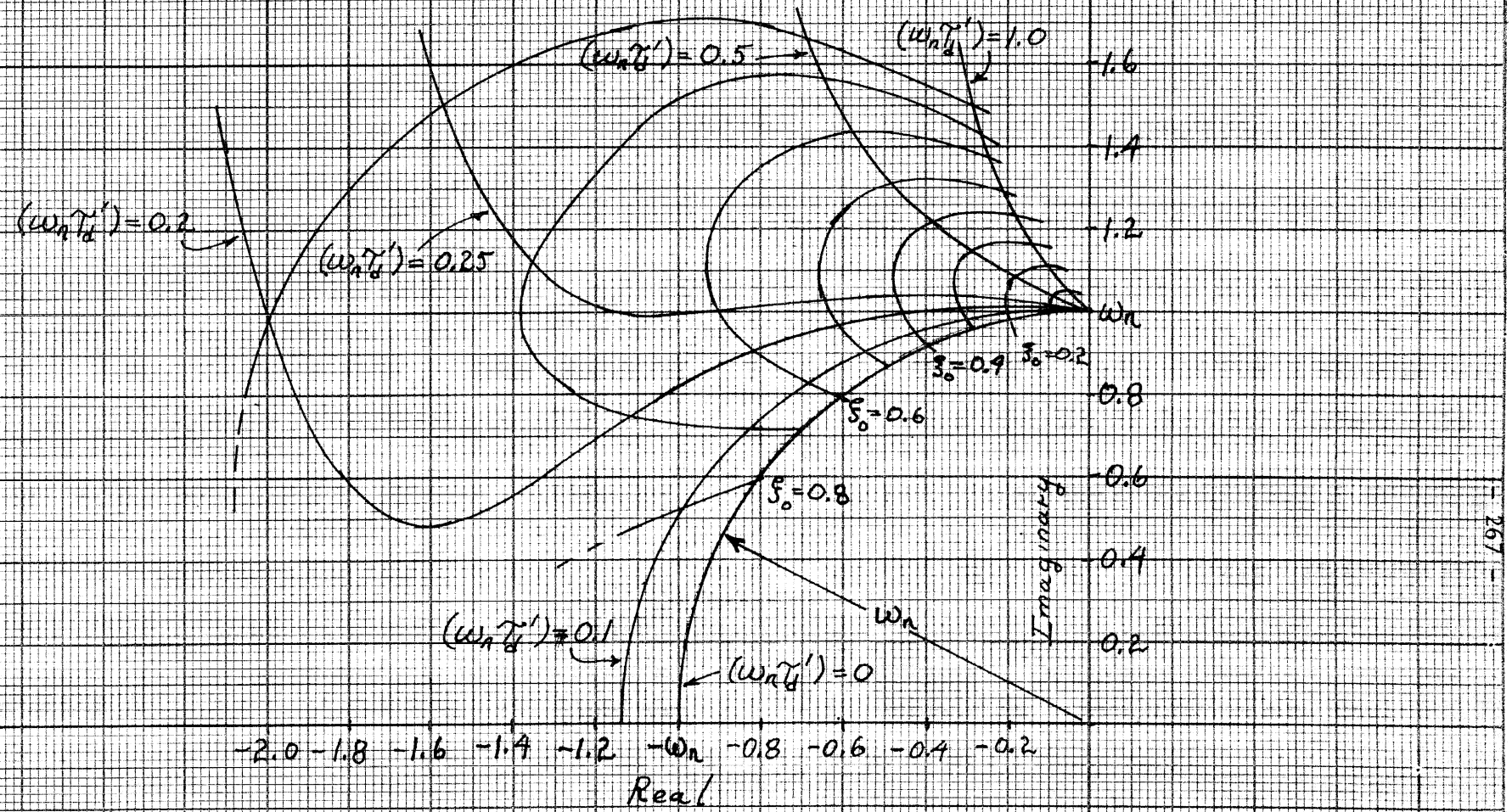

FIG 03 ROOT LOCI OF $\left(s' + 1/(\omega_n\tau_d')\right)(s'^2+1) + \frac{2\zeta_0}{(\omega_n\tau_d')}s' = 0$

FOR VARIOUS VALUES OF $(\omega_n\tau_d')$ AND ζ_0; $s' \equiv \left(\frac{s}{\omega_n}\right)$

Fig D4 Damping Ratio and Relative Oscillation Frequency for the Characteristic Response of a Synchronous Machine without Damper Windings and Negligible Armature Resistance

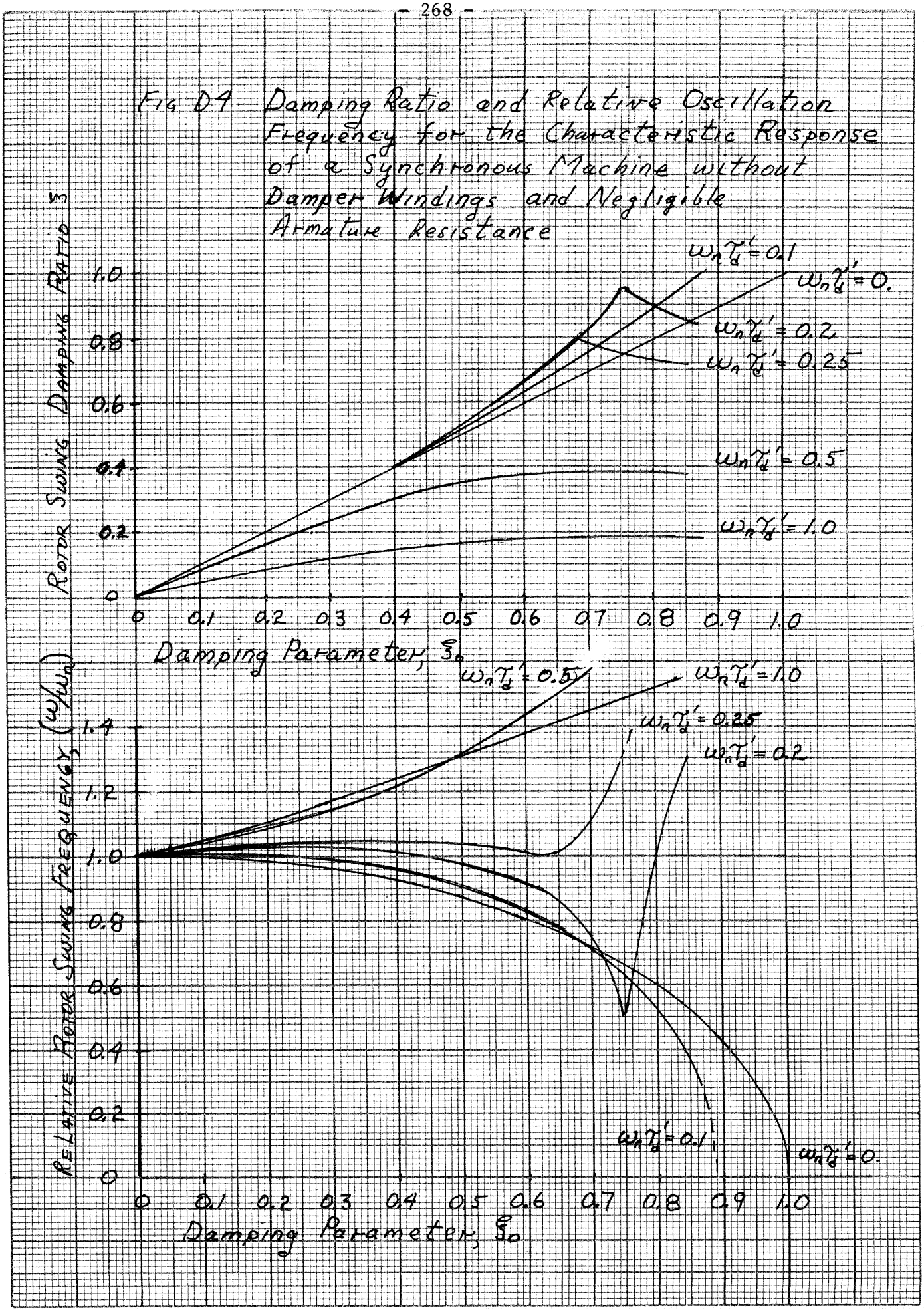

APPENDIX E

BOND GRAPHS AND THEIR APPLICATION IN DESCRIBING COMPUTATIONAL CAUSALITY REQUIREMENTS OF MULTI-MACHINE SYSTEM SIMULATIONS

Without going into the entire subject of bond-graphs in detail, the application of bond graphs to the determination of causality requirements in a system of many interconnected components may be briefly explained as follows. Components of physical models may be represented as energy multi-ports; the simplest multiport is a one-port; for example any two terminal network such as a single inductor, resistor or capacitor. As indicated in Section 1 of Chapter 2, the four-winding electrical machine may be represented as a multi-port having four electrical ports (winding terminals) and one mechanical port (rotor shaft). A connection for energy transfer to any port of a multiport model component is graphically represented by a short line segment called a "bond". Thus, the interconnections between the different model components in a system are represented by "bonds" which interconnect the ports of those models. An illustration of a bond graph for a very simple system, and its conventional circuit equivalent, is shown below.

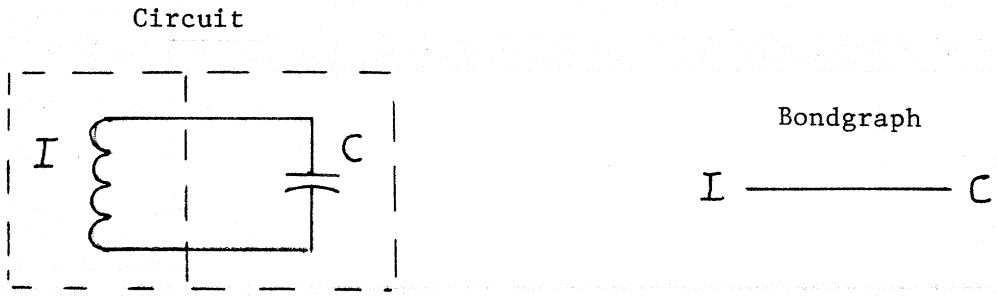

Fig. E1 Circuit Diagram and Bondgraph of a Simple Oscillator

This bond describes the path for energy transfer between the two ports which it connects. Associated with each bond are a physical effort and a physical flow variable (ie voltage and current, torque and speed), the product of these two variables is power and represents the energy transport on that bond. Thus the energy flow (power) on a bond is quantitatively defined by the product of the bond's effort and flow variables.

One of the advantages of a bond-graph representation of a complex system consisting of many interconnected components is that the computational causality flow through a model of the system can be easily and clearly determined in a systematic manner. Consequently, causal inconsistencies produced by attempting to connect a bond between two components having identical and thus conflicting causalities, become immediately evident.

As stated above, each bond is characterized by two variables, an effort and a flow. Furthermore, when one end of a bond is connected to a port, one of these bond variables will be the input or independent variable for that port, and the remaining variable will be the computed output or dependent variable with respect to that port. Now when two ports are connected by a bond, the computed output or dependent variable of one of the ports must be the input variable to the other port, and conversely. A causal conflict results when two ports having the same causality are directly connected to each other; both require the same input variable, and no means of computing that variable is available.

In a bond-graph representation of a system model, the computational causality of the various model components is indicated at the ports of those components as follows. A "causal tie" or short stroke

is drawn perpendicular to that end of a bond adjacent to the port for which the designated input is an effort variable. The designated input to the port connected at the other end of the bond will then implicitly be a flow variable. Thus, the absence of a "causal tic" at the end of a bond indicates that the flow variable is a designated input to the port connected at that end. Since what is a designated input at one end of a bond must be an output from the port at the other end, the "causal tic" may only appear at one end of a given bond for a causally consistent connection.

In the following description, the input/output assignments of effort and flow variables to the ports of the model components will be those required by integration causality. Thus in the previous example for the simple oscillator, the designation of effort as the input variable to the inductor, or equivalently as the computed output from the capacitor, is illustrated as follows:

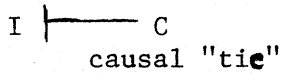

In general, the requirements of integration causality for inertive and compliant one-ports, z_I and z_C, are indicated as follows:

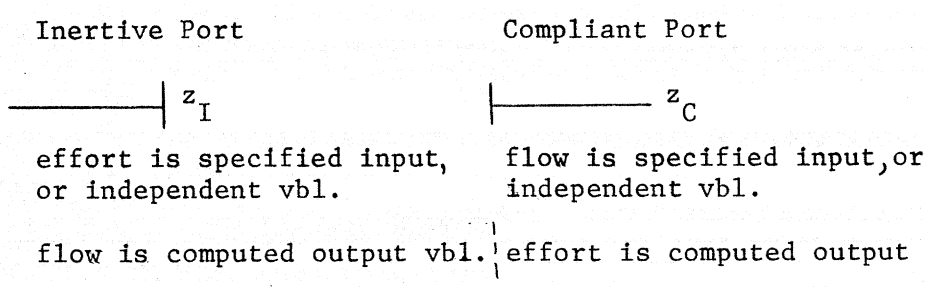

Similarly the five port machine model (which includes not only the loss-less multiport of Section 1, but also winding resistances, rotor inertia

and friction) is represented as:

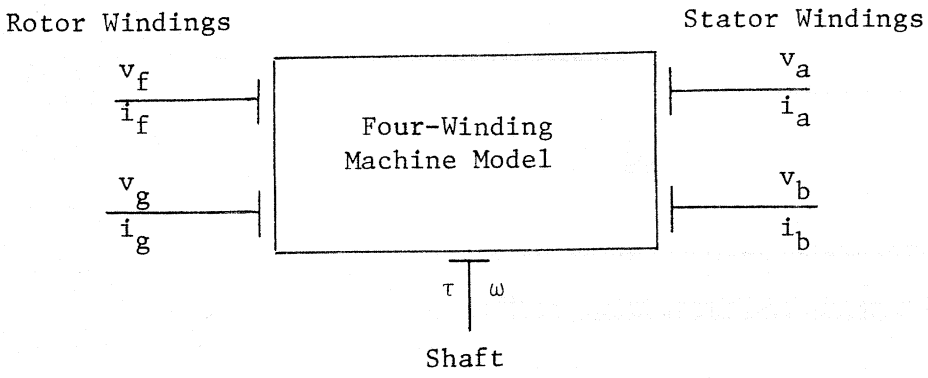

Fig. E2 Bondgraph of Four-Winding Machine Model

The above illustration indicates that the machine is an inertive multi-port, the position of the causal tics indicated the specification of effort variables (voltage, torque) as inputs in order to satisfy the integration causality requirements of the model equations.

The machines and impedance network elements in an interconnected system composed of several machines are joined by means of "series" and "parallel" connections. These two types of connections are represented by the following two types of bond graph junction structures; the "1" junction representing a series connection and the "0" junction representing a parallel connection. Both of these junction structures are ideal in the sense that power flows (product of effort and flow) in the bonds attached to these junctions must sum to zero. However, we shall only be concerned with the causal implications of these two types of junction structures. A series connection is characterized by the fact that the flow or current is the same for each element in a series string; thus the flow variable or current may only be specified once for a series connection of components. The bond graph representation of a series connection involving n ports is a "1" junction having n bonds. Because

the flow variable in all of these bonds must be the same, the flow variable may be independently specified on only one of the bonds connected to the "1" junction. Consequently, one and only one of the bonds on a "1" junction must have a causal "tic" away from the junction; the causal "tics" on the n-1 remaining bonds must be positioned adjacent to the junction. The situation for a parallel connection, which is represented by a bond-graph "0" junction, is exactly the dual of that for the series connection. A parallel connection is characterized by the fact that the effort variable is common to all components so connected, consequently the common effort variable or voltage for this connection may only be specified once. The bond graph representation of a parallel connection involving n ports is a "0" junction having n bonds. The common effort variable for the junction may only be independently specified on one of the n bonds of the "0" junction. Consequently one and only one of the n bonds on the "0" junction must have its causal "tic" towards the junction; the causal "tics" on the remaining n-1 bonds must be positioned away from the junction. These properties of "0" and "1" junctions, together with the corresponding circuit representations, are illustrated in Fig. E3.

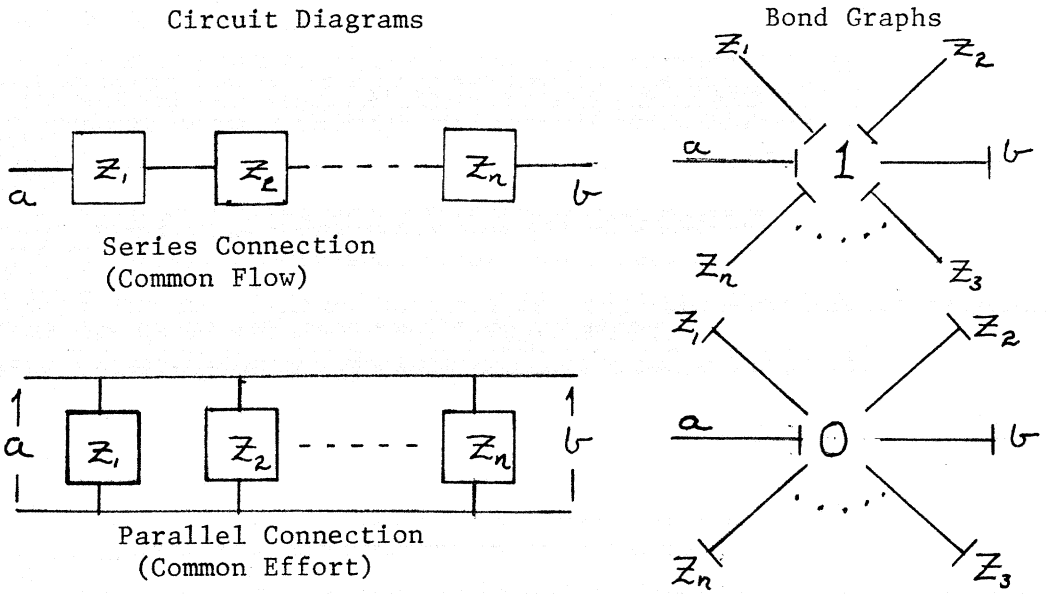

Fig. E3 Circuit Diagrams and Bond Graphs
for Series and Parallel Connections

It should be noted that the causality requirements of the above junction structures, unlike those of the energy storage elements, are independent of computational considerations and may not be violated under any circumstances. In effect, these requirements are constraints imposed by the nature of the physical connections represented by these junction structures.

The causal bond-graph of a system of interconnected components is formed by using the "0" and "1" junction structures, described above, to interconnect the bonds emanating from the ports of the individual components. For the model of the resulting connected system to be causally compatible, the assignment of causality on each bond, as indicated by the placement of the "tics", must be such as to satisfy the causality requirements of every junction structure and component in the system. Consequently the causal compatibility of a model for a system composed of many interconnected components may be determined directly from the bond-graph

of the system without having to examine the actual dynamical equations of the individual components.

Because the computational causality assignments on the ports of the energy storage components of the model were those required by integration of the model equations, the presence of a causal inconsistency in the bond-graph for an interconnected system often indicates the presence of redundant state variables in the system model. A relevant example of exactly this situation is a system composed of two machines having directly interconnected stator windings, as in the case of a pair of selsyns. The bond-graph representation of this system, shown below, clearly indicates causal incompatibility.

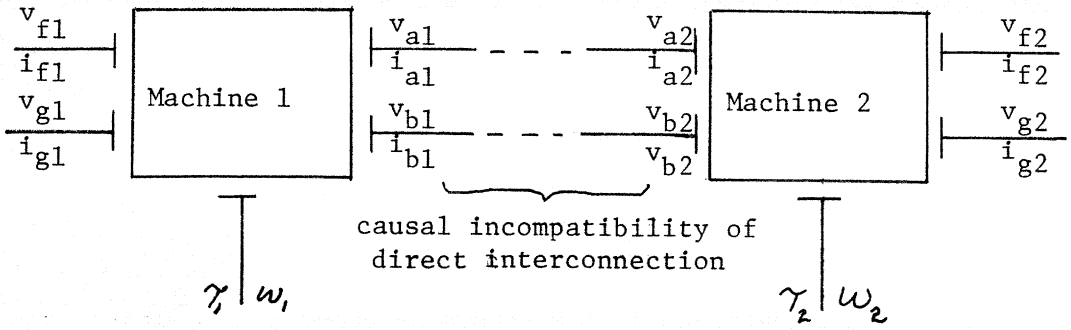

Fig. E4 Direct Interconnection of Two Single-Machine Models

Essentially the nature of the causal incompatability is that both machine models require specification of terminal voltages as input variables, and the above system model does not provide a means by which these required voltages may be computed - the computed "outputs" from both machines are the currents. Of course, one way of resolving this dilemna is to represent one of the two machines by a model having derivative

causality, thereby making the interconnection between the two machines causally compatable.

Another way of handling this problem is to eliminate the redundant state variables directly by analytically combining the model equations of both machines with the constraint equations of the interconnection. The result of such a combination is that the two interconnected single machine models are replaced by a single two-machine model as illustrated below.

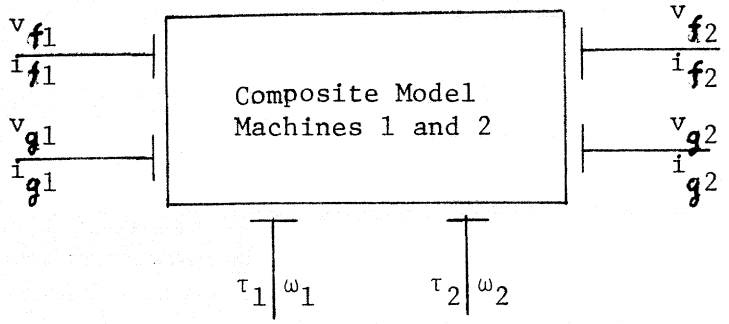

Fig. E5 Combined Two-Machine Model

Although the analytical combination of several interconnected single machine models into a single multi-machine model is always possible in principle, this technique often becomes impractical because of the tremendous complexity of the resulting equations.

Finally, the causality dilemna in this example may also be resolved by inserting a shunt resistor or capacitor in the interconnection between the two machines. The resolution of the original causal incompatability provided by the addition of such a simple shunt network is again clearly illustrated by the bond graph of the modified system. However, the resultant model is now no longer the same as that of the original system.

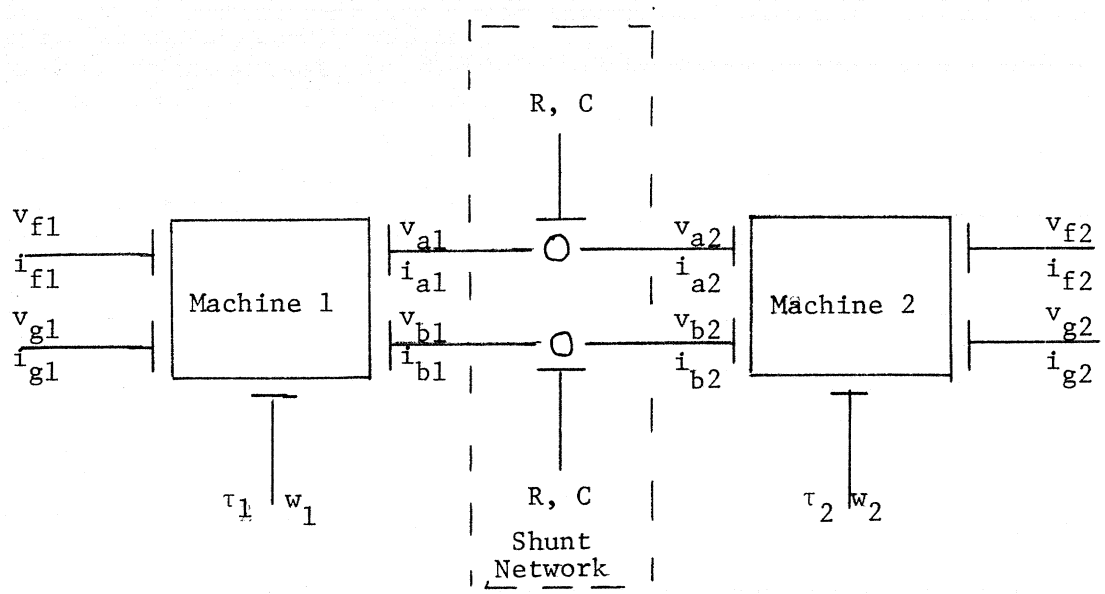

Fig. E6 Interconnected Two-Machine System with Shunt Load

The intent of the preceding paragraphs has been to very briefly describe how bond-graphs may be used to determine the flow of computational causality in simulation models for systems composed of several interconnected physical components, with particular emphasis on the simulation of multi-machine systems. The description given was limited, being specifically tailored to the problem of multi-machine simulation, and is thus far from comprehensive. For a more complete explanation of the bond graph method and its general application in physical system modelling, the interested reader should consult [5].